GEOLOGICAL SURVEY OF CANADA
COMMISSION GÉOLOGIQUE DU CANADA

# CURRENT RESEARCH 1996-A
# CORDILLERA AND PACIFIC MARGIN

---

# RECHERCHES EN COURS 1996-A
# CORDILLÈRE ET MARGE DU PACIFIQUE

1996

Natural Resources Canada Ressources naturelles Canada

Canada

## NOTICE TO LIBRARIANS AND INDEXERS

The Geological Survey's Current Research series contains many reports comparable in scope and subject matter to those appearing in scientific journals and other serials. Most contributions to Current Research include an abstract and bibliographic citation. It is hoped that these will assist you in cataloguing and indexing these reports and that this will result in a still wider dissemination of the results of the Geological Survey's research activities.

## AVIS AUX BIBLIOTHÉCAIRES ET PRÉPARATEURS D'INDEX

La série Recherches en cours de la Commission géologique contient plusieurs rapports dont la portée et la nature sont comparables à ceux qui paraissent dans les revues scientifiques et autres périodiques. La plupart des articles publiés dans Recherches en cours sont accompagnés d'un résumé et d'une bibliographie, ce qui vous permettra, on l'espère, de cataloguer et d'indexer ces rapports, d'où une meilleure diffusion des résultats de recherche de la Commission géologique.

GEOLOGICAL SURVEY OF CANADA
COMMISSION GÉOLOGIQUE DU CANADA

# CURRENT RESEARCH 1996-A
# CORDILLERA AND PACIFIC MARGIN

---

# RECHERCHES EN COURS 1996-A
# CORDILLÈRE ET MARGE DU PACIFIQUE

1996

Available in Canada from

Geological Survey of Canada offices:

601 Booth Street
Ottawa, Canada K1A 0E8

3303-33rd Street N.W.
Calgary, Alberta T2L 2A7

100 West Pender Street
Vancouver, B.C. V6B 1R8

or from

Canada Communication Group – Publishing
Ottawa, Canada K1A 0S9

and through authorized bookstore agents
and other bookstores

A deposit copy of this publication is also available for reference
in public libraries across Canada

Cat. No. M44-1996/1E
ISBN 0-660-16287-3

Price subject to change without notice

**Cover description**

Kshwan Glacier rock avalanche, Cambria Icefield, 25 km southeast of Stewart, British Columbia. Photo by Charlie Greig in August 1993. See paper by T.E. Mauthner, this volume. GSC 1995-361

Avalanche de pierres survenue dans la région du glacier Kshwan, champ de glace Cambria, 25 km au sud-est de Stewart, en Colombie-Britannique. Photo prise par Charlie Greig en août 1993. Voir l'article de T.E. Mauthner du présent volume de «Recherches en cours». (GSC 1995-361)

## Separates

A limited number of separates of the papers that appear in this volume are available by direct request to the individual authors. The addresses of the Geological Survey of Canada offices follow:

Geological Survey of Canada
601 Booth Street
OTTAWA, Ontario
K1A 0E8
(FAX: 613-996-9990)

Geological Survey of Canada (Calgary)
3303-33rd Street N.W.
CALGARY, Alberta
T2L 2A7
(FAX: 403-292-5377)

Geological Survey of Canada (Victoria)
100 West Pender Street
VANCOUVER, B.C.
V6B 1R8
(FAX: 604-666-1124)

Geological Survey of Canada (Victoria)
P.O. Box 6000
9860 Saanich Road
SIDNEY, B.C.
V8L 4B2
(Fax: 604-363-6565)

Geological Survey of Canada (Atlantic)
Bedford Institute of Oceanography
P.O. Box 1006
DARTMOUTH, N.S.
B2Y 4A2
(FAX: 902-426-2256)

Quebec Geoscience Centre/INRS
2535, boulevard Laurier
C.P. 7500
Sainte-Foy (Québec)
G1V 4C7
(FAX: 418-654-2615)

## Tirés à part

On peut obtenir un nombre limité de «tirés à part» des articles qui paraissent dans cette publication en s'adressant directement à chaque auteur. Les adresses des différents bureaux de la Commission géologique du Canada sont les suivantes :

Commission géologique du Canada
601, rue Booth
OTTAWA, Ontario
K1A 0E8
(facsimilé : 613-996-9990)

Commission géologique du Canada (Calgary)
3303-33rd St. N.W.,
CALGARY, Alberta
T2L 2A7
(facsimilé : 403-292-5377)

Commission géologique du Canada (Victoria)
100 West Pender Street
VANCOUVER, British Columbia
V6B 1R8
(facsimilé : 604-666-1124)

Commission géologique du Canada (Victoria)
P.O. Box 6000
9860 Saanich Road
SIDNEY, British Columbia
V8L 4B2
(facsimilé : 604-363-6565)

Commission géologique du Canada (Atlantique)
Institut océanographique Bedford
P.O. Box 1006
DARTMOUTH, Nova Scotia
B2Y 4A2
(facsimilé : 902-426-2256)

Centre géoscientifique de Québec/INRS
2535, boulevard Laurier
C.P. 7500
Sainte-Foy (Québec)
G1V 4C7
(facsimilé : 418-654-2615)

# CONTENTS

# Carlin-type gold deposits and their potential occurrence in the Canadian Cordillera

K. Howard Poulsen
Mineral Resources Division, Ottawa

*Poulsen, K.H., 1996: Carlin-type gold deposits and their potential occurrence in the Canadian Cordillera; in Current Research 1996-A; Geological Survey of Canada, p. 1-9.*

**Abstract:** Carlin-type deposits are characterized by pyrite and micron-sized gold particles disseminated in de-calcified zones in otherwise carbonate-bearing rocks. Silicification in the form of stratabound jasperoid replacements of bedded rocks and as discordant hydrothermal breccias is a common affiliate of ore. Carlin-type deposits are commonly enriched in arsenic, antimony, and mercury and this is reflected in part by the presence of coarse stibnite and orpiment / realgar in late-stage veins. Carlin-type deposits are controlled structurally by thrusts, upright folds and, most important, high-angle normal faults. They occur in distinct mineral belts in the Paleozoic miogeocline of the western United States where they co-exist with Paleozoic sedex deposits and Mesozoic through Cenozoic intrusion-related porphyry Cu-Mo, skarn Cu, skarn Au, skarn Pb-Zn, and vein and manto Ag-Pb-Zn deposits. Although definitive examples of Carlin-type deposits are unknown in Canada, analogous geological environments exist in the Omineca Belt of the Canadian Cordillera.

**Résumé :** Les gisements de type Carlin sont caractérisés par la présence de pyrite et de particules microniques d'or disséminées dans les zones décalcifiées de roches autrement carbonatées. La silicification, sous la forme de substitutions en jaspéroïdes stratoïdes de roches stratifiées et sous la forme de brèches hydrothermales discordantes, accompagne souvent la minéralisation. Les gisements de type Carlin sont habituellement riches en arsenic, en antimoine et en mercure, ce qui s'explique en partie par la présence de stibine et d'orpiment-réalgar (grain grossier) dans les filons tardifs. Les gisements de type Carlin sont contrôlés structuralement par des chevauchements, des plis droits et surtout des failles normales à pendage fort. Ils sont situés dans des zones minérales distinctes du miogéosynclinal paléozoïque de l'ouest des États-Unis, où ils coexistent avec des gisements exhalatifs sédimentaires (SEDEX) du Paléozoïque et des gisements du Mésozoïque au Cénozoïque (porphyres à Cu-Mo, skarns cuprifères, skarns aurifères, skarns plombo-zincifères ainsi que filons et mantos minéralisés en Ag-Pb-Zn). On ne connaît aucun exemple définitif de gisements de type Carlin au Canada, mais des milieux géologiques analogues existent dans le domaine d'Omineca de la Cordillère canadienne.

## INTRODUCTION

Carlin-type deposits are the major source of current gold production in the Great Basin segment of the United States Cordillera (Fig. 1, 2) but are not known in Canada despite many similarities in geology and metallogeny (Dawson et al., 1991). The author therefore spent the 1995 field season examining the potential for this type of deposit in Canada. This progress report is an overview of Carlin-type deposits based both on literature review and on direct observations in the Great Basin, followed by a discussion of application of this information to the Canadian Cordillera, particularly in the northern part of the Omineca Belt.

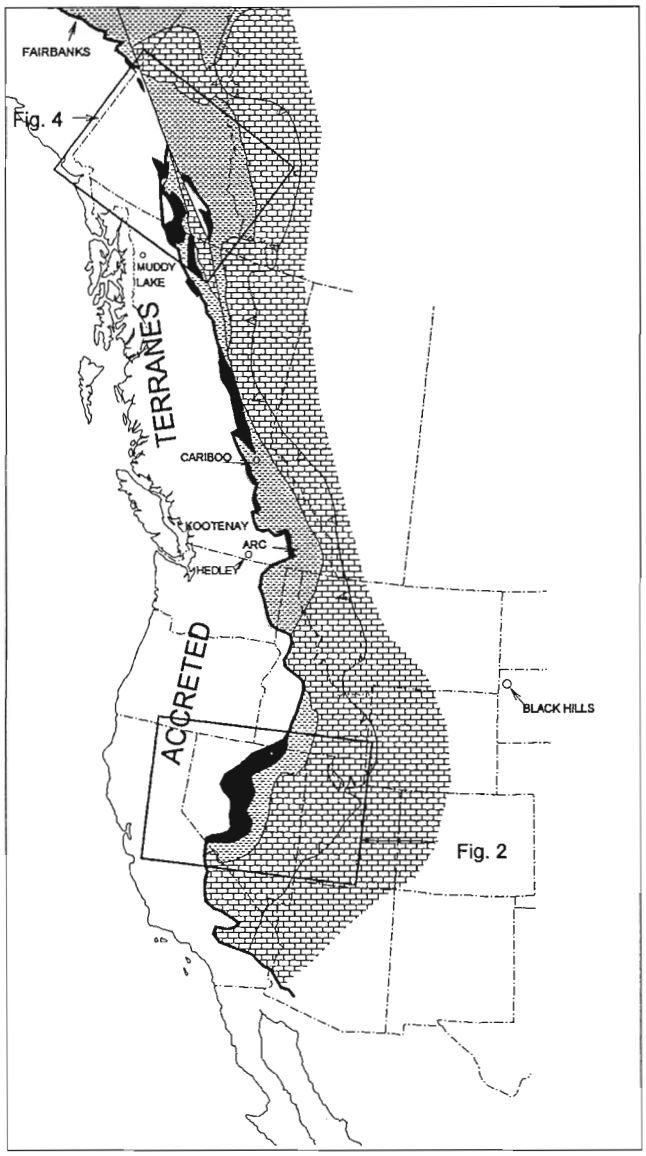


***Figure 1.*** *Sketch map of the western margin of ancestral North America showing the locations of major mineral districts discussed in the text (adapted from Turner et al., 1989; Gabrielse and Yorath, 1991).*

## CARLIN-TYPE DEPOSITS

Carlin, Nevada, is synonymous with a particular type of mineral deposit in which fine-grained gold is dispersed mainly in calcareous sedimentary rocks. Prior to the 1960s, a few similar deposits of this type were successfully mined in the Bingham Canyon area of Utah (Mercur), in the Black Hills of South Dakota (Golden Reward / Annie Creek), and in the Cortez area of Nevada (Gold Acres). Lindgren (1933) classified them as mesothermal "siliceous limestone replacement" deposits. A few other deposits of this type were known but metallurgical treatment was commonly difficult due to the refractory nature of some of the ore types. The discovery of the Carlin Mine and new processing techniques in the 1960s led to the modern recognition of a specific class of gold deposit which is commonly termed as "Carlin-type" (Berger and Bagby, 1991).

### *Definition*

No strong consensus exists as to the defining characteristics of this deposit type owing to geological differences from deposit to deposit in the Carlin area, and to even greater differences when deposits beyond the Carlin area are considered. A practical definition is that Carlin-type deposits are irregular bodies of disseminated pyrite and micron-sized gold particles in de-calcified sedimentary rocks that were once carbonate-bearing. Gold occurs mainly in discordant breccia zones and stratabound concordant zones and is found most commonly within the arsenian rims of pyrite grains, encapsulated in fine-grained quartz and as free grains.

### *Host rocks*

The host rocks in north-central Nevada range in age from Cambrian to Triassic and commonly consist of calcareous siltstone to dolomitic limestone: units that are bedded (1 cm to 1 m) appear to be more favourable hosts than thick massive ones. In a few cases, sandstone and conglomerate possessing calcareous matrix or cement are good hosts and there are local cases where Carlin-type mineralization is hosted by greenstone of volcanic origin. Granitoid intrusions and associated skarn and calc-silicate hornfels occur adjacent to many deposits (Fig. 3); although sedimentary hosts rocks are most common, there are places where Carlin-type mineralization extends out of a sedimentary host into igneous rocks such as felsic dykes and sills.

### *Alteration*

The effects of hydrothermal alteration in and around Carlin-type deposits are visually subtle but mineralogically distinctive. The most common alteration products are "de-calcified" carbonate rocks in which calcium carbonate has been removed to produce a bleached, "sanded" rock (Kuehn and Rose, 1992); in places the bleaching is obscured by the presence of particulate carbon so that the rock takes on a charcoal colour. Decalcification is also responsible for a peculiar texture at several deposits : centimetre-thick lenses

and layers of black crystalline calcite are separated by 10 to 20 cm-thick layers of buff, gritty decalcified rock that was formerly limestone. Such crystalline calcite may result from carbonate dissolved from the limestone and reprecipitated elsewhere.

A more extreme and readily recognizable form of alteration is jasperoid (Fig. 3), a product of silicification of carbonate lithologies (Kuehn and Rose, 1992). This has been observed to varying degrees at most deposits and appears to be an important guide to ore even where, as is most common, it contains low concentrations of gold. Jasperoid superficially resembles chert (which also occurs in the stratigraphic section near some deposits) but can be distinguished on the basis of complete replacement of many consecutive beds, by the presence of silicified fossil pseudomorphs and, most important, by the presence of cavities lined by fine-grained sugary quartz and limonite after sulphide minerals. Even more extreme forms of hydrothermal alteration, likely assisted by faulting, are jasperoidal hydrothermal breccias: they are composed of angular fragments of jasperoid that, in turn, are cemented by fine-grained, "cherty" silica. The breccias are discordant and appear to have a closer affinity with gold mineralization and, in some cases, constitute ore in contrast to the more massive stratabound jasperoid replacement zones which contain only chemically anomalous amounts of gold. Argillic alteration commonly accompanies fault-controlled silicification (Keuhn and Rose, 1992).

### *Structure*

A high degree of structural control on the sites of Carlin-type mineralization is indicated by the spatial association of deposits with, in order of decreasing age, thrusts, upright folds, and high-angle normal faults.

Thrusts are present in many Carlin-type deposits and in most cases occur within, or define the boundaries of, the mineralized zone. The specific role of thrusts is difficult to judge but regional structures such as the Golconda Thrust (Permian Sonoman Orogeny), the Roberts Mountains Thrust (RMT; Devono-Mississippian Antler Orogeny), and the Sevier Fold and Thrust Belt (Cretaceous) are regional loci for gold (Fig. 2). For example, rocks of the Roberts Mountains Allochthon above the Roberts Mountain Thrust are mainly Ordovician siliciclastics whereas the carbonate-bearing strata directly below it are as young as Devonian and are preferential hosts to ore; similar relationships are present at other type localities and have also been verified in a general way at several mines. Most thrusts in the Great Basin deposits are

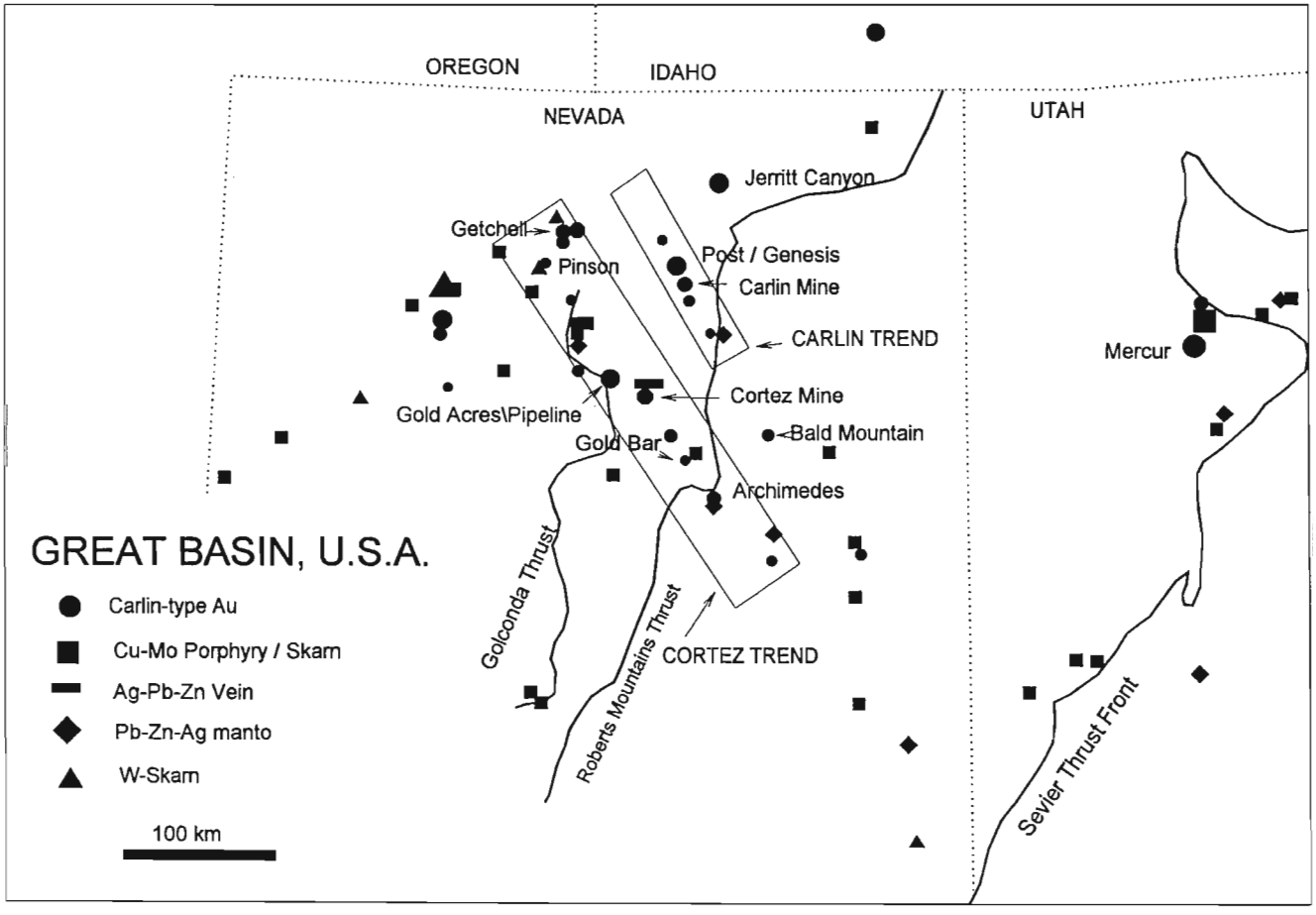


***Figure 2.*** *Map of part of the Great Basin showing major structural features and Carlin-type gold deposits in relation to other mineral deposit types (adapted from Berger and Bagby, 1991 Peters et al., 1995).*

ductile shear zones at shallow angles to bedding; within them strata are strongly transposed and contorted. Mesoscopic intrafolial isoclines and thrust duplexes were observed in such shear zones at several localities.

Upright anticlines of 10 to 100 m amplitude were observed in more than half of the deposits visited. Such folds trend north-northwest parallel to the Carlin and Cortez gold belts and, as demonstrated by S.G. Peters (in Peters et al., 1995), are particularly common in the Carlin area. The Tuscarora and Betze anticlines are ore-controlling structures in the Genesis and Post-Betze deposits respectively and similar structures are present at Gold Acres and Cortez (Howald et al., 1995). It is possible that the control results from the fact that these folds reflect the presence of larger doubly plunging anticlinoria, the eroded cores of which define "windows" of favourable carbonate rocks below the Roberts Mountains Thrust. Most geologists consider the upright folds to postdate the thrusts but some could be related to thrusts as accommodation structures or anticlinal thrust terminations.

The most ubiquitous structural features associated with Carlin-type deposits are high-angle normal faults. These faults commonly strike either northeast, northwest, or north and they are regarded as direct controls of ore because grade-thickness contours typically mimic one or more of these trends. It is also clear that these are not basin-and-range faults (Miocene) which cut and offset orebodies and ore-related faults. Graubard and Smith (1995) have suggested that the regular orientations of these ore-related faults may reflect primary trends in underlying Precambrian basement as well as the configuration of the Proterozoic rifted margin of North America.

### *Geochemistry*

Apart from gold, Carlin-type deposits are geochemically enriched in arsenic, antimony, and mercury. Arsenic abundance is also reflected microscopically by arsenian rims (containing inclusion gold) on pyrite, locally by the presence of arsenopyrite and mesoscopically by common late-stage (post ore?) calcite veinlets containing orpiment and realgar. Likewise, coarse stibnite in late fractures is a reflection of antimony abundance at some deposits. The As-Sb-Hg enrichment is commonly cited as the Carlin suite of trace elements but Ba and W have also been reported at some deposits (Berger and Bagby, 1991), perhaps more as a reflection of local geology than of Carlin-type mineralization. Although base metal deposits occur in proximity in some cases, Carlin-type ores have notably low contents of Cu, Pb, and Zn and Ag.

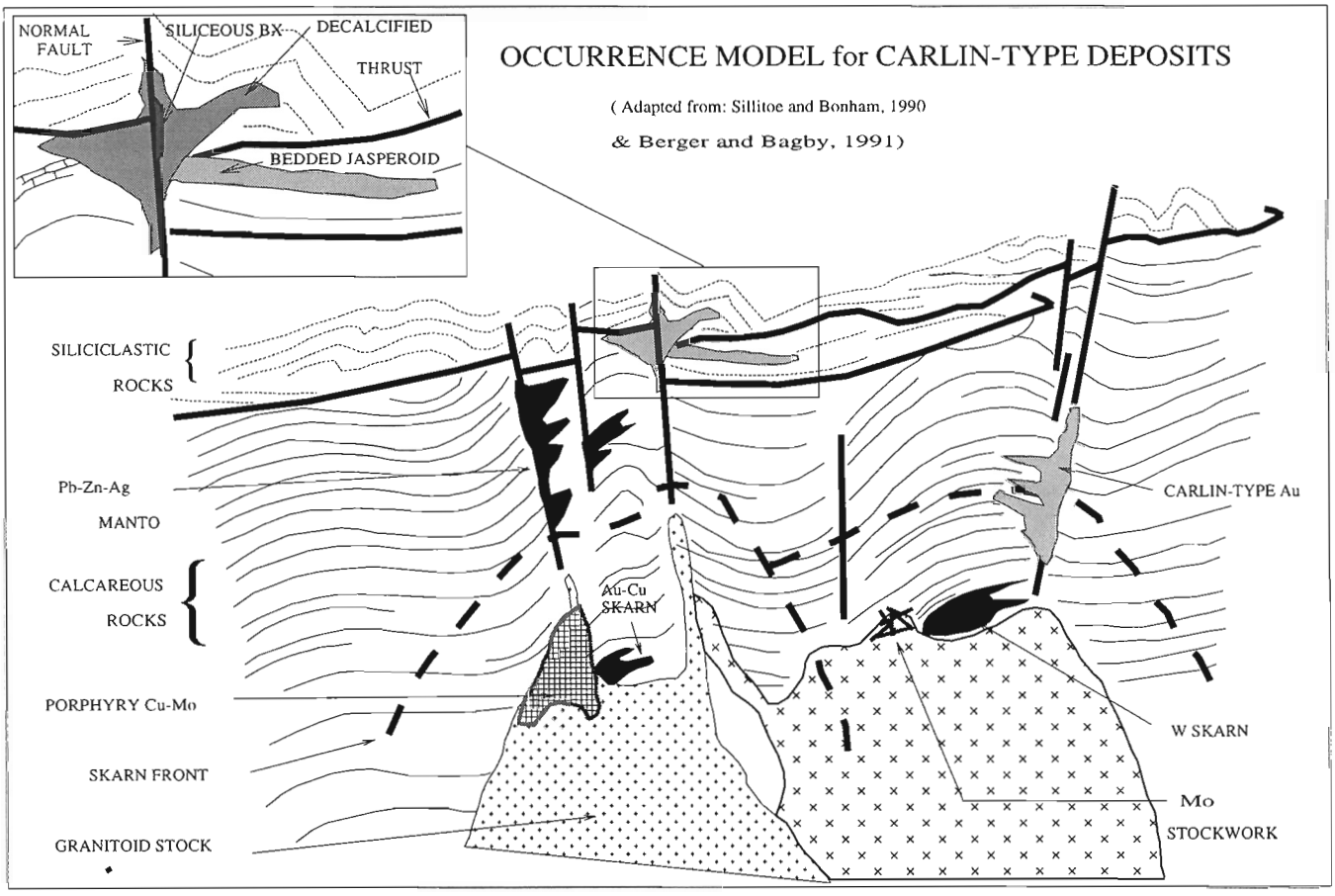


***Figure 3.*** *Schematic diagram illustrating the occurrence of Carlin-type deposits in relation to granitoid intrusions, structures and contact metamorphic features.*

### *Size*

The deep Tertiary weathering of the Carlin-type deposits of north-central Nevada and the mining of many of them by open-pit operations has led to the mistaken impression that, geologically, Carlin-type deposits are inherently of large tonnage and low grade. This is an artifact of open pit – heap leach oxide mining and processing methods; however many operations, particularly at mature mines, are shifting to underground mining to exploit deep high-grade hypogene ores that grade between 15 and 30 g/t Au. The range of tonnage-grade characteristics of Carlin-type deposits therefore would be effectively the same as Canadian Shield gold deposits if only hypogene ores were compared.

### *Metallogeny*

Carlin-type gold deposits in north-central Nevada are but one component of a larger metallogenic province that is more or less coincident with the Great Basin physiographic region (Fig. 1). The variety of commodities and many of the ore deposit types occurring within the Great Basin have little direct connection with the Miocene extension that formed it and Carlin-type deposits are no exception.

A first-order spatial control on the distribution Carlin-type deposits is their location within carbonate rocks that were deposited on the passive continental margin of North America (Fig. 1). In the case of north-central Nevada, the deposits occur near the interface, partly depositional and partly tectonic, of easterly transported offshore siliciclastic rocks and autochthonous shelf carbonate rocks as well as in "Antler" overlap molasse basins near this interface. As such they tend to overlap spatially in a broad way with Paleozoic sedex deposits which, in Nevada, are composed mainly of barite.

A second-order control is their location within a broad belt of Mesozoic-Cenozoic magmatism that has overprinted the continental margin. As such, Carlin-type deposits broadly co-exist with skarn W deposits (mainly Cretaceous), porphyry Cu-Mo and related skarn deposits (Jurassic, Cretaceous, Paleogene), and vein / manto / chimney deposits of Ag-Pb-Zn (Fig. 3).

A third-order spatial control is their occurrence in northwest-striking polymetallic mineral belts, most prominent of which are the Carlin and Cortez trends (Fig. 2) which contain the Carlin and Cortez gold districts respectively. Contrary to many published accounts, these mineral belts do appear to correspond with physically identifiable features. Most important from the point of view of Carlin-type deposits is the fact that the mineral belts are marked by aligned trains of anticlinoral windows that expose carbonate rocks below the Roberts Mountains Thrust – the windows are likely culminations in northwest folds with further control by northwest high-angle faults. Another feature of the mineral belts is that they correspond to chains of felsic stocks. Three main age ranges are represented: Jurassic (170-150 Ma), Cretaceous (110-90 Ma) and Tertiary (40-30 Ma). Some of these intrusions have associated porphyry Cu-Mo mineralization and skarns whereas others are barren and have weakly developed skarn and hornfels at their margins. Many of the Carlin-type deposits in the Great Basin occur within 1 to 2 km of intrusions, particularly those of Mesozoic age. Important examples include the Post-Betze-Genesis group of deposits (167 Ma Goldstrike stock), Bald Mountain deposits (155 Ma stock with minor W and Pb-Zn skarn), Getchell and Pinson deposits (90 Ma stock with major W skarn), Cortez (Jurassic-Cretaceous stock with peripheral vein / manto Ag-Pb-Zn), Gold Acres and Pipeline deposits (99 Ma Gold Acres stock with minor Mo-W skarn and Pb-Zn skarn), Archimedes (100 Ma stock with Pb-Zn skarn and peripheral vein / manto Ag-Au-Pb-Zn), and Gold Quarry (stock of unknown age with Cu-Au skarn). The last three cases are of interest because the presence of intrusions is not evident from bedrock geology maps: they have been intersected in drill core, either deeply buried or shallow and covered by pediment. Nonetheless there are some important cases (e.g. Jerritt Canyon, Gold Bar, the Carlin Mine) where there is no direct evidence whatsoever of intrusions spatially associated with Carlin-type mineralization.

Although an overall spatial correlation between Carlin-type deposits and felsic plutons finds good empirical support, there is little hard evidence to support a direct genetic link between the two. Therefore the timing of Carlin-type deposits is a key metallogenic question but this remains largely unresolved. Like the case for Canadian Shield gold deposits, this is currently one of the most contentious research issues surrounding Carlin-type deposits. The best indirect evidence is that in the cases of the Jurassic Goldstrike and Bald Mountain stocks, a significant amount of ore-grade mineralization is hosted by the intrusive rocks and this is continuous with Carlin-type mineralization in adjacent calcareous rocks. The other bracket is provided by Tertiary felsic dikes (40-30 Ma) which commonly cut orebodies; in no cases are these significantly mineralized although in some cases they are reported to be hydrothermally altered. The results of direct dating of Carlin-type deposits are highly controversial but two views are prominent: one is that all deposits are Oligocene (40-30 Ma; Thorman et al., 1995), the other is that the deposits range in age from Jurassic through Oligocene (Berger and Bagby, 1991).

### *Ore genesis*

The early view that Carlin-type deposits are of epithermal origin and of Miocene age related to basin-and-range extension has been largely refuted on geological grounds and few geologists hold this view. There are, however, two other prominent views on the origin of these deposits: one intrusion-related, the other a deep-crustal fluid-fault model.

The first view, that Carlin-type deposits are distal replacement deposits that formed in the proximity of felsic intrusions, is probably best embodied in the model of Sillitoe and Bonham (1990). These authors emphasized that there is a strong spatial association between intrusions and Carlin-type mineralization which they viewed essentially as distal skarns (Fig. 3). One of the implications of this genetic model is that it allows for a variety of deposit ages. Another is that intrusive systems known to have associated (even weakly developed) porphyry or skarn mineralization are prospective

sites for Carlin-type deposits. It is not clear whether any particular metal association is a requirement; however, in some cases the metal related to the intrusion is Cu, in others it is Pb and/or Zn, and yet in others W (Berger and Bagby, 1991).

The second view (Thorman et al., 1995) is that Carlin-type deposits in north-central Nevada formed from deeply convecting crustal-scale hydrothermal cells that operated during a very restricted interval in the late Eocene to early Oligocene. Although recognizing that this activity is temporally and spatially coincident with magmatism, this model denies any direct link between Carlin-type deposits and plutonic rocks. Rather the deposits are viewed as the products of a unique period of pre-basin-and-range crustal thinning in this area in the Paleogene. This thinning is thought to have lead to increased geothermal gradients and to the development of large-scale hydrothermal cells controlled by existing Paleozoic and Mesozoic structures. This model envisions regional flow of meteoric waters, large-scale interaction between fluids and rocks, and deposition of gold at 2 to 6 km in the crust.

The question of the genesis of Carlin-type deposits remains to be resolved but, from an empirical point of view, an occurrence model that relates them spatially to felsic intrusive rocks, skarns, and contact aureoles is fully consistent with the field observations at most of the Great Basin deposits that were examined. This model therefore can serve as a starting point for evaluating analogous Canadian environments.

## POTENTIAL FOR CARLIN-TYPE DEPOSITS IN THE CANADIAN CORDILLERA

A complete assessment of potential for Carlin-type deposits in the Canadian Cordillera will require much more in-depth study but, on the basis of information gathered during the past field season, a few preliminary points can be considered. The first is that the outcome of the assessment depends strongly on a choice of deposit model. The "intrusion-related" model allows for diverse ages and local settings for deposits of this type whereas the "deep-crustal extensional" model is much more restrictive and corresponds to a unique temporal and tectonic combination that corresponds specifically to the Great Basin. Certainly, an important "Nevada-only" aspect is the deep Tertiary weathering that allowed exploitation of so many otherwise non-economic gold deposits. By the same token, however, this unique exploitation of oxide ores has led to the discovery of higher-grade hypogene ores which likely would have otherwise escaped detection. These hypogene deposits, as yet incompletely documented, should form the basis of search for Carlin-type mineralization in Canada, where the "intrusion-related" view of Carlin-type deposits could find direct application.

If one focuses on the subset of hypogene Carlin-type deposits and on the model of an intrusion association, then two major geological settings stand out as being prospective. The first is in those parts of the accreted terranes that have a basement containing carbonate lithologies that have been overprinted by Mesozoic and Cenozoic plutonism. For example, gold mineralization that is Carlin-like has been described in the upper Paleozoic carbonate rocks of the Asitka group of the Stikine terrane in the Muddy Lake area of northern British Columbia (Schroeter, 1986). One might also expect Carlin-type mineralization in similar settings in the Stikine and Quesnel terranes in southern British Columbia, especially distal to known examples of gold-rich skarns as in the Hedley District (Dawson et al., 1991).

The second major prospective setting for Carlin-type mineralization in the Canadian Cordillera is in miogeoclinal and adjacent pericratonic terranes of the Omineca Belt (Gabrielse and Yorath, 1991) where there are direct analogues to the Great Basin:

1. The same stratigraphic elements are present in this portion of the deformed continental margin of ancestral North America as exist in the Great Basin: in the late Paleozoic, westerly derived clastic rocks overlap easterly derived early Paleozoic shelf carbonate to offshore clastic transitions (Gordey et al., 1987; Turner et al., 1989; Gabrielse and Yorath, 1991).
2. Overprinting Mesozoic magmatism has, not surprisingly, resulted in large-scale metallogenic signatures similar to those in the Great Basin. The Selwyn Basin is an area of the Yukon where a variety of Au- and W-bearing Cretaceous skarns (Sinclair, 1986) exists and where intrusion-related disseminated gold has already been discovered. The Ketza River (Pelly Mountains) and Midway (Cassiar Platform) areas are also particularly attractive because of the of the presence of known Ag-Pb-Zn mantos, some of which are auriferous (Abbott, 1986; Cathro, 1988): the analogies with Nevada's Ruby Hill district are strong. Likewise the Cariboo district (Fig. 1) hosts auriferous sulphide deposits that are similar in some respects to the Ruby Hill mantos and, although this is a deformed terrane, it could host Carlin-type ores. The collective presence of favourable carbonate stratigraphy, Mesozoic intrusions, skarn W, Ag-Pb-Zn veins as well as known vein-type gold deposits (e.g. Ymir) makes the Kootenay arc another attractive site for Carlin-style mineralization.

Despite these compelling tectonic and metallogenic analogues, definitive examples of Carlin-type mineralization have yet to be reported in the Omineca Belt. The next section therefore examines the specific case of the northern part of the Omineca with an analysis of the important controlling factors which might indicate the presence of this type of mineralization.

### *The example of the northern Omineca Belt*

Like the Cortez Trend of Nevada (Fig. 2), the miogeoclinal portion of the northern Omineca Belt in Yukon Territory and adjacent parts of the Northwest Territories, British Columbia and Alaska is overprinted by a metalliferous Cretaceous magmatic arc (Fig. 4; Sinclair, 1986; Gordey and Anderson, 1993). This belt contains mineral deposits including skarn W, skarn Pb-Zn-Ag, and vein Ag-Pb-Zn as well as diverse types of gold mineralization including intrusion-related sheeted

veins, skarns, and mantos. An occurrence model that shows the distribution of the various styles of mineralization in schematic form relative to a hypothetical felsic stock (Fig. 5) has been established through direct observation and an analysis of mineral file data. Note that most known gold deposits and occurrences are located inboard of contact metamorphic aureoles around Cretaceous stocks. Most prominent are deposits composed of Au-Bi-Mo-W (e.g. Dublin Gulch, Clear Creek) in sheeted quartz veinlets mainly within porphyritic intrusive rocks but locally extending outward into adjacent hornfels. These are examples of the "Fort Knox" style of mineralization found near Fairbanks, Alaska (J.K. Mortensen, pers. comm., 1995) and thought to be in the broadest sense porphyry-type gold mineralization (Hollister, 1991): W-skarn (Ray Gulch, Scheelite Dome) occurs in the same environment (Fig. 5). Gold is also present in skarns (Brown and Nesbitt, 1987) and mantos (Cathro, 1988) that are likely related to intrusions of similar age and type.

Some of the oxidized gold deposits of the Brewery Creek District (Fig. 4) are atypical in that they are found beyond the extremities of a contact metamorphic aureole (Fig. 5). Apart from local intrusion-hosted "Fort Knox style" mineralization (e.g. the Classic zone), most known mineralization is of Au-As-Sb affinity in fault-controlled veinlet zones in dykes and sills of porphyritic quartz monzonite that are of similar age to nearby stocks but lack the related contact aureoles. The sills and dykes intrude near the contact between argillite, siltstone, and dolomitic siltstone of the Ordovician-Silurian Road River Group and argillite, chert-pebble conglomerate, and arenite that are correlative with the Devono-Mississipian Earn Group (T. Bremner, pers. comm., 1995). Although most of geological reserves of gold mineralization at Brewery Creek are confined to intrusive hosts, up to 20 per cent (the Blue and Pacific zones) occurs as disseminations and in zones of weak brecciation in Earn Group siliciclastic rocks; this sediment-hosted mineralization is also geochemically anomalous in As and Sb and is strongly controlled by faults (R. Diment, pers. comm., 1995). At best it can be viewed as "Carlin-like" in that the hosts are non- to weakly calcareous and there is little obvious evidence of silicification. However, the fact that such mineralization does exist in the distal portions of a larger intrusion-centred hydrothermal system, emphasizes that this is the kind of setting that may host "Carlin-type" mineralization, as defined in a stricter sense, in more calcareous lithologies. Such lithologies are abundant throughout the northern Cordilleran Miogeocline because the

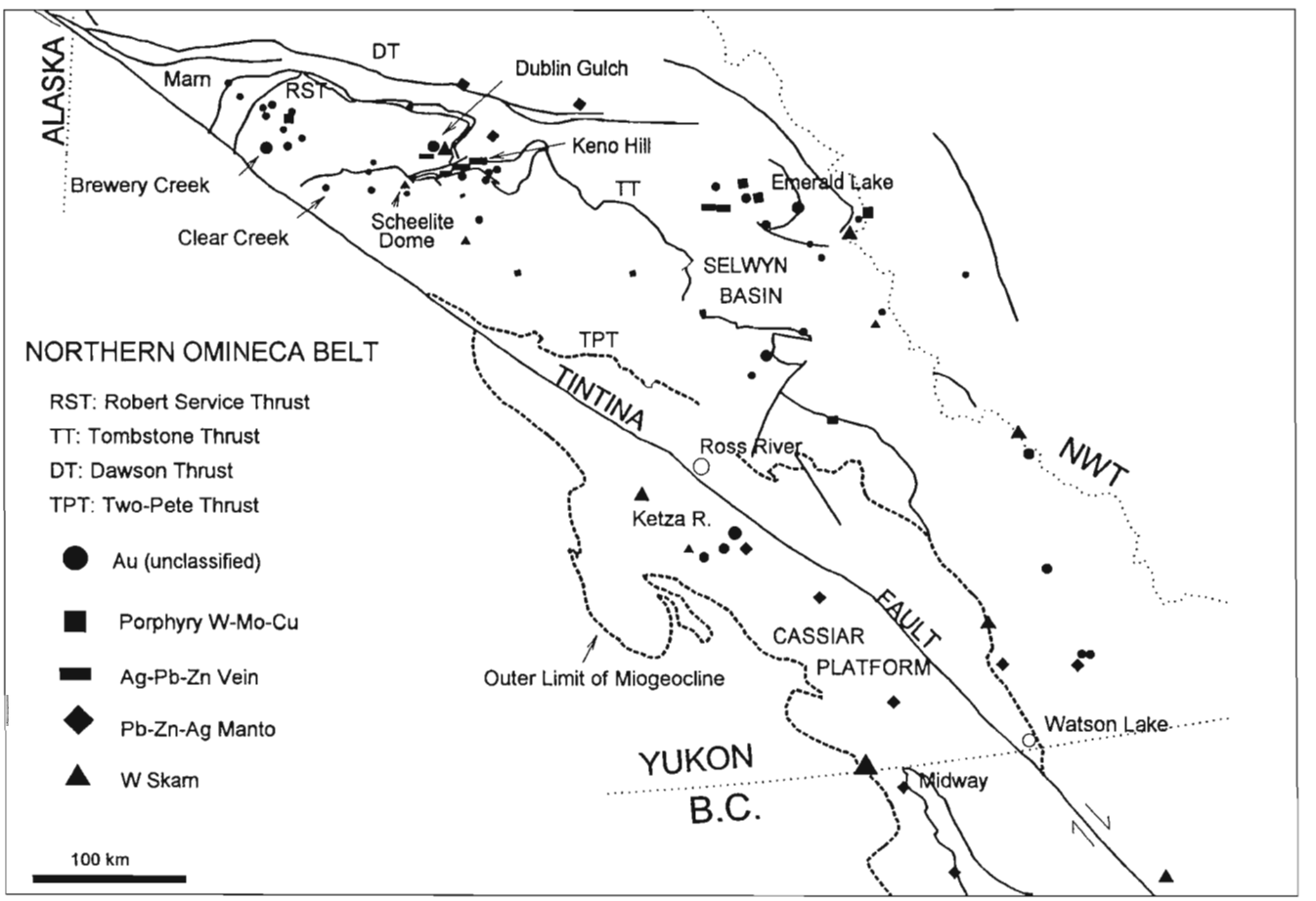


***Figure 4.*** *Sketch map of part of the northern Omineca Belt showing major structural features and known gold deposits / occurrences in relation to other mineral deposit types (adapted from Sinclair, 1986; Dawson et al., 1993).*

facies boundary between siliciclastic and carbonate lithologies has remained stationary for a long time (Gordey and Anderson, 1993). Intercalations of argillite, local coarse clastic rocks, and impure carbonate rocks are therefore common in sequences ranging from the Late Precambrian (Hyland Group) through the Triassic. Further tectonic imbrication of these lithologies has taken place locally in northern Cordillera, as in Nevada, during the emplacement of major allochthons (Fig. 4) such as those soled by the Robert Service and Tombstone thrusts (D. Murphy, pers. comm., 1995). Potentially favourable host units for disseminated gold mineralizaton include the carbonate members of the Precambian Yusezyu Formation, the Cambro-Ordovician Rabbitkettle Formation, and the Silurian Steel Formation as described by Gordey and Anderson (1993). The orange- to buff-weathering wispy laminated mudstone (locally dolomitic) Steel Formation is particularly noteworthy in that it strongly resembles, both in age and lithology, the highly productive Roberts Mountains Formation in Nevada. In addition, this unit is noted for the widespread occurrence of diagenetic pyrite (Gordey and Anderson, 1993); this provides attractive sites for nucleation of gold derived from hydrothermal fluids.

## DISCUSSION

The foregoing is recognized to be a much simplified analysis of the complex question of potential for Carlin-type mineralization in the Canadian Cordillera. Nonetheless, there is little doubt that the geological settings offered by the Selwyn Basin and Cassiar Platform are strongly analogous to those of the Carlin-type deposits of the Great Basin and the economic consequences of this should be seriously entertained. The presence or absence of Carlin-type mineralization in these Canadian terranes also has considerable bearing on the questions surrounding the origin of Carlin-type mineralization in general: is the intrusion-related Carlin model valid? are the analogous Canadian terranes simply too deeply eroded to have this type of mineralization preserved? is a major zone of crustal extension like that experienced in the Great Basin one of the key elements for Carlin-type mineralization but one that is absent in the Canadian Cordillera? Answers to these questions must await the results of a more thorough search for Carlin-type mineralization in Canada.

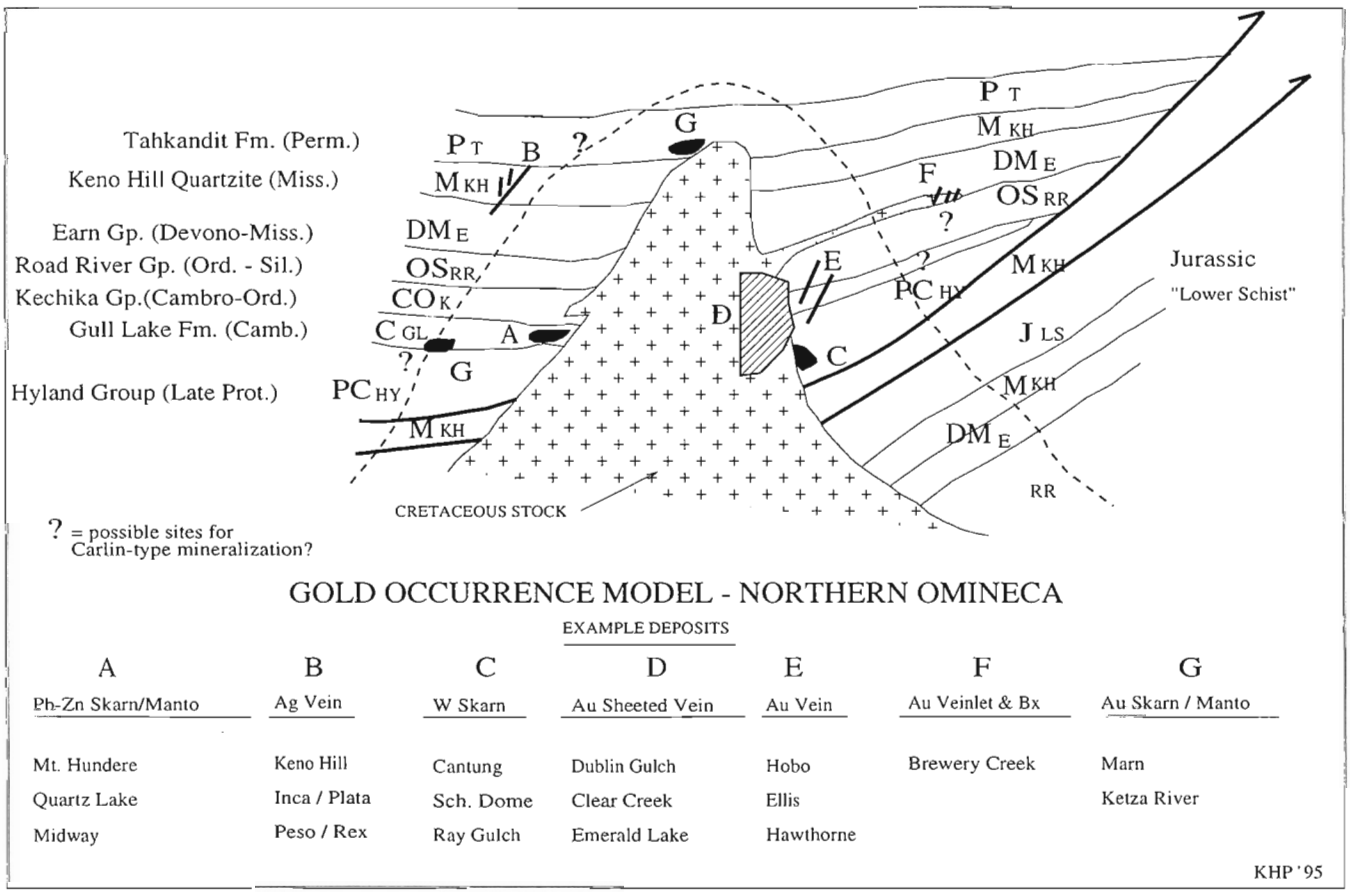


***Figure 5.*** *Schematic diagram illustrating an occurrence model for gold and related deposits in the Selwyn Basin and Cassiar Platform.*

## ACKNOWLEDGMENTS

Field work in 1995 was conducted collaboratively with J.K. Mortensen (University of British Columbia), D. Murphy (Canada / Yukon Geoscience Office) and Trevor Bremner (Department of Indian Affairs and Northern Development). The author is indebted to each of them for sharing vital information and expertise on the northern Cordillera and its mineral deposits and for serving as "reality checks" for some of the ideas presented herein. Steve Gordey and Hugh Gabrielse (GSC Vancouver) and Dave Lefebure (B.C. Geological Survey) provided valuable advice on regional aspects of the study and François Robert has contributed substantially to the elaboration of the mineral deposits concepts. Field examination of several of the mineral deposits referred to in the text was made possible through the kind co-operation and hospitality of the following mining companies: Loki Gold Corporation; Kennecott Canada, First Dynasty Mines Ltd., Keno Hill Mines Ltd., Regent Ventures, Inc., APC Ventures, Inc., and YGC Resources Ltd. F. Robert, J. Mortensen, D. Murphy, D. Sinclair, T. Bremner, and B. Dubé reviewed the manuscript and provided helpful suggestions.

## REFERENCES

**Abbott, J.G.**
1986: Epigenetic mineral deposits of the Ketza-Seagull District, Yukon; in Yukon Geology, Vol. 1; Exploration and Geological Services Division, Yukon, Indian and Northern Affairs Canada, p. 56-66.

**Berger, B.R. and Bagby, W.C.**
1991: The geology and origin of Carlin-type gold deposits; in Gold Metallogeny and Exploration, (ed.) R.P. Foster; Blackie, Glasgow and London, p. 210-248.

**Brown, I.J. and Nesbitt, B.E.**
1987: Gold-copper-bismuth mineralization in hedenbergitic skarn, Tombstone Mountains, Yukon; Canadian Journal of Earth Sciences, v. 24, p. 2362-2372.

**Cathro, M.S.**
1988: Gold, silver and lead deposits of the Ketza River District, Yukon: Preliminary results of field work; in Yukon Geology, Vol. 2; Exploration and Geological Services Division, Yukon, Indian and Northern Affairs Canada, p. 8-25.

**Dawson, K.M., Panteleyev, A., Sutherland Brown, A., and Woodsworth, G.W.**
1991: Regional Metallogeny, Chapter 19 in Geology of the Cordilleran Orogen in Canada, (ed.) H. Gabrielse and C.J. Yorath; Geological Survey of Canada, Geology of Canada, No. 4, p. 707-768 (also Geological Society of America, The Geology of North America, v. G-2)

**Gabrielse, H. and Yorath, C.J.**
1991: Tectonic synthesis, Chapter 18 in Geology of the Cordilleran Orogen in Canada, (ed.) H. Gabrielse and C.J. Yorath; Geological Survey of Canada, Geology of Canada, No. 4, p. 677-705 (also Geological Society of America, The Geology of North America, v. G-2)

**Gordey, S.P. and Anderson, R.G.**
1993: Evolution of the Northern Cordilleran miogeocline, Nahanni map area (105I), Yukon and Northwest Territories; Geological Survey of Canada, Memoir 428, 214 p.

**Gordey, S.P., Abbott, J.G., Tempelman-Kluit, D.J., and Gabrielse, H.**
1987: "Antler" clastics in the Canadian Cordillera; Geology, v. 15, p.103-107.

**Graubard, C.M. and Smith, G.M.**
1995: Northeast Nevada crustal-scale gold anomaly and Bolivian analog: element recycling within a Precambrian basement-structure template; Geology and Ore Deposits of the America Cordillera, Reno / Sparks, Nevada, 1995, Program with Abstracts, p. A34.

**Hollister, V.F.**
1991: Origin of placer gold in the Fairbanks, Alaska, area: a newly proposed lode source; Economic Geology, v. 86, p.402-405.

**Howald, W.C., Foo, S.T., and Craig, L.D.**
1995: Gold Deposits of the Cortez Trend: Relationship to Regional Structure Framework; Geological Society of Nevada, Field Trip Guide Book G, Geology and Ore Deposits of the American Cordillera, 580 p.

**Kuehn, C.A. and Rose, A.W.**
1992: Geology and geochemistry of wall-rock alteration at the Carlin gold deposit, Nevada; Economic Geology, v. 87, p. 1697- 1721.

**Lindgren, W.**
1933: Mineral Deposits; McGraw-Hill, New York and London, 930 p.

**Peters, S.G., Williams, C.L., and Volk, J.**
1995: Structural Geology of the Carlin Trend; Geological Society of Nevada, Field Trip Guide Book B, Geology and Ore Deposits of the American Cordillera, 520 p.

**Schroeter, T.G.**
1986: Muddy Lake Project; in Geological Fieldwork, 1985; British Columbia Ministry of Energy, Mines and Petroleum Resources, Paper 1986-1, p.175-183.

**Sillitoe, R.H. and Bonham, H.F. Jr.**
1990: Sediment-hosted gold deposits: Distal products of magmatic-hydrothermal systems; Geology, v. 18, p.157-161.

**Sinclair, W.D.**
1986: Molybdenum, tungsten and tin deposits and associated granitoid intrusions in the northern Canadian Cordillera and adjacent parts of Alaska; in Mineral Deposits of Northern Cordillera, (ed.) J.A. Morin; Canadian Institute of Mining and Metallurgy, Special Volume 37, p. 216-233.

**Thorman, C.H., Brooks, W.E., Snee, L.W., Hofstra, A.H., Christensen, O.D., and Wilton, D.T.**
1995: Eocene-Oligocene model for Carlin-type deposits in northern Nevada; Geology and Ore Deposits of the America Cordillera, Reno / Sparks, Nevada, 1995, Program with Abstracts, p. A75.

**Turner, R.J.W., Madrid, R.J., and Miller, E.L.**
1989: Roberts Mountains allochthon: Stratigraphic comparison with the lower Paleozoic outer continental margin strata of the northern Canadian Cordillera; Geology, v. 17, p. 341-344.

Geological Survey of Canada Project 940003

# Middle Triassic (Ladinian) volcanic strata in southern Yukon Territory, and their Cordilleran correlatives[1]

Craig J.R. Hart[2] and M.J. Orchard
GSC Victoria, Vancouver

*Hart, C.J.R. and Orchard, M.J., 1996: Middle Triassic (Ladinian) volcanic strata in southern Yukon Territory, and their Cordilleran correlatives; in Current Research 1996-A; Geological Survey of Canada, p. 11-18.*

**Abstract:** Geological mapping of Whitehorse Trough strata of Stikinia in southern Yukon has identified an unusual succession dominated by mafic volcanic rocks. The succession, here termed the Joe Mountain volcanic complex, is at least 3 km thick and underlies a region approximately 20 by 40 km. The section comprises pillowed, massive and autobrecciated basalt flows, massive microdiorite and diabase, clastic and calcareous sedimentary rocks and gabbro. Major element geochemistry suggests that the volcanic rocks are dominantly sub-alkalic, iron-enriched tholeiitic basalt and basaltic andesite. Conodonts obtained from intercalated carbonate strata indicate that the Joe Mountain volcanic complex is Middle Triassic (Ladinian) in age. Rocks of this age are poorly represented within the accreted Cordilleran terranes. Correlative strata are dominated by chert and argillite, and/or different volcanic suites. The Joe Mountain volcanic strata have no obvious Cordilleran counterparts.

**Résumé :** La cartographie géologique des couches de la cuvette de Whitehorse (Stikinie, partie sud du Yukon) a permis d'identifier une succession inhabituelle où dominent les volcanites mafiques. La succession, appelée ici complexe volcanique de Joe Mountain, mesure au moins trois kilomètres d'épaisseur et couvre une région d'environ 20 km sur 40 km. La coupe comprend des coulées de basalte coussiné, massif et autobréchifié; de la microdiorite et de la diabase massives; des roches sédimentaires clastiques et calcaires ainsi que du gabbro. La géochimie des éléments majeurs révèle que les roches volcaniques sont surtout des basaltes tholéiitiques et des andésites basaltiques de composition subalcaline et riches en fer. Les conodontes provenant des strates carbonatées intercalées indiquent que le complexe volcanique de Joe Mountain remonte au Trias moyen (Ladinien). Les roches de cet âge sont mal représentées dans les terranes accrétés de la Cordillère. Dans les strates corrélatives dominent le chert et l'argilite ou différentes suites volcaniques. Les strates volcaniques de Joe Mountain n'ont pas de contreparties évidentes dans la Cordillère.

[1] Contribution to Canada-Yukon Mineral Resource Development Cooperation Agreement (1991-1996), a subsidiary agreement under the Canada-Yukon Economic Development Agreement.
[2] Canada/Yukon Geoscience Office, P.O. Box 2703 (F-3), Whitehorse, Yukon Y1A 2C6

## INTRODUCTION

Recent geological mapping in the southern Yukon (Whitehorse map area, NTS 105D) has identified an unusual succession of strata dominated by mafic volcanic rocks. Conodonts obtained from intercalated sedimentary rocks indicate a Middle Triassic (Ladinian) age, an interval that is poorly represented within the accreted terranes of the Canadian Cordillera. This paper documents the geology and conodont biochronology of this new occurrence and compares it with correlative Ladinian rocks within the accreted terranes of the Cordillera.

## TECTONIC SETTING AND REGIONAL GEOLOGY

South-central Yukon Territory is underlain by a diverse array of terranes that comprise the Intermontane Superterrane (Fig. 1). Stikinia and Cache Creek Terrane are two large components of the Intermontane Superterrane. Stikinia in Yukon is dominated by an Upper Triassic volcanic assemblage (Lewes River arc), and the adjacent Upper Triassic to Middle Jurassic marginal basin assemblage (Whitehorse Trough). Cache Creek is dominated by structurally complex, Upper Paleozoic oceanic basalt, ultramafite, carbonate, and chert overlain by a Triassic-Middle Jurassic chert-greywacke assemblage. The two terranes are juxtaposed along the Nahlin and Crag Lake faults. Although there are occurrences of Cache Creek Terrane rocks north of the Crag Lake Fault, these are considered by Gordey and Stevens (1994) to occur as down-dropped klippe.

Successions of volcanic rocks in the region north of the Crag Lake Fault east of Whitehorse are largely undated and confident assignment to a specific group, formation or terrane is not possible. Much of these volcanic strata were mapped as "Volcanics of uncertain age" by Wheeler (1961). More recently, components have been assigned Cretaceous and Triassic ages (Wheeler and McFeely, 1991). Other volcanic assemblages in the region are assigned to the Paleozoic Cache Creek Group, Upper Triassic Lewes River Group, Cretaceous Hutshi Group, Cretaceous Mount Nansen Formation and the Paleocene Skukum Group (Wheeler, 1961; Tempelman-Kluit, 1984; Wheeler and McFeely, 1991).

Recent 1:50 000 mapping by Hart and Hunt (1994a,b, 1995a,b) assigned portions of the "Volcanics of uncertain age", Cretaceous Hutshi and Mount Nansen groups to a single distinctive succession of volcanic and sedimentary strata that they called the Joe Mountain volcanic complex (Fig. 2).

## JOE MOUNTAIN VOLCANIC COMPLEX

The high-standing massifs in the Joe Mountain, Mount Byng, and Teslin Mountain areas are largely underlain by a 20 km wide by 40 km long, northwest-trending region of mafic volcanic rocks, their intrusive equivalents, and clastic and calcareous sedimentary rocks. Collectively these rocks comprise the Joe Mountain volcanic complex (JMVC). The complex is generally in fault contact with sedimentary rocks of the Whitehorse Trough although locally it is intruded by Cretaceous plutons. Stratigraphic continuity with the sedimentary rocks is possible but has not been confidently demonstrated.

The Joe Mountain volcanic complex is composed of four units: 1) a lower unit of dark basaltic flows; 2) a clastic and calcareous sedimentary package; 3) a thick massive package of basalt flows, microdiorite, and diabase; and 4) gabbro (Fig. 3).

1. The lower unit of dark basalt (informally called the "Old Pillows" by Hart and Hunt, 1994a,b) forms a thick sequence of stacked pillows and lesser massive flows and breccia over a large region south of Joe Mountain. The base of this unit is not exposed and its thickness is likely >500 m. Black and brown-green weathering, fine grained, dense, generally aphyric, grey-green pillow basalt contains rare, thin (max. 10 cm) and discontinuous

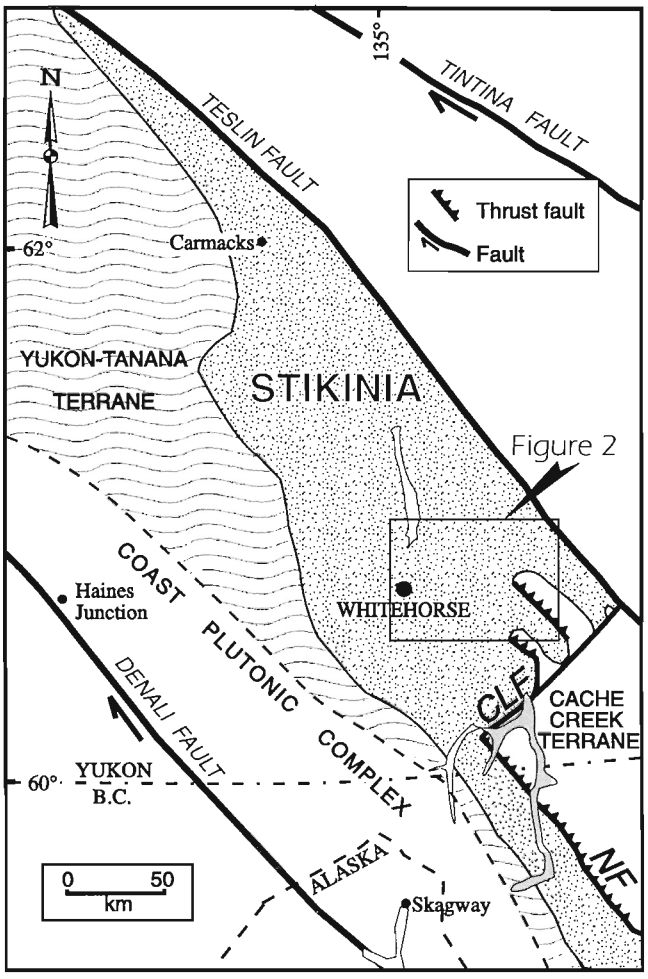


***Figure 1.*** *The Intermontane Superterrane in southern Yukon is composed of Stikinia, Yukon-Tanana, and Cache Creek terranes. The study area (Fig. 2) includes various assemblages of Triassic and older volcanic rocks among the Upper Triassic to Middle Jurassic rocks of the Whitehorse Trough. CLF=Crag Lake Fault, NF=Nahlin Fault.*

interbedded sediments that are typically cherty or limy (now recrystallized to sparry calcite). Calcite veinlets are common and reptile-like scaly chlorite is typical on pillow surfaces. This unit is moderately to steeply dipping and locally vertical. Pillows have been flattened and thinned adjacent to steep strike-slip shear zones. Fault zones in this unit are characterized by ankeritic breccias and gossans with quartz veining and jasper.

2. A chaotic sequence of clastic and calcareous sedimentary rocks conformably overlies the Old Pillows (Fig. 4). South of Joe Mountain, the moderately dipping sedimentary sequence is approximately 2 km thick although it has been inflated somewhat by intercalated volcanic flows. The sedimentary sequence is dominated by recessive thin-bedded, tan-brown and grey-black argillite punctuated by resistant, 1-5 m thick beds of massive hyaloclastic tuff and conglomerate, pebbly sandstone, and sandy limestone. The clastic rocks are poorly sorted and typically composed of angular volcanic fragments. Limestone is generally dark grey, well-bedded, sandy and shaley, and contains rare, poorly preserved, thick-shelled bivalves. Other, well-preserved bivalves (*Daonella*? sp.) were also observed in the lower part of this unit.

3. The bulk of the Joe Mountain volcanic complex is composed of dark, blocky and resistant weathering, massive, but locally pillowed, light green, relatively unaltered basalt, microdiorite, and diabase (Fig. 5a). The microdiorite is fine- to medium-grained, generally non-magnetic and although dominantly aphyric, locally sparsely feldspar and pyroxene-phyric. The pillows tend to be large (1-2 m), and generally difficult to observe among the thick accumulations of otherwise massive and autobrecciated flows. Thin (20-200 m thick) sedimentary units, similar to those previously described, occur within

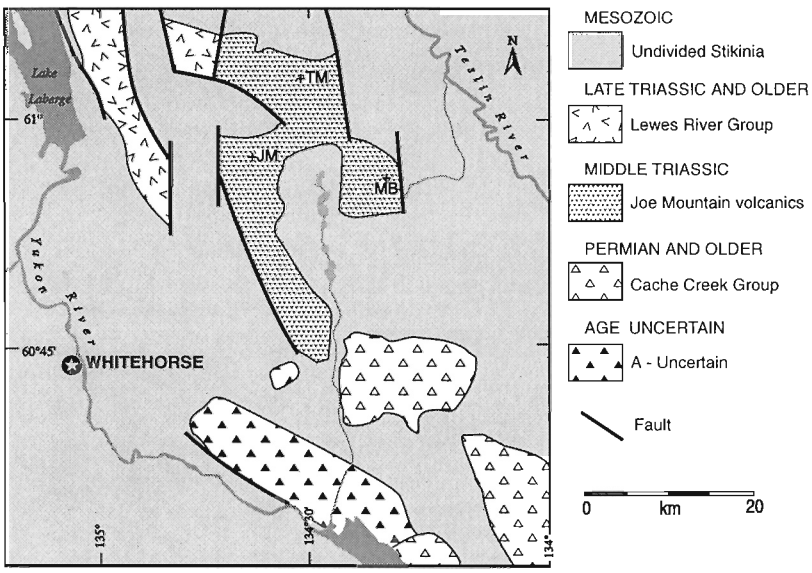


*Figure 2.*

*Occurrences of Triassic and older volcanic rocks in the northeast Whitehorse (105D) and southeast Laberge (105E) map areas. The Joe Mountain volcanic complex comprises rocks previously mapped as "Volcanics of uncertain age", Hutshi Group and Mount Nansen Group. Geology compiled and modified from Wheeler (1961), Tempelman-Kluit (1984), and Hart and Hunt (1994a, 1995a). TM = Teslin Mtn., JM = Joe Mtn., MB = Mount Byng.*

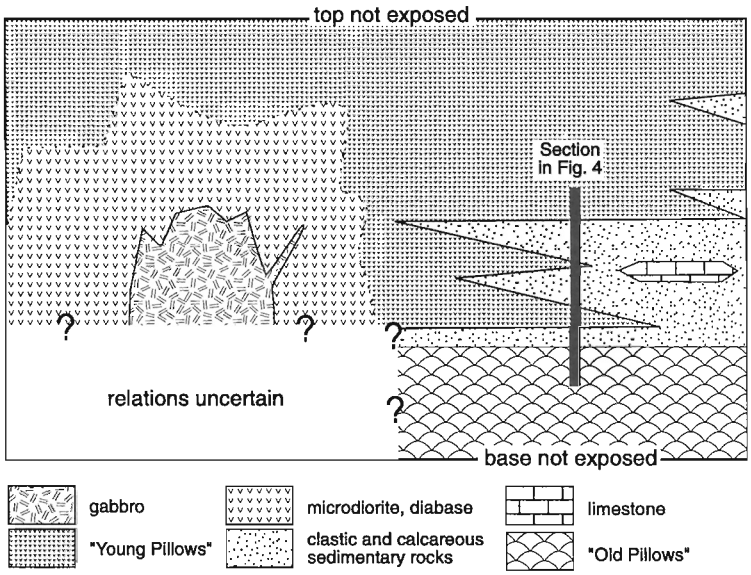


*Figure 3.*

*Schematic cross-section displaying the gross stratigraphy and relations between the various units within the Joe Mountain volcanic complex. The "Young Pillows" and the microdiorite, diabase units are essentially equivalent but represent extrusive and intrusive phases respectively.*

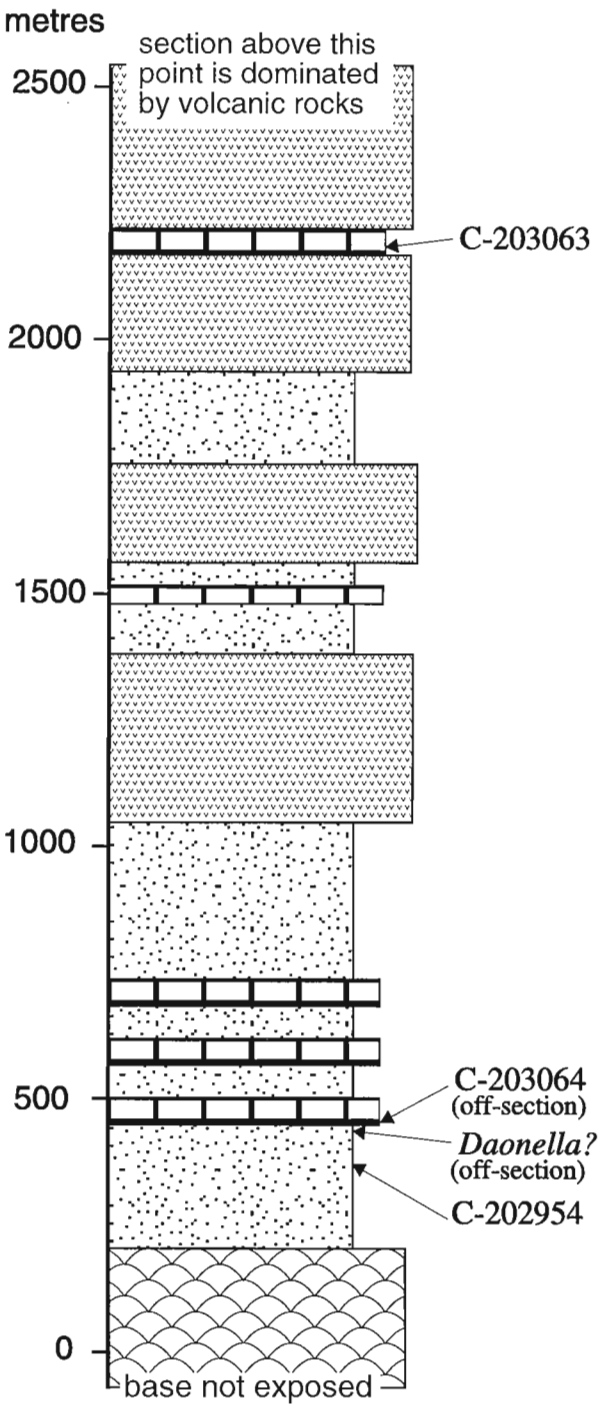


***Figure 4.*** *Section and sample localities from the predominantly sedimentary portion of the Joe Mountain volcanic complex. The section is compiled from 1:25 000 mapping by the first author starting from 60°54.5′N, 134°43.0′W. Rock patterns are the same as those in Figure 3.*

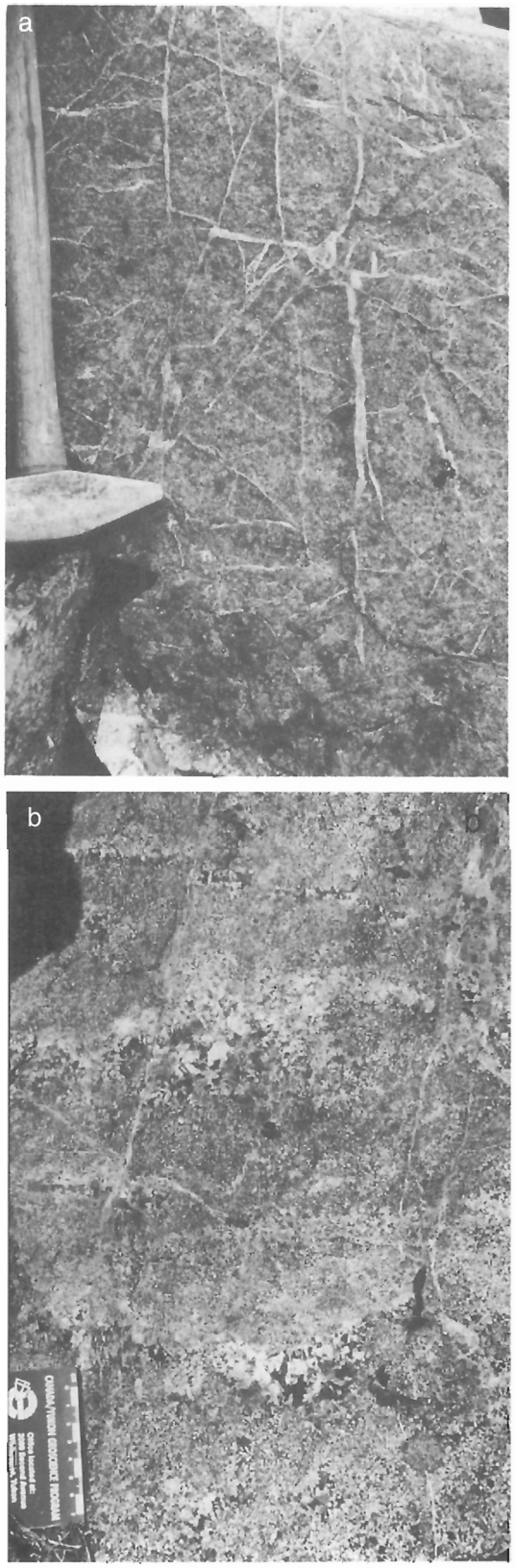


***Figure 5.*** *Typical rock types of the Joe Mountain volcanic complex include:* ***a)*** *microdiorite which is typically crosscut by reticulate networks of thin white veinlets; and* ***b)*** *texturally variable, coarsely crystalline pyroxene gabbro.*

the sequence of flows. Subvolcanic phases are cut by reticulate networks of thin white veinlets of an unknown mineral (albite?). The thickness of the microdiorite unit is variable but likely in excess of 700 m. In the Joe Mountain and Mount Byng areas, the basalt/microdiorite is thick and massive and interpreted to be subvolcanic in origin.

4. The gabbro is exposed over much of the upland plateau north of Joe Mountain, and north and west of Mount Byng. It is characterized by leucocratic, coarse-grained and texturally variable, pyroxene gabbro (Fig. 5b). This unit underlies and intrudes the microdiorite and basalt flows. Locally, small marginal bodies of coarse grained anorthosite and pyroxenite (bronzite?) are associated with the gabbro. The textural variation and intrusive relationship of the gabbro with the microdiorite indicates that the gabbro likely represents the hypabyssal portion of the magma chamber that fed the Joe Mountain volcanic complex.

Preliminary major-element whole-rock geochemical analysis indicates that the volcanic rocks of the Joe Mountain volcanic complex are dominated by sub-alkalic basalt and basaltic andesite (Fig. 6a). On a calc-alkaline/tholeiitic plot, data are almost entirely within the iron-enriched tholeiite field (Fig. 6b). The tectonic discriminate diagram suggests that the minor element composition of the Joe Mountain volcanic complex rocks are typical of island arc tholeiite and mid-ocean ridge (or marginal basin) basalt (Fig. 6c).

## GEOCHRONOMETRY

The Joe Mountain volcanic complex is devoid of minerals suitable for isotopic dating. Whole-rock analyses of samples of basalt and andesite yielded reset K-Ar ages between 52 and 143 Ma indicating that the rocks have been variably affected by younger thermal events (J. Mortensen, pers. comm., 1995). A K-Ar whole-rock analysis of the gabbro gave a slightly older age of 168 ± 6 Ma (Bremner, 1991) but the date is still significantly younger than the ages given by fossils. A model whole-rock Rb-Sr date from a single analysis of andesite yielded an upper Permian age of 252 ± 10 Ma (Bremner, 1991) but lack additional constraining points.

## BIOCHRONOLOGY

Cratonal successions in western Canada include fossiliferous Middle Triassic strata that form the basis of a detailed ammonoid biochronology (Tozer, 1994). Conodonts from

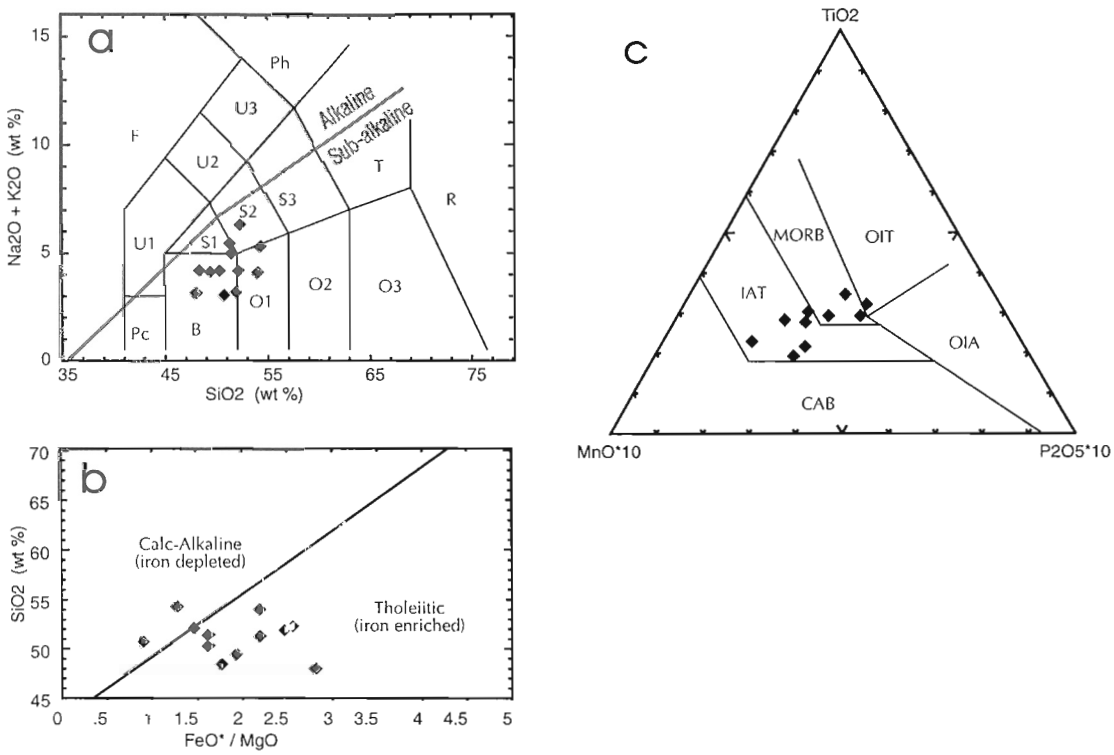


***Figure 6.*** *All data are plotted as anhydrous.* ***a)*** *Total alkalis vs silica classification diagram with subdivisions of Le Maitre (1989); B = basalt, O1 = basaltic andesite, S1 = trachybasalt, S2 = basaltic trachyandesite. Alkaline/subalkaline curve from Irving and Baragar (1971).* ***b)*** *Calc-alkaline/tholeiitic discrimination diagram (Miyashiro, 1974).* ***c)*** *Minor element discriminate plot for basaltic rocks (45-54% $SiO_2$; Mullen, 1983). CAB = calc-alkaline basalt, IAT = island arc tholeiite, MORB = mid-ocean ridge basalt, OIT = ocean island tholeiite, OIA = ocean island andesite.*

**Table 1.** Numeric data on Ladinian conodont taxa (left column) from the six GSC localities (top row) in the Joe Mountain volcanic complex.

| | C-202954 | C-203051 | C-203056 | C-203062 | C-203063 | C-203064 |
|---|---|---|---|---|---|---|
| *B.* aff. *hungaricus* | | | | | | 2 |
| *B.*aff.*mungoensis* | 1 | | | | | |
| *N.*aff.*acuta* | | | 2 | | | |
| *N.*exgr.*constricta* | | | | | 2 | 6 |
| *N.*exgr.*inclinata* | 10 | 1 | 9 | 1 | 3 | 2 |
| *N.*sp.indet. | 10 | | 10 | 2 | 2 | 7 |
| *Paragondolella?*sp. | 4 | | | | 1 | |
| ramiforms | 22 | | 1 | 1 | 2 | 1 |

these sections, supplemented by Nevadan successions (e.g., Orchard and Bucher, 1992), may be used to date isolated conodont faunas in terms of standard Triassic chronostratigraphy. Six isolated conodont collections (Table 1) have been recovered from the sedimentary intercalations of the Joe Mountain volcanic complex, three of which are located relative to the stratigraphic section shown in Figure 4. Structural complexity precludes confident relative placement of all the collections, but the entire suite of samples can confidently be assigned to the Ladinian.

The most diagnostic conodonts in the present collections are specimens of *Budurovignathus*, present in C-202954 and C-203064, which lie in (or are projected to lie within) the basal part of the succession. This cosmopolitan genus ranges from the Ladinian through basal Carnian. In the Carnian, it is associated with *Metapolygnathus* species, but none of these occur in the present collections. Several species of *Budurovignathus* are identified through the Ladinian, and these can be partly related to ammonoid zones. A primitive, unornamented species (cf. *B. hungaricus* (Kozur and Vegh)) occurs at the type locality of the Poseidon ammonoid Zone at Tuchodi Bluff (Tuchodi Lake map area) in northeast British Columbia, whereas *B. mungoensis* (Diebel) is characteristic of the top Ladinian Sutherlandi Zone, as for example at Brown Hill on Williston Lake (Halfway River map area). The intervening ammonoid zones of *Meginoceras meginae* and *Maclearnoceras maclearni* (Tozer, 1994, p. 32-34) have not yielded species of *Budurovignathus*, although weakly ornamented forms might be anticipated in that interval. Specimens of *Budurovignathus* from Joe Mountain volcanic complex are assigned to *B.* aff. *hungaricus* and to *B.* aff. *mungoensis* based on differing degrees of anterior platform ornamentation.

All the collections from Joe Mountain volcanic complex contain a variety of other platform species, including *Neogondolella* ex gr. *constricta* (Mosher and Clark), *Neogondolella* ex gr. *inclinata* (Kovacs), and possible *Paragondolella* sp. (Table 1). Many other specimens are too poorly preserved to identify. The first species, good examples of which occur in sample C-203063, ranges from upper Anisian into Ladinian strata in Nevada. In British Columbia, the last representatives of the *N.* ex gr. *constricta* occur within the Meginae Zone. *N.* ex gr. *inclinata* replaces the former species as the dominant neogondolellid in younger Ladinian strata: typical species are commonly associated with *B. mungoensis* in the Sutherlandi Zone. *Paragondolella* ranges through the Ladinian. Little is known of the forms assigned to *N.* aff. *acuta* (Kozur).

In summary, the age of the Joe Mountain volcanic complex conodont collections is 'mid'-Ladinian, post-Poseidon Zone and probably pre-Sutherlandi Zone. A Meginae Zone age is probable for at least one collection. In terms of the Tethyan sequence, at least the older collections from the Joe Mountain volcanic complex are equivalent to the Fassanian substage of the Ladinian; *B. mungoensis* characterizes the Longobardian substage (March et al., 1990).

## CORRELATION

Ladinian conodonts are relatively uncommon in the Canadian Cordillera, and the rock packages that they date are not known in detail. The following provides an updated inventory (see also Orchard, 1991) of known Ladinian units, all of which are broadly correlative with the Joe Mountain volcanic complex.

*Budurovignathus* spp. are known from several localities on the autochthon, mainly from the Liard Formation in northeast British Columbia. There are also several occurrences in the parautochthonous Hoole Formation and correlatives in the Pelly Mountains (Watson Lake, Finlayson Lake, Quiet Lake map areas). Outboard of these Cassiar Terrane localities, the Ladinian is recognized in Quesnel Terrane in siliciclastic and carbonate sedimentary strata of the Quesnel Lake Group (Quesnel Lake map area), Brooklyn Formation and Olalla limestone (Penticton map area; Pohler et al., 1989), and other limestones within the dominantly calc-alkaline arc volcanics of the Nicola Group (Ashcroft map area; Orchard and Danner, 1991); all these localities yield *Budurovignathus* spp. Most of these are records of late Ladinian *B. mungoensis* but at least one from the Brooklyn Limestone is very close to the Joe Mountain volcanic complex forms, implying a pre-Sutherlandi Zone age.

The Cache Creek Group contains chert that has been dated as Ladinian both in the type area in southern British Columbia (Orchard, 1986; Beyers and Orchard, 1991; Cordey and Read, 1992) and in the north near the

B.C.-Yukon border (Cordey et al., 1991). Cherts of the Bridge River Group have also yielded Ladinian radiolarians (Cordey, 1986). There is little information on the detailed stratigraphy and precise age of these Middle Triassic chert packages, but in no case are there associated volcanic rocks that are clearly dated as Ladinian.

There is also a single locality of Middle Triassic chert known from the Terrace area, but much more data are available from farther north in Stikinia where Middle Triassic strata occur in the Iskut River area. There, the "Tsaybahe group" is an assemblage of Upper Anisian to Ladinian argillite, greywacke, and limestone intercalated with, and overlain by, augite and plagioclase-phyric flows and tuff (Read, 1984; Read et al., 1989). These rocks unconformably underlie the lower part of the better known Stuhini Group of Late Triassic age. Ladinian, *Daonella*-bearing siliceous argillite is also described from the Scud River (Brown et al., 1991) and Telegraph Creek (Souther, 1972) areas. In the latter area, *Budurovignathus mungoensis* is also recorded.

In the Insular Belt, *Daonella*-bearing Ladinian shale underlies volcanic rocks of the Karmutsen Formation on Vancouver Island, and the Nikolai Greenstone in the Saint Elias and Wrangell mountains. Although this basaltic volcanism has been suggested to be partially Ladinian in age, it could be entirely Carnian. Possible Ladinian conodonts are also known from the Coast Mountains in sedimentary strata of the Perseverance group of Taku Terrane (Gehrels et al., 1992). Ladinian fossils are also known from strata southeast of Skagway that is correlated with Alexander Terrane (Brew et al., 1985).

## DISCUSSION AND CONCLUSION

Rocks of the Joe Mountain volcanic complex are Ladinian in age. Rocks of this age are not common among the accreted terranes of the Canadian Cordillera. Throughout much of Stikinia, the Ladinian is largely represented by the angular and erosional unconformity between Paleozoic Stikine Assemblage and Upper Triassic Stuhini/Lewes River groups. Known occurrences of Ladinian strata in both Stikinia and Cache Creek are of chert and siliceous argillite. In the Iskut area, Middle Triassic volcanic strata (Tsaybahe group) are, in part, older than Ladinian and are dominated by augite and plagioclase-phyric volcanic rocks. These rocks are lithologically similar to the Stuhini Group which have a high-potassium calc-alkaline geochemical signature (Souther, 1977; Logan and Koyanagi, 1994), but unlike rocks of the Joe Mountain volcanic complex which are aphyric and have a tholeiitic geochemical signature. Similar differences apply to the coeval parts of the Nicola Group in Quesnel Terrane. Consequently, the volcanic strata of the Joe Mountain volcanic complex represent a unique succession with no obvious counterpart in the Cordillera.

The terrane affiliation of the Joe Mountain volcanic complex is problematic. It is fault-bound within Upper Triassic Whitehorse Trough sedimentary rocks (Stikinia), but a depositional link cannot be confidently demonstrated. If an association with Stikinia is confirmed then the Joe Mountain volcanic complex represents the oldest exposed strata of the terranes in Yukon. However, rocks of the complex are along strike with, but separated by a Cretaceous intrusion from, volcanic and ultramafic rocks of the Cache Creek Terrane. Furthermore, rocks of the Joe Mountain volcanic complex are lithologically identical to fault-bound successions in northernmost British Columbia which were assigned to the Cache Creek Terrane (Conrad series of Hart and Pelletier, 1989; Graham Creek igneous suite of Mihalynuk et al., 1991). If rocks of the Joe Mountain volcanic complex are assigned to Cache Creek Terrane they are the youngest igneous rocks and the most northerly representatives of that terrane.

## ACKNOWLEDGMENTS

Fieldwork was supported by the Canada-Yukon Mineral Resource Development Cooperation Agreement (1991-1996) funding to the Canada/Yukon Geoscience Office. Julie Hunt assisted in the geological mapping and helped to develop the concept of the Joe Mountain volcanic complex. Steve Gordey is thanked for his review of the manuscript. Further thanks to Peter Read, Mitch Mihalynuk, Dave Brew, and Fabrice Cordey for conversations about Middle Triassic rocks in the Cordillera.

## REFERENCES

**Beyers, J.M. and Orchard, M.J.**
1991: Upper Permian and Triassic conodont faunas from the type-area of the Cache Creek Complex, south-central British Columbia, Canada; in Ordovician to Triassic Conodont Paleontology of the Canadian Cordillera, M.J. Orchard and A.D. McCracken (ed.); Geological Survey of Canada, Bulletin 417, p. 269-297.

**Bremner, T.**
1991: Mount Byng mineral occurrence; in Yukon Geology 1990; Exploration and Geological Services Division, Yukon, Indian and Northern Affairs Canada, p. 52-56.

**Brew, D.A., Ford, A.B., and Garwin, S.L.**
1985: Fossiliferous Middle and (or) Upper Triassic rocks within the Coast Plutonic-Metamorphic Complex southeast of Skagway; United States Geological Survey, Circular 967, p. 86-89.

**Brown, D.A., Logan, J.M., Gunning, M.H., Orchard, M.J., and Bamber, W.E.**
1991: Stratigraphic evolution of the Paleozoic Stikine assemblage in the Stikine and Iskut rivers area, northwestern British Columbia; Canadian Journal of Earth Sciences, v. 28, p. 958-972.

**Cordey, F.**
1986: Radiolarian ages from the Cache Creek and Bridge River complexes and from chert pebbles in Cretaceous conglomerates, southwestern British Columbia; in Current Research, Part A; Geological Survey of Canada, Paper 86-1A, p. 595-602.

**Cordey, F. and Read, P.B.**
1992: Permian and Triassic radiolarian ages from the Cache Creek Complex, Dog Creek and Alkali Lake areas, southwestern British Columbia; in Current Research, Part E; Geological Survey of Canada, Paper 92-1E, p. 41-51.

**Cordey, F., Gordey, S.P., and Orchard, M.J.**
1991: New biostratigraphic data for the northern Cache Creek Terrane, Teslin map area, southern Yukon; in Current Research, Part E; Geological Survey of Canada, Paper 91-1E, p. 67-76.

**Gehrels, G.E., McClelland, W.C., Samson, S.D., Patchett, J., and Orchard, M.J.**
1992: Geology of the western flank of the Coast Mountains between Cape Fanshaw and Taku Inlet, southeastern Alaska; Tectonics, v. 11, p. 567-585.

**Gordey, S.P. and Stevens, R.A.**
1994: Preliminary interpretation of bedrock geology of the Teslin area (105C), 1:250 000 scale; Geological Survey of Canada, Open File 2886.

**Hart, C.J.R. and Pelletier, K.S.**
1989: Geology of Carcross (105D/2) and part of Robinson (105D/7) map areas; Exploration and Geological Services Division, Yukon, Indian and Northern Affairs, Open File 1989-1, 84 p.

**Hart, C.J.R. and Hunt, J.A.**
1994a: Geology of the Joe Mountain map area (105D/15), southern Yukon Territory, 1:50 000 geological map; Exploration and Geological Services Division, Yukon, Indian and Northern Affairs Canada, Open File 1994-4 (G).
1994b: Geology of the Joe Mountain map area (105D/15), southern Yukon Territory; in Yukon Exploration and Geology, 1993; Exploration and Geological Services Division, Yukon, Indian and Northern Affairs Canada, p. 47-66.
1995a: Geology of the Mount M'Clintock map area (105D/16), southern Yukon Territory, 1:50 000 geological map; Exploration and Geological Services Division, Yukon, Indian and Northern Affairs Canada, Open File 1995-4 (G).
1995b: Geology of the Mount M'Clintock map area (105D/16), southern Yukon Territory; in Yukon Exploration and Geology 1994; Exploration and Geological Services Division, Yukon, Indian and Northern Affairs Canada, p. 87-104.

**Irving, T.N. and Baragar, W.R.A.**
1971: A guide to the chemical classification of the common volcanic rocks; Canadian Journal of Earth Sciences, v. 8, p. 523-548.

**Le Maitre, R.W.**
1989: A Classification of Igneous Rocks and Glossary of Terms; Blackwell, Oxford, 193 p.

**Logan, J.M. and Koyanagi, V.M.**
1994: Geology and mineral deposits of the Galore Creek area (104G/3, 4); British Columbia Ministry of Energy, Mines and Petroleum Resources, Bulletin 92.

**March, M., Budurov, K., and Hirsch, F.**
1990: *Sephardiella* nov. gen. (Conodonta), emendation of *Carinella* (Budurov, 1973) from the Ladinian (Middle Triassic) type area in Catalonia (N.E. Spain), Sephardic Province; Courier Forschunginstitut Senckenberg, v. 118, p. 197-201.

**Mihalynuk, M.G., Mountjoy, K.J., McMillan, W.J., Ash, C.J., and Hammack, J.L.**
1991: Highlights of 1990 Fieldwork in the Atlin area (104N/12W); in Geological Fieldwork 1990; British Columbia Ministry of Energy, Mines and Petroleum Resources, p. 145-152.

**Miyashiro, A.**
1974: Volcanic rock series in island arcs and active continental margins; American Journal of Science, v. 274, p. 321-355.

**Mullen, E.D.**
1983: $MnO/TiO_2/P_2O_5$: a minor element discriminate for basaltic rocks of oceanic environments and its implications for petrogenesis; Earth and Planetary Science Letters, v. 62, p. 53-62.

**Orchard, M.J.**
1986: Conodonts from Western Canadian chert: their nature, distribution and stratigraphic application; in Conodonts, Investigative Techniques and Applications, R.L. Austin (ed.); Proceedings of the Fourth European Conodont Symposium (ECOS 1V), Chapter 5; p. 96-121. Ellis-Horwood, Chichester, England.
1991: Conodonts, time and terranes: an overview of the biostratigraphic record in the western Canadian Cordillera; in Ordovician to Triassic Conodont Paleontology of the Canadian Cordillera, M.J. Orchard and A.D. McCracken, (ed.); Geological Survey of Canada, Bulletin 417, p. 1-26.

**Orchard, M.J. and Bucher, H.**
1992: Conodont-ammonoid intercalibration around the Lower-Middle Triassic boundary: Nevadan clocks help tell British Columbian time; in Current Research, Part E; Geological Survey of Canada, Paper 92-1E, p. 133-140.

**Orchard, M.J. and Danner, W.R.**
1991: The paleontology of Quesnellia; in A Field Guide to the Paleontology of Southwestern Canada, P.L. Smith, (ed.); Canadian Paleontology Conference I, Vancouver, p. 139-168.

**Pohler, S.M.L., Orchard, M.J., and Tempelman-Kluit, D.J.**
1989: Ordovician conodonts identify the oldest sediments in the Intermontane Belt, Olalla, south-central British Columbia; in Current Research, Part E; Geological Survey of Canada, Paper 89-1E, p. 61-67.

**Read, P.B.**
1984: Geology Klastline River (104G/16E), Ealue Lake (104H/13W), Cake Hill (1041/4W), and Stikine Canyon (104J/1E), British Columbia; Geological Survey of Canada, Open File 1080.

**Read, P.B., Brown, R.L., Psutka, J.F., Moore, J.M., Journeay, M., Lane, L.S., and Orchard, M.J.**
1989: Geology of More and Forrest Kerr creeks (parts of 104B/10, 15, 16 and 104G/1, 2), northwestern British Columbia; Geological Survey of Canada, Open File 2094.

**Souther, J.G.**
1972: Geology and mineral deposits of Tulsequah map-area, British Columbia; Geological Survey of Canada, Memoir 362, 84 p.
1977: Volcanism and tectonic environments in the Canadian Cordillera – a second look; in Volcanic Regimes in Canada, W.R.A. Baragar, L.C. Coleman, and J.M. Hall (ed.); Geological Association of Canada, Special Paper 16, p. 3-24.

**Tempelman-Kluit, D.J.**
1984: Laberge (105E) and Carmacks (115I) map-areas, two 1:250 000 maps and legend; Geological Survey of Canada, Open File 1101.

**Tozer, E.T.**
1994: Canadian Triassic ammonoid faunas; Geological Survey of Canada, Bulletin 467.

**Wheeler, J.O.**
1961: Whitehorse map-area, Yukon Territory; Geological Survey of Canada, Memoir 312, 156 p.

**Wheeler, J.O. and McFeely, P.**
1991: Tectonic assemblage map of the Canadian Cordillera; Geological Survey of Canada, Map 1712A.

Geological Survey of Canada Project 810028

# Structural evolution and rock types of the Slide Mountain and Yukon-Tanana terranes in the Campbell Range, southeastern Yukon Territory

Heather E. Plint[1] and Terence M. Gordon[1]
GSC Victoria

*Plint, H.E. and Gordon, T.M., 1996: Structural evolution and rock types of the Slide Mountain and Yukon-Tanana terranes in the Campbell Range, southeastern Yukon Territory; in Current Research 1996-A; Geological Survey of Canada, p. 19-28.*

**Abstract:** Mapping at 1:50 000 scale in the Campbell Range, Yukon Territory examined the Finlayson Lake fault zone and the Slide Mountain and Yukon-Tanana terranes. Map units identified are: (a) Yukon-Tanana terrane: $DT_p$ chlorite-actinolite phyllite, $DT_a$ argillite, $DT_c$ metachert and slate; (b) Slide Mountain terrane: $DPs_c$ and $DPs_p$ metachert, argillite, and phyllite, $DPs_g$ greenstone, breccia, gabbro, and meta-sedimentary rocks, $DPs_{lg}$ leucogabbro, and $DPs_s$ serpentinite; and (c) Earn Group: $DMe_c$ metachert and argillite, and $DMe_s$ sandstone, siltstone, and shale.

Unit $DPs_g$ is thrust over $DT_p$ and $DT_a$ in the west and $DPs_c$ in the east. The map pattern of $DT_c$ suggests a klippe preserved from erosion by normal faulting along its southern boundary. These structures may represent a flower structure or an originally east-directed thrust sequence disrupted by west-directed back thrusts with continued shortening.

**Résumé :** La cartographie à l'échelle de 1:50 000 dans le chaînon Campbell (Yukon) a permis d'analyser la zone de failles du lac Finlayson ainsi que les terranes de Slide Mountain et de Yukon-Tanana. Les unités cartographiques établies sont les suivantes : a) terrane de Yukon-Tanana : $DT_p$ phyllade à chlorite-actinolite, $DT_a$ argilite, $DT_c$ métachert et ardoise; b) terrane de Slide Mountain : $DPs_c$ et $DPs_p$ métachert, argilite et phyllade, $DPs_g$ roches vertes, brèche, gabbro et roches métasédimentaires, $DPs_{lg}$ leucogabbro, $DPs_s$ serpentinite; c) Groupe d'Earn : $DME_c$ métachert et argilite, $DME_s$ grès, siltstone et shale.

L'unité $DPs_g$ chevauche, d'une part, les roches associées à $DT_p$ et à $DT_a$ dans l'ouest et, d'autre part, à $DPs_c$ dans l'est. La géométrie de $DT_c$ sur la carte suggère une klippe protégée contre l'érosion par des failles normales le long de sa limite méridionale. Ces structures peuvent représenter une structure en forme de palmier ou une séquence de chevauchement initialement vers l'est et perturbée par des rétrochevauchements d'orientation ouest accompagnés d'un raccourcissement continu.

[1] Department of Geology and Geophysics, University of Calgary, 2500 University Drive, N.W., Calgary, Alberta T2N 1N4; e-mail: Plint@geo.ucalgary.ca; TMG@geo.ucalgary.ca.

## INTRODUCTION

In the northern Cordillera, Late Devonian to Late Triassic, massive greenstone, mafic to ultramafic plutonic rocks, and sedimentary rocks of the Slide Mountain terrane are faulted between autochthonous North American strata and the Yukon-Tanana terrane. In southeastern Yukon, the boundary between the North American rocks and accreted rocks is the Finlayson Lake fault zone (Fig. 1). The fault zone is interpreted to be the displaced northern extension of the Teslin structural zone of south-central Yukon, that has been offset 450 km to the southeast along the mid-Cretaceous to Tertiary dextral strike-slip Tintina fault (e.g., Tempelman-Kluit, 1979).

The Finlayson Lake fault zone incorporates and deforms rocks of the Slide Mountain and Yukon-Tanana terranes and locally contains eclogitic rocks. The timing and nature of motion along the fault zone is poorly understood. At its northern end, it is marked by north-northwest-trending, anastomosing, steeply dipping faults interpreted to have mainly strike-slip displacement (e.g., Tempelman-Kluit, 1972). Farther south, in the northern Campbell Range, the fault zone comprises north-northwest trending faults, some of which are thrust faults that place Slide Mountain terrane over rocks of Yukon-Tanana terrane in the west and other rocks of the Slide Mountain terrane to the east (Plint, 1995). The fault zone is thought to be a transpressive zone (Mortensen and Jilson, 1985) although the details of its structural evolution remain unknown. Geological mapping in the Campbell Range, southeastern Yukon (Fig. 2), is part of an ongoing study of the depositional setting of the Slide Mountain terrane and the structural evolution of the fault zone.

## LOCATION AND ACCESS

The study area is located 175 km north of Watson Lake, Yukon Territory between the Campbell Highway to the east and Wolverine Lake to the west (Fig. 2). Mapping at 1:50 000 scale covering parts of NTS sheets 105G/8/9 and 105H/5/12, was carried out for six weeks during the 1995 field season from helicopter-supported fly camps and the Campbell Highway. Outcrop is excellent to sporadic above treeline (ca. 1600 m), moderate to absent on mountain slopes, and locally present along creeks.

## TECTONIC SETTING AND PREVIOUS WORK

The rocks underlying the map area have been assigned to the Slide Mountain and Yukon-Tanana terranes (e.g., Wheeler and McFeely, 1991). The Slide Mountain terrane in southeastern Yukon consists of greenstone, ultramafic and mafic plutonic rocks, ribbon chert, and minor marble (Mortensen, 1992a). The Yukon-Tanana terrane is a pericratonic terrane of polydeformed and metamorphosed rocks derived from

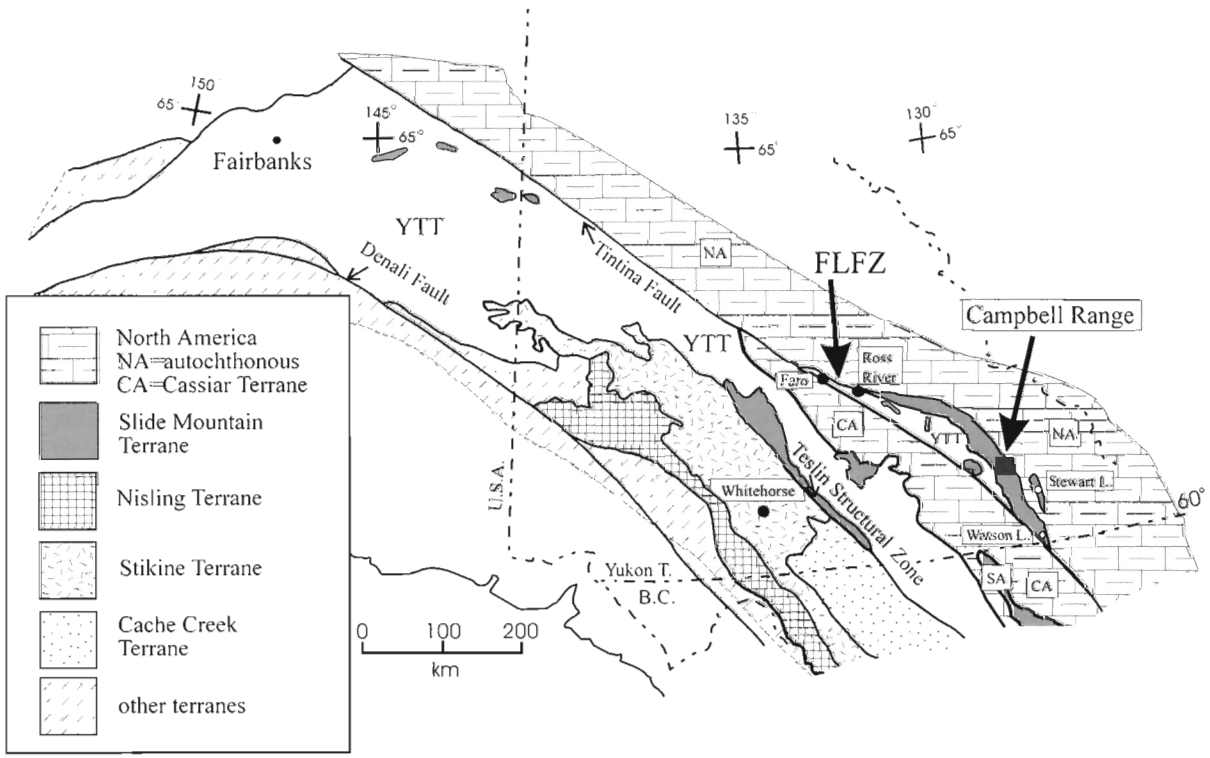


***Figure 1.*** *Terranes of the northern Cordillera. NA is autochthonous North American strata; CA is allochthonous North American strata (= Cassiar terrane); YTT is Yukon-Tanana terrane. FLFZ is the Finlayson Lake fault zone. SA = Sylvester Allochthon. Modified from Mortensen (1992b).*

pre-Devonian to Upper Triassic sedimentary, volcanic, and plutonic protoliths (e.g., Hansen, 1990). The Slide Mountain terrane is interpreted to be the remnants of oceanic crust that separated the Yukon-Tanana terrane from North America (e.g., Nelson, 1993). The Yukon-Tanana terrane may be a distal equivalent of North America or an unrelated allochthonous terrane (e.g., Hansen, 1990; Hansen et al., 1991).

Early geological mapping by the Geological Survey of Canada reported greenstone, metadiorite, minor serpentinite, and minor amphibolite throughout most of the map area (Wheeler et al., 1960; Roots et al., 1966). Regional mapping in the study area by Mortensen and Jilson (1985) defined the "Campbell Range belt" as consisting of a unit of greenstone, serpentinite, chert, minor diabase, and minor gabbro structurally interleaved with units of grey chert and metachert and of massive carbonate. Age determinations indicate that the rocks of the Campbell Range belt range from latest Devonian to Early Permian age (Mortensen and Jilson, 1985; Mortensen, 1992a). The greenstone unit is correlated with the Slide Mountain terrane (Monger, 1984; Plint, 1995). Plint and Gordon (1995) interpreted the greenstone unit to have formed in a deep submarine environment with some terrigenous influx based on the presence of radiolarian chert, serpentinite, breccias with pillow fragments, altered glass shards and dendritic pyroxene microphenocrysts, and quartz-chert greywacke layers containing detrital epidote, plagioclase, tourmaline, and rare volcanic clasts.

The regional correlation of the carbonate and chert/metachert units is uncertain. Correlations of the chert/metachert unit with Devonian-Mississippian North American stratigraphy, mid-Paleozoic units of the Yukon-Tanana terrane, and the Late Devonian to Late Triassic Slide Mountain terrane have been suggested (J.K. Mortensen, pers. comm., 1994). Plint (1995) divided the chert/metachert unit into two units, at least one of which was interpreted to be part of the Slide Mountain terrane.

Mortensen and Jilson (1985, their Fig. 2) interpreted the Finlayson Lake fault zone as a zone of steep faults developed in the chert/metachert unit and truncated by a folded thrust fault at the base of a klippe of greenstone. Plint (1995) reported that the base of the greenstone is marked by diverging thrust faults and included them, along with inferred steep, north-northwest-trending faults, as part of the fault zone.

## MAP UNITS

Five map units (units 1 to 5) were identified and described by Plint (1995) from the 1994 field season. Mapping in 1995 has revealed the presence of thin, distinctive lithological units at the top of the former unit 1 and structurally below unit 3, and identified 4 new units. The units have been renamed to reflect their inferred depositional age. The terminology from Plint (1995) is given in brackets:

| | |
|---|---|
| $Dt_p$ | chloritic phyllite and schist (unit 1) |
| $Dt_a$ | grey argillite and metasiltstone (new unit) |
| $Dt_c$ | metachert and grey slate (unit 2) |
| $Dps_c$ | tan- to yellow-weathering metachert and maroon siliceous and argillaceous metasiltstone and argillite (unit 3) |
| $DPs_p$ | pink-, orange-, or tan-weathering metachert and tan or grey argillite and phyllite (new unit) |
| $Dps_g$ | greenstone (unit 4) |
| $Dps_{lg}$ | leucogabbro (new unit) |
| $Dps_s$ | serpentinite (unit 5) |
| $Dme_c$ | black metachert and argillite (new unit) |
| $Dme_s$ | siltstone, shale, and basalt (new unit) |

Unit $DPs_g$ is thrust to the southwest over units $DT_p$ and $DT_a$ and to the northeast over unit $DPs_c$ (Plint, 1995). Faults, one of which is interpreted to be a normal fault, are inferred to bound unit $DT_c$. Serpentinite is exposed as small slivers in unit $DPs_g$ and is structurally interleaved with rocks in unit $DT_c$. It is designated as a separate unit due to its varied mode of occurrence, although it rarely forms map-scale bodies.

### *Chlorite-actinolite phyllite and schist ($DT_p$)*

This unit has been correlated with the Yukon-Tanana terrane (Mortensen, 1992a) and the middle unit of the "layered metamorphic suite" of Mortensen and Jilson (1985). The unit is renamed "chlorite-actinolite phyllite and schist" to better reflect the abundance of actinolite in many samples. Mariposite is present locally. In addition to the muscovite-quartz-chlorite phyllite, black carbonaceous argillite and minor metachert described in Plint (1995), the unit is expanded to include white, homogeneous quartzite, with or without grey argillaceous partings. The quartzite is exposed in scattered outcrops along the western edge of the ridge east of Wolverine Lake.

Two sub-map scale bodies of feldspar porphyry are present as structural lenses in unit $DT_p$. The northern porphyry is approximately 150 m thick and 200 m long. The rock is light grey or white, resistant weathering, and poorly to strongly foliated. It contains subhedral potassium-feldspar phenocrysts up to 1 cm in the longest dimension and minor, embayed quartz microphenocrysts in a microcrystalline quartzofeldspathic matrix. The porphyry grades downwards into a phyllite. The porphyry differs from those in unit $DT_c$ in that it lacks plagioclase phenocrysts, contains quartz microphenocrysts and has a microcrystalline, rather than fine grained, matrix. Its protolith is interpreted to be a phyric felsic volcanic flow.

The southern porphyry is exposed as a boulder train approximately 200 m wide and 500 m long between units $DT_p$ and $DT_a$. The rock is weakly to moderately foliated and contains clinopyroxene phenocrysts strongly altered to actinolite and subhedral plagioclase in a very fine grained quartzofeldspathic matrix. It is similar to porphyries in unit $DT_c$ in containing plagioclase and mafic phenocrysts but unlike those in unit $DT_c$, it contains no potassium feldspar in the matrix. Its protolith is interpreted to be a high-level intrusive rock.


10 km
Finlayson River
Campbell Highway
Wolverine Lake
limit of mapping
61°35'N
130°20'W
424600E
6826500N
458750E
6807750N
61°25'W
130°05'N
DPSp
DPSlg
DPSg
DPSc
DPSs
DMEs
DMEc
DTc
DTp
DTlg

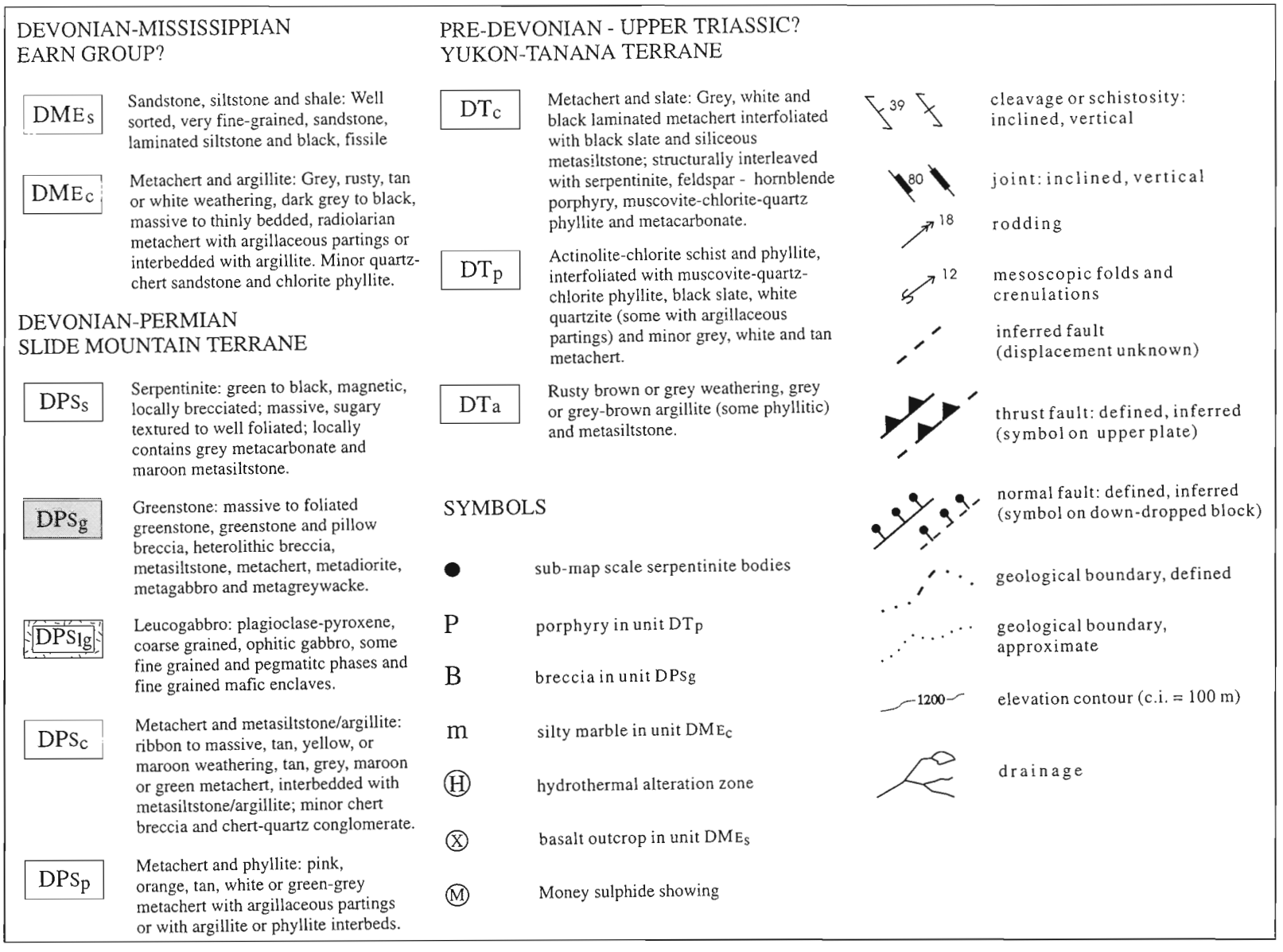


***Figure 2.*** *Geology of study area. In the legend, age assignments are from Mortensen (1992a, b) and terrane assignments are discussed in the text.*

### *Grey argillite and metasiltstone ($DT_a$)*

A unit of rusty brown- or grey-weathering, grey or greyish-brown argillite and minor metasiltstone is differentiated from unit $DT_p$. It is exposed directly below the western thrust fault. Well exposed sections indicate this unit is up to 60 m thick; it was traced over a strike length of at least 9 km.

### *Metachert and slate ($DT_c$)*

This unit is included in the chert/metachert unit of Mortensen and Jilson (1985). Plint (1995) hypothesized it may correlate with the lower division of the Slide Mountain terrane as defined in the Sylvester allochthon (e.g., Nelson, 1993). The unit consists predominantly of grey, white, and black laminated metachert, grey siliceous metasiltstone, and rusty brown- to grey-weathering, grey to black carbonaceous slate or argillite, structurally interleaved with serpentinite, hornblende-plagioclase and plagioclase-potassium feldspar porphyry, muscovite-quartz-chlorite phyllite, quartz-eye muscovite-chlorite phyllitic schist, chloritic schist, and minor grey, calcareous metacarbonate and greyish-green metachert. Subhedral feldspar and less common, embayed quartz porphyroclasts are present in phyllite and schist. The protoliths for phyllite and schist are interpreted to be felsic to mafic phyric flows.

### *Tan- to yellow-weathering metachert and maroon siliceous and argillaceous metasiltstone ($DPs_c$) and pink-, orange-, or tan-weathering metachert and tan or grey argillite and phyllite ($DPs_p$)*

These units are included in the chert/metachert unit by Mortensen and Jilson (1985) and correlate with the Slide Mountain terrane (Plint, 1995). Unit $DPs_c$ consists of massive or thinly to moderately bedded, rusty brown-, yellow-, tan-, and maroon-weathering metachert, commonly with manganese staining along joints and fracture surfaces, and is rhythmically interbedded with grey, tan, and maroon metasiltstone and argillite. Its exposed thickness is approximately 650 m, although it is likely thickened by thrust faults and folding. The metachert locally contains recrystallized radiolaria. One 15 m thick bed of massive chert-quartz conglomerate containing minor, rounded fine grained argillaceous and gabbroic clasts, was observed in unit $DPs_c$.

Unit $DPs_c$ is structurally underlain by a newly recognized unit ($DPs_p$) approximately 375 m thick of pink, orange, tan, white, or rarely greenish-grey metachert with argillaceous partings or thinly to moderately interbedded with tan or grey argillite and phyllite. Bedding is commonly planar or slightly undulating and locally, lensic. Dolomite-quartz veins, up to 1 cm thick and associated with copper?-bearing minerals in one outcrop of unit $DPs_p$, suggest localized hydrothermal alteration.

### *Greenstone ($DPs_g$) and serpentinite ($DPs_s$)*

Units $DPs_g$ and $DPs_s$ are correlative with the upper divisions of the Slide Mountain terrane (Plint, 1995). Unit $DPs_g$ comprises massive to moderately foliated greenstone, greenstone breccia, pillow breccia, heterolithic breccia, maroon metasiltstone and minor maroon, grey, green, pink, and white metachert, metagabbro, metadiorite, and metagreywacke. Intrusive contacts between metadiorite and metachert are well exposed locally in unit $DPs_g$.

Two rusty-weathering, alteration zones with associated copper-staining were observed in the greenstone. The altered rock, exposed over an area of less than 20 $m^2$, is brecciated, highly calcareous, and cut by calcite veins. These zones are interpreted to have formed by seafloor hydrothermal alteration.

Another localized, rusty weathering zone was examined in pillowed to massive greenstone at the "Money showing" in the southern part of the map area (Fig. 2). The zone is less than 10 m thick and disappears about 100 m along strike. Sulphide mineralization is developed in foliation concordant, siliceous lenses in a very fine grained, well foliated, rusty-weathering, dark green rock composed of chlorite, muscovite, quartz, and sphene. The rock contains minor subhedral, microscopic quartz crystals and is interpreted as a tuffaceous lens in the greenstone.

### *Leucogabbro ($DPs_{lg}$)*

Massive, coarse grained, ophitic leucogabbro underlies most of one mountain in the northeastern part of the map area. The rock consists of approximately equal parts plagioclase and clinopyroxene, with plagioclase typically enclosing subhedral pyroxene.

The map pattern shows that greenstone surrounds the leucogabbro (Fig. 2). An intrusive relationship is further supported by both the common occurrence of fine grained phases in an otherwise coarse grained leucogabbro near its inferred contact and by basaltic xenoliths and metre-scale blocks locally in the leucogabbro.

North of the leucogabbro and near a zone of hydrothermal alteration, the greenstone contains an 8 m thick, 100 m long slice of highly fractured and altered leucogabbro juxtaposed against a sub-map scale body of serpentinite (Fig. 2). Although no kinematic indicators are present, the density of northwest-trending, vertical fractures in the leucogabbro increase towards the contact with the serpentinite, suggesting the leucogabbro is fault-bounded. An outcrop of fish-scale serpentinite is exposed also in the main leucogabbro body (Fig. 2). These observations suggest that the leucogabbro is tectonically disrupted and probably intruded the greenstone prior to their thrust emplacement onto unit $DPs_c$.

### *Black metachert and argillite ($DMe_c$)*

This unit is included by Mortensen and Jilson (1985) in the chert/metachert unit and is tentatively correlated here with the Earn Group (see below). Contacts with other units are not exposed.

The unit consists of black-, grey-, rusty brown-, tan-, or white-weathering, dark grey to black, massive to thinly bedded, locally laminated, radiolarian-bearing metachert with argillaceous partings or interbedded with rusty-weathering, dark grey to black argillite. Quartz veins cut bedding and intrude along joint surfaces. One 50 cm bed of medium- to coarse-grained quartz-chert sandstone with angular to subrounded grains was observed in the black metachert. Quartz grains are polycrystalline and in some, the quartz subgrains define a foliation suggesting a tectonized, continental(?) detrital source.

Minor chloritic phyllite is interlayered on the centimetre- to metre-scale with argillite. Foliation in argillite and phyllite is parallel to bedding in metachert. An outcrop of massive, tan-coloured, silty (meta)limestone, about 15 m thick (horizontal distance) is exposed in this unit near its western boundary (Fig. 2). The limestone exhibits a weak northwest-striking, steeply southwest-dipping spaced cleavage.

### *Siltstone, shale, basalt ($DMe_s$)*

This unit is included by Mortensen and Jilson (1985) in the chert/metachert unit. It may correlate with the Devonian-Mississippian Earn Group (see below).

Five outcrops in unit $DMe_s$ were examined; its contacts are not exposed. The unit consists of well sorted, very fine grained, laminated grey sandstone to siltstone and black fissile shale. Included in the unit is a outcrop of pristine, strongly jointed, black basalt (Fig. 2).

## STRUCTURAL GEOLOGY

Macroscopic structures consist of (a) thrust faults at the base of the greenstone unit, (b) inferred northwest- and east-striking faults that bound unit $DT_c$ and northwest-plunging folds in unit $DT_c$, and (c) folds and faults in unit $DMe_c$.

### *Thrust faults*

A top-to-the-southwest thrust fault separates units $DT_p$ and $DT_a$ from greenstone along the western margin of the map area. The fault is exposed in the head wall of an northeasterly trending valley near the southerly mapped extent of unit $DT_a$ (Fig. 2, 3). Here the thrust at the base of the massive, fractured greenstone is subparallel to the cleavage in grey- to rusty brown-weathering grey argillite (unit $DT_a$).

Evidence for top-to-the-southwest thrust displacement appears in many outcrops of chlorite-actinolite phyllite where the steeply northeast-dipping cleavage is cut and deflected in a dextral sense by a subparallel, low-angle cleavage (Fig. 4). Evidence is also found at the northern plagioclase porphyry

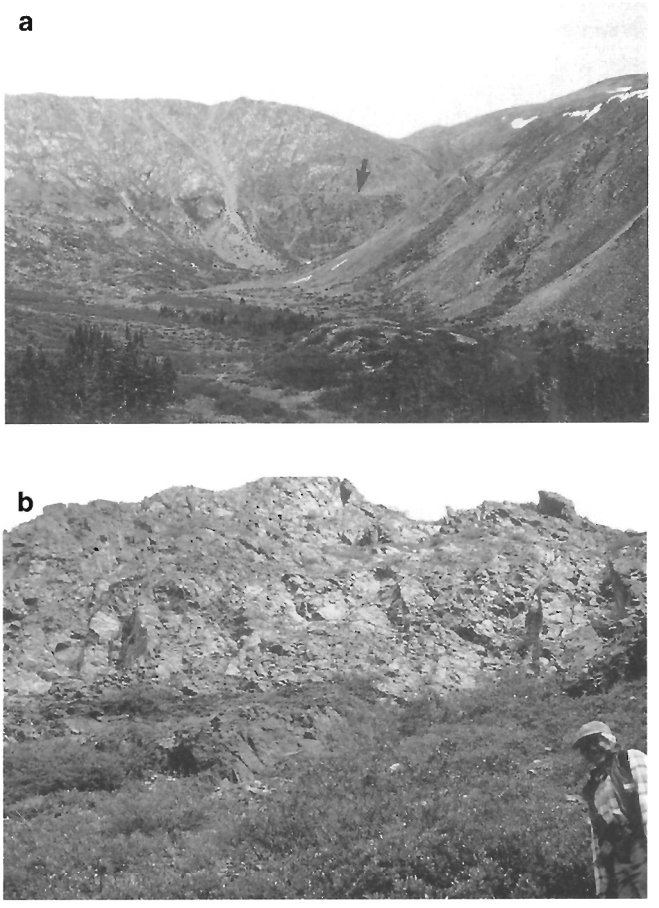


***Figure 3.*** ***a)*** *Looking east at massive greenstone of unit DPsg (top) and argillite of unit DTa separated by a top-to-the-southwest thrust fault (arrow).* ***b)*** *Close view of the contact.*

***Figure 4.*** *Looking northwest at vertical joint surface. Steeply dipping foliation in chlorite-actinolite phyllite of unit $DT_p$ is cut by parallel lower angle cleavage, causing a lozenge shaped weathering habit. The low-angle cleavage deflects the steep cleavage in a sinistral (top-to-the-southwest) shear sense (cf. Plint, 1995, Fig. 8).*

in unit $DT_p$. The argillite, structurally overlying the porphyry contain tight to isoclinal intrafolial folds of compositional layering suggesting dip-parallel transposition along the foliation. The porphyry is not lineated but is increasing foliated towards its base. Quartzofeldspathic layers in argillite directly below the porphyry are isoclinally folded into northwest-trending, southwest-verging folds whose axial surfaces are truncated and dextrally deflected into sigmoidal forms by a low-angle cleavage. These structures record top-to-the-southwest shear at the porphyry margins.

A top-to-the-northeast thrust fault, that places greenstone over unit $DPs_c$ in the eastern part of the map area, has been refined. The serpentinite thought to lie along the thrust fault is now interpreted to mark another sub-map scale, top-to-the-northeast thrust fault (untraceable along strike) in the greenstone unit (see Plint, 1995, Fig. 9). The regional thrust fault and unit $DPs_c$ that forms the footwall are exposed farther to the east that originally interpreted. Outcrop-scale, listric, top-to-the-west back thrusts associated with the regional thrust fault are well exposed in river canyons that transect unit $DPs_c$ (see Plint, 1995, Fig. 9).

The contact between units $DPs_p$ and $DMe_c$ is interpreted to be a thrust fault because its inferred trace is subparallel to the thrust fault between units $DPs_c$ and $DPs_g$ and because small scale, top-to-the-northeast reverse faults are observed in argillite in unit $DMe_c$ (see below).

### *Faults and folds in unit $DT_c$*

The paucity of exposure in areas of inferred contacts of unit $DT_c$ hinders structural interpretations. However, small scale structures are relatively well developed in unit $DT_c$ and yield some clues as to the nature of the contacts.

Moderately, easterly plunging, upright, gentle folds to tight crenulations deform the cleavage in slate in unit $DT_c$. Quartz rodding in metachert and in foliation-parallel quartz veins in slate have a similar orientation and may have developed synchronously with the easterly plunging folds.

Foliation parallel or subparallel, northeast or southwest-dipping faults truncate the easterly plunging folds and juxtapose massive hornblende-plagioclase or potassium feldspar-plagioclase porphyry, serpentinite, slate, and metachert. At one outcrop, massive serpentinite becomes strongly foliated towards the unexposed contact with slate suggesting a faulted contact. Kinematic indicators are lacking for these faults. They are probably thrust faults however, as they imbricate a wide variety of rock types on a scale of metres.

Northwest-trending, horizontal to moderately north-plunging, commonly upright to steeply inclined folds, deform the foliation on the outcrop and regional scale. Towards the western margin of unit $DT_c$, the folds vary from upright to northeast-verging. The timing of folding about northwest-trending axes relative to foliation-parallel faults and easterly plunging folds is unclear. However, because evidence for foliation parallel faulting is found along both northeast- and southwest-dipping foliation surfaces, it is probable that the faults are folded by the northwest-trending folds.

The east-striking fault that forms the southern contact is interpreted to be a north-side-down normal fault because the map pattern requires an sharp contact at a high angle to the regional foliation. Similarly oriented normal faults are common in the region (e.g., Tempelman-Kluit, 1979; Mortensen, 1992a) and small scale, top-down-to-north normal faults and shear bands occur in unit $DT_c$. The small scale normal faults and shear bands may be younger than the northwest-trending folds (see discussion).

### *Faults and folds in unit $DMe_c$*

West- and northwest-trending, moderately plunging, open to tight folds deform the bedding on a regional and outcrop scale in unit $DMe_c$. Locally, outcrop scale, northwest-striking, southwest-dipping, reverse faults are exposed in argillite in the unit. The cleavage is deflected or folded and truncated across the fault surfaces in a sinistral shear sense (Fig. 5). Localized dip-parallel (southwest-plunging) rodding on foliation surfaces observed in metachert is inferred to result from foliation-parallel thrusting within unit $DMe_c$.

## METAMORPHISM

Metamorphic grade increases from subgreenschist prehnite-pumpellyite facies in the east through pumpellyite-actinolite facies to greenschist epidote-actinolite facies in the west. Foliation in subgreenschist facies greenstone is defined by a planar parting visible in outcrop but rarely in thin section. Synmetamorphic epidote veins are common along foliation surfaces and, in well foliated samples of greenstone breccia, foliation is defined by flattened glass shards now replaced predominately by chlorite, quartz, and pumpellyite. Foliation in chlorite-actinolite phyllite of unit $DT_p$ is defined by actinolite, chlorite, and flattened relict amygdules. This foliation wraps around epidote porphyroblasts containing chlorite-filled extensional fractures (Plint and Gordon, 1995) suggesting that metamorphism was syn- to post-tectonic with respect

***Figure 5.*** *Discordant cleavage in argillite in unit $DMe_c$ (below and left of hammer) resulting from folding and shear along mesoscopic top-to-the-east reverse faults.*

to the foliation in the region. Therefore, the metamorphic assemblages are interpreted to result from regional, rather than seafloor, metamorphism. This is further supported by the widespread development of the assemblage pumpellyite-quartz-chlorite which would be unstable, or only stable over a narrow depth range, under the high geothermal gradients associated with seafloor alteration (e.g., Liou et al., 1987).

No metamorphic grade change can be determined across the eastern regional thrust fault or the boundaries of unit DTc due to differences in rock type. The western regional thrust fault juxtaposes rocks of the same (epidote-actinolite) facies. Either it is a postmetamorphic fault that fortuitously juxtaposes rocks of the same grade or it is a pre- or syn-metamorphic fault. A synmetamorphic fault is most probable because structures in unit DTp that formed during regional thrusting caused ductile deformation of pre-existing fabrics.

## REGIONAL CORRELATIONS

Without age control, regional correlation of map units depends upon matching lithological associations. The documentation of metaplutonic rock (porphyry) in unit $DT_p$ further supports its correlation with the Yukon-Tanana terrane (cf. Mortensen, 1992a). Plint (1995) hypothesized that unit $DT_c$ may be correlated with the lower division of the Slide Mountain terrane as documented in the Sylvester Allochthon (e.g., Nelson, 1993). However, the absence of calc-arenite and *radiolarian* chert and the presence of metavolcanic rocks and feldspar-hornblende porphyry in unit $DT_c$ suggest that it is more probably correlative with the Yukon-Tanana terrane.

Units $DPs_c$, $DPs_p$, $DPs_g$, $DPs_{lg}$, and $DPs_s$ are lithologically identical to the upper divisions of the Slide Mountain terrane in British Columbia (e.g., Nelson, 1993; Ferri and Melville, 1994) and are thus correlated with the Slide Mountain terrane (Plint, 1995). Unit $DMe_c$ is similar lithologically to the lower Devonian-Mississippian Earn Group whereas unit $DME_s$ could correlate with either division of the Earn Group (e.g., Gordey et al., 1982). The pristine nature of the basalt included in unit $DMe_s$ (Fig. 2), suggests that it is probably a late Cretaceous or early Tertiary flow (cf. Mortensen and Jilson, 1985).

## DISCUSSION

Regional mapping by Mortensen and Jilson (1985) reveals an abundance of both easterly and westerly dipping thrust faulted contacts in the Campbell Range. Some of these are interpreted to be klippe folded about northwest-trending axes. The exposure of unit $DT_c$ in the map area was interpreted to represent the core of one of these synformally folded klippe of greenstone (Mortensen and Jilson, 1985, p. 807). Mortensen and Jilson (1985) evoked steep (strike-slip?) faults underlying and truncated by the basal thrust to account for the discontinuity of units beneath the klippe.

Our data indicate that the base of the greenstone unit is marked by northwest-striking, moderate to shallowly dipping thrust faults with hanging wall displacements to the southwest and northeast. No evidence for steep, northerly trending faults is found in the footwall rocks. This contradicts the folded thrust fault and klippe interpretation. However, the map pattern of unit $DT_c$ is most readily explained as a klippe preserved from erosion by normal faulting along its southern boundary. Given that northwest-trending thrust faults characterize the regional structure and that northwest-trending folds are widespread in unit $DT_c$, it is reasonable to assume that the northwest-trending boundaries of unit $DT_c$ are also reverse faults. Whether they are diverging faults or a single synformally folded thrust fault is indeterminate.

We propose two hypotheses that can explain these observations:

1. The divergently dipping thrust faults are not folded but define a flower-type structure truncated locally by easterly-trending normal faults. If this is correct, then some of the "steep fault contacts" mapped by Mortensen and Jilson (1985) may be strike-slip faults.
2. The divergently dipping thrust faults record an originally east-vergent thrust sequence in which continued shortening was accommodated by west-directed back-thrusts. In this scenario, we envisage both sinistral reactivation of the western (east-dipping) limbs of the klippe in addition to the generation of new, west-directed thrusts. This sort of "tectonic wedge" model requires a wedge-shaped basement geometry and has been proposed for the boundary between paleo-North America and accreted terranes in British Columbia (e.g., Bellefontaine, 1990; Price, 1986). Although we have no constraints on the basement geometry in the study area, a wedge model could account for the folded klippe documented by Mortensen and Jilson (1985) and divergent thrust faults, northwest-trending folds in unit DTc and general map pattern documented in this study.

## ACKNOWLEDGMENTS

Funding was provided by LITHOPROBE and NSERC grants to T.M. Gordon. Thanks are due to S. Loudon for the cheery field assistance, to Equity Engineering and Westmin Resources for the hospitality and logistical support and to everyone at Frontier Helicopters in Watson Lake for the excellent helicopter support and hospitality. Many thanks to C. Roots for a critical review that improved the manuscript.

## REFERENCES

**Bellefontaine, K.A.**
1990: The tectonic evolution of the Ingenika Group and its implications for the boundary between the Omineca and Intermontane Belts, north-central British Columbia; MSc. thesis, McGill University, Montreal, Quebec, 94 p.

**Ferri, F. and Melville, D.M.**
1994: Bedrock geology of the Germansen Landing-Manson Creek area, British Columbia (94N/9,10,15; 94C/2); in British Columbia Ministry of Energy, Mines and Petroleum Resources, Bulletin 91, p. 32-41.

**Gordey, S.P., Abbott, J.G., and Orchard, M.J.**
1982: Devono-Mississippian (Earn Group) and Younger strata in east-central Yukon; in Current Research, Part B; Geological Survey of Canada, Paper 82-1B, p. 93-100.

**Hansen, V.L.**
1990: Yukon-Tanana terrane: a partial acquittal; Geology, v. 18, p. 365-369.

**Hansen, V.L., Heizler, M.T., and Harrison, T.M.**
1991: Mesozoic thermal evolution of the Yukon-Tanana composite terrane: new evidence from $^{40}Ar/^{39}Ar$ data; Tectonics, v. 10, p. 51-76.

**Liou, J.G., Maruyama, S., and Cho, M.**
1987: Very low grade metamorphism of volcanic and volcaniclastic rocks - mineral assemblages and mineral facies; in Low-Temperature Metamorphism, (ed.) M. Frey; Blackie and Son, Glasgow, p. 59-113.

**Monger, J.W.H.**
1984: Cordilleran tectonics: a Canadian perspective; Société Géologique de France, Bulletin, v. 26, p. 255-278.

**Mortensen, J.K.**
1992a: New U-Pb ages for the Slide Mountain Terrane in southeastern Yukon Territory; in Radiogenic and Isotopic Studies, Report 5; Geological Survey of Canada, Paper 91-2, p. 167-173.
1992b: Pre-mid-Mesozoic tectonic evolution of the Yukon-Tanana terrane, Yukon and Alaska; Tectonics, v. 11, p. 836-853.

**Mortensen, J.K. and Jilson, G.A.**
1985: Evolution of the Yukon-Tanana terrane: Evidence from southeastern Yukon Territory; Geology, v. 13, p. 806-810.

**Nelson, J.L.**
1993: The Sylvester Allochthon: upper Paleozoic marginal-basin and island-arc terranes in northern British Columbia; Canadian Journal of Earth Sciences, v. 30, p. 631-643.

**Plint, H.E.**
1995: Geological mapping in the Campbell Range, southeastern Yukon (Parts of 105G/8/9 and 105H/5/12); in Yukon Mining and Exploration Geology 1994, Part C; Exploration and Geological Services Division, Indian and Northern Affairs Canada, Whitehorse, Yukon, p. 47-57.

**Plint, H.E. and Gordon, T.M.**
1995: The Slide Mountain terrane and Finlayson Lake fault zone: marginal basin rocks in a transpressive setting? Evidence from the Campbell Range, southeastern Yukon; in LITHOPROBE Slave-Northern Cordillera Lithospheric Evolution Report No. 44, p. 33-50.

**Price, R.A.**
1986: The southeastern Canadian Cordillera: thrust faulting, tectonic wedging, and delamination of the lithosphere; Journal of Structural Geology, v. 8, p. 239-254.

**Roots, E.F., Green, L.H., Roddick, J.A., and Blusson, S.L.**
1966: Frances Lake, 105H; Geological Survey of Canada, Map 6-1966, scale 1:253 440.

**Tempelman-Kluit, D.J.**
1972: Geology and origin of the Faro, Vangorda and Swim concordant zinc-lead deposits, central Yukon Territory; Geological Survey of Canada, Bulletin, 208, 73 p.
1979: Transported cataclasite, ophiolite and granodiorite in Yukon: Evidence of arc-continent collision; Geological Survey of Canada, Paper 79-14, 27 p.

**Wheeler, J.O. and McFeely, P.** (comp.)
1991: Tectonic assemblage map of the Canadian Cordillera and adjacent parts of the United States of America; Geological Survey of Canada, Map 1712A, scale 1:2 000 000.

**Wheeler, J.O., Green, L.H., and Roddick, J.A.**
1960: Geological Survey of Canada, Map 8-1960, Finlayson Lake, 105G. scale 1:253 440.

LITHOPROBE and NSERC Grant #GP0046219

# Late Tertiary to Quaternary volcanism in the Atlin area, northwestern British Columbia

B.R. Edwards[1], T.S. Hamilton, J. Nicholls[2], M.Z. Stout[2], J.K. Russell[3], and K. Simpson[3]
GSC Victoria, Sidney

*Edwards, B.R., Hamilton, T.S., Nicholls, J., Stout, M.Z., Russell, J.K., and Simpson, K., 1996: Late Tertiary to Quaternary volcanism in the Atlin area, northwestern British Columbia; in Current Research 1996-A; Geological Survey of Canada, p. 29-36.*

**Abstract:** We extend the previous descriptions and report preliminary interpretations for age constraints based on field data for several occurrences of Late Tertiary to Quaternary volcanic deposits in the Atlin area: Ruby Mountain, Cracker Creek, Volcanic Creek, Llangorse Mountain, and Chikoida Mountain. The deposits include a collection of extensively eroded feeder pipes (Chikoida), a tall, columnar-jointed vent plug or a vent proximal lava flow (Llangorse), isolated cinder cones with associated lava flows (Cracker and Volcanic creeks), and a partly eroded stratovolcano (Ruby Mountain). The volcanic products at two localities, Ruby and Chikoida mountains, contain crustal xenoliths. Peridotite xenoliths are present at all five localities.

Two of the deposits, Volcanic and Cracker creeks, appear to be postglacial, whereas Ruby and Llangorse mountains have undergone moderate glacial modification. An approximate age for the bodies exposed at Chikoida Mountain is indeterminate but they appear to have been extensively glaciated.

**Résumé :** Le présent article vise à étoffer les descriptions antérieures et à faire état des premières interprétations des datations de plusieurs gisements volcaniques du Tertiaire tardif au Quaternaire de la région d'Atlin (gisements du mont Ruby, du ruisseau Cracker, du ruisseau Volcanic, du mont Llangorse et du mont Chikoida); les interprétations sont basées sur des données de terrain. Les gisements sont divers : groupe de cheminées nourricières considérablement érodées (Chikoida), culot de cheminée de grande taille et à structure prismatique ou coulée de lave proximale de cheminée (Llangorse), cônes de cendre isolés accompagnés de coulées de lave apparentées (ruisseaux Cracker et Volcanic) et strato-volcan partiellement érodé (mont Ruby). Aux sites des monts Ruby et Chikoida, les produits volcaniques contiennent des xénolites crustaux. Des xénolites de péridotite sont signalés à chacun des cinq sites.

Deux des gisements, ceux des ruisseaux Volcanic et Cracker, semblent être postérieurs à la glaciation; quant aux gisements des monts Ruby et Llangorse, ils ont été modérément modifiés par la glaciation. L'âge des massifs affleurant au mont Chikoida est indéterminé mais ils semblent avoir été recouverts de glace.

[1] Department of Geological Sciences, University of British Columbia, 6339 Stores Road, Vancouver, British Columbia V6T 1Z4; e-mail: bedwards@earth.geology.ubc.ca
[2] Department of Geology and Geophysics, University of Calgary, 2500 University Drive N.W., Calgary, Alberta T2N 1N4
[3] Department of Geological Sciences, University of British Columbia, 6339 Stores Road, Vancouver, British Columbia V6T 1Z4

## INTRODUCTION

Late Tertiary and Quaternary volcanism occurs throughout the western half of the northern Cordillera (Fig. 1 inset). Many of these volcanic centres have been studied in detail including: Volcano Mountain (Trupia and Nicholls, in press) and Ne Ch'e Ddhäwa (i.e., Wootton's cone; Jackson, 1989; Francis and Ludden, 1990) in the Fort Selkirk volcanic complex (Francis and Ludden, 1990), Alligator Lake (Eiché et al., 1987; Francis, 1987), Tuya Buttes and vicinity (Mathews, 1947; De P. Watson and Mathews, 1948; Moore et al., in press), Level Mountain (Hamilton, 1981), Heart Peaks (Casey, 1980), Mount Edziza (Souther and Hickson, 1984; Souther, 1992), Hoodoo Mountain (Edwards and Russell, 1994; Edwards et al., 1995), the Iskut-Unuk River centres (Hauksdóttir et al., 1994; Hauksdóttir, 1994), and the Aiyansh/Tseax River flows (Sutherland-Brown, 1969). However, the Late Tertiary to Quaternary volcanic occurrences in the Atlin area have not been extensively studied with the exception of work in the Ruby Mountain area (Nicholls et al., 1982; Levson, 1992) and brief descriptions of the Late Tertiary-Quaternary volcanic units by Aitken (1959).

The regional geology of the Atlin area was first outlined in detail by Aitken (1959). More recent studies include Bultman (1979), Bloodgood et al. (1989), Bloodgood and Bellefontaine (1990), Ash and Arksey (1990), Levson (1992), Mihalynuk and Smith (1992), and Mihalynuk et al. (1992). These studies demonstrate that the basement geology in the Atlin area comprises predominantly upper Paleozoic Cache Creek Group (Mississippian to Late Triassic) and Mesozoic intrusions that together form the Atlin terrane (Ash and Arksey, 1990; Bloodgood and Bellefontaine, 1990; Mihalynuk et al., 1992). Important Tertiary to Quaternary units include intermediate to felsic volcanic rocks of the Sloko Group (Aitken, 1959; Mihalynuk et al., 1992), Middle Tertiary-Quaternary olivine basalts and basanites (Aitken, 1959; Bultman, 1979; Nicholls et al., 1982; Bloodgood et al., 1989), Tertiary Au-bearing sediments, and glacial deposits (Aitken, 1959; Levson, 1992).

The purpose of this paper is to describe Late Tertiary to Quaternary volcanic rocks found in the Atlin area at the following five localities: Ruby Mountain, Cracker Creek, Volcanic Creek, Chikoida Mountain, and Llangorse Mountain. The five localities include a diverse group of volcanic features including a stratovolcano (Ruby Mountain), cinder cones

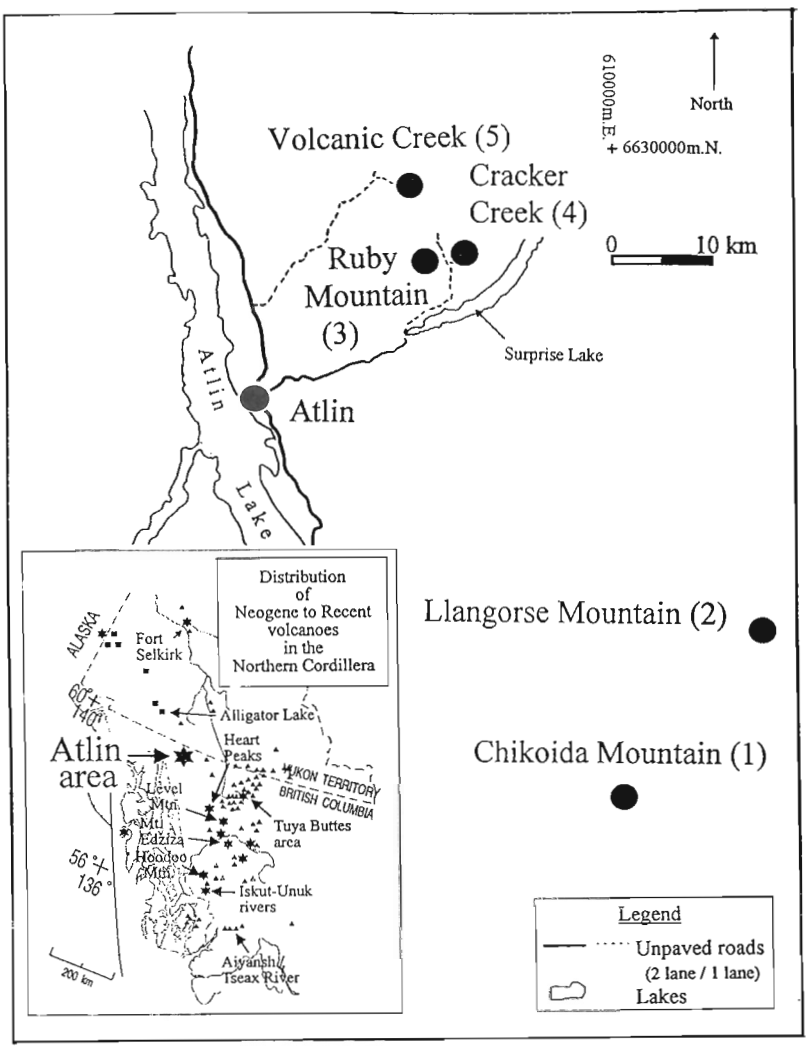


***Figure 1.***

*Regional location map for volcanic centres within the Atlin area; numbers refer to the five volcanic centres described in the text, including: 1) Chikoida Mountain, 2) Llangorse Mountain, 3) Ruby Mountain, 4) Cracker Creek, and 5) Volcanic Creek. Inset map of the northern Cordilleran volcanoes is modified from C. Hickson.*

(Cracker and Volcanic creeks), and feeder pipes (Chikoida Mountain). The formation at Llangorse Mountain is either a vent plug or a vent-proximal lava flow. Field relationships for four of the five locations indicate that the volcanism is Quaternary and at all of the locations both crustal and mantle xenoliths were collected.

This study comprises part of a larger project to collect lava and xenoliths samples from the Quaternary basaltic occurrences in the northern Cordillera as a supporting geoscience investigation for the LITHOPROBE SNORCLE transects. The samples collected in the Atlin area as well as from several other centres are to be used to characterize the subsurface geology along the SNORCLE transect. Both mantle and crustal xenoliths can provide critical constraints for the construction of stratigraphic models from geophysical data of the crust and upper mantle underlying the northern Cordillera.

## VOLCANIC CENTRES IN THE ATLIN AREA

Oligocene to Holocene mafic magmatism has been reported from twelve locations in the Atlin area. Seven of those localities were not visited during this study but are briefly summarized from other sources (Aitken, 1959; Bultman, 1979; Bloodgood and Bellefontaine, 1990; Ash and Arksey, 1990). Aitken (1959) mentioned the occurrence of Tertiary (?) basaltic volcanic deposits immediately west of Line Lake and to the south and west of Mount Llangorse. Two small occurrences of olivine-phyric basaltic lava (27.5 ± 4.3 Ma to 16.2 ± 2 Ma, whole rock K-Ar; Bultman, 1979) occur on the southeast shore of Atlin Lake, one in Anderson Bay and the other to the south in Moose Bay (Bultman, 1979; Bloodgood and Bellefontaine, 1990). Ash and Arksey (1990) tentatively correlated plagioclase-phyric basaltic dykes in the Monarch Mountain area south of Atlin with the volcanism at Ruby Mountain. Finally, according to a story in The Klondike Nugget (Anonymous, January 28, 1899) a historic volcanic eruption in the Atlin area may have occurred in 1898, approximately 50 miles south of Gladys Lake. The eruption produced sporadic airfalls for several days and "...the miners were working nights, gladly profiting by the mellow twilight caused by the volcano's glare, which turned night into day." (The Klondike Nugget, p. 4).

Five volcanic rock occurrences were visited briefly in mid-July and early August 1995; the locations are shown in Figure 1. All five sites are situated within the Atlin map sheet (104N) and four of the five locations are shown on the 1:250 000 geological map of the Atlin area by Aitken (1959); the fifth location, Chikoida Mountain, was mapped only recently by M. Mihalynuk (pers. comm., 1994). Brief field descriptions of each of the five sites visited during 1995 are given below starting with the oldest (?) occurrence, at Chikoida Mountain.

### *Chikoida Mountain*

Chikoida Mountain (map sheet 104N/3; UTM centre 612500E/6565000N) is approximately 60 km by air southeast of Atlin, British Columbia and is not accessible by road (Fig. 1). Four subvolcanic, oval-shaped outcrops of basalt occur approximately 100 m due south of the 1880 m summit cairn on Chikoida Mountain at an elevation of 1830 m. The outcrops of basalt at Chikoida Mountain are not shown on Aitken's (1959) geological map of the Atlin area but were first recognized by M. Mihalynuk (pers. comm., 1994).

The four discrete, oval-shaped bodies of weathered, chocolate brown to black olivine-phyric basalt are generally less than 20 m in diameter. The bodies are contained within quartz diorite of the Chikoida Mountain stock and are aligned approximately parallel to the contact of the host stock with underlying metasediments of the Cache Creek Group. The basalt units contain up to 40% clasts of quartz diorite and have abundant olivine phenocrysts/xenocrysts, black, glassy clinopyroxene megacrysts up to 1 cm in length, and rare, small (<5 cm) peridotite xenoliths (Fig. 2). These exposures probably represent hypabyssal feeder pipes to a volcanic centre which has been totally removed by glaciation.

The pipes intrude the Chikoida Mountain stock, which is inferred to be Triassic to Cretaceous in age, providing a maximum age. Field evidence constraining the minimum age of eruption of the Chikoida Mountain pipes is meager, however, all of the outcrops have been glaciated, and no lava flows or tephra are present. The pipes could be correlative with brown-weathering, olivine-phyric basalts on the eastern shore of Atlin Lake in Moose Bay and Anderson Bay which are Oligocene to Miocene, based on the brief description of the Atlin Lake occurrences by Bultman (1979).

### *Llangorse Mountain*

Llangorse Mountain (map sheet 104N/7; UTM centre 626000E/6582500N) is situated approximately 60 km by air southeast of Atlin, British Columbia. It not accessible by road. Aitken (1959) mapped three areas of olivine basalt south of the summit on Llangorse Mountain. These locations are 4 km south, 8 km southwest, and 10 km south of the summit of Llangorse Mountain at elevations of approximately 1400 m

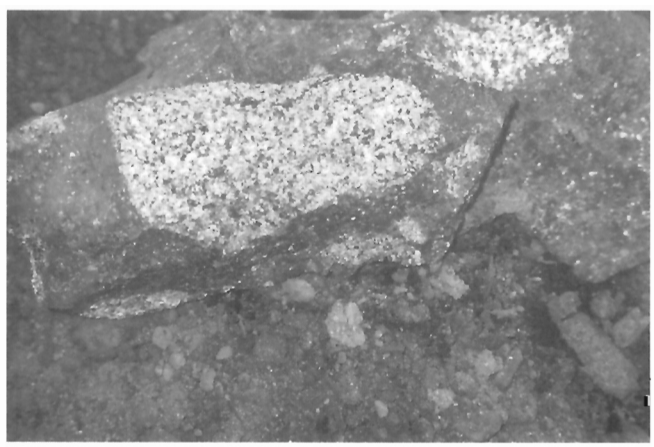

***Figure 2.*** *Field photograph of granodiorite xenoliths in basalt at Chikoida Mountain. Central xenolith is 9.5 cm long by 4.5 cm wide.*

(Aitken, 1959). The location closest to the summit and situated at the south edge of a cirque valley was examined in detail (Fig. 1).

The dark grey basalt forms a north-facing wall approximately 70 m high (Fig. 3). Columnar joints flare downward from the top to the base where they are 2 m wide. The basalt overlies a diamict at the lip of the cirque on both the east and southwest sides of the lava flow. The diamict is approximately 20 m thick at the southwest outcrop and contains cobble and boulder-size clasts of the Mount Llangorse quartz diorite (Fig. 4). The diamict also contains fragments of basalt and altered peridotite and strikes 255°, dipping 30°N at the southwest exposure. The basalt has a chilled zone approximately 1 m thick in contact with the diamict. Most of the xenoliths are in the chilled zone. Above the chilled zone is a 1 m thick vesicular zone overlain by columnar jointed basalt. The north face of the basalt has a base of talus 20-40 m high composed of basalt and less frequently coarser grained, gabbroic boulders derived from dykes (?) that cut the columnar-jointed basalt; some of the boulders contain peridotite blocks up to tens of centimetres in diameter. Most peridotite is dunite; lherzolite characterized by clinopyroxene-rich bands is less abundant.

***Figure 3.*** *View to the south of columnar jointed basalt 4 km south of the summit of Llangorse Mountain. Exposure is approximately 70 m from the base to the top.*

The age of the volcanism on Llangorse Mountain is indeterminate. Aitken (1959) cited evidence for a Late Tertiary age based on what he interpreted as a secondary northward dip direction to the basalt and the diamicton exposed on the west side of the basalt. However, our observations suggest that the orientation of the basalt and diamicton is a primary depositional feature, based on the extensive, vertical columnar joints on the north face. The basalt appears to have filled a U-shaped valley, overriding the diamict that partly filled the valley. The clasts of basalt and altered peridotite in the diamict and their stratigraphic relationships require the nearly contemporaneous formation of the rock bodies. Perhaps the flow entered a pre-existing cirque, which was at least partly filled with ice that melted to form the diamict. The chilled margin of the flow could be the result of cooling by meltwater. The large size of the peridotite xenoliths in the basalt argues against significant transport from the vent as the dense peridotite clasts would have settled out of the flow quickly. No evidence for ice-contact volcanism was found. The basalt probably is Quaternary.

### *Ruby Mountain*

Ruby Mountain (map sheet 104N/11; UTM centre 591650E/6618250N; base at 1000 m above sea level) is a partly dissected stratovolcano (Fig. 5). The volcano is approximately 26 km by road east of Atlin, British Columbia, and can be accessed by 4-wheel-drive vehicle from mining roads along either Boulder Creek or Ruby Creek (Fig. 1). The summit of the volcano is 1880 m above sea level (Fig. 6, location 1). Associated lava flows and airfall deposits occur to the east along Ruby Creek at 1100 m elevation. The total volume of the volcano is approximately 1 $km^3$. The name "Ruby" was presumably given to the mountain because of the

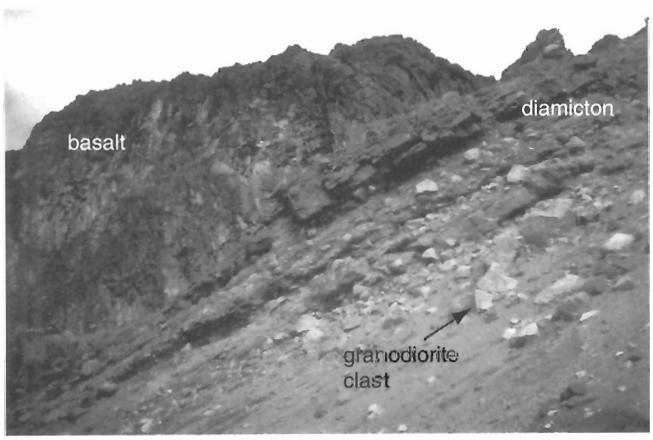


***Figure 4.*** *View to the east of poorly sorted, well bedded diamicton exposed on the west side of Llangorse Mountain volcanic centre.*

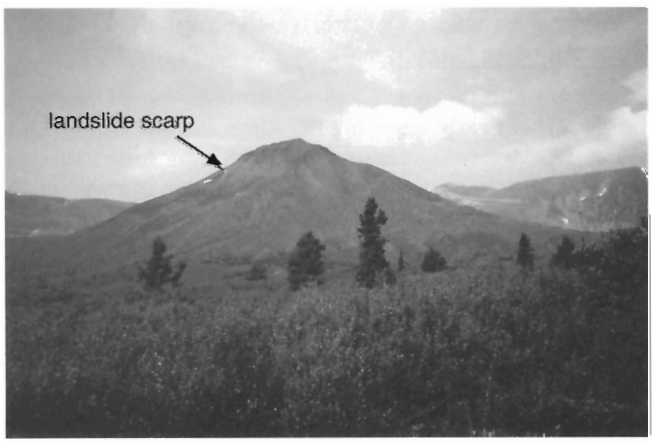


***Figure 5.*** *View of Ruby Mountain volcano from Ruby Creek looking to the west.*

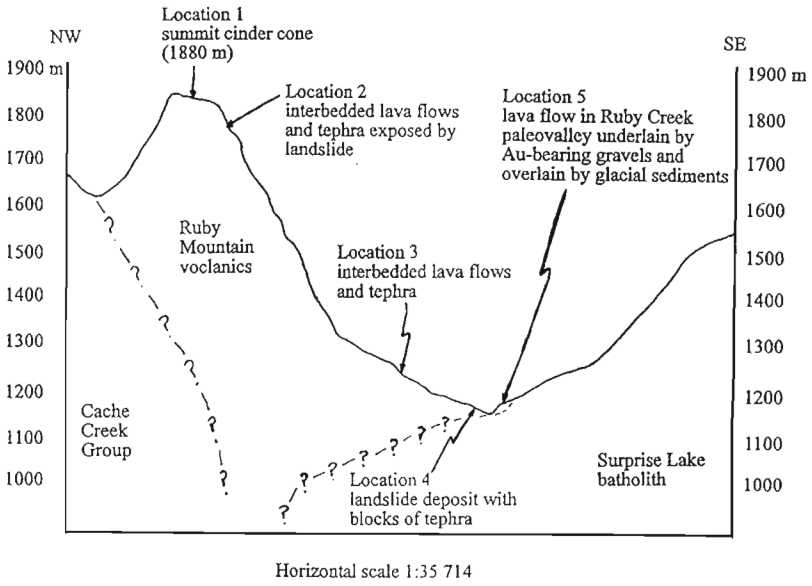


***Figure 6.***

*Schematic cross-section (NW-SE) for Ruby Mountain. Vertical exaggeration is 3.5 times. Locations of features described in the text are labelled.*

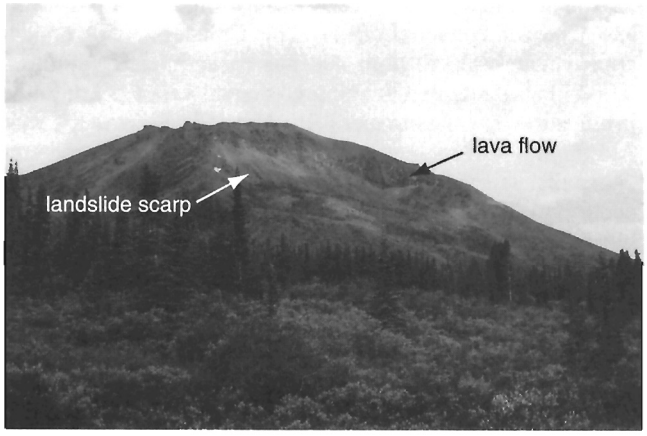


***Figure 7.*** *View looking to the west of Ruby Mountain volcano showing the sequence of lava flows that comprise the top of the volcano.*

striking red-brown tephra which is abundant both at the top of the volcano and on its eastern and northern flanks. The stratigraphy of the upper third of the volcano is well exposed on three sides. To the west the fourth side abuts the bedrock ridge forming the divide between Ruby and Boulder creeks. Although gullies draining the northern side of the volcano expose lava flows and are relatively free of vegetation, the lower eastern flanks are heavily vegetated.

As recognized by Aitken (1959), Ruby Mountain is a stratovolcano characterized by both pyroclastic deposits and lava flows. The lava are olivine-phyric basanites based on mineralogical and geochemical descriptions by Nicholls et al. (1982). The summit of the volcano is a glacially-modified cinder cone with a small, remnant crater. The floor of the crater is now covered with periglacial frost polygons and the north side is a cirque which hosts a rock glacier (Levson, 1992). The rim of the crater comprises agglutinated bombs up to 2 m in length and lava flows. One of the lava flows, exposed on the upper east side of the volcano in a landslide scarp, is at least 10 m thick and shows columnar jointing (Fig. 6, location 2 and Fig. 7). The thick flow is overlain by five thinner flows (1-5 m thick), each separated by layers of red scoria.

Tephra and lava flows predominate below the summit crater. Well sorted, partly welded lapilli tuffs interbedded with thin (<1 m) lava flows occur near Ruby Creek (Fig. 6, location 3). Cockscomb dykes are exposed on the upper northern slopes of the volcano and loose tephra is pervasive. The lower northern slopes of the volcano comprise loose cinder and appear to have been carried down the slopes by mass wasting. Lava flows are preserved on both the northern and eastern slopes of the volcano. On the west bank of Ruby Creek, due east of the summit of Ruby Mountain, a diamict contains blocks greater than 1 m in size of bedded, well-sorted lapilli tuff (Fig. 6, location 4). In at least one of the blocks, the bedding is now vertical. The diamict is probably part of a large landslide deposit noted by Levson (1992) which covers much of the lower eastern flank of Ruby Mountain and the lava flow along Ruby Creek.

An olivine-phyric basanite lava flow is exposed to the west of Cracker Creek cone along Ruby Creek and contains smaller crustal xenoliths and rare peridotite xenoliths up to 1.5 cm across (Fig. 6, location 5) (Nicholls et al., 1982; Mortensen, 1992). The basalt is light grey and aphanitic with autoliths of highly vesicular basalt to 25 cm across. It is columnar jointed and 20-40 m thick, with some of the jointing flaring near the base due to irregular cooling surfaces on the old valley floor and wall. The lava flow covers Au-bearing stream gravels and is overlain by glacial till (Fig. 8) (Aitken, 1959; Levson, 1992). Levson (1992) found clasts of basalt in the uppermost portion of the stream gravels. He also noted that locally the contact between the gravels and the overlying basalt was marked by scoriaceous sand and gravel.

Ruby Mountain volcano sits immediately on and against metasediments of the Cache Creek Group and alaskite of the Surprise Lake batholith (Fig. 6) (Aitken, 1959; Bloodgood et al., 1989). These contact relationships are best seen on the

steep western side of the valley through which Ruby Creek presently flows. Xenoliths of the basement lithologies are abundant in scoria near the crater and range up to 1 m in maximum dimension. The felsic xenoliths have textures which vary from totally unreacted to partly melted. In hand samples of basalt, white feldspar crystals with irregular shapes are common and may be xenocrysts from dissaggregated xenoliths as opposed to phenocrysts. Peridotite xenoliths are much less common, are rarely greater than 3 cm in maximum dimension, and are found in lava flows, in tephra, and in bombs.

Ruby Mountain volcano is partially dissected by post-Wisconsin alpine glaciation, which has repeatedly filled the Ruby Creek drainage and formed lateral terraces along the creek (Aitken, 1959; Levson, 1992). However, Ruby Mountain volcano may be old enough that it was affected by the Wisconsinian regional glaciation event as well. The top of the crater at Ruby Mountain is situated above the 1680 m (5500 ft.) level that was identified by Aitken (1959) as demarcating "continental" glaciation features from alpine glaciation features. At Ruby Mountain, the crater rim has been glaciated on all but the west side, suggesting that glacial ice reached this critical elevation after the crater formation. Alternatively, the crater may have acted as a cirque for a small alpine glacier, thus explaining the eroded crater walls.

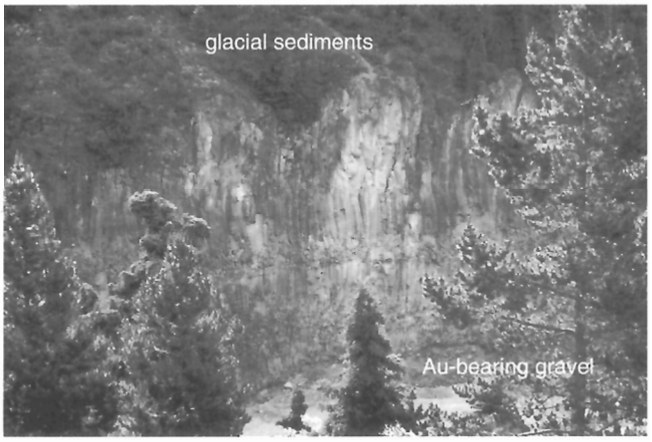


***Figure 8.*** *View looking to the east into the drainage of Ruby Creek showing the columnar jointed lava flow filling the lower part of Ruby Creek. The flow is approximately 30 m thick.*

***Figure 9.*** *View of Cracker Creek cone from the west.*

The Ruby Creek lava flow was interpreted as originating from the Cracker Creek vent by Aitken (1959). He considered Ruby Mountain volcano to be older than the lava flow exposed along Ruby Creek. However, the lava has been dated (K-Ar method) at 540 ka BP ± 200 ka (Mortensen, 1992) and based on this age date is more likely to have originated from Ruby Mountain, which has been glaciated, as opposed to the Cracker Creek cone, which has not.

### *Cracker Creek*

A small cinder cone occurs on the drainage divide between the south fork of Cracker Creek and Ruby Creek (map sheet 104 N/11; UTM centre 594750E/6618900N; base at 1290 m above sea level) (Fig. 9). It is 3 km due east of Ruby Mountain, on the eastern side of Ruby Creek. The cone is approximately 28 km east of Atlin and is accessed by mining roads up Ruby and Cracker creeks (Fig. 1). The Cracker Creek cone is approximately 30 m high and has an estimated volume of 0.003 $km^3$. It sits in a hanging U-shaped valley 80 m higher in elevation than the broader Ruby Creek drainage to the west. Although it still maintains a distinct conical shape, the cone is heavily vegetated and poorly exposed. No glacial erratics occur on it and it does not appear to have ever been covered by sediments of any kind. The cone comprises red-brown, variably oxidized, highly vesicular basaltic tephra. Crustal xenoliths are less abundant than in volcanic rocks from Ruby Mountain volcano; some of the xenoliths are partly fused. Peridotite xenoliths are rare.

Cracker Creek cone is not modified by glacial action and is the youngest volcanic feature found during this study. Field observations are consistent with the cone having formed since the last major period of regional glaciation, and possibly even since the last advance of the alpine glaciers. This would give it a maximum age of 10 ka BP (Clague, 1991).

### *Volcanic Creek*

Two nested cinder cones and an accompanying lava flow occur in the septum of two glaciated valleys that meet at the northwestern end of Mount Barham, near the headwaters of Volcanic Creek (map sheet 104N/14; UTM centre 589500E/6625000N), approximately 28 km by road to the north and east of Atlin. The cones are accessible to within 3 km by 4-wheel-drive roads via Fourth of July Creek and Volcanic Creek (Fig. 1). The uppermost cone is approximately 100 m high, 100 m in diameter, and sits on at the confluence of two glaciated valleys at approximately 1500 m elevation. The total estimated volume of lava and tephra at Volcanic Creek is 0.02 $km^3$.

Immediately east of the cones on Mount Barham, Cache Creek Group metasediments and metavolcanics are exposed. The upper valley walls both north and south of the cones expose dioritic units of the Fourth of July batholith

***Figure 10.*** *Lava flow underlain and overlain by red tephra, Volcanic Creek. Lava flow is approximately 1 m thick.*

(Mihalynuk et al., 1992). The cones are well preserved, consist of lapilli to block size, red-brown basaltic tephra, and appear not to have been modified by glaciers. A grey, basaltic lava flow, exposed along Volcanic Creek, has been dissected by the creek. The dissected lava flow varies in thickness from 1 to 3 m near the cones to more than 10 m approximately 1 km downstream. The lava flow can be traced intermittently downstream for more than 2 km and locally has well developed columnar jointing. It is both underlain and overlain by red-brown, slightly welded tephra (Fig. 10). Crustal and peridotite xenoliths are rare in the scoria and lava flow at Volcanic Creek.

The Volcanic Creek nested cones appear to be postglacial. The scoria cones are little modified by erosion or mass wasting and most bombs appear to lie in the position they fell. Possibly, because the cones lie at the junction of two U-shaped valleys, they were protected from glacial erosion from Mount Barham, immediately to the east. However, it seems likely that the scoria cones would not have survived regional glaciation. This leads to the conclusion that the volcanism at Volcanic Creek is also younger than the last regional glaciation (10 ka BP; Clague, 1991).

## VOLCANOLOGICAL-PETROLOGICAL PROBLEMS IN THE ATLIN AREA

Volcanological-petrological problems associated with Middle Tertiary-Quaternary volcanic rocks in the Atlin area concern: 1) the origin of the xenoliths found in the volcanic units; 2) the ages of glaciation and volcanism; and 3) the pre-eruptive magmatic histories of the volcanic rocks.

The first of these problems is important on a regional scale, and is currently addressed by several supporting geoscience investigations for the LITHOPROBE SNORCLE transects. The xenoliths from these centres as well as from other Neogene and Quaternary volcanic centres in the northern Cordillera are critical to geoscientists interested in the structure of the Cordilleran crust because they provide the only direct access to the subsurface geology of the Cordillera and will provide important details for interpretations of subsequent geophysical surveys.

The second problem represented in the Atlin area, the temporal relationship between glaciation and volcanism, is also of regional significance. Several workers have postulated a genetic link between glaciation and volcanism in the northern Cordillera (Grove, 1974) and in other parts of the northern hemisphere (e.g., Iceland, Sigvaldason et al., 1992). Four of the five volcanic features in the Atlin area described above occur in areas that were glaciated prior to volcanic activity and at least two of the four experienced subsequent glacial modification.

No detailed petrological investigations of any of the volcanic centres in the Atlin area have been published. Such studies could help to constrain the possible petrogenetic links between different centres and help to define the tectonic regime responsible for the magmatism. The detailed magmatic histories for all of the occurrences awaits further field-based and geochronological studies.

## ACKNOWLEDGMENTS

We wish to acknowledge M. Mihalynuk for providing background information on the geology of the Atlin area and informing us of the Chikoida Mountain and Atlin Lake locations. The editorial suggests of C. Hickson greatly improved the manuscript as did those of B. Vanlier. We also thank D. Francis for information concerning Ruby and Llangorse mountains. B.R. Edwards was supported in part by a University Graduate Fellowship from the University of British Columbia. Ancillary research costs were born by NSERC Research Grant 0000820 to J.K.R., NSERC Research Grant A7372 to J.N., and LITHOPROBE. This is LITHOPROBE contribution 703.

## REFERENCES

**Aitken, J.D.**
1959: Atlin, British Columbia; Geological Survey of Canada, Memoir 307, 89 p.

**Anonymous**
1899: An active volcano; The Klondike Nugget, January 28, p. 4.

**Ash, C.H. and Arksey, R.L.**
1990: The Atlin ultramafic allochthon: ophiolitic basement within the Cache Creek terrane; tectonic and metallogenic significance (104N/12); in Geological Fieldwork 1989; British Columbia Ministry of Energy, Mines, and Petroleum Resources, Paper 1990-1, p. 365-374.

**Bloodgood, M.A. and Bellefontaine, K.A.**
1990: The geology of the Atlin area (Dixie Lake and Teresa Island) (104N/6 and parts of 104N/5 and 12); in Geological Fieldwork 1989; British Columbia Ministry of Energy, Mines, and Petroleum Resources, Paper 1990-1, p. 205-215.

**Bloodgood, M.A., Rees, C.J., and Lefebure, D.V.**
1989: Geology and mineralization of the Atlin area, northwestern British Columbia (104N/11W and 12E); in Geological Fieldwork 1988; British Columbia Ministry of Energy, Mines, and Petroleum Resources, Paper 1989-1, p. 311-322.

**Bultman, T.R.**
1979: Geology and tectonic history of the Whitehorse trough west of Atlin, British Columbia; PhD. thesis, Yale University, New Haven, Connecticut.

**Casey, J.J.**
1980: Geology of the Heart Peaks volcanic centre, northwestern British Columbia; MSc. thesis, University of Alberta, Edmonton, Alberta.

**Clague, J.J.**
1991: Quaternary glaciation and sedimentation; Chapter 12 in Geology of the Cordilleran Orogen in Canada, H. Gabrielse and C.J. Yorath (ed.); Geological Survey of Canada, Geology of Canada, no. 4, p. 419-434 (also Geological Society of America, The Geology of North America, v. G-2).

**De P. Watson, K. and Mathews, W.H.**
1948: Partly vitrified xenoliths in pillow basalt; American Journal of Science, v. 244, p. 601-614.

**Edwards, B.R. and Russell, J.K.**
1994: Preliminary stratigraphy of Hoodoo Mountain volcanic centre, northwestern British Columbia; in Current Research 1994-A; Geological Survey of Canada, p. 69-76.

**Edwards, B.R., Edwards, G., and Russell, J.K.**
1995: Revised stratigraphy for the Hoodoo Mountain volcanic centre, northwestern British Columbia; in Current Research 1995-A; Geological Survey of Canada, p. 105-115.

**Eiché, G.E., Francis, D.M., and Ludden, J.N.**
1987: Primary alkaline magmas associated with the Quaternary Alligator Lake volcanic complex, Yukon Territory, Canada; Contributions to Mineralogy and Petrology, v. 95, p. 191-201.

**Francis, D.**
1987: Mantle-melt interaction recorded in spinel lherzolite xenoliths from the Alligator Lake volcanic complex, Yukon, Canada; Journal of Petrology, v. 28, p. 569-597.

**Francis, D. and Ludden, J.**
1990: The mantle source for olivine nephelinite, basanite and alkaline olivine basalts at Fort Selkirk, Yukon, Canada; Journal of Petrology, v. 31.

**Grove, E.W.**
1974: Deglaciation - a possible triggering mechanism for Recent volcanism; International Association of Volcanology and Chemistry of the Earth's Interior, Proceedings of the Symposium on Andean and Antarctic Volcanology Problems, Santiago, Chile, September 1974, p. 88-97.

**Hamilton, T.S.**
1981: Late Cenozoic alkaline volcanics of the Level Mountain Range, northwestern British Columbia: geology, petrology and paleomagnetism; PhD. thesis, University of Alberta, Edmonton, Alberta.

**Hauksdóttir, S.**
1994: Petrography, geochemistry and petrogenesis of the Iskut-Unuk rivers volcanic centres, northwestern British Columbia; MSc. thesis, University of British Columbia, Vancouver, British Columbia.

**Hauksdóttir, S., Enegren, E.G., and Russell, J.K.**
1994: Recent basaltic volcanism in the Iskut-Unuk rivers area, northwestern British Columbia; in Current Research 1994-A; Geological Survey of Canada, p. 57-67.

**Jackson, L.E., Jr.**
1989: Pleistocene subglacial volcanism near Fort Selkirk, Yukon Territory; in Current Research, Part E; Geological Survey of Canada, Paper 89-1E, p. 251-256.

**Levson, V.M.**
1992: Quaternary geology of the Atlin area (104N/11W, 12E); in Geological Fieldwork 1992; British Columbia Ministry of Energy, Mines, and Petroleum Resources, Paper 1992-1, p. 375-390.

**Mathews, W.H.**
1947: "Tuyas", flat-topped volcanoes in northern British Columbia; American Journal of Science, v. 245, p. 560-570.

**Mihalynuk, M.G. and Smith, M.T.**
1992: Highlights of 1991 mapping in the Atlin-West map area (104N/12); in Geological Fieldwork 1992; British Columbia Ministry of Energy, Mines, and Petroleum Resources, Paper 1992-1, p. 221-227.

**Mihalynuk, M.G., Smith, M.T., Gabites, J.E., Runkle, D., and Lefebure, D.**
1992: Age of emplacement and basement character of the Cache Creek terrane as constrained by new isotopic and geochemical data; Canadian Journal of Earth Sciences, v. 29, p. 2463-2477.

**Moore, J.G., Hickson, C.J., and Calk, L.**
in press: Tholeiitic-alkalic transition at subglacial volcanoes, Tuya region, British Columbia; Journal of Geophysical Research, Solid Earth.

**Mortensen, J.K.**
1992: British Columbia, GSC 92-29; in Radiogenic Age and Isotopic Studies: Report 6; Geological Survey of Canada, Paper 92-2, p. 192.

**Nicholls, J., Stout, M.Z., and Fiesinger, D.W.**
1982: Petrologic variations in Quaternary volcanic rocks, British Columbia, and the nature of the underlying upper mantle; Contributions to Mineralogy and Petrology, v. 79, p. 201-218.

**Sigvaldason, G.E., Annertz, K., and Nilsson, M.**
1992: Effect of glacier loading/deloading on volcanism: postglacial volcanic production rate of the Dyngjufjoll area, central Iceland; Bulletin of Volcanology, v. 54, p. 385-392.

**Souther, J.G.**
1992: The late Cenozoic Mount Edziza Volcanic Complex, British Columbia; Geological Survey of Canada, Memoir 420, 320 p.

**Souther, J.G. and Hickson, C.J.**
1984: Crystal fractionation of the basalt comendite series of the Mount Edziza volcanic complex, British Columbia: major and trace elements; Journal of Volcanology and Geothermal Research, v. 21, p. 79-106.

**Sutherland-Brown, A.**
1969: Aiyansh lava flow, British Columbia; Canadian Journal of Earth Sciences, v. 6, p. 1460-1468.

**Trupia, S. and Nicholls, J.**
in press: Petrology of Recent lava flows, Volcano Mountain, Yukon Territory, Canada; Lithos.

Geological Survey of Canada Project 820018

# Kshwan Glacier rock avalanche, southeast of Stewart, British Columbia

Tanya E. Mauthner[1]
GSC Victoria

*Mauthner, T.E., 1996: Kshwan Glacier rock avalanche, southeast of Stewart, British Columbia; in Current Research 1996-A; Geological Survey of Canada, p. 37-44.*

**Abstract:** During the winter of 1992-1993, a rock avalanche slid onto and crossed the Kshwan Glacier. Between 1 and 3 million cubic metres of hornblende-biotite granodiorite of the Eocene Kshwan Glacier pluton detached along joints from an oversteepened slope debuttressed by downwasting and retreating glaciers. Modelling of the Kshwan Glacier rock avalanche and comparison with other avalanches suggest that it had a coefficient of friction and runout characteristic of rock avalanches occurring in glacial environments. Examination of the geological and geomorphic conditions causing mass movements such as the Kshwan Glacier rock avalanche substantiates the need for caution in the development of recently glaciated terrain such as in the Coast Mountains.

**Résumé :** Durant l'hiver de 1992-1993, une avalanche de pierres a traversé la surface du glacier Kshwan. Entre un et trois millions de mètres cubes de granodiorite à hornblende-biotite du pluton éocène de Kshwan Glacier se sont détachés le long des joints à partir d'une pente surraidie aux saillies nivelées par les glaciers en période de fonte et de recul. La modélisation de cette avalanche et sa comparaison avec d'autres indiquent que son coefficient de frottement et d'écoulement est caractéristique des glissements de ce type se produisant en milieu glaciaire. L'analyse des conditions géologiques et géomorphologiques à l'origine des mouvements de masse comme l'avalanche de pierres du glacier Kshwan confirme la nécessité de faire preuve de prudence dans la mise en valeur des terrains récemment recouverts de glace comme ceux que l'on trouve dans la chaîne Côtière.

[1] #401 - 1680 Balsam Street, Vancouver, British Columbia V6K 3M1; e-mail: mauthner@unixg.ubc.ca

## INTRODUCTION

The deposit of a recent, large-scale rock avalanche, or "sturzstrom", here referred to as the Kshwan Glacier rock avalanche, was discovered in the spring of 1993 by a helicopter pilot operating in the Coast Mountains southeast of Stewart, British Columbia (Fig. 1-3). Between 1 and 3 million cubic metres of rock slid onto and across the Kshwan Glacier, which is located in the southern extremes of the Cambria Icefield. Debris from the Kshwan Glacier rock avalanche failed from a height of as much as 675 m above the glacier, travelled over a horizontal distance of 2205 m, and crossed the glacier's 1.2 km width, approximately 4.5 km up ice from the present toe. The avalanche and similar events, such as the Tim Williams Glacier rock avalanche 90 km to the north (Evans and Clague, 1990), attest to potential avalanche hazards in the steep and rugged glacial terrain of this part of the Coast Mountains, and are particularly relevant because they have occurred close to areas of intense mineral exploration and possible mine development. For example, Lac Minerals Ltd.'s Red Mountain Gold Project is located 20 km north of the Kshwan Glacier rock avalanche, and the past-producing Torbrit and Dolly Varden mines are about 10 km to the east-southeast. This report summarizes the characteristics of the Kshwan Glacier rock avalanche, and is based on observations made on the detachment surface and debris lobe during three days of fieldwork in August 1994 (Mauthner, 1995).

## TIMING

The Kshwan Glacier rock avalanche was not observed by local helicopter pilots during the summer of 1992, and is therefore inferred to have occurred between the autumn of 1992 and the spring of 1993. What triggered the rock avalanche remains unknown. A seismic trigger, a mechanism which is commonly the cause of rock avalanches (Shreve, 1966), is not suspected to have played a role in the initiation of the Kshwan Glacier rock avalanche, because there is no record of a significant earthquake (greater than 4.0 on the Richter Scale) having occurred in the area during the winter of 1992-93 (L. Finn, pers. comm., 1995).

## LOCAL GEOLOGY

The Cambria Icefield area is situated along the Coast-Intermontane belt boundary, with Jurassic and Tertiary plutons of the Coast Belt intruding mainly Lower and Middle Jurassic stratified rocks of Stikinia (Greig et al., 1994). The debris of the Kshwan Glacier rock avalanche consists almost exclusively of blocks from the Kshwan Glacier pluton, an unfoliated, medium grained, hornblende-biotite granodiorite (range in composition: tonalite to quartz monzodiorite) of Eocene age. The pluton intrudes the Early Jurassic Bulldog Creek pluton to the west and south, and Triassic and/or Lower Jurassic clastic and volcaniclastic rocks to the north and east (Greig et al., 1995).

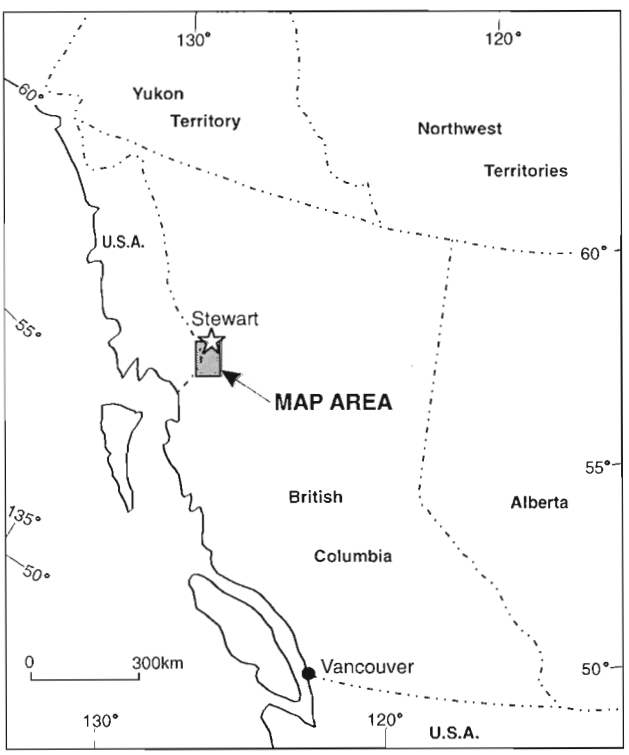


*Figure 1. Location map of the study area in northwestern British Columbia. Shaded box outlines area of Figure 2.*

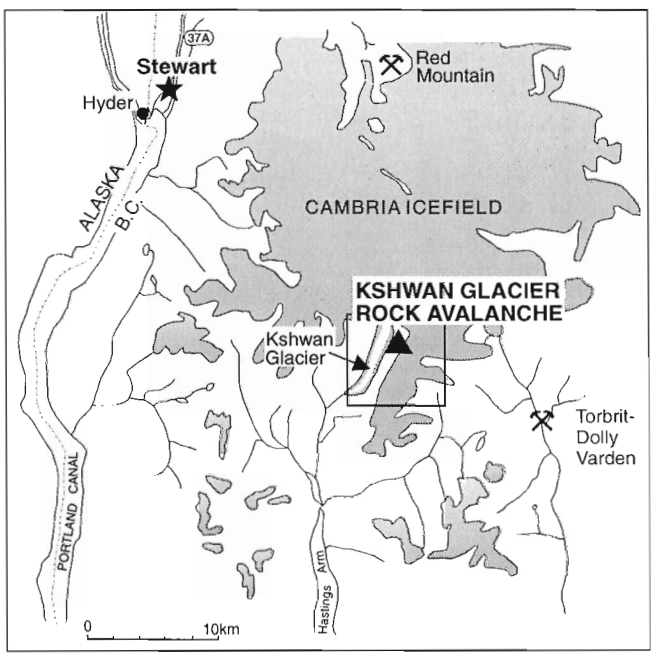


*Figure 2. Location of Kshwan Glacier rock avalanche southeast of Stewart, British Columbia; box outlines location of Figure 6.*

***Figure 3.*** *Oblique photo of the Kshwan Glacier rock avalanche, taken in August 1993, facing north.*

### *Discontinuities: dykes and joints*

The Kshwan Glacier pluton is intruded by several generations of dykes. The oldest dykes are centimetre- to decimetre-scale coarse grained pegmatites, consisting of potassium feldspar, plagioclase, and quartz. Near the north-northwest-trending (340°), moderately west-dipping (30-60°) head scarp of the detachment, pegmatites have intruded parallel to a joint set which strikes north-northeast and dips 50° to the west. On ridges adjacent to the avalanche scarp, the most common dykes are 2-6 m thick, north-northwest-trending, steeply southwest dipping, pale grey, porphyritic dacites, with phenocrysts of plagioclase feldspar, hornblende, biotite, and quartz. Thinner, possibly related dykes include fine grained, dark grey to green, biotite-phyric andesites(?), which are exposed near the base of the detachment surface and strike easterly.

The average dip-slope joint set along the north side and base of the detachment surface is oriented 168°/45°W (Mauthner, 1995). The joints are continuous and planar, and range in dip from approximately 60° at the head scarp (Fig. 4)

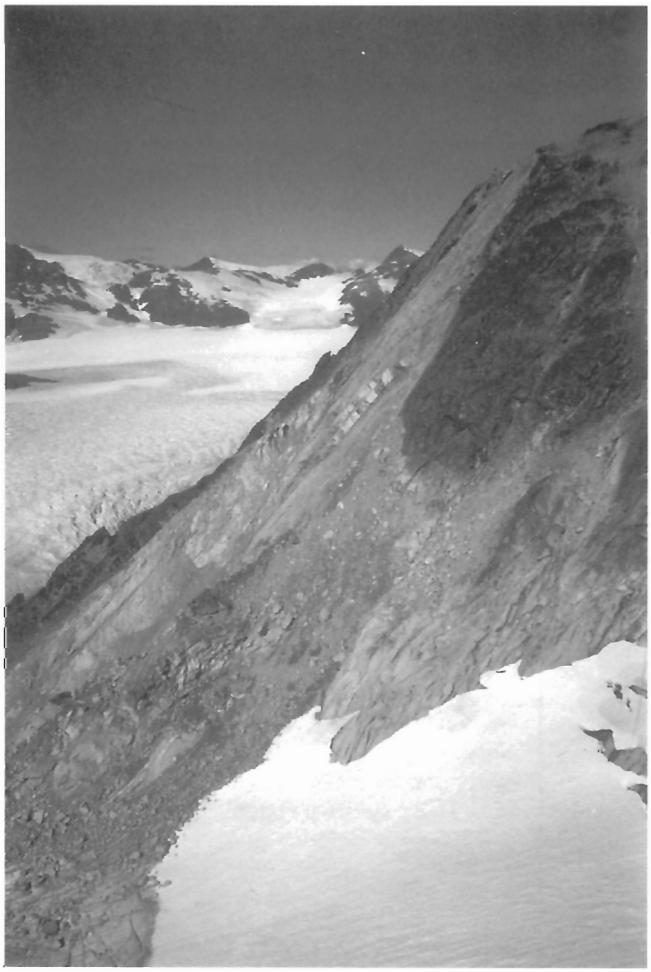

***Figure 4.*** *Photo of smooth, planar joint surface at head scarp of avalanche detachment surface; scarp dips at an average of 60° southwest.*

***Figure 5.*** *Photo of the detachment surface, facing east.*

to 30° at the base of the detachment surface. At the head scarp, the dip-slope joint set is planar, smooth, and has an average spacing of 1 m. Some joint surfaces have a thin film of chlorite; others appear to be coated with up to 5 cm of quartz, or are strongly weathered, leaving smooth quartz surfaces "pock-marked" by preferential weathering of coarse grained mafic minerals. The dip-slope joint set at the base of the slope is smooth, curviplanar (with an amplitude of 30 cm across 10 m), locally chloritic, and has a spacing ranging from 10 cm to 4 m. The joint set forming the southern wall of the detachment, which is below a hanging glacier adjacent to the avalanche site (Fig. 5), is oriented 016°/35°W. All of the dip-slope joint sets are intersected by steeper, less continuous, wavy joints oriented approximately 000°/70°W. The steeper joint set parallels a 1 m andesitic dyke visible in southern slope. Elsewhere in the pluton, the most common joint sets are north-northwest-trending, steeply southwest-dipping (paralleling the dacite dykes), and north-northeast-trending, steeply northwest- or southeast-dipping. Major lineaments oriented north-northwest and northeast are visible on airphotos (Fig. 6), and occur on both sides of the Kshwan Glacier. These lineaments may be faults, but subparallel regional joint sets are also visible in the air photos and if they are faults, they may be reactivated joints.

## DETACHMENT ZONE

The Kshwan Glacier rock avalanche occurred on an oversteepened slope, at an elevation between 1243 m and 1675 m (Fig. 5, 7). The detachment zone is adjacent to a hanging glacier to the south, and lies above and to the east of the Kshwan Glacier. Figure 7 shows a longitudinal profile of the slide from head scarp to the debris toe. The profile of the mountain slope prior to failure was taken from the 1:50 000 topographic map (NTS 103P/13), and it was drawn to correspond with the estimated centreline of the rock avalanche path (Fig. 6).

Aerial photographs and reconnaissance geological mapping demonstrate that the regional joint pattern is consistent in orientation on either side of the valley of the Kshwan Glacier. The dip-slope joint set on the detachment surface appears to be a type of sheet jointing related to the stress regime recorded in the pluton (as in Twidale, 1973). Isostatic rebound of the pluton after recent deglaciation may have played a role in weakening the dip-slope joints, and therefore may have contributed to the failure. In addition, the upper slopes of the mountain have been deglaciated, whereas the lower slopes have not, suggesting the possibility that differential stresses between the base and peak of the mountain further contributed to slope failure.

In their study of the Tim Williams Glacier rock avalanche, Evans and Clague (1990) suggested that relatively incompetent rocks within the Hazelton Group, such as pyroclastic rocks and argillite, are particularly landslide prone. However, in this case, the massive Eocene Kshwan Glacier pluton is a less deformed and more competent lithology than the Lower Jurassic rocks of the Hazelton Group, into which it was emplaced. This suggests that it was not rock type which controlled the type of failure, but deglaciation, which allowed for debuttressing of glacially over-steepened slopes, and which led to failure along appropriately oriented structural discontinuities.

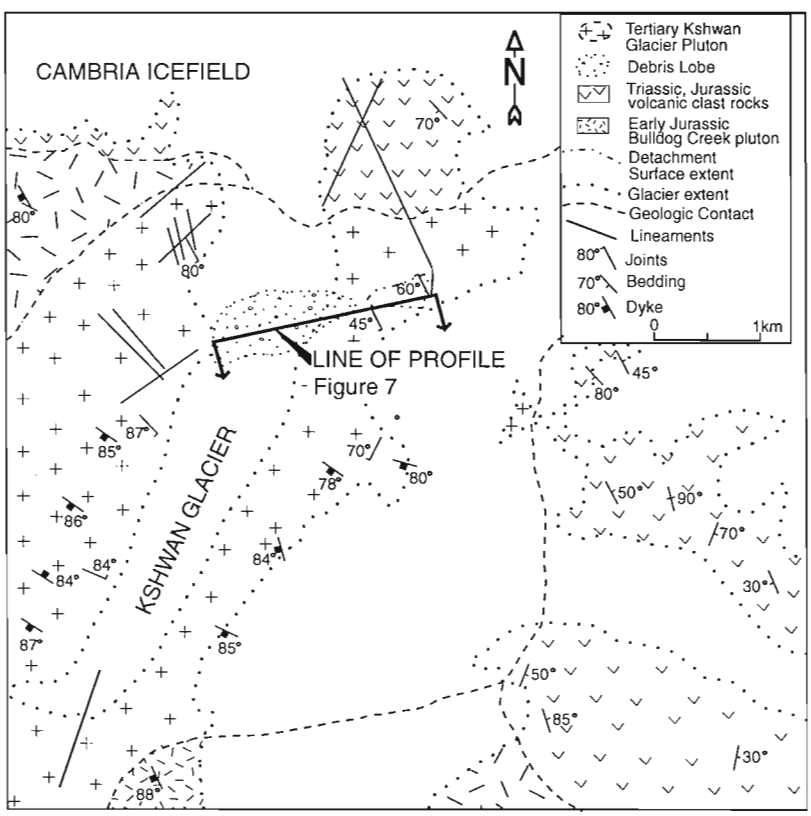


*Figure 6.*

*Diagram showing extent of the Kshwan Glacier pluton, the detachment surface and the debris lobe. Major lineaments and joint patterns from airphotos BC 2179-83,-84 (1954); geology from C.J. Greig (written comm., 1995).*

## DEBRIS LOBE CHARACTERISTICS

The avalanche debris lobe is 1400 m long, a maximum of 400 m wide, and consists of a chaotic mass of material ranging in size from silt and coarse grained sand, to angular blocks 10 m in diameter (Fig. 3, 8). It is apparent from airphotos which predate the failure (airphotos 1982 BC 82019 no. 267-268) that the debris followed a topographic low in the glacier ice; therefore, the geometry of the lobe was controlled by the topography of the glacier as well as by the direction of the debris fall. Photographs from 1993 and 1994 show the debris lobe in approximately the same location, so the slide has not moved significantly down-ice since the slope failure although, slight curvature of the lobe may reflect somewhat more rapid movement of the central part of the glacier. A second debris fan overlying the main debris lobe is evident near the eastern lateral moraine (Fig. 3). Rock destabilized by the first failure may have become detached somewhat later, suggesting that further small failures may occur in the detachment area.

Large blocks in the debris lobe are lithologically uniform and have fresh, conchoidally fractured surfaces with angular to slightly rounded edges. Approximately 1% of the debris has smooth, planar, chloritic surfaces. Less than 1% of the rocks seen along the perimeter of the debris lobe are subrounded, rust coloured, and weathered, and are identical to those in the lateral moraine along the east side of the valley. They probably represent debris incorporated from the lateral moraine during the slide event. Large blocks are scattered across the entire surface of the debris lobe, but there is a greater concentration along the margins. Isolated blocks in the centre of the lobe lie on a bed of finer grained rubble; larger blocks near the perimeter of the lobe are locally blanketed by up to 1 cm of coarse grained sand. The concentration of 2-10 m blocks near the margins of the lobe form sharp, steep levees similar to ones formed by debris flow channels, but lacking grain size grading. The southern debris levee is approximately 7 m thick (Fig. 9), and the northern levee is somewhat smaller, rising approximately 4 m above the glacier surface. There is also a smaller average block size in the northern levee. The total thickness of the levees, and of the debris lobe in general, is difficult to ascertain. Glacial ice appears to slope up beneath the lobe, particularly along its southern margin, so it is possible that entrained ice and snow in the avalanche was subsequently insulated by the debris lobe from melting. Alternatively, there may have been very little entrainment, and the upward-sloping ice may have resulted entirely from preferential insulation. The fact that ice along the northern margin receives less exposure to direct summer sunlight than that along the southern margin and shows less evidence for upward-sloping ice, supports a theory of preferential insulation.

Crevasses within the glacier appear to be continuous with those within and beneath the debris lobe. That the ice pattern is reflected in the debris lobe suggests that debris has either fallen into the crevasses or that the crevasses have opened up since the avalanche. In either case, the observations suggest that the lobe is quite thin, perhaps on the order of 4-7 m.

The detached mass abuts the opposite (west) side of the valley, but no evidence other than the levee exists for thickening at the debris toe. Outcrop surfaces along the west wall of the valley are unweathered but little damage appears to have been caused by the impact of the rock avalanche. At most, a small amount of rock may have fallen as a result of the impact, but this may also be due to planar failure during exfoliation. These observations are important in understanding the method by which the value of the friction coefficient was determined in Mauthner (1995). If the rock

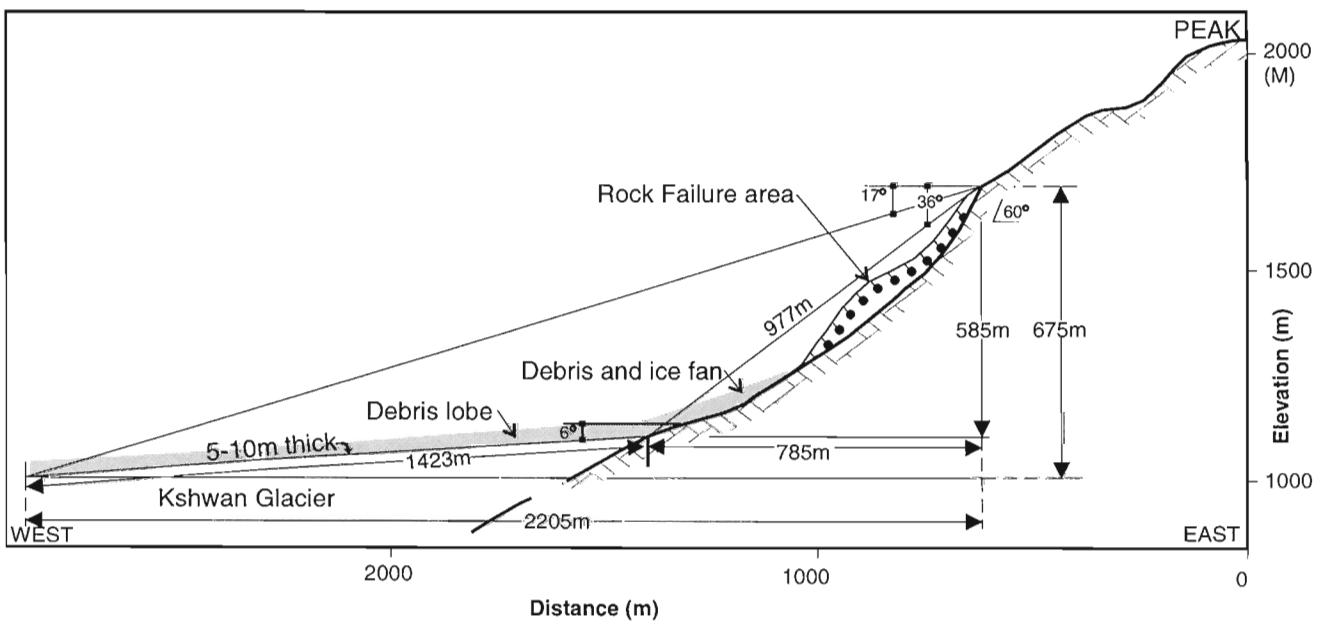


*Figure 7. Longitudinal profile of the detachment surface and debris lobe along the oriented NE-SW centreline of the rock avalanche fall path. See Figure 6 for line of profile.*

avalanche had impacted against the west valley wall, it would be necessary to estimate the distance the debris would have travelled had the wall not been there, the loss of debris momentum due to the impact. Unlike the Tim Williams Glacier rock avalanche (Evans and Clague, 1990), there was not enough momentum to cause the rock debris to rebound off the opposite valley wall and be deflected down-ice.

## COMPARISON WITH ROCK AVALANCHES IN GLACIAL AND NONGLACIAL ENVIRONMENTS

Around the perimeter of the debris lobe, some large boulders are blanketed/covered by a thin layer of coarse sand with an overall granodiorite composition. This observation appears to be common in rock avalanches. Shreve (1966) noted the presence of debris cones, with graded bedding, on top of large sturzstrom blocks in the Sherman Glacier rock avalanche, and Heim (1932) described the presence of large angular blocks embedded within a matrix of pulverized rock in the Flims sturzstrom. The presence of coarse sand on top of large boulders in the Kshwan Glacier rock avalanche suggests that a dense suspension of sand and dust settled after the sturzstrom ceased moving. The deposits are thin relative to those of the Sherman Glacier rock avalanche, most likely because of differences in rock properties, such as strength, mineral composition, and grain size.

Many rock avalanches that have occurred in glacial environments have incorporated ice and snow with the rock debris. The ice and snow may be part of the detached mass, or they may be acquired during the passage of the rock avalanche. McSaveney (1978) noted ice and snow within debris piles and covered with slumping debris along the margins of the Sherman Glacier rock avalanche in Alaska, and he estimated that 20% of the detached mass was glacier ice. For the Mt. Cook rock avalanche in New Zealand, Hancox et al. (1991) describe a widely variable ice content ranging up to 80% by volume. For the Kshwan Glacier rock avalanche, there is no evidence that a significant portion of the debris consisted of snow or ice.

The coefficient of friction for the Sherman Glacier rock avalanche was estimated to be 0.11 (McSaveney, 1978), and a dynamic analysis of the Kshwan Glacier rock avalanche determined a significantly greater coefficient of friction (0.31), with a time of emplacement of 59 seconds (method of Heim (1932), details in Mauthner (1995)). The difference probably reflects the relatively high percentage of ice and snow incorporated in the Sherman Glacier debris lobe, which likely decreased the frictional resistance within and at the base of the debris lobe.

The frictional resistance of a rock avalanche moving over ice should be significantly less than that of a rock avalanche travelling over rock or soil. Budd et al. (1979) determined that the maximum value of the coefficient of friction for ice/rock interfaces varies from 0.18 and 0.42, and Barton and Choubey (1977) showed that values for rock/rock interfaces, such as those between rock/joint surfaces, are somewhat greater. Voigt and Faust (1982) proposed that water and steam pressures generated from melted ice and snow due to frictional heating at the base of the falling debris may reduce the coefficient of friction. Figure 10 is a reproduction of a graph by Evans et al. (1989). It compares the logarithms of mobility and volume of rock avalanches that occurred in glacial and nonglacial environments, and shows that for rock avalanches of similar volume, those that occurred in glacial environments generally travelled farther (i.e., reflecting a smaller fahrboeschung or H/L ratio). The data for the Kshwan Glacier rock avalanche (2 million $m^3$, H/L=0.31) are consistent with events that occurred in glacial environments.

***Figure 8.*** *One of the largest debris blocks along the perimeter of the debris lobe. Person for scale in lower left centre of photo.*

***Figure 9.*** *Southern debris levee at the centre of Kshwan Glacier.*

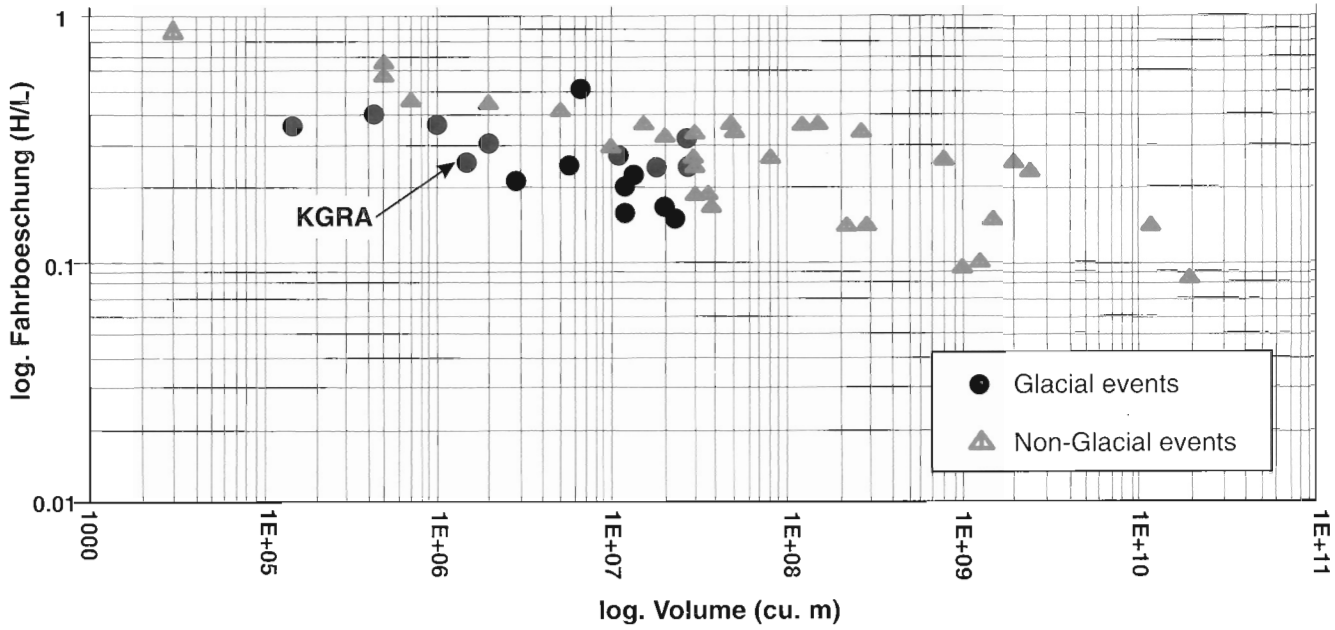


***Figure 10.*** *Plot of mobility (log. Fahrboeschung H/L) versus volume (log. volume) of rock avalanches in glacial and nonglacial environments. Data for the graph was taken from Clague and Evans (1988) for "glacial" events, and from Scheidegger (1973) for "nonglacial" events. The arrow points to the data point for the Kshwan Glacier rock avalanche (KGRA).*

## CONCLUSIONS

Major mechanisms contributing to slope failure in the Kshwan Glacier rock avalanche were:

1. glacial undercutting by the Kshwan Glacier and tributary glaciers which resulted in the oversteepening and exposure of dip-slope joint surfaces at the base of the impending failure surface.
2. debuttressing of the mountain slope by down-wasting of supporting glacial masses.

The observations made on the Kshwan Glacier rock avalanche suggest that the potential is high for catastrophic rock avalanches in the oversteepened, outlying glacial valleys radiating from icefields such as the Cambria. Encroaching human activity, such as mining exploration, recreation, and settlement into recently deglaciated areas, may be severely impacted by the occurrence of unpredicted and rapid slope failure. This highlights the need for careful site investigation prior to exploitation. An understanding of the operative mechanisms helps to identify areas of potential hazard, which are most likely to be where glaciers have carved steep valleys into the underlying bedrock, then retreated, and where local discontinuities are subparallel to valley walls.

## ACKNOWLEDGMENTS

The author would like to acknowledge Charlie Greig of the Geological Survey of Canada, who suggested the project, edited the manuscript and arranged for drafting. Also thanked are Hans Smit, Dave Cawood, and Kate Bull of Lac Minerals Ltd., for their support. Thanks are also due to Marc Pritchard of Klohn Crippen for comments on project structure, to Darwin Green and Claire Floriet for assistance in the field, to Rob Thorne of Vancouver Island Helicopters for his expert flying, to Ted Clarke for reproducing photographs, to Peter Mustard for review of the final copy, to Lindsie Nicholson for drafting figures, and to Bev Vanlier for proof reading. Particular thanks goes to my thesis advisor, K. Wayne Savigny, for his help and insight.

## REFERENCES

**Barton, N. and Choubey, V.**
1977: The shear strength of rock joints in theory and practise; Rock Mechanics, v. 10, p. 1-54.

**Budd, W.F., Keage, P.L., and Blundy, N.A.**
1979: Empirical studies of ice sliding; Journal of Glaciology, v. 23, p. 157-169.

**Clague, J.J. and Evans, S.G.**
1988: Catastrophic rock avalanches in glacial environments, in Landslides, (ed.) C. Bonnard; Proceedings, 5th International Symposium of Landslides, Lausanne, v. 2, p. 1153-1159.

**Evans, S.G., Clague, J.J., Woodsworth, G.J., and Hungr, O.**
1989: The Pandemonium Creek rock avalanche, British Columbia; Canadian Geotechnical Journal, v. 26, p. 427-446.

**Evans, S.G. and Clague, J.J.**
1990: Reconnaissance observations on the Tim Williams Glacier rock avalanche, near Stewart, British Columbia; in Current Research, Part E; Geological Survey of Canada, Paper 90-1E, p. 351-354.

**Greig, C.J., Anderson, R.G., Daubeny, P.H., Bull, K.F., and Hinderman, T.K.**
1994: Geology of the Cambria Icefield: regional setting for Red Mountain gold deposit, northwestern British Columbia; in Current Research 1994-A; Geological Survey of Canada, p. 45-56.

**Greig, C.J., McNicoll, V.J., Anderson, R.G., Daubeny, P.H., Harakal, J.E., and Runkle, D.**
1995: New K-Ar and U-Pb dates for the Cambria Icefield area, northwestern British Columbia; in Current Research 1995-A; Geological Survey of Canada, p. 97-103.

**Hancox, G.T., Chinn, T.J., and McSaveney, M.J.**
1991: Mt. Cook Rock Avalanche, 14 December, 1991; Immediate Report, DSIR Geology and Geophysics, File Reference H36/942, Project 361.110, Christchurch, New Zealand.

**Heim, A.**
1932: Bergsturz und Menschenleben; Bitech Publishers, Vancouver, British Columbia, 1989. (English translation by Nigel Skermer).

**Mauthner, T.E.**
1995: Observations and preliminary assessment of the Kshwan Glacier rock avalanche near Stewart in northwestern British Columbia; BASc. thesis, Department of Geological Engineering, University of British Columbia, Vancouver, British Columbia, 41 p.

**McSaveney, M.J.**
1978: Sherman Glacier rock avalanche, Alaska, U.S.A.; in Natural Phenomena, Elsevier, Amsterdam, The Netherlands, p. 197-258.

**Scheidegger, A.E.**
1973: On the prediction of the reach and velocity of catastrophic landslides; Rock Mechanics, v. 5, p. 231-273.

**Shreve, R.L.**
1966: The Sherman Landslide, Alaska; Science, v. 154, p. 1639-1643.

**Twidale, G.R.**
1973: On the origin of sheet jointing; Rock Mechanics, v. 5, p. 163-187.

**Voight, B. and Faust, C.**
1982: Frictional heat and strength loss in some rapid landslides; Geotechnique, v. 33, p. 243-273.

Geological Survey of Canada Project 840046-XM

# Bedrock geology of north-central and west-central Nass River map area, British Columbia

Carol A. Evenchick and Peter S. Mustard[1]
GSC Victoria, Vancouver

*Evenchick, C.A. and Mustard, P.S., 1996: Bedrock geology of north-central and west-central Nass River map area, British Columbia; in Current Research 1996-A; Geological Survey of Canada, p. 45-55.*

**Abstract:** Jurassic (and earliest Cretaceous(?)) Bowser Lake Group rocks underlie more than 90% of north-central and west-central Nass River map area. Tertiary, Quaternary(?), and Recent igneous rocks comprise 10% of bedrock.

Bowser Lake Group is composed entirely of turbidites. They are commonly lithic to arkosic arenites; minor variations include thick mud-rich intervals, sandstone with detrital muscovite, and turbidites derived from a volcanic source. The structure is dominated by chevron-style parallel folds which accommodated significant horizontal shortening. In the northeast, folds are upright, trend northwest, and have gentle plunge. In the southwest, folds are gently inclined (varying to overturned), trend northeast, and verge southeast. Interference between the two orientations is apparent in the southwest.

Hyder pluton is composed of massive biotite hornblende granite and quartz monzonite with peraluminous and K-feldspar megacrystic phases. Extrusive rocks are erosional remnants of upper Tertiary or Quaternary and Recent basaltic flows.

**Résumé :** Les roches du Groupe de Bowser Lake du Jurassique (et du Crétacé initial(?)) couvrent plus de 90 % des secteurs centre nord et centre ouest de la région cartographique de la rivière Nass. Les lithologies ignées tertiaires, quaternaires(?) et holocènes comprennent 10 % de roche de socle.

Le Groupe de Bowser Lake ne contient que des turbidites, surtout des arénites lithiques à arkosiques; les variations mineures incluent des intervalles puissants riches en boue, des grès à muscovite détritique et des turbidites d'origine volcanique. Le style structural se caractérise par des plis parallèles en chevron, résultant d'un raccourcissement horizontal important. Dans le nord-est, les plis sont droits, d'orientation nord-ouest et à plongement faible. Dans le sud-ouest, ils sont légèrement inclinés (et peuvent être jusqu'à déversés), d'orientation nord-est et à vergence sud-est. L'interférence entre les deux orientations est apparente dans le sud-ouest.

Le pluton de Hyder est composé de granite massif à biotite et hornblende ainsi que de monzonite quartzique incluant des phases mégacristallines hyperalumineuses et à feldspaths potassiques. Les roches extrusives sont des lambeaux d'érosion du Tertiaire supérieur ou des coulées basaltiques du Quaternaire et de l'Holocène.

[1] Earth Sciences, Simon Fraser University, Burnaby, British Columbia V5A 1S6

## INTRODUCTION

Nass River map area (103P, Fig. 1) is the site of a new regional mapping project in the Cordillera. Rationale for the project is the lack of a regional (1:250 000) geological map and corresponding lack of information about the stratigraphy and structure and their relationships to other elements within the broader framework of the Cordillera. The northwest corner of the map area encompasses a region of precious and base metal exploration and production, and therefore has been studied at several levels of detail since the early 1900s. The remainder of the area, however, has been mapped little beyond McEvoy's 1893 survey along major waterways (McEvoy, 1894, 1912); consequently the relationship of strata in the northwest to elsewhere is poorly understood. The northwest corner is also the junction of a seismic experiment (ACCRETE) along the western boundary of Nass River map area with a proposed Lithoprobe project (SNORCLE) across the northern Canadian Cordillera.

In the current project, regional bedrock and surficial mapping surveys will be integrated with associated thematic studies, including stratigraphy, sedimentology, structure, geochronology, mineral deposit studies, geophysical studies, neotectonic studies, and environmental studies.

In 1995 the objective was to assemble a working team and to begin bedrock mapping; other elements of the project will begin in 1996. The area mapped (Fig. 1) was chosen with the aim of crossing a broad spectrum of geology, and of working outward from the most recently mapped areas: Cambria Icefield region (Fig. 2; Greig et al., 1994), and Bowser Lake map area (Evenchick et al., 1992). G.J. Woodsworth began studying young volcanic rocks as part of a neotectonics study, and D.J. Alldrick spent two weeks examining mineralized rocks in central and west Anyox pendant and the Georgie River mine.

## REGIONAL GEOLOGICAL FRAMEWORK AND PREVIOUS WORK – NASS RIVER AREA

Most bedrock in Nass River is divided into three broad groupings (Fig. 1): 1) Triassic and Lower to Middle Jurassic rocks of Stikinia; 2) Middle Jurassic to Lower Cretaceous rocks of the Bowser basin; and 3) Mesozoic and Cenozoic granitoid rocks of the Coast Belt. Minor constituents are Cretaceous rocks of the Skeena Group, upper Tertiary or Quaternary and Recent volcanic rocks, and metamorphic rocks of unknown age.

### *Stikinia*

Triassic and Lower to Middle Jurassic stratified rocks of Stikinia constitute the last volcanic arcs of the suspect terrane Stikinia before it amalgamated with the western margin of North America. They are widespread around the Bowser basin, and in detail exhibit a complex volcanogenic stratigraphy. Triassic strata are mafic, intermediate, and bimodal

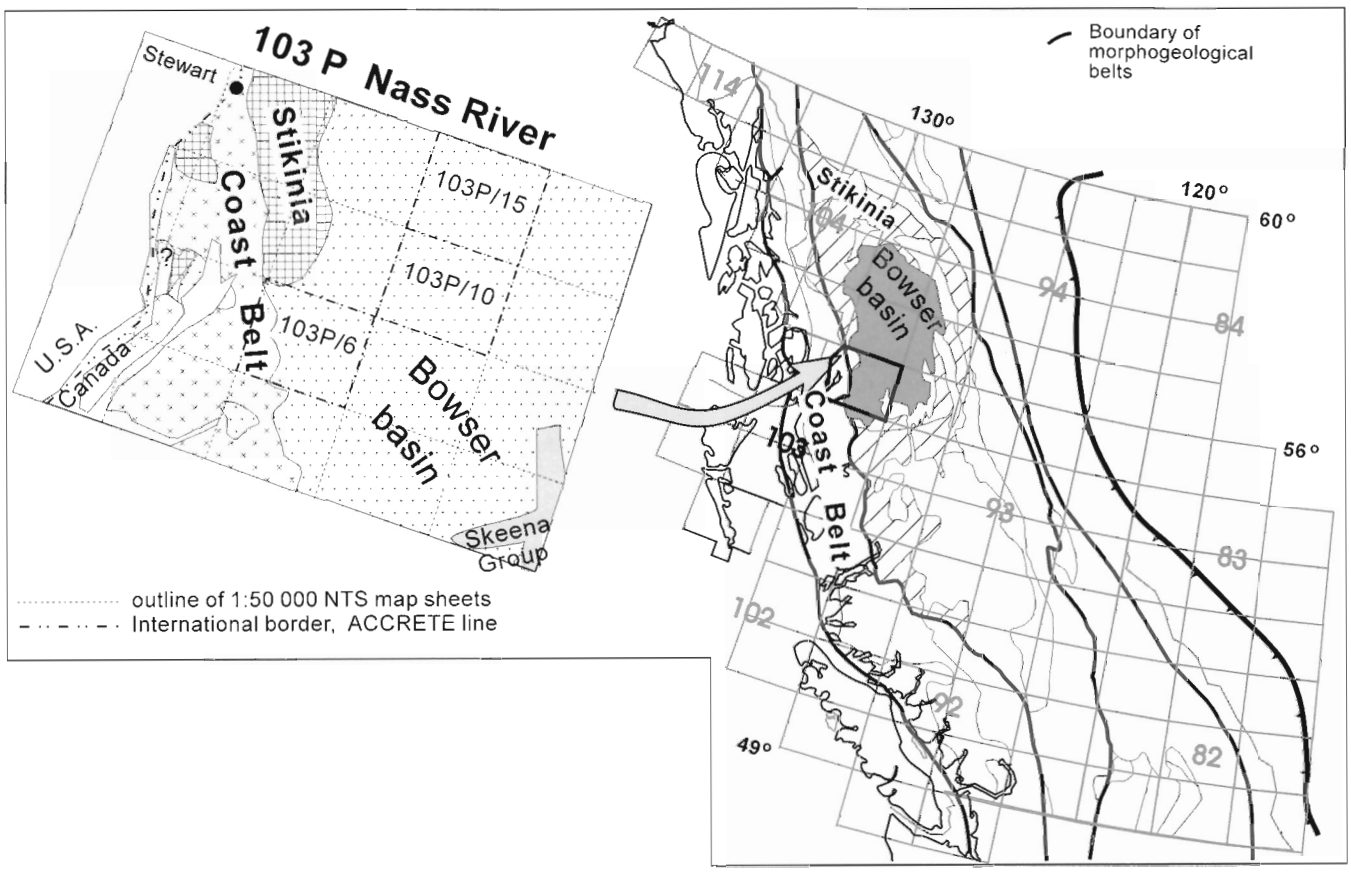

volcanic rocks and medium- and fine-grained clastic rocks; Jurassic strata comprise bimodal to felsic volcanic rocks, coarse- to fine-grained volcanic clastic, and sedimentary rocks (Anderson, 1993; and references therein).

In Nass River map area, Jurassic volcanic and related clastic strata occur in the northwest quadrant as a structural culmination bounded on the east by clastic rocks of the Bowser basin, and on the west by plutonic rock of the Coast Belt. A long history of examination of these rocks follows a pattern of dividing sedimentary and volcanic units into stratigraphic units, and subsequent recognition that such units have little stratigraphic significance (McConnell, 1913; Hanson, 1935; Grove, 1986; Dawson and Alldrick, 1986; Greig et al., 1994). In general, the strata comprise a Lower to Middle Jurassic succession of mafic to felsic submarine volcanic rocks intercalated with sedimentary rocks derived from the volcanics. Most recently, Dawson and Alldrick (1986) divided strata between Alice Arm and Cambria Icefield into five stratigraphic units; three dominantly sedimentary units are separated by two dominantly volcanic units. Farther north, Greig et al. (1994) divided Hazelton Group around Cambria Icefield into ten lithological units ranging from mafic to felsic volcanic rocks, and related clastic rocks. Minor Triassic volcanic and clastic rocks occur near Kinskuch Lake and northern Cambria Icefield (Greig, 1992; Greig et al., 1994).

### *Bowser basin*

When Stikinia amalgamated with North America, the northern part became the site of widespread deposition of detritus from the north, east, and south. The resulting depocenter, apparently open to the west, is called Bowser basin, and strata deposited in the basin are called Bowser Lake Group (Tipper and Richards, 1976). In the northern two-thirds of the basin the major source was the Cache Creek terrane, and in the south the source included an uplifted part of Stikinia called the Skeena Arch. The majority of the Bowser Lake Group is Middle Jurassic to latest Jurassic or earliest Cretaceous in age, although one area contains strata as young as mid-Cretaceous (Tipper and Richards, 1976; Evenchick and Thorkelson, 1993 and references therein). In general, Jurassic to earliest Cretaceous strata in the basin record southwest progradation

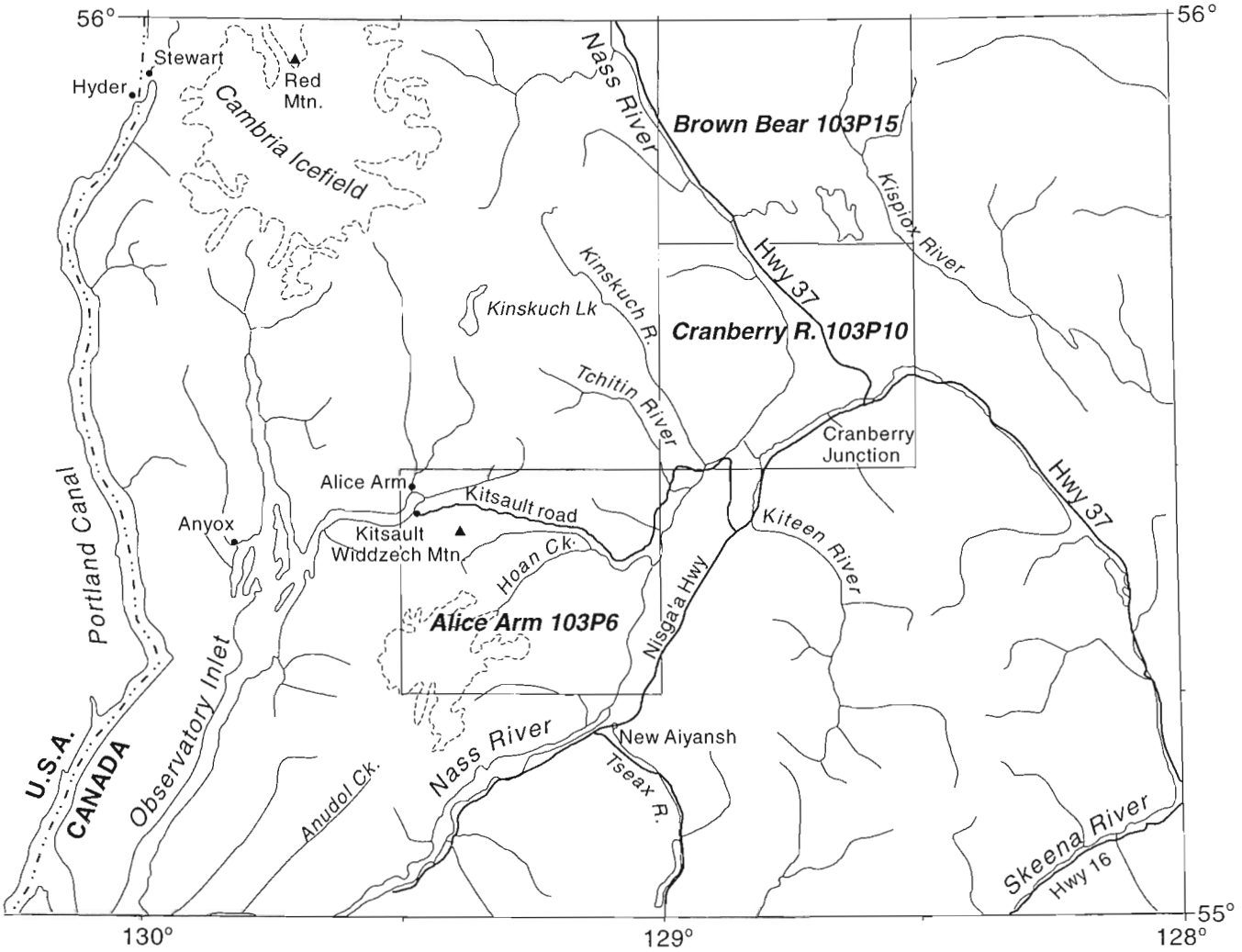


***Figure 2.*** *Location of geographic features in Nass River map area referred to in text.*

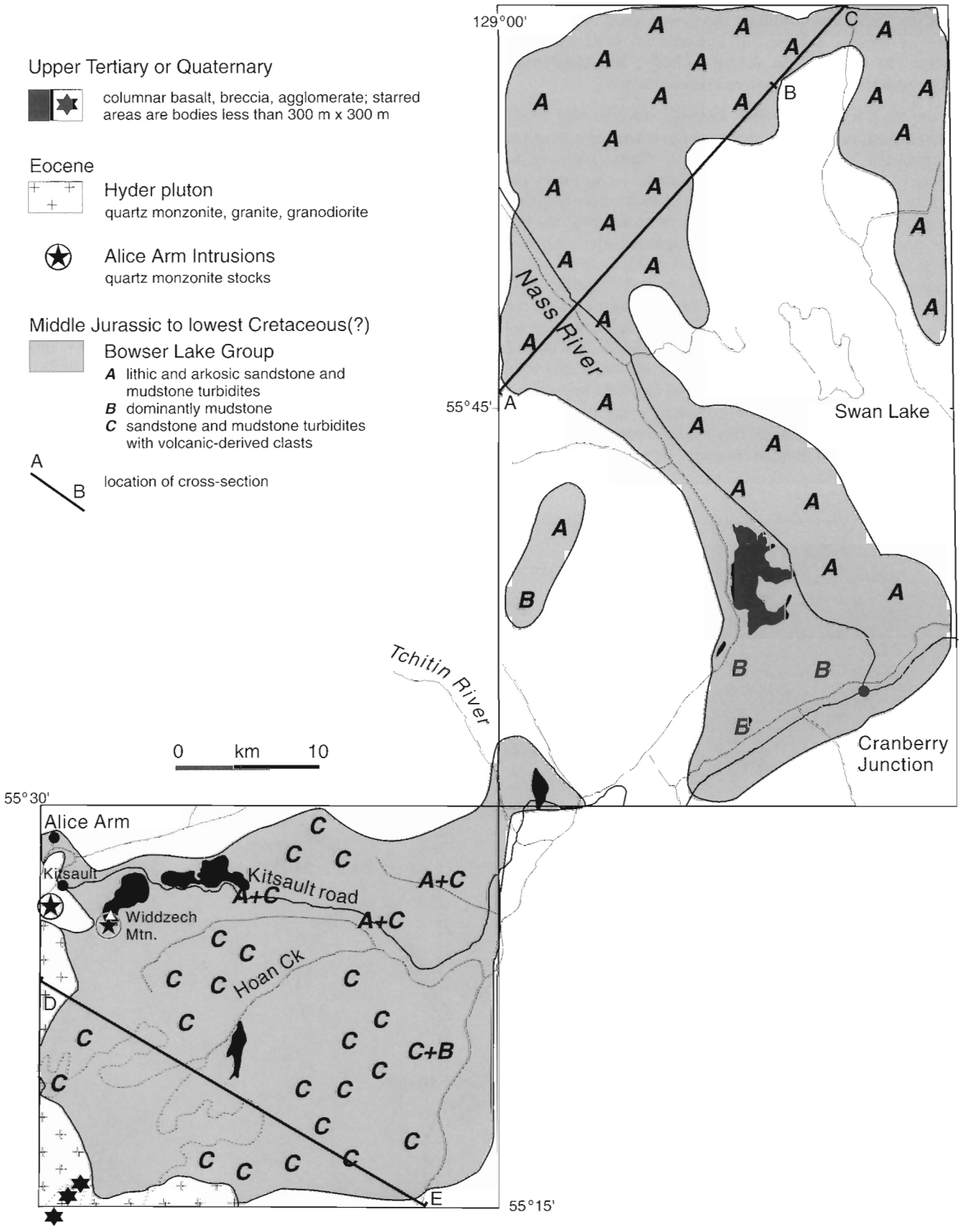


***Figure 3.*** *Sketch map of geology in map areas 103P/6,10,15, and location of cross-sections (Fig. 9).*

of shallow marine and deltaic strata over continental slope and rise deposits; mid-Cretaceous strata were deposited within a subsequent fold and thrust belt (Evenchick, 1994). The present distribution of lithofacies assemblages is a result of this depositional history as well as contractional structures. Bowser Lake Group immediately north of Nass River map area is mainly turbidites (Evenchick et al., 1992); those east and south are undivided Bowser Lake Group (Woodsworth et al., 1985; Richards et al., 1996). Bowser Lake Group in Nass River map area has only been examined in cursory fashion, and only within 10 km of the Hazelton Group or Coast Belt (Grove, 1986; Greig et al., 1994). Grove (1986) referred to Upper Jurassic clastic rocks in western Nass River area as Nass Formation of the Hazelton Group (after McConnell, 1913; Hanson, 1935).

### *Skeena Fold Belt*

Cretaceous and older strata in the region were deformed in Early to latest Cretaceous time to form the Skeena Fold Belt (Evenchick, 1991). It is characterized by northeast-verging folds and thrust faults; folds in thinly layered rocks are less than one, to several kilometres in wavelength, gently plunging, and upright or overturned to the northeast. Northeast-trending folds are present locally on the west side of the fold belt. The fold belt is thin-skinned, involved Stikinia, and accommodated at least 50% (165 km) northeastward shortening. Fold trends in northwest Nass River area are shown by Carter and Grove (1972), Grove (1986), and Greig et al. (1994); fold trends and structural style are unknown in the remaining two-thirds of the map area.

### *Plutonic rocks*

Plutonic rocks in the region comprise: 1) Mesozoic plutons which are part of the magmatic arcs associated with Stikinian volcanism; 2) Cenozoic plutons in the eastern Coast Plutonic Complex; and 3) Cenozoic stocks and dykes east of the Coast Plutonic Complex. In Nass River map area most dated plutonic rocks are Eocene (Carter, 1981). About twenty K-Ar age determinations from 49 to 55 Ma have been made in and around porphyry Cu and Mo deposits in the Alice Arm area, southwest of New Aiyansh, and in the Kitsault River area (Carter, 1981; recalculated using decay constants of Steiger and Jäger, 1977). The deposits are in porphyritic quartz monzonite stocks of the Alice Arm Intrusions, which intrude Hazelton and Bowser Lake groups. In Cambria Icefield area several stocks, the Bitter Creek pluton, and Portland Canal dyke swarm are 48-50 Ma (K-Ar and U-Pb methods; Greig et al., 1995; Green et al., 1995). The east side of the Coast Plutonic Complex comprises a composite plutonic body of mainly quartz monzonite, granodiorite, and granite called Hyder pluton (Grove, 1986). Six K-Ar age determinations range from 47-52 Ma (Smith, 1977; recalculated using decay constants of Steiger and Jäger, 1977; Carter, 1981). Eocene intrusions in the Stewart region comprise a suite of compositionally similar, coeval rocks, informally called Hyder plutonic suite, which is distinguished from Mesozoic intrusions by a greater proportion of biotite and quartz (Anderson, 1989). The Goldslide Intrusions in northwest Cambria icefield are the only Early Jurassic plutons (Greig et al., 1995, and references therein).

Youngest strata in the region are late Tertiary or Quaternary and Recent basaltic to andesitic lava flows. They occur 5-15 km east-southeast of Alice Arm, near Cranberry Junction, Tchitin River, and Mt. Priestly, and 20 km northwest and 25 km west-northwest of New Aiyansh (Fig. 2, 3). Most occur in broad valleys at 200-750 m elevation. Six remnants in southwest 103P/6 appear to have filled paleovalleys now at 500-1000 m and 1200-1400 m elevation (described below). The Recent flow is in Tseax and Nass river valleys. Distribution of young volcanic rocks was defined by McEvoy (1894, 1912), Hanson (1935), Sutherland Brown (1969), and Carter and Grove (1972). New localities are described in this report. Descriptions of the flows southeast of Alice Arm were given by Hanson (1935), Drummond (1961), and Carter (1964). Aiyansh lava flow was mapped and described in detail by Sutherland Brown (1969). The flows are flat-lying, several metres to 100 m thick, and columnar basalt is common everywhere except in the Aiyansh flow. Most are pre- or syn-Pleistocene as evidenced by glacial striations and erratics. Whole-rock K-Ar ages on Alice Arm flows are 0.62 ± 0.6, and 1.6 ± 0.8 Ma (Carter, 1981). The Aiyansh flow is 200 ± 130 years old (Sutherland Brown, 1969).

## GEOLOGY IN ALICE ARM, CRANBERRY RIVER, AND BROWN BEAR MAP AREAS (103P/6, 10, 15)

Most of the bedrock in the Nass Valley is covered by an extensive blanket of surficial deposits. Bedrock-cored drumlins afford rare, poor bedrock exposure except where transected by roads; roadcuts and the Nass River account for most of the less than 10% of bedrock exposure in Brown Bear (103P/15) map area. Cranberry River area (103P/10) has similarly meagre bedrock exposure, but rare high treed ridges in the southwest have large continuous outcrop. Alice Arm area (103P/6) has excellent exposure in alpine areas, along shoreline in Alice Arm, and on the Kitsault road.

### *Stratigraphy*

Most bedrock is turbidites of the Bowser Lake Group (Fig. 3). Less than 10% is Eocene granitoid rocks of the Hyder pluton, late Tertiary or Quaternary volcanic rocks, and dykes.

#### Bowser Lake Group

*Cranberry River and Brown Bear map areas*

Rocks in Cranberry River and Brown Bear map areas are predominantly intercalated medium grey sandstone and dark grey siltstone to silt-rich mudstone. A monotonous single map unit of bedded sandstone and mudstone underlies more than 95% of the area and continues into immediately adjacent map areas. Its thickness is difficult to estimate due to tight folding,

large areas of poor exposure, and the possibility of repetition by unrecognized thrust faults. We estimate a minimum thickness of 1500 m. Massive to poorly stratified units of dark grey silt-rich mudstone tens to hundreds of metres thick occur in a few places. In the southwest part of Cranberry River area it forms a persistent unit probably several hundred metres thick which appears to grade vertically and laterally(?) into the bedded sandstone unit.

Sandstone occurs as thin to thick beds of medium- to fine-grained (less commonly coarse grained) lithic to arkosic arenite. Beds are laterally persistent sheets which are traceable for hundreds of metres in the few areas of continuous exposure. Most beds contain a massive, nongraded to subtly normal graded base. Angular rip-up clasts of mudstone are common in the lower part of many sandstones, especially medium- to thick-bedded ones. Most sandstone beds are either entirely massive or change in the upper 10-20% to faintly laminated to very thin bedded, fine grained sandstone which either grades up to, or is sharply capped by, siltstone or silt-rich dark grey mudstone. Less commonly, upper parts of sandstone beds show gradation in size and stratification types typical of Bouma turbidite sequences with horizontal lamination or thin beds of fine grained sandstone changing upward to a layer of ripple or cross-ripple stratification, or to convolutely deformed bedding. The upper parts of these beds tend to be laminated, very fine grained sandstone or coarse siltstone which either grades subtly upward into, or is sharply capped by, several to tens of centimetres of dark grey silt-rich mudstone. Comminuted carbonaceous plant fragments are common in some capping mudstone. Using Bouma turbidite sequence terminology, $T_{ABE}$ or $T_{AE}$ turbidites are most common, with less common $T_{ABCE}$ and rare $T_{ABCDE}$ turbidites.

Paleoflow directions were determined from flutes, grooves and chevron marks on the bases of sandstone beds (Fig. 4), and from ripple cross-stratification within sandstones where three-dimensional orientations were apparent. Several hundred measurements from several dozen sites scattered throughout the map areas were corrected for folding and tilting of bedding. A strong and persistent southwest to west paleoflow trend is apparent. Synsedimentary folding is common locally, including sheath folds and convolute folded intervals several metres thick; fold vergence is consistently towards the southwest. Collectively, the paleocurrent data suggest a broadly southwest dipping paleoslope and an eastern source area for all sediments.

All sandstones are interpreted as sediment gravity flow deposits, either turbidites or possibly density modified grain flows for some of the massive thick-bedded sandstones. No features indicating sub-wave base conditions were observed, and combined with the scarcity of body or traces fossils and the abundance of slump structures, a deep shelf or slope depositional environment is inferred.

*Alice Arm map area*

Sedimentary rocks are dominated by intercalated turbidite sandstone and mudstone as described above. In the east they comprise lithic arenites and silt-rich mudstones similar to those in Cranberry River and Brown Bear map areas. Paleocurrent data also indicate flow towards the west or southwest. In the western two-thirds of the map area sandstone and mudstone turbidite successions also dominate (Fig. 5), but in extensive ridge exposures above treeline the sandstones contain a notable component of coarse grained angular feldspar and quartz grains, many subhedral to euhedral. Some mudstone in this succession is white-weathering and highly siliceous. We interpret these rocks as products of first cycle erosion of a nearby volcanic source area. The siliceous mudstone is probably reworked tuffaceous material. Paleocurrents indicate that they may be partly derived from a western volcanic source area (though possibly an inactive remnant of a volcanic arc as there is no evidence of active volcanism associated with these rocks). This volcaniclastic succession is probably greater than 1500 m thick (see cross-section and Fig. 5). The relationship of this unit to the more typical Bowser Lake Group is not well constrained. There appears to be a higher proportion of volcanic-derived strata in alpine regions southwest and north of the Kitsault road. Gentle

***Figure 4.*** *View northwest to grooves on bases of medium grained sandstone turbidites in Cranberry River area.*

***Figure 5.*** *View northeast of thick turbidite succession in Alice Arm area; width of field in background is about 1 km; in foreground is 15 m.*

northeasterly plunge of folds south of the road, and moderate southwest plunge of folds north of the road suggest that rocks in the alpine areas are stratigraphically lower than those on the road. There is probably a thick gradational contact from turbidites with some volcanic component into typical lithic arenite successions of the Bowser Lake Group which are more common on the road. Precise definition of the stratigraphic relationship of the volcaniclastic succession to the main Bowser Lake Group succession to the east is also hampered by the abundant folds and poor exposure in the eastern part of the map area. Until either age or stratigraphic position are well constrained, possible interpretations for these rocks include: 1) that they represent vertical and/or lateral transitions from west-derived clastics of the Hazelton Group upward and/or eastward into more typical Bowser Lake Group; 2) apparent intertonguing is a result of structural relief; 3) they represent a part of the Bowser Lake Group which is not a transition from the Hazelton Group, but is derived in part from a volcanic source (similar to Bowser Lake Group of the southern basin which is derived from the Skeena Arch). Continued mapping of this unit to the north and southeast should provide better constraints on its stratigraphic position and relationship to typical Bowser Lake Group. Strata in the vicinity of Alice Arm are fine grained sandstone and siltstone and may constitute a separate map unit with further study.

### Hyder pluton

Southwestern Alice Arm area is underlain by Hyder pluton. It is leucocratic, fresh, equigranular to porphyritic granite, granodiorite, and quartz monzonite with 5 to 15% fresh biotite and hornblende, and <1% megascopic sphene. It is massive and cut by finer grained granitoid dykes of similar composition, aplite dykes, lamprophyre, and diorite dykes. The pluton has sharp intrusive contacts with clastic rocks, and dykes are moderately abundant within 1 km of the contact. Contact metamorphism is apparent within 1.5 km of the contact, as is a notable change in structural style. Hornfelsed fine grained clastic rocks have a pink tinge which is assumed to be biotite; mesoscopic andalusite porphyroblasts occur on the ridge 15 km south of Kitsault. Carter (1964) noted a biotite isograd 900-1800 m from the pluton about 5 km south of Kitsault. K-feldspar megacrysts and peraluminous (garnet-bearing) granite on the west shore of Observatory Inlet are indications that the Hyder pluton may be divisible into mappable phases.

### Dykes

Eighty-five dykes were observed in the study area (with the exception of those marginal to the Hyder pluton); all but four occur in Alice Arm map area. Dykes in sedimentary rocks have strong preferred orientation parallel with bedding, or rarely, cleavage (Fig. 6). Two main types are 1) medium grained and white-weathering, and 2) fine grained and dark-weathering. Medium grained, white-weathering dykes are massive granite or quartz monzonite similar to Hyder pluton. They constitute a dense network of dykes of various orientations emanating from the pluton within 500 m of the contact (Fig. 7); dykes farther east are parallel with bedding. Fine- and medium-grained varieties occur within the Hyder pluton. Granitoid dykes are commonly 50 cm to several metres thick, but locally up to 100 m thick.

Fine grained, dark-weathering dykes are diorite and lamprophyre. They are green-brown-weathering, aphanitic to very fine grained, and some contain mafic or feldspar phenocrysts. Most are 40 to 80 cm thick. In Hyder pluton they are the youngest igneous rocks. Two localities of rusty/white-weathering dykes occur 500 and 800 m from the volcanic flow east of Tchitin River. The dykes have about 40-60% pyroxene phenocrysts in matrix of fine grained plagioclase crystals, and are 30 cm to 1 m thick.

### Late Tertiary or Quaternary volcanic rocks

Young flows of columnar basalt occur in broad valleys at relatively low elevation, and appear to have filled smaller paleovalleys at higher elevation. Flows in broad valleys include those near Cranberry Junction, Tchitin River, and Alice Arm. Flows in higher paleovalleys occur in the southwest quadrant of Alice Arm map area.

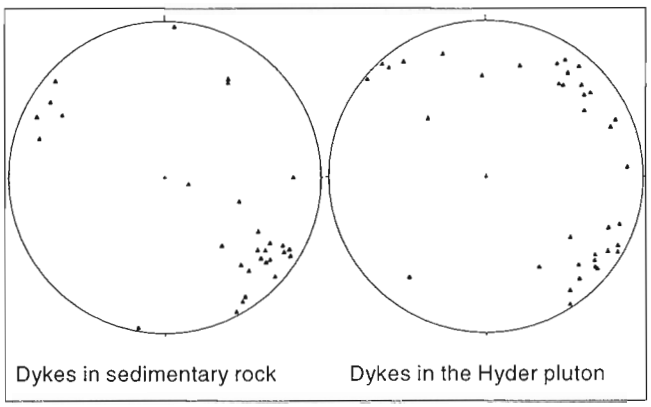


***Figure 6.*** *Lower hemisphere projections of poles to dykes (mostly in Alice Arm area).*

***Figure 7.*** *View north of dykes emanating from the Hyder pluton into clastic rock of the Bowser Lake Group; width of view is 800 m.*

Northwest of Cranberry Junction are two remnants of a flow which once covered at least 20 km$^2$. The largest body is east of Nass River between 200 and 330 m elevation; west of the river is a body about 300 m$^2$. The flow consists of grey-weathering columnar basalt with phenocrysts of feldspar to 15 mm, in an aphanitic, locally vesicular matrix. Individual flows are up to 50 m thick.

Between Tchitin and Kinskuch rivers is a lava flow about 2 km$^2$ whose base is between 200 and 220 m elevation. It is similar to the Cranberry Junction flow in weathering character and composition, and includes rare phenocrysts of olivine or pyroxene up to 1 mm diameter.

Lava flows east of Alice Arm cover about 12 km$^2$. Their base is at 750 to 800 m elevation and thickness about 150 m. The largest body is at Widdzech Mountain, which is described by Carter (1964) and in detail by Drummond (1961) as trachyte and basalt with trachytic and porphyritic textures. Phenocrysts of plagioclase (Carter, 1964) or sanidine (Drummond, 1961) occur in a fine grained matrix of clinopyroxene, olivine, and magnetite.

*Figure 8. View southwest of erosional remnants of columnar basalt on the northwest side of Anudol valley; width of view is 1 km.*

On the south side of Hoan Creek is a north-trending belt of volcanic and clastic rocks 3 km long and up to 900 m wide which defines a paleovalley with at least 200 m of relief across individual points, and 450 m relief (between 550 m and 1000 m elevation) along its length. It is composed of poorly lithified clastic rocks, agglomerate, and columnar basalt.

Southwest of the crest of the icefield at the head of Hoan and Anudol creeks are five erosional remnants of volcanic rock. At the head of the valley is a 200 x 300 m nunatak revealed by ablation of the icefield since 1982 (when high level airphotos were flown). It is at 1460 to 1500 m elevation, and composed of agglomerate and columnar basalt; the base is not exposed. Two kilometres to the southwest is a remnant of similar rock 200 m x 600 m resting nonconformably on Hyder pluton on the northwest wall of the valley between 1200 and 1350 m elevation. The basal contact dips about 20° southeast, into the main valley. Another 3 km southwest (in 103P/3) are three erosional fragments of what, from a distance, appears to mainly columnar basalt (Fig. 8). They occur in a hanging valley on the northwest side of the Anudol valley, between 1200 and 1350 m elevation and each is about 200 m diameter.

## *Structural geology*

The study area encompasses three regions of strikingly different structural geometry. The major differences are expressed in cross-sections and stereonets of Figures 9 and 10. Most of the area is composed of parallel folds with wavelengths about 500 to 1500 m, but those in the northeast trend northwest whereas folds in the southwest trend northeast; the boundary is near the border of Alice Arm and Cranberry River map

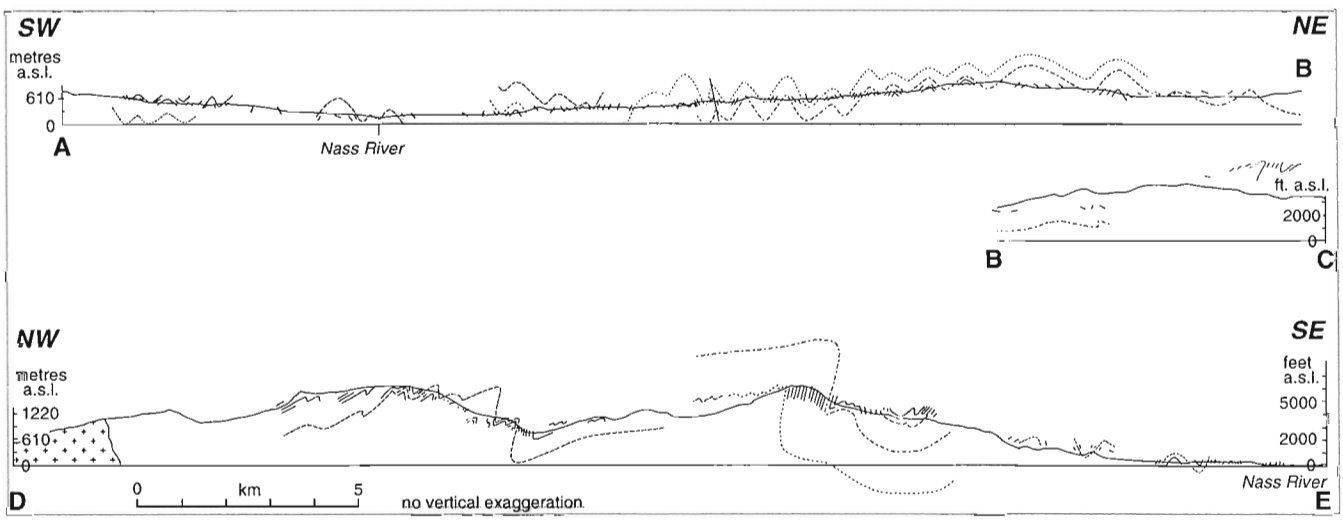


*Figure 9. Cross-sections of study area, locations are shown in Figure 3. Small solid lines are bedding measurements. Broken lines are form-lines of large scale structure interpreted from outcrop observations and bedding measurements.*

areas. The third major type of structural geometry is near the Hyder pluton, where folds are similar-style, and wavelength is as small as decimetres.

### Cranberry River and Brown Bear areas

The structure is dominated by chevron-style parallel folds which accommodated significant horizontal shortening (Fig. 9). The folds trend northwest and have gentle plunge, as displayed in domains 1 to 7 of Figure 10. They are generally upright, tight to close "m" folds, repeating the same 1000 m of section across most of the area examined. An exception is in the northeast corner of Brown Bear area where overturned folds which verge consistently to the northeast are well exposed on ridges. Fold hinges are rarely exposed in roadcuts; the few observed folds have faults in the hinge area to accommodate space problems (Fig. 11). Common outcrop features are cleavage parallel with the axial surface (or fanned across axial surfaces), joints perpendicular to fold axes, and abundant polished and grooved bedding surfaces, some with slickensides of fibrous quartz. The latter are inferred to be a result of flexural-slip folding.

### Alice Arm and southwest Cranberry River areas

Structure in Alice Arm area (except near Hyder pluton and Alice Arm) and southwesternmost Cranberry River area is dominated by chevron-style parallel folds which trend northeast and are upright to overturned to the southeast (Fig. 10, domains 8-13,15). They consistently verge to the southeast

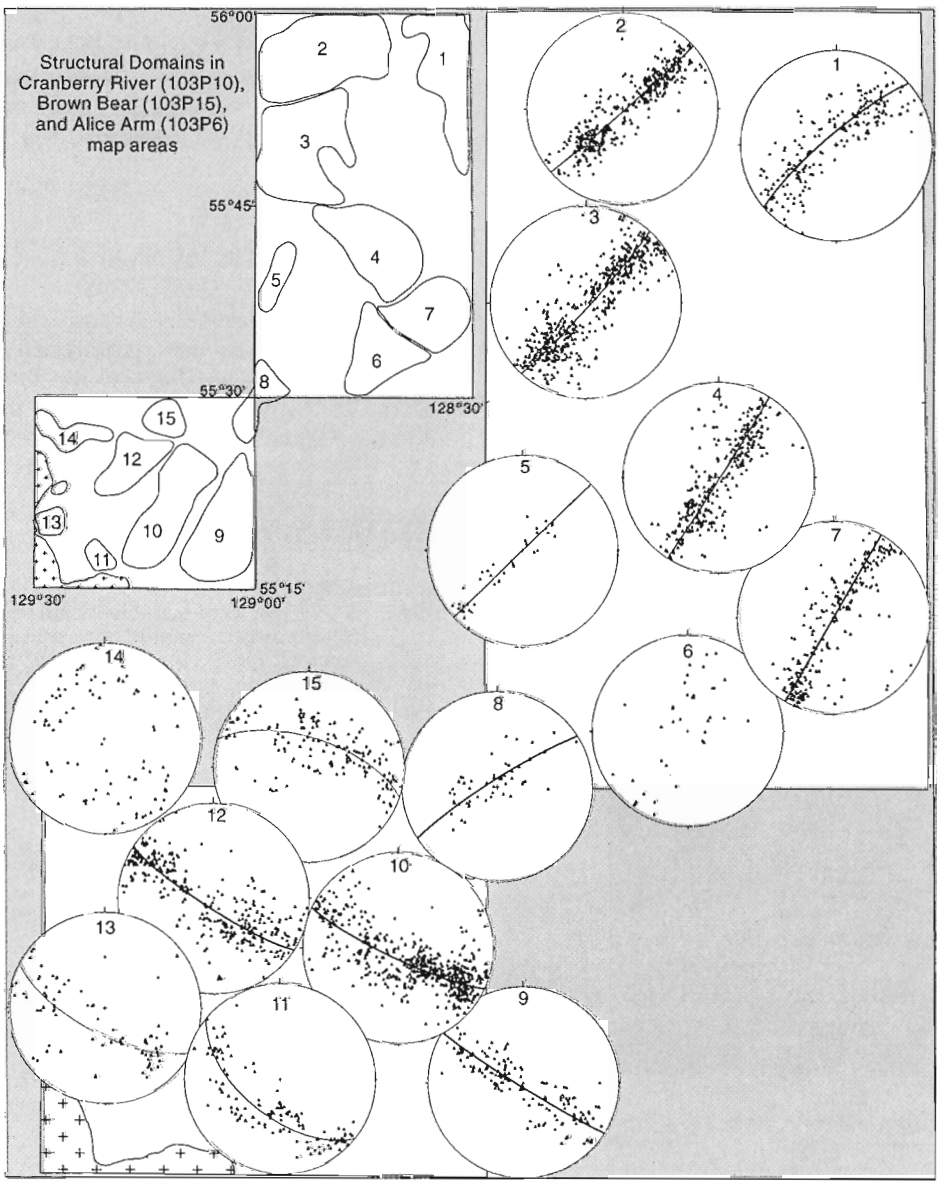


***Figure 10.*** *Map of structural domains with stereonets. Stereonets are lower hemisphere projections of poles to bedding, plotted on Schmidt nets.*

*Figure 11. View southeast of fold hinge in northern Cranberry River area.*

*Figure 12. View northeast of southeast verging structures in Alice Arm area; width is 1 km.*

*Figure 13. Ductile, rootless structures 1 km from the Hyder pluton.*

(Fig. 9, 12). Most are 300 to 800 m in wavelength, but parasitic structures are locally as small as 10 m in wavelength, and one major fold of several kilometres wavelength has an overturned limb more than 1000 m thick (Fig. 5). Locally, gently dipping limbs are warped by northeast-trending folds, which results in some of the dispersion apparent in poles to bedding in domains 10 and 12. Outcrop features in Alice Arm area are the same as those described for Cranberry River and Brown Bear areas, except that cleavage is not consistently parallel with the axial surface, and it is locally penetrative. Northeast-trending folds occur sporadically on the west side of the Skeena Fold Belt. A speculative explanation for these atypical structures is that they are a result of sinistral oblique convergence on the Cordilleran margin in Early to mid-Cretaceous time (Evenchick, 1995).

### Alice Arm area near the Hyder pluton

Structures within 1.5 km of the Hyder pluton are parallel and similar folds which vary from close to isoclinal and are locally rootless; similar folds are more common near the contact (Fig. 13). Outcrop and larger scale fold interference patterns are common.

## ACKNOWLEDGMENTS

Kris Holm and Chris Huggins provided able assistance in the field. We appreciate the co-operation of John Wheatly, the facilities maintenance foreman for Kitsault, who provided access to the Kitsault mine and to camping facilities in Kitsault. Glenn Woodsworth reviewed the manuscript.

## REFERENCES

**Anderson, R.G.**
1989: A stratigraphic, plutonic, and structural framework for the Iskut River map area, northwestern British Columbia; in Current Research, Part E; Geological Survey of Canada, Paper 89-1E, p. 145-154.
1993: A Mesozoic stratigraphic and plutonic framework for northwestern Stikinia (Iskut River area), northwestern British Columbia, Canada; in Mesozoic Paleogeography of the Western United States-II, (ed.) G. Dunne and K. McDougall; Pacific Section, Society of Economic Paleontologists and Mineralogists, v. 71, p. 477-494.

**Carter, N.C.**
1964: Geology of the Lime Creek area; Minister of Mines and Petroleum Resources, British Columbia, Annual Report 1964, p. 21-41.
1981: Porphyry copper and molybdenum deposits of west-central British Columbia; British Columbia Ministry of Energy, Mines and Petroleum Resources, Bulletin 64, 150 p.

**Carter, N.C. and Grove, E.W. (comp.)**
1972: Geological compilation map of the Stewart, Anyox, Alice Arm, and Terrace areas; British Columbia Department of Mines and Petroleum Resources, Preliminary Map No. 8.

**Dawson, G.L. and Alldrick, D.J.**
1986: Geology and mineral deposits of the Kitsault Valley; in Geological Fieldwork 1985; British Columbia Ministry of Energy, Mines and Petroleum Resources, Paper 1986-1, p. 219-224.

**Drummond, A.D.**
1961: Geology of the Alice Arm molybdenum prospect; MSc. thesis, University of British Columbia, Vancouver, British Columbia, 100 p.

**Evenchick, C.A.**
1991: Geometry, evolution, and tectonic framework of the Skeena Fold Belt, north-central British Columbia; Tectonics, v. 10, p. 527-546.
1994: Depositional history of the northern two-thirds of the Bowser basin and its implications for Jurassic western North American tectonics; Geological Society of America, Abstracts with Programs, v. 26, no. 7, p. A148.
1995: Structural evidence of Early Cretaceous sinistral displacement in the northern Canadian Cordillera?; Geological Association of Canada, Program with Abstracts, p. A30.

**Evenchick, C.A. and Thorkelson, D.J.**
1993: Geology, Spatsizi River, British Columbia (104H); Geological Survey of Canada, Open File 2719, scale 1:250 000.

**Evenchick, C.A., Mustard, P.S., Porter, J.S., and Greig, C.J.**
1992: Regional Jurassic and Cretaceous facies assemblages, and structural geology in Bowser Lake map area (104A), B.C.; Geological Survey of Canada, Open File 2582.

**Green, D., Greig, C.J., and Friedman, R.M.**
1995: Portland Canal dyke swarm, Stewart area, northwestern British Columbia: geological setting, geochronology, and thermal modelling; in Current Research 1995-E; Geological Survey of Canada, p. 47-57.

**Greig, C.J.**
1992: Fieldwork in the Oweegee and Snowslide ranges and Kinskuch Lake area, northwestern British Columbia; in Current Research, Part A; Geological Survey of Canada, Paper 92-1A, p. 145-155.

**Greig, C.J., Anderson, R.G., Daubeny, P.H., Bull, K.F., and Hinderman, T.K.**
1994: Geology of the Cambria Icefield: regional setting for Red Mountain gold deposit, northwestern British Columbia; in Current Research, 1994-A; Geological Survey of Canada, p. 45-56.

**Greig, C.J., McNicoll, V.J., Anderson, R.G., Daubeny, P.H., Harakal, J.E., and Runkle, D.**
1995: New K-Ar and U-Pb dates for the Cambria Icefield area, northwestern British Columbia; in Current Research 1995-A; Geological Survey of Canada, p. 97-103.

**Grove, E.W.**
1986: Geology and mineral deposits of the Unuk River-Salmon River-Anyox Area; British Columbia Ministry of Energy, Mines and Petroleum Resources, Bulletin 63.

**Hanson, G.**
1935: Portland Canal area, British Columbia; Geological Survey of Canada, Memoir 175.

**McConnell, R.G.**
1913: Portions of Portland Canal and Skeena Mining Division, Skeena District, British Columbia; Geological Survey of Canada, Memoir 32.

**McEvoy, J.**
1894: Geological Survey of Canada, Annual Report, v. VI, pt. A, p. 13-16.
1912: Route map of part of Nass River, British Columbia; Geological Survey of Canada, Map 69A.

**Richards, T.A., Woodsworth, G.J., and Tipper, H.W.**
1996: Geology, Hazelton, British Columbia; Geological Survey of Canada, Map 1852A, scale 1:250 000.

**Smith, J.G.**
1977: Geology of the Ketchikan D-1 and Bradfield Canal A-1 quadrangles, southeastern Alaska; United States Geological Survey, Bulletin 1425, 49 p.

**Steiger, R.H. and Jäger, E.**
1977: Subcommission on geochronology: convention on the use of decay constants in geo- and cosmochronology; Earth and Planetary Science Letters, v. 36, p. 359-362.

**Sutherland Brown, A.**
1969: Aiyansh lava flow, British Columbia; Canadian Journal of Earth Sciences, v. 6, p. 1460-1468.

**Tipper, H.W. and Richards, T.A.**
1976: Jurassic stratigraphy and history of north-central British Columbia; Geological Survey of Canada, Bulletin 270.

**Woodsworth, G.J., Hill, M.L., and van der Heyden, P.**
1985: Preliminary geological map of Terrace (NTS 103I east half) map area, British Columbia; Geological Survey of Canada, Open File 1136.

Geological Survey of Canada Project 950037

# Nechako Project overview, central British Columbia[1, 2]

L.C. Struik and W.J. McMillan[3]
GSC Victoria, Vancouver

*Struik, L.C. and McMillan, W.J., 1996: Nechako Project overview, central British Columbia; in Current Research 1996-A; Geological Survey of Canada, p. 57-62.*

**Abstract:** The Geological Survey of Canada and British Columbia Geological Survey Branch together with researchers in university and industry have initiated new geological mapping in central British Columbia (NTS 93F, 93K, and parts of 93G, 93L, 93M, 93N). The project is co-ordinated and financially augmented through the Geological Survey of Canada's National Mapping Program (NATMAP). Bedrock and surficial mapping are enhanced by geophysical and geochemical interpretations and site studies.

**Résumé :** La Commission géologique du Canada, de concert avec la *Geological Survey Branch* de la Colombie-Britannique ainsi que des chercheurs du milieu universitaire et de l'industrie, a entrepris de cartographier à nouveau la géologie du centre de la Colombie-Britannique (SNRC 93F, 93K et des parties de 93G, 93L, 93M, 93N). Le projet est coordonné et financièrement appuyé par le Programme national de cartographie géoscientifique (CARNAT) de la Commission géologique du Canada. La cartographie du socle et des dépôts superficiels bénéficie de l'apport d'interprétations géophysiques et géochimiques de même que d'études de sites.

[1] Contribution to the Nechako NATMAP Project
[2] This is a joint mapping project of the Geological Survey of Canada and British Columbia Geological Survey Branch.
[3] British Columbia Geological Survey Branch, British Columbia Ministry of Energy Mines and Petroleum Resources, 1810 Blanshard Street, Victoria, British Columbia V8V 1X4

## INTRODUCTION

A consortium of geoscientists have joined expertise to improve the geological understanding of the central Canadian Cordillera (Fig. 1). In particular they will address questions of Tertiary crustal extension, Mesozoic compression and the manner of accretion of exotic terranes, the geological and geophysical definition of the terranes, the sequence of changing Pleistocene glacial ice flow directions, and the character and dispersion of glacial deposits.

Over fifty scientists from the Geological Survey of Canada, British Columbia Geological Survey Branch, Canadian Forestry Service, universities in North America, Asia, and Europe, and mineral development companies have major or "in kind" involvement in the project. Over five years, new regional and local detailed geological and geophysical maps will be published for the Nechako River (93F), Fort Fraser (93K) and parts of Prince George (93G/12,13), Smithers (93L/16), Hazelton (93M/1), and Manson River (93N/4,5,12) map areas (Fig. 1).

Throughout the paper the following abbreviations will be used:

| | |
|---|---|
| BCGSB | British Columbia Geological Survey Branch |
| GIS | Computer Geographic Information Systems |
| GSC | Geological Survey of Canada |
| MDRU | Mineral Deposits Research Unit at UBC |
| UA | University of Alberta |
| UBC | University of British Columbia |
| UNB | University of New Brunswick |

## NECHAKO NATMAP OBJECTIVES

We will test the hypothesis that the Eocene volcanic complex in central British Columbia represents the tectonic/magmatic expression of an Eocene regional extensional event (Fig. 2; Struik, 1994). Understanding this geology will lead to an understanding of the regional Eocene tectonics, the structural relationships of the upper and lower plates of the extension complex, and precious metal epithermal mineral deposit possibilities associated with the contact zone between the upper and lower plates.

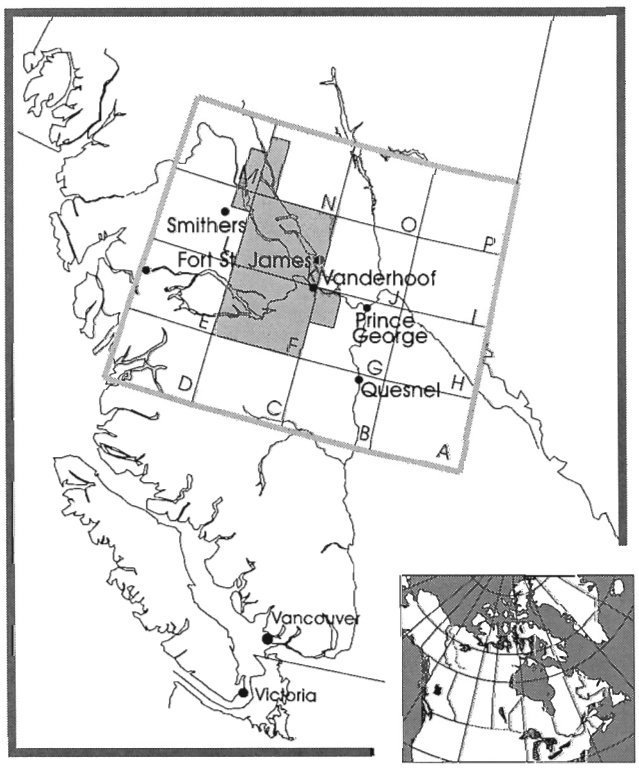


***Figure 1.*** *Location of the Nechako NATMAP project.*

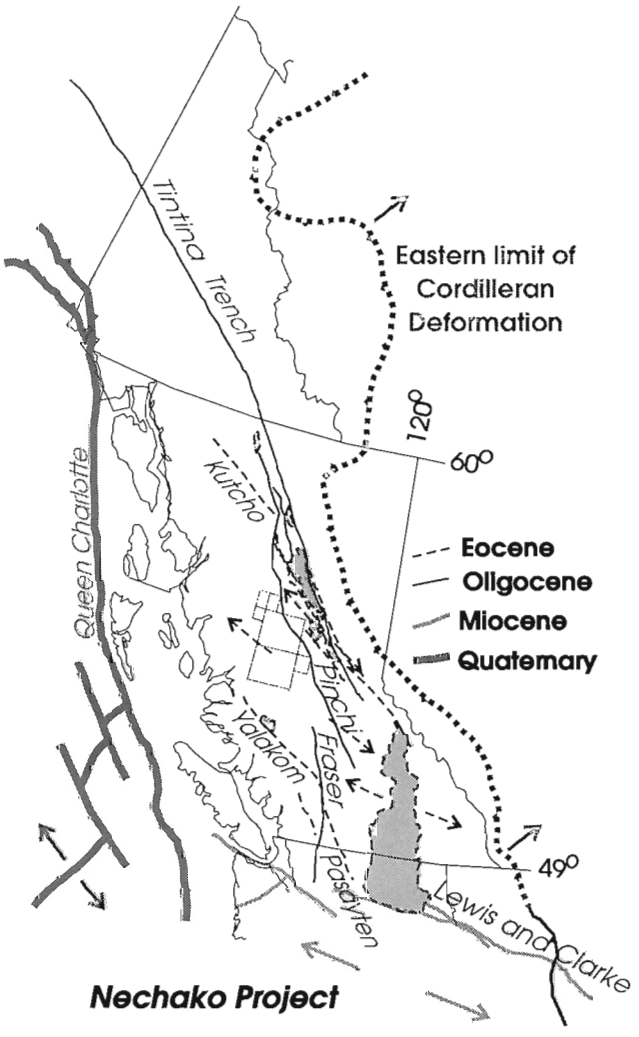


***Figure 2.*** *Relationship of the study area to the Eocene tectonic environment in the North American Cordillera. Shaded areas are metamorphic core complexes.*

To realize this objective we will need to accomplish four subobjectives:

1. Bring obsolete 1:250 000 scale geological maps to modern standards (existing maps are based on fieldwork from the 1940s and 1950s (Armstrong, 1949; Tipper, 1963)). These include bedrock maps for 93F and 93K, and surficial maps for 93F. This area was identified as a high priority area for new mapping by the GSC and BCGSB co-operation committee (Tempelman-Kluit and Matysek, 1994). It was sanctioned by the industry liaison committees of both organizations and the local mineral industry.
2. Characterize the Skeena Arch Triassic-Jurassic volcanic arc sequence by studying stratigraphy, plutonic character, tectonic history, rock distribution, and Cu-Au associations that are noted so clearly in surrounding areas. More money has been earned from Jurassic mineral deposits in British Columbia than from deposits of any other age.
3. Test the hypothesis that the boundary between Stikine and Cache Creek terranes is a regional thrust fault like the King Salmon fault in northern British Columbia, and from characteristics of the three major terranes of the area determine their tectonic histories.
4. Determine the regional Pleistocene ice flow directions in central British Columbia where we know ice sheets from three different directions coalesced, testing the hypothesis of multiple directions of flow through time as indicated by recent interpretations of Alain Plouffe (1995). Retreat of these ice sheets left much of the area covered by unconsolidated glacial deposits. Ice flow information is very important in drift prospecting, in understanding chemical dispersion patterns, and in tracing units through covered areas during regional bedrock mapping.

Only by accomplishing these subobjectives will we be able to interpret the nature of the Tertiary tectonics. These fundamental geological questions will require a broad range of expertise and techniques to solve because bedrock exposure in central British Columbia is poor due to an extensive cover of Quaternary deposits. The Mesozoic bedrock locally is covered by Tertiary plateau basalts. Few sections of the Quaternary deposits are exposed because little of it has been transected by roadcuts or stream valleys.

To accomplish these objectives we plan to apply a range of geoscientific studies where we will:

1. Map the bedrock and surficial geology in scales appropriate to the problem. This will be done interactively by a consortium of experts applying a broad range of techniques.
2. Map the surficial geology to determine the glacial history. Till geochemistry and heavy mineral content, combined with glacial flow directions will be used to trace hidden bedrock lithologies.
3. Interpret aeromagnetic and gravity data to trace units beneath the cover rocks, to map subsurface structures and to provide feedback to improve the interpretations of geology based on mapping of exposed rock.
4. Conduct radiometric surveys to assist in the differentiation of plutonic units directly through their exposed chemical signature and indirectly through their distributed chemical signature in the surficial sediments.
5. Carry out local gravity and electromagnetic surveys to assist in the delineation of geological structures to depth and to test regional geophysical models. These data will be needed to construct controlled and reasonable interpretative cross-sections.
6. Determine paleomagnetic orientations on suites of rock to determine their genetic and tectonic relationships. This information will be used to help determine the significance and degrees of offset on terrane contacts, and to test for structural rotations that may have accompanied Eocene extension.
7. Conduct seismic P-wave crustal studies as a relatively inexpensive way to map the third dimension; information needed to solve the contact relationships of the Cache Creek Terrane, and the structural characteristics and geometry of the Eocene extension complex and its Upper Plate.
8. Isotopically date the plutonic suites and characterize them chemically. This information will constrain many of the tectonic events when we have a clear interpretation of the pluton genesis and contact relations with the country rock.
9. Increase paleontological control through contracts for radiolarian and fusulinid expertise, and support for GSC and university paleontological research and determinations. This biostratigraphic information is needed to unravel the internal structure of the Stikine and Cache Creek terranes.
10. Conduct image analysis of satellite spectral and radar data to provide information on the regional distribution of lithologies, structures, and lineaments.
11. Collate all data, using computer technology, into GIS databases that will permit the fusion of geoscience information into thematic maps; provide these GIS data sets to involved researchers and clients in a simple, easily used format to encourage analysis of interrelationships of the geoscience data sets.

This research will be published as a series of maps, GIS databases and reports (Fig. 3). We will reinterpret the various data sources from the viewpoint of environmental and land use impact to make pertinent information more widely accessible.

## OVERVIEW OF NATMAP RESULTS TO DATE

### *Bedrock mapping*

Don MacIntyre, Ian Webster, and Kim Bellefontaine of the BCGSB with the assistance of summer student John Bryant completed 1:50 000 scale geological mapping of NTS map sheet 93L/16 (Fig. 3D) (MacIntyre et al., 1996). Significant revisions were made to Carter's (1973) Preliminary Map 12

which was the only published geology map of the porphyry belt other than the 1:250 000 GSC Open File maps. Carter's geology was placed into a modern stratigraphic framework. Samples were collected for radiometric dating by Mike Villeneuve of the GSC and this information will help to further refine the geology of the area. Several new epithermal systems were located and these appear to be related to either early Jurassic or post-Eocene hydrothermal events. A stratigraphy was developed for the Eocene Newman volcanics, the extrusive equivalent of the Babine Intrusions. Emplacement of porphyries and related extrusive activity appears to predate the main episode of Eocene extensional faulting in the area. Mapping in 1996 will move northward into NTS map sheet 93M/1.

Paul Schiarizza (BCGSB) spent 8 days examining the geology east of Takla Lake (93N/5, 12, 13) in preparation for a geological mapping program planned in subsequent years (Fig. 3E). This program will concentrate on metavolcanic and metasedimentary rocks of the Sitlika assemblage, with the goal of developing an internal stratigraphy and assessing its

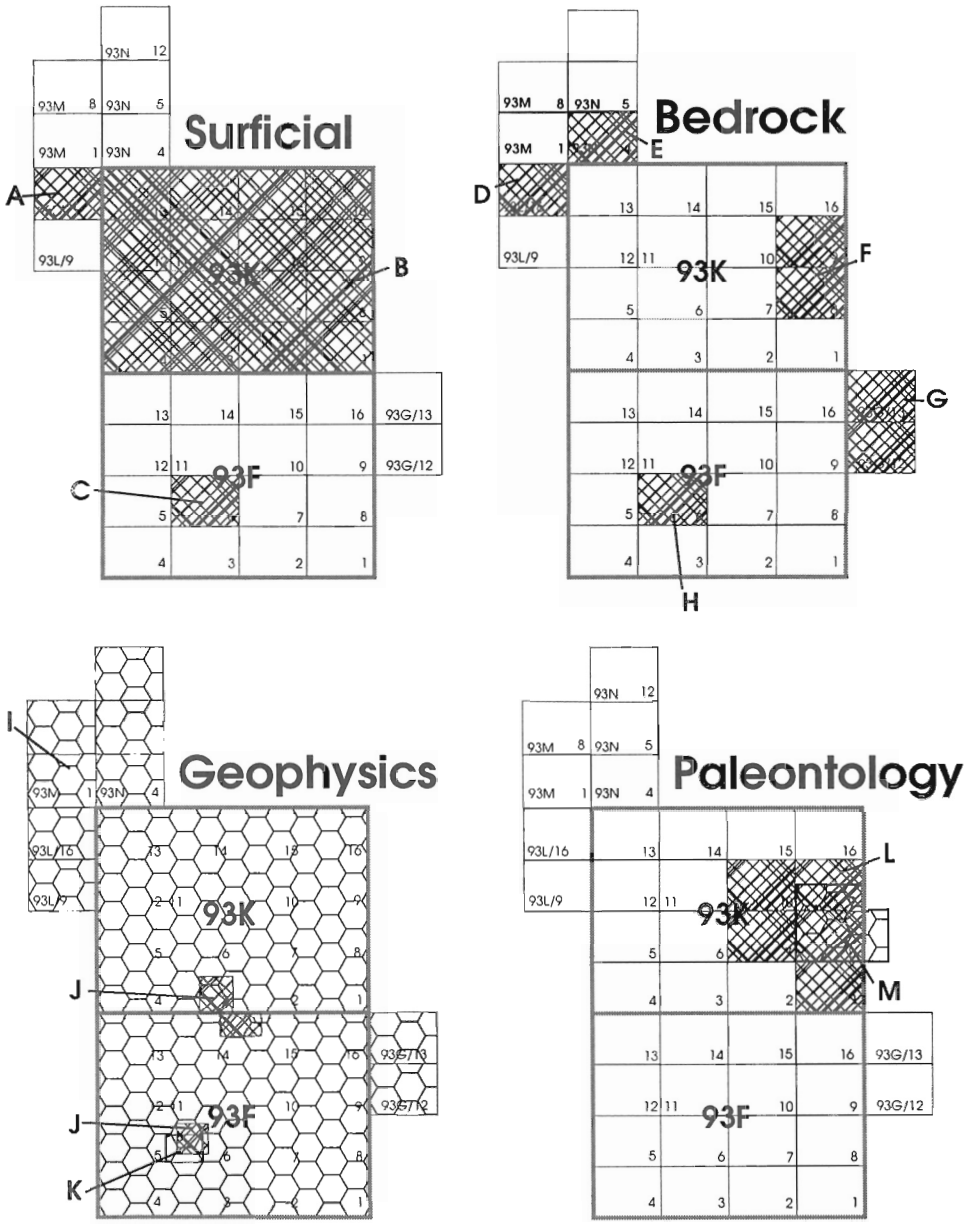


*Figure 3. Location of various Nechako subprojects active in 1995. Letters are referenced in the text: A) D. Huntley et al. [BCGSB, UNB]; B) A. Plouffe [GSC]; C) V. Levson [BSGSB; D) D. MacIntyre et al. [BCGSB]; E) P. Schiarizza [BCGSB]; F) L. Struik et al. [GSC]; G) S. Wetherup et al. [UA, GSC]; H) L. Diakow et al. [BCGSB, GSC]; I) C. Lowe and D. Seemann [GSC]; J) R. Shives [GSC]; K) R. Enkin [GSC]; L) F. Cordey [contract]; and M) M. Orchard [GSC].*

potential to host volcanogenic massive sulphide deposits. It will also establish the relationships between the Sitlika assemblage and adjacent rocks of Cache Creek and Stikine terranes, as well as test the proposed correlation between the Sitlika assemblage and the Kutcho Formation, which hosts the Kutcho Creek volcanogenic massive sulphide deposit in northern British Columbia.

Larry Diakow (BCGSB), in concert with Terry Poulton and Howard Tipper of the GSC, spent five days revisiting fossil sites in the southern Nechako Plateau area in an effort to better constrain the ages of Lower and Middle Jurassic sedimentary sequences (Fig. 3H). Biostratigraphy is critically important because isotopic dating in interlayered bimodal volcanics has been inconclusive. This work completes a 1:50 000 scale Canada-British Columbia Mineral Development Agreement funded bedrock mapping program in the Nechako River area. The updated geological framework provided by this project will be expanded during the NATMAP program by additional bedrock mapping in mapsheets 93E/4, 5, 12 and 13.

Bert Struik (GSC) and a crew of three university students conducted bedrock mapping of the Vanderhoof Gneiss Complex (93G/12, 13 and parts of 93G/5, 6 and 11) (Wetherup and Struik, 1996; Fig. 3G), and began work in Fort Fraser map area (93K) near Fort St. James (Struik et al., 1996; Fig. 3F). The Vanderhoof orthogneiss and paragneiss are clearly in fault contact with overlying ultramafic rocks of the Cache Creek Group. Ductile shear in the lower plate gneiss increases toward the contact, and upper plate shear at the contact consists of a narrow zone of brittle gouge. On the eastern side of the complex the upper plate motion was down to the east-southeast. Wetherup will be continuing studies of these rocks in the Masters program at the University of Alberta under the supervision of Phillipe Erdmer. Brian Traub mapped the area of metamorphic rocks of southern Babine Lake for a Bachelors thesis project, also supervised by Phillipe Erdmer. This work expands on the reconnaissance conducted by Struik and Erdmer (1990). As part of the regional mapping of the Cache Creek Group, a contract research project has been conducted by Fabrice Cordey on the radiolarian biostratigraphy (Fig. 3L). This work will assist in defining the age range, paleogeographic setting, biostratigraphy, and structures of the Cache Creek Terrane in the central Canadian Cordillera. Preliminary results from this summer are reported in Cordey and Struik (1996). Newly determined age relationships have been used to locate a thrust fault, and have established a Triassic age range for ribbon cherts of the Cache Creek Group in the vicinity of Fort St. James.

Ed Kimura and Sharon Gardiner (Placer Dome), Glenn Johnston (Endako Mines), and Placer Dome Inc. have contributed data from their regional geological mapping of the area around the Endako Molybdenum deposit which is underlain by Mesozoic rocks (93F, 93K). We are working with Placer Dome in the digitization of that data, some of which will appear in the geological compilations for the Nechako NATMAP project.

Joe Whalen (GSC) conducted a reconnaissance of plutonic suites in the Endako/Fraser Lake area (93F/14 and 93K/3) in preparation for mapping and lithogeochemical studies in subsequent years. The plutonic suites show a wide range of genetic types and compositions.

### *Surficial mapping*

Dave Huntley and Vic Levson (BCGSB) co-ordinated regional surficial mapping, drift geochemical sampling, and glacial studies in the Babine Porphyry Belt (93M/01 and 93L/16) (Fig. 3A) (Huntley et al., 1996). They worked closely with doctoral candidate Andy Stumpf and Masters candidates Erin O'Brien and Gordon Weary under the supervision of Bruce Broster, of University of New Brunswick (Stumpf et al., 1996).

Surficial geology maps for these two areas show surficial cover, landforms, ice flow patterns, and the distribution of mineralized glacial erratics and will be completed for Cordilleran Roundup 1996. Geochemical results from ICP and INA analyses of some 900 samples of basal till (800), mineralized erratics (40) and other sample media collected in areas of good mineral potential will be released when data become available. Interpretation of regional paleo-ice flow patterns, physiographic controls of deposition, and the deglacial history of Lake Babine are in progress. These data will be used to interpret the geochemical results to aid future exploration in the area.

Steve Cook (BCGSB) conducted followup studies as an outcome of the Mineral Development Agreement (MDA) supported, lake geochemical surveys (Fig. 3C). As an adjunct to the NATMAP project and funded through the MDA, he and Wayne Jackaman (BCGSB), together with Peter Friske (GSC), Martin McCurdy (GSC), and Steve Day (GSC) conducted a regional lake sediment and water geochemistry survey over the northeastern part of the Fort Fraser map area (NTS 93K/9, 10, 15, 16). The survey is a contribution to the continuing objective of completing Regional Geochemical Survey (RGS) coverage of the northern interior. The survey area also covers the Pinchi fault zone mercury deposits, and will provide valuable baseline regional data for anticipated studies of naturally occurring mercury in the environment.

Alain Plouffe (GSC) has compiled and published the surficial geology of the Fort Fraser map area (93K) at 1:100 000 scale (Fig. 3B). That work is the culmination of mapping that he conducted under the 1991-1995 MDA program. In addition to the geological maps, Plouffe, with Bruce Ballantyne (GSC), has published the results of regional till geochemical surveys done in the same map area. Those geochemical distributions are being put into a regional glacial flow direction history (Plouffe, 1995).

### *Geophysical studies*

Rob Shives (GSC) conducted a contract radiometric, aeromagnetic, and VLF (very low frequency electromagnetic) study over a pluton-dominated area near Fraser Lake (93K/3, 93F/14) and south of the Kemano Reservoir (93F/6) (Fig. 3J). These studies will be used in the mapping of the various plutonic suites in these regions. The surveys were flown in late September and results were unavailable at the time of writing.

Randy Enkin (GSC) worked with Larry Diakow to sample rocks of the Entiako Spur and Nagliko Uplift for paleomagnetic studies of the Jurassic sequences (93F/6) (Fig. 3K). This work will test the hypotheses of plate translations related to terrane accretion, and block rotations possibly related to Tertiary strike-slip faulting.

Carmel Lowe (GSC) has begun interpretation of the existing gravity and aeromagnetic data (93G, 93F, 93K, 93L, 93M, 93N) (Fig. 3I). This information will be used to aid the bedrock and surficial mapping, and assist in the interpretation of the geology to depth.

### *Geochronology*

Mike Orchard (GSC) has compiled a database of existing paleontological determinations from the project area, and has concentrated on documenting conodont fauna from the Cache Creek limestone (Orchard and Struik, 1996; Fig. 3M).

Mike Villeneuve (GSC) and Jim Mortensen (UBC, MDRU) have conducted reconnaissance sampling programs for isotopic age dating of igneous and metamorphic suites throughout the project area. These works will initially concentrate on defining ages for the numerous plutonic and extrusive suites in the area and establishing the relationship between plutonism and ore generation. Villeneuve is co-ordinating the isotopic dating for the project and has begun compiling a computer database of existing isotopic dates for the area (93G, 93F, 93K, 93L, 93M, 93N). That database will become part of the Canadian database of isotopic ages co-ordinated by the geochronology section of the GSC.

### *Geographic Information Systems*

Stephen Williams (GSC) is working with scientific staff of both the GSC and BCGSB in the compilation of computer geological, geochemical, and geophysical data to be published on CD-ROM. That data will be integrated with a common GIS platform. It will contain information relevant to the Quesnel Trough of central British Columbia including NTS map areas 93K, 93N, 93J, 93O(SW), and 94C. The computer information will be available in several formats and will be accessible with software included with the CD-ROM.

## ACKNOWLEDGMENTS

We would like to thank all those people who worked hard to make this project a reality and for the support of the GSC, BCGSB, and geoscience community. We make a special note of thanks to Cominco (Ken Pride) and Placer Dome (Ed Kimura) for their willingness to make company geological mapping information available to this project.

## REFERENCES

**Armstrong, J.E.**
1949: Fort St. James map-area, Cassiar and Coast districts, British Columbia; Geological Survey of Canada, Memoir 252.

**Carter, N.**
1973: Preliminary geological map of northern Babine Lake area (93L/NE, 93M/SE); British Columbia Department of Mines, Preliminary Map 12.

**Cordey, F. and Struik, L.C.**
1996: Scope and preliminary results radiolarian biostratigraphic studies, Fort Fraser and Prince George map areas, central British Columbia; in Current Research 1996-A; Geological Survey of Canada.

**Huntley, D.H., Levson, V.M., Stumpf, A.J., and Broster, B.E.**
1996: Quaternary geology and regional till geochemical sampling, Babine Lake, British Columbia; in Geological Fieldwork 1995; British Columbia Ministry of Energy, Mines and Petroleum Resources, Paper 1996-1.

**MacIntyre, D.G., Webster, I.C.L., and Bellefontaine, K.A.**
1996: Babine Porphyry Belt project, bedrock geology of the Fulton Lake map area (NTS 93L16); in Geological Fieldwork 1995; British Columbia Ministry of Energy, Mines and Petroleum Resources, Paper 1996-1.

**Orchard, M.J. and Struik, L.C.**
1996: Conodont biostratigraphy, lithostratigraphy, and correlation of the Cache Creek Group near Fort St. James, British Columbia; in Current Research 1996-A; Geological Survey of Canada.

**Plouffe, A.**
1995: Glacial history of north-central British Columbia; in Final Program and Abstracts, Geological Association of Canada, v. 20, p. A84.

**Struik, L.C.**
1994: Intersecting intracratonal Tertiary transform fault systems in the North American Cordillera; Canadian Journal of Earth Sciences, v. 30, p. 1262-1274.

**Struik, L.C. and Erdmer, P.**
1990: Metasediments, granitoids, and shear zones, southern Babine Lake, British Columbia; in Current Research, Part E; Geological Survey of Canada, Paper 90-1E, p. 59-63.

**Struik, L.C., Floriet, C., and Cordey, F.**
1996: Geology near Fort St. James, central British Columbia; in Current Research 1996-A; Geological Survey of Canada.

**Stumpf, A.J., Huntley, D.H., Levson, V.M., and Broster, B.E.**
1996: Detailed surficial mapping and drift exploration in the Babine Porphyry Belt; in Geological Fieldwork 1995; British Columbia Ministry of Energy, Mines and Petroleum Resources, Paper 1996-1.

**Tempelman-Kluit, D.J. and Matysek, P.**
1994: Geoscience information needs for the future of British Columbia; Geological Survey of Canada and British Columbia Ministry of Energy Mines and Petroleum Resources, Internal Report.

**Tipper, H.W.**
1963: Nechako River map area, British Columbia; Geological Survey of Canada, Map 1131A.

**Wetherup, S. and Struik, L.C.**
1996: Vanderhoof Metamorphic Complex and surrounding rocks, central British Columbia; in Current Research 1996-A; Geological Survey of Canada.

Geological Survey of Canada Project Number 950036

# Vanderhoof Metamorphic Complex and surrounding rocks, central British Columbia[1,2]

S. Wetherup[3] and L.C. Struik
GSC Victoria, Vancouver

*Wetherup, S. and Struik, L.C., 1996: Vanderhoof Metamorphic Complex and surrounding rocks, central British Columbia; in Current Research 1996-A; Geological Survey of Canada, p. 63-70.*

**Abstract:** Vanderhoof Metamorphic Complex is defined here as a suite of paragneiss and orthogneiss units underlying the area south and southeast of Vanderhoof, British Columbia (93F/9, 16 and 93G/5, 6, 12, 13). These rocks are in fault contact with structurally overlying ultramafic rocks and basalt of the Cache Creek Group. The fault contact is a low angle detachment that has down to the southeast motion in the central part of the exposed complex. The paragneiss of the complex has fine grained clastic rock, limestone, marl and possibly basalt protoliths. Orthogneiss of the complex is mostly biotite granite and granodiorite, which forms sills, dykes, and plutonic masses. Metamorphic grade is indeterminate from field evidence. These rocks are intruded and overlain by felsic to intermediate volcanic and intrusive rocks, probably of Tertiary age.

**Résumé :** Le complexe métamorphique de Vanderhoof est défini, dans le présent article, comme une suite de paragneiss et d'orthogneiss observés dans la région au sud et au sud-est de Vanderhoof, en Colombie-Britannique (93F/9, 16 et 93G/5, 6, 12, 13). Ces unités sont en contact de faille avec les roches ultramafiques et les basaltes structuralement sus-jacents du Groupe de Cache Creek. Le contact de faille est un décollement à angle faible dont le déplacement vers le bas est orienté vers le sud-est dans la partie centrale du complexe affleurant. Les protolites du paragneiss du complexe consistent en des clastites à grain fin, des calcaires, des marnes et peut-être des basaltes. Les orthogneiss du complexe sont surtout des granites à biotite et des granodiorites qui forment des filons-couches, des dykes et des massifs plutoniques. Les indices recueillis sur le terrain sont insuffisants pour déterminer l'intensité du métamorphisme. Ces unités sont recoupées et surmontées par des roches volcaniques et intrusives felsiques à intermédiaires, d'âge probablement tertiaire.

[1] Contribution to the Nechako NATMAP Project
[2] This is a joint mapping project of the Geological Survey of Canada and British Columbia Geological Survey Branch
[3] Department of Geology, University of Alberta, Edmonton, Alberta T6G 2E3

## INTRODUCTION

The Vanderhoof Metamorphic Complex and surrounding rocks of central British Columbia are being mapped as part of the Nechako NATMAP project (Fig. 1; Struik and McMillan, 1996). These rocks were formerly included in plutonic suites during early reconnaissance mapping (Tipper, 1961, 1963). They were later differentiated as a metamorphic suite during compilation of various small scale maps of the Canadian Cordillera (Tipper et al., 1979; Wheeler and McFeely, 1991).

Surrounding rocks of the region include oceanic and island arc volcanic and sedimentary sequences. These are part of the Cache Creek and Takla groups, and Tertiary rocks dominated by basalts and dacites. In this progress report we describe the geology of two 1:50 000 scale map areas of the northwestern Prince George map area: NTS 93G/12 and 13, and report on our preliminary attempts to understand the tectonic history of the Vanderhoof Metamorphic Complex.

## GEOLOGY

Western Prince George map area is underlain by six assemblages ranging in age from Pliocene to middle Paleozoic (or older). They consist of the Chilcotin Group plateau basalt, Miocene and Pliocene sedimentary rocks, early and middle Tertiary granite and Ootsa Lake Group intermediate volcanic rocks, Cache Creek Group oceanic assemblage rocks, and Vanderhoof Metamorphic Complex paragneiss and orthogneiss. Much of the area is covered by glaciofluvial and glaciolacustrine deposits, and various tills and alluvium (Tipper, 1961). Bedrock is generally exposed on the few ridge tops and some stream beds. Isolated exposures through the glacial deposits are uncommon. All of the discussion here will concern the bedrock.

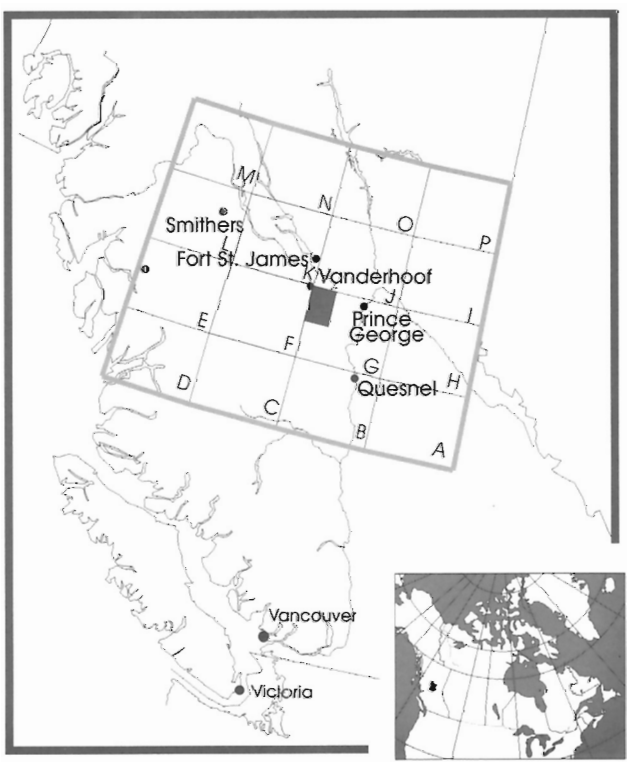


***Figure 1.*** *Location map of the study area.*

### *Miocene and Pliocene*

#### Chilcotin Group

Chilcotin Group of the map area consists mainly of various basalt units. It underlies much of the central portion of 93G/12 and the northern and northeastern areas of 93G/13 (Fig. 2, 3). The best exposures of this generally poorly exposed unit are found along tributaries of the Chilako River (extreme south-central) and the Nechako River (at Carole Falls). Tipper (1961), included these rocks in the Chilcotin basalt. Chilcotin Group basalt is distinguished from other basalt units in the area by its fresh appearance, lack of deformational features, common hexagonal columnar jointing pattern, and common olivine and pyroxene phenocrysts. This unit is generally found in low-lying areas surrounding the ridges and peaks. It is interpreted as a series of basaltic flows that covered most of the low-lying paleotopography.

The basalt formed flows that weather dark rusty brown, and are black to very dark green on fresh surfaces. Phenocrysts consist of olivine (0.5-10%, 0.5-2 mm) and pyroxene (0-2%, 0.5-1 mm). Vesicles are abundant especially near flow tops where they occupy 20-30% of the rock. They are locally filled with either very fine grained chlorite or zeolites. Flows are often columnar jointed with rusty red flow tops. Curved segregation pipes (or degassing pipes) are common. No deformational or metamorphic features were observed in the Chilcotin basalt, but some minor hydrothermal alteration occurs in small localized areas. No new information has been gathered to refine the previously interpreted Miocene age (Tipper, 1961; Wheeler and McFeely, 1991).

#### Sedimentary rocks

Rare outcrops of these rocks are located in the north-central region, in railway cuts by the Nechako River and in the banks of the Nechako and Cluculz rivers. These rocks consist of siltstone, sandstone, and conglomerate. They are included in undifferentiated Miocene sedimentary rocks (Tipper, 1961). These rocks are distinguished from overlying glacial sediments by their better sorting and greater induration.

The siltstone unit is very light beige on both fresh and weathered surfaces. Beds are from 1 mm to 2 cm thick and contain light rusty red lamellae. Local rare pebbles or granules occur in the generally very well sorted siltstone. The siltstones are gradational with well sorted sandstones. Sandstones are light brown on fresh and weathered surfaces. Grain sizes vary from very fine to coarse. Beds are generally 1 cm thick but may vary between 3 mm to 2 cm. Clasts are dominantly quartz and feldspar with minor amounts of fine grained mafic and calcite clasts. Grains are moderately cemented with calcite. Some medium- to fine-grained sandstone units contain

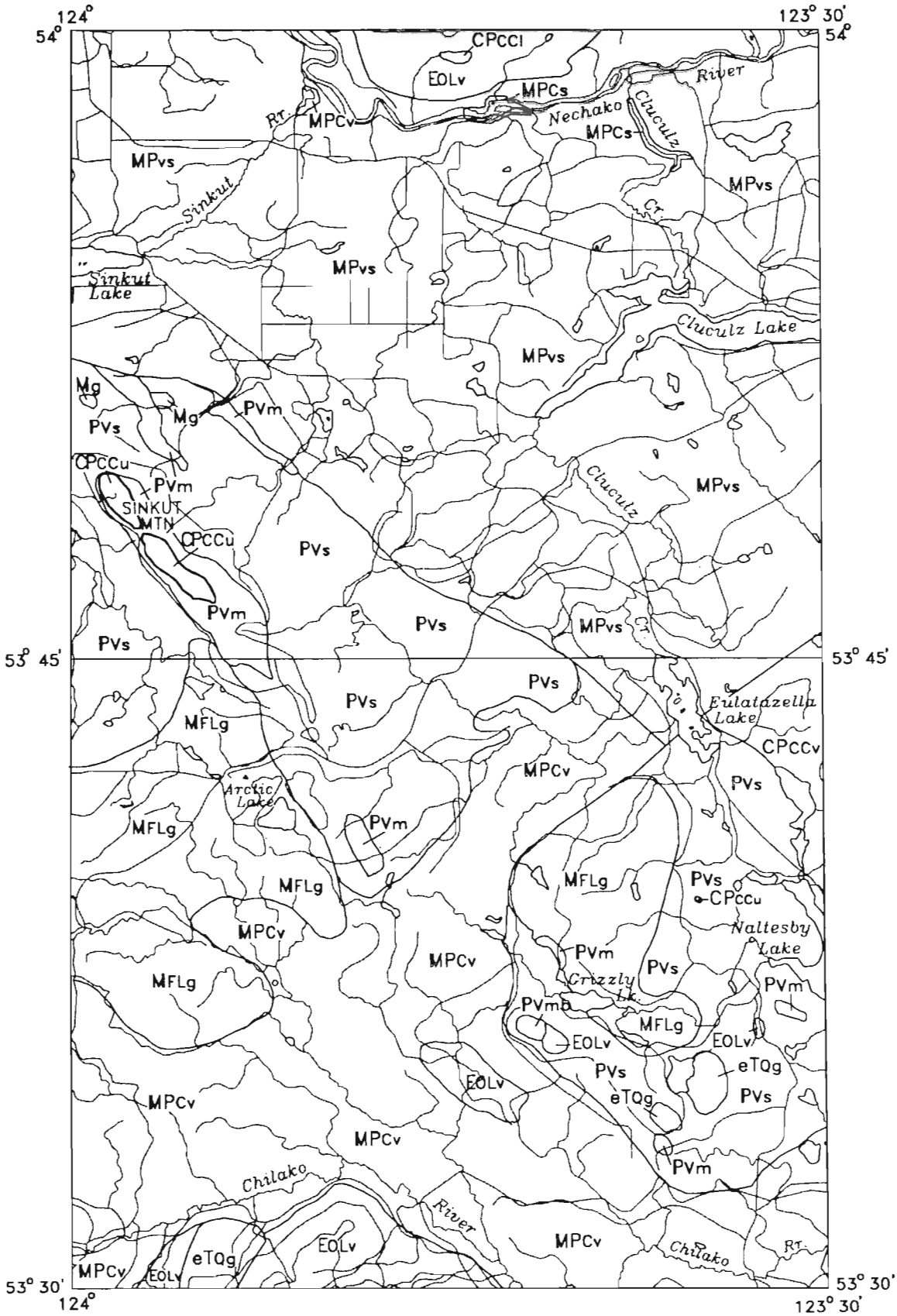


***Figure 2.*** *Bedrock geological interpretations of NTS map areas 93G/12 and 13. Map scale is approximately 1:250 000. For legend to this map see Figure 3.*

carbonized plant fossils. Coarse grained sandstone grades into granule conglomerate and fine grained pebble conglomerate. Clasts are very similar in composition to the sandstone except for the addition of quartzite.

Beds within the Miocene sediments are nearly horizontal to shallowly east-dipping. These sediments appear to have undergone no greater than diagenetic metamorphism.

In the map area these are interpreted to be the youngest rocks as they overlie the Chilcotin basalt at the Nechako River. Tipper (1961) interpreted these rocks to underlie the Chilcotin basalt, but it is possible that the sedimentary regime overlaps that of the basalt flows.

## *Eocene*

### Ootsa Lake Group

Rocks of the Ootsa Lake Group mainly outcrop in the southern part of the map area except for some outcrops north of the Nechako River (Fig. 2). They consist of basalt, andesite, rhyolite, and dacite flows and locally minor volcaniclastic rocks. The best exposures are located on the high ridge south of the Chilako River. The sequence is estimated to be approximately 300 m thick at that locality. These rocks were mapped by Tipper (1961) as the undifferentiated Paleocene and Eocene volcanics (unit 9). Subsequently Tipper et al. (1979) mapped them as Cretaceous/Tertiary Ootsa Lake Group, and Wheeler and McFeely (1991) included them as part of the Paleocene Tertiary Kamloops assemblage. South of the Chilako River this unit overlies quartzite and siltite that may be part of the Vanderhoof Metamorphic Complex. Its upper contact is not exposed.

The andesite is green and weathers light green and consists generally of an aphanitic matrix with phenocrysts of plagioclase (1-3 mm, 10-20%, euhedral) and minor quartz. The plagioclase has random orientations and is inhomogeneously distributed through the rock. Minor constituents include pyroxene, magnetite, and secondary epidote. Fragments of rhyolite are found in the andesite in the eastern exposures south of the Chilako River.

The dacite has a light green matrix and has crystals of feldspar (0.5-2 mm, 5%) and quartz (0.5-1 mm, 1%) and fragments of andesite (5-30 mm, 1%). Rhyolite units are flow banded, cream to tan, and contain fine crystals of quartz and feldspar. In some places, both the dacite and rhyolite have vesicles, some of which have quartz fillings.

There is no new information on the dating of this sequence.

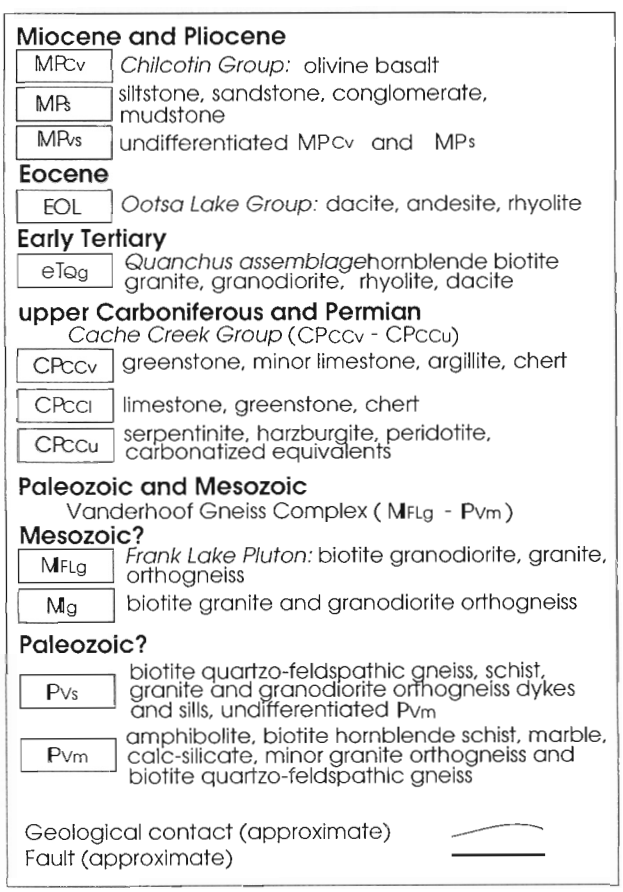


***Figure 3.*** *Legend for the geology map of Figure 2.*

## *Early Tertiary*

### Quanchus assemblage

Quanchus assemblage granite bodies were mapped in the southern part of the map area (Fig. 2) and to the south and southeast. Of these outcrops, a small exposure of granite located in the extreme southwest of the map area (Fig. 2) and continuing to the south is informally referred to here as the Chilako granite. Excellent exposure of the Chilako granite is found within the Nataniko River valley. A distinctive granite body, here named the Barton Lake granite, outcrops just to the southeast of the area shown in Figure 2 and is best exposed at the northern tip of the Telegraph Range. Tipper (1961) grouped these granites with the Topley Intrusions and Tipper et al. (1979) included one of them with the Quanchus Intrusions. These rocks are typified by their lack of significant fabric and by common feldspar porphyry xenoliths. These granite bodies crosscut gneiss, Cache Creek sedimentary and ultramafic rocks and Ootsa Lake volcanic rocks as interpreted from xenoliths.

The Chilako granite weathers light grey and is white to light pink. It comprises roughly equal proportions of plagioclase (1-4 mm) and K-feldspar which combine to form 60-85% of the rock. The remainder of the rock is composed of quartz (1-4 mm, 15-20%), biotite (5-15%), hornblende (0-5%), and minor amounts of fine grained magnetite.

Barton Lake granite is light grey on weathering surfaces and white on fresh surfaces. The rock contains white feldspar (50-60%), quartz (20-25%), hornblende (0-10%), euhedral biotite (5-15%), and minor magnetite. Grain size in the matrix is generally between 1 and 4 mm, but feldspar phenocrysts are up to 6 mm. The most distinctive feature of this granite is the hexagonal biotite phenocrysts. The granite does not appear to

be appreciably deformed or metamorphosed. From crosscutting relationships, and the feldspar porphyry xenoliths found within the granite, the age of the granite has been interpreted to be Tertiary and perhaps Eocene.

Biotite quartz porphyry microgranite bodies southeast of Grizzly Lake are included within this unit. They intrude quartzite of the Vanderhoof Complex and are fresh and undeformed rocks.

## *Upper Carboniferous and Permian*

### Cache Creek Group

*Limestone unit*

Limestone forms a small part of the Cache Creek Group in the area. It is more prevalent to the east where more basalt and sedimentary rocks of the Cache Creek Group are exposed. The limestone is light grey weathering, grey and light grey. Mostly it is cleaved and the crinoidal debris is flattened and broken. The limestone is interlayered with basalt and minor ribbon chert.

*Greenstone unit*

Greenstone occupies a large area of the Cache Creek Group exposures to the east of the map area shown in Figure 2. It is strongly deformed, displaying a well developed foliation with disruption of possible primary layering. Plagioclase and pyroxene crystals are visible in places although these have been mostly replaced with low metamorphic grade alteration minerals. It is invaded by many quartz veins, themselves disrupted by foliation parallel flow. Original volcanic textures are mostly obliterated.

*Ultramafic unit*

Cache Creek ultramafic rocks are found on Sinkut Mountain and to the southeast of the map area. A large, well exposed area of highly resistant rocks lies to the east of Naltesby Lake, at Bobtail Mountain (Fig. 4). There is little compositional variation noted within the ultramafic rocks. Tipper (1961) mapped these rocks as Cache Creek serpentinite and ultramafic rocks. Distinguishing these rocks is their dun coloured weathering surface, massive nature, and composition of altered pyroxenes, fibrous amphiboles, and serpentine.

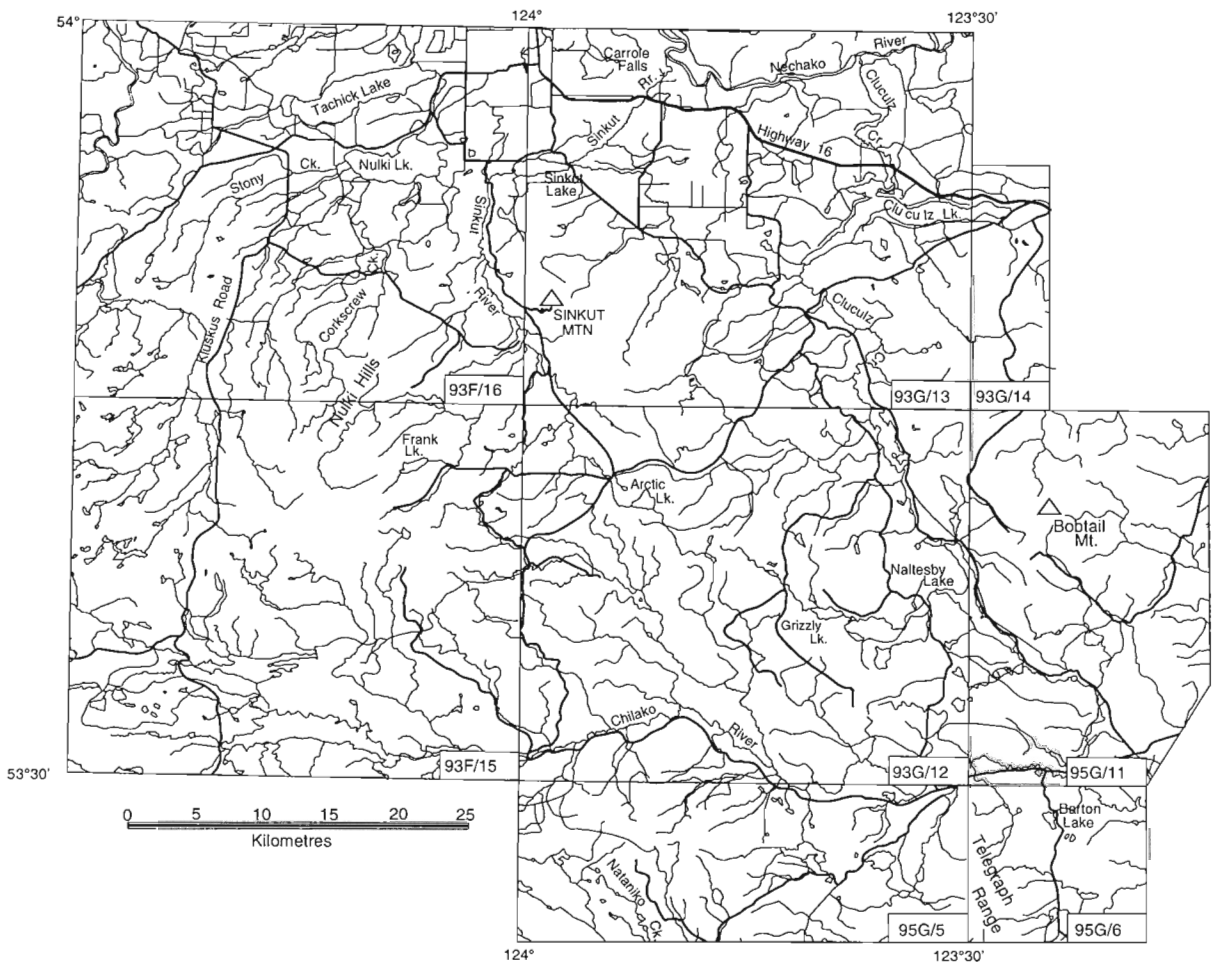


***Figure 4.*** *Index map of geographic and geological features of the area referred to in the text.*

Contacts, in the few places seen, are faults. A shear zone contact between ultramafic rock and Vanderhoof gneiss is exposed on Sinkut Mountain.

Cache Creek ultramafic rocks weather orange-red or dun and are very dark green to green on fresh surfaces. Mineralogy of these rocks varies by original composition and by the degree of alteration. Most are altered to some degree, with amphibole, serpentine, talc, and carbonate. Remnant minerals include pyroxene, olivine, magnetite, and possibly chromite. Crystals range from very coarse to medium and locally fine grained. Structurally, these rocks are massive with some joints and discrete shear zones. The shears in the Sinkut rocks are generally oriented near horizontal and near vertical, striking roughly north. Metamorphism has, locally, completely hydrated any prior olivine or pyroxene, but relict crystals or pseudomorphs of pyroxene are occasionally found.

The age of the Cache Creek Group is constrained, in the area to the northwest, as Pennsylvanian to Upper Triassic (Cordey and Struik, 1996; Orchard and Struik, 1996).

## *Paleozoic and Mesozoic*

### Vanderhoof Metamorphic Complex

Vanderhoof Metamorphic Complex consists of paragneiss and orthogneiss and some undifferentiated Tertiary intrusions. The complex underlies a broad area south and southeast of Vanderhoof (Fig. 2). These rocks were included by Tipper (1961) as part of the Topley Intrusions, by Wheeler and McFeely (1991) as part of an unnamed suite of orthogneiss southwest of Prince George and by Bellefontaine et al. (1995) as Vanderhoof Metamorphic Complex. The complex has been differentiated into three units: 1) siliciclastic paragneiss and 2) calcic paragneiss, both recessive and poorly exposed, intruded by 3) a large orthogneiss and granite body here called the Frank Lake pluton. A subunit of the calcic gneiss is an amphibolite that may have been derived from a basalt.

### Frank Lake pluton

Frank Lake pluton outcrops through much of the area to the south and west. The type locality for the Frank Lake pluton is in the Nulki Hills surrounding Frank Lake in 93F/9. Characterizing this granite are its white feldspars, accessory minerals magnetite and titanite, and its subhedral biotite or hornblende. Evidence that the Frank Lake pluton intruded the Vanderhoof paragneiss is given by: (1) undeformed to deformed dykes intruded into the gneiss, (2) stoped fragments of the gneiss within the granite near paragneiss contacts, and (3) pegmatite veins, which are interpreted to be a separate late phase of the granite, crosscutting the gneiss. Frank Lake pluton is mylonitized near the shallowly dipping contact with overlying Cache Creek Group ultramafic rocks.

Frank Lake pluton is greyish-white, weathering white. Most of the rock is white feldspar (50-60%) and quartz (10-30%). Generally, accessory minerals consist of biotite (5-20%) and minor amounts of magnetite and titanite. Some outcrops contain hornblende as well as biotite. Crystal sizes range between 1 and 4 mm.

The granite appears relatively unmetamorphosed, but is locally deformed. Deformation occurs near the upper contact with the ultramafic rocks along Sinkut ridge (Fig. 2), and in the western Nulki Hills (along the Kluskus Road). Foliations in the Nulki Hills (in 93F/9 and F/16) strike roughly north and dip shallowly west, with lineations plunging shallowly northward. On Sinkut Ridge the foliations strike northeast, and dip shallowly to moderately eastward, with lineations plunging shallowly northward. Frank Lake pluton is assumed to be Mesozoic in age. Permian orthogneiss has been dated in the area of Arctic Lake (R. Friedman, pers. comm., 1995), and may be part of the Frank Lake suite. It is possible that Frank Lake pluton is not a single pluton as here described.

## *Permo-Carboniferous*

### Siliciclastic Vanderhoof gneiss

Vanderhoof siliciclastic gneiss is exposed from Sinkut Mountain south and southeast through the map area. The unit consists mainly of biotite schist, biotite hornblende gneiss, quartz feldspar gneiss, and quartzite. It includes undifferentiated marble, calc-silicate rocks, and amphibolite of the calc-silicate unit. These rocks are well exposed along the northern base of Sinkut Mountain. Rocks of this unit are distinguished from the Frank Lake pluton by their better developed foliation, generally finer grain size, and well developed heterolithic layering. Contacts with other units of the Vanderhoof gneiss are gradational or intrusive. Contacts with overlying units are faults and the basal contact was not seen.

The biotite schist is dark grey to black and weathers rusty brown. It consists of biotite (30%-50%, 2-3 mm) with the remainder of the rock composed of feldspar, quartz, and hornblende in various proportions. Biotite hornblende gneiss (gradational with amphibolite) consists of 10-25% biotite and 5-20% 1-2 mm hornblende.

The quartz feldspar gneiss is light brown and weathers rusty brown. It consists of feldspars (40-60% 0.2-2 mm), biotite (4-20%), and quartz. Quartzites are dark grey to light grey and weather rusty brown. They contain 4-15% feldspar and 5-10% biotite. Layers of these rock units are between 3 mm to several metres thick.

### Calcic Vanderhoof gneiss

This unit occurs throughout the area of the Vanderhoof Metamorphic Complex from Sinkut Mountain southeastward through Grizzly Lake (Fig. 2). Three lithologies characterize this unit: marbles, calc-silicate rocks, and amphibolites. The best exposures are found north of Sinkut Mountain and southeast of Arctic Lake. Nowhere is the full unit well exposed. The unit occurs within the siliciclastic unit, possibly high in the sequence. Contacts with the siliciclastic unit are not exposed, but are inferred to be gradational as amphibolite

layers are found with the siliciclastic rocks. The upper contact at Sinkut Mountain is a low angle fault (further described in section on structure).

Marbles in these gneiss units are white and consist of calcite and minor diopside, grossular, phlogopite, and plagioclase. Generally, the calcite is coarsely crystalline (2-5 mm), with the accessory minerals rarely larger than 1.5 mm.

Calc-silicate rock weathers grey and is greyish-green on fresh surfaces. It is usually poorly layered consisting of very fine grained tremolite, calcite, diopside, grossular, epidote, and occasionally some quartz. Thin units of this rock can be found flanking some of the marble or amphibolite outcrops.

The amphibolites are grey-green on weathered surfaces and dark grey-green when fresh. They consist of finely crystalline hornblende, biotite, and plagioclase with some finer grained lenses, and layers of plagioclase, diopside, epidote, ±grossular. They are interlayered with the marble and calc-silicate rock. In these rocks the aligned mica and amphibole define the primary foliation which is locally crenulated and locally has a secondary crenulation cleavage. The metamorphic facies appears to be near lower amphibolite and perhaps higher in grade.

Within this unit are possible metabasaltic amphibolite exposed southwest of Grizzly Lake (Fig. 2) and at the northernmost tip of the Telegraph Range in 93G/6. Both exposures are similar in appearance and in mineral assemblage, and are not associated with marble or calc-silicate rock. Lenses and veinlets of calc-silicate material occur within these amphibolites and these form outlines of what may have been interpillow material of a pillow basalt. These rocks are intruded by the Frank Lake pluton and the Barton Lake granite and in the Telegraph Range appear to be faulted against Cache Creek ultramafic rocks.

The metabasalt weathers grey and has dark green fresh surfaces. Minerals within the unit consist of long dark green amphibole (80-90% 0.2-3 mm), with fine grained epidote and plagioclase (10-20%). Primary foliation is defined by aligned amphibole.

The age of the calcic unit is inferred from intrusive relations. It is older than the Mesozoic or Permian plutonic units that intrude it (Wheeler and McFeely, 1991). The unit structurally underlies the Carboniferous to Triassic Cache Creek Group. With no other information the unit's age is interpreted as upper Paleozoic.

## STRUCTURE

### *Tertiary units*

The Chilcotin Group basalt units are everywhere nearly flat lying, and appear undeformed. Miocene sedimentary rocks are mostly flat lying to shallowly dipping. Early Tertiary Ootsa Lake Group volcanic rocks are steep to shallowly dipping, and are locally sheared by dextral strike-slip faults.

Deformation of the Cache Creek Group rocks varies substantially by composition. Ultramafic rocks show little foliation, although they are tilted and cut by shear zones. In places the ultramafic rocks have lenses of closely spaced minor shears and joints with attitudes at high angles to the regional structures. Cache Creek basalt, limestone, and slate have a well developed foliation. The ribbon chert beds are disrupted by irregular boudinage and disruption of folds.

Gneiss of the Vanderhoof Metamorphic Complex is generally shallowly dipping throughout the west and has steeper dips in the Grizzly Lake area to the southeast. Foliations in the paragneiss are generally parallel to layering and are defined by biotite and hornblende mineral alignment and by flattening of quartz and feldspar crystals. Dismembered interfolial folds developed during and after formation of the foliation. Mineral lineations are common, generally parallel to stretching directions of quartz. Crenulations of the regional foliation occur locally and are common in the Grizzly Lake area, with shear bands and shear folds.

Orthogneiss of the Vanderhoof complex ranges in texture from weakly foliated granites to augen mylonite. Stretching lineations are common and locally the rocks are L-tectonites; mostly they exhibit some degree of flattening. Deformation in the orthogneiss increases toward higher structural levels. At Frank Lake the Frank Lake pluton has a weak foliation. To the east the deformation increases, and at Arctic Lake and northward to Sinkut Ridge it has a well developed foliation, is flattened and locally mylonitic. Orthogneiss intrudes the various paragneiss units of the Vanderhoof Metamorphic Complex.

### Sinkut detachment

On Sinkut Mountain, sheared amphibolite and interlayered quartzofeldspathic gneiss directly underlie Cache Creek ultramafic rocks in a 4 m thick gouge zone overlain by 3 m of sheared but coherent ultramafics. Rotational extensional shear fabric in the amphibolite indicates a top to the southeast sense of motion (Fig. 5). We infer this contact to represent an

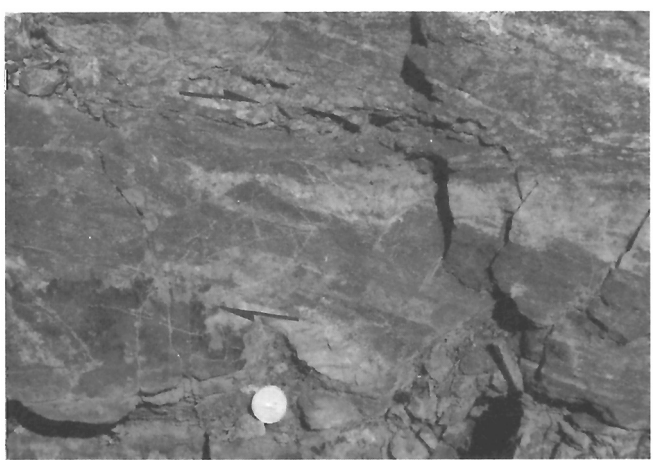

***Figure 5.*** *Shear structures in amphibolite of the Vanderhoof Complex directly under the fault contact with ultramafic rocks of the Cache Creek Group on Sinkut Mountain. Motion is top to the right (east-southeast), as indicated by half arrows.*

extensional detachment fault, and that the Vanderhoof Metamorphic Complex was uplifted during regional crustal extension. The Cache Creek Group lies wholly within the upper plate of the extensional structure.

The Vanderhoof gneiss directly beneath the contact with the Cache Creek Group ultramafic rocks is everywhere highly sheared and the orthogneiss is mylonitized. The placement of brittle gouge of the upper plate rocks onto the ductile mylonitic fabric of the lower plate is typical of extensional complexes. The juxtaposition of low grade metamorphic rocks of the Cache Creek Group onto higher grade rocks of the Vanderhoof Metamorphic Complex is also typical of extensional complexes.

## CONCLUSIONS

Vanderhoof Metamorphic Complex consists of a biotite quartzofeldspathic and marble/amphibolite paragneiss sequence intruded by mainly biotite and granite and granodiorite orthogneiss. Paragneisses of the complex have a fine grained siliciclastic rock, limestone, marl, and possibly basalt protoliths. Those protoliths are distinct from the Cache Creek Group. This sequence is structurally overlain by the Carboniferous to Triassic Cache Creek Group. The Vanderhoof Complex appears to represent the metamorphic core of an extensional complex, of which the Cache Creek Group in this area forms the upper plate, and the Sinkut Detachment forms the primary extensional detachment fault.

## ACKNOWLEDGMENTS

Dick Armstrong recognized the extensional tectonic significance of the Vanderhoof Gneiss more than a decade ago. Rich Friedman kindly shared unpublished information on isotopic age dates he obtained from orthogneiss in the area. Claire Floriet and Bryan Traub provided excellent assistance in the field.

## REFERENCES

**Bellefontaine, K.A., Legun, A., Massey, N., and Desjardins, P.**
1995: Digital Geological Compilation of northeast B.C. - southern half (NTS 83D, E, 93F, G, H, I, J, K, N, O, P); British Columbia Ministry of Energy Mines and Petroleum Resources, Open File 1995-24.

**Cordey, F. and Struik, L.C.**
1996: Scope and preliminary results of radiolarian biostratigraphic studies, Fort Fraser (93K) and Prince George (93G) map areas, central British Columbia; in Current Research 1996-A; Geological Survey of Canada.

**Orchard, M.J. and Struik, L.C.**
1996: Conodont biostratigraphy, lithostratigraphy, and correlation of the Cache Creek Group Fort St. James, British Columbia; in Current Research 1996-A; Geological Survey of Canada.

**Struik, L.C. and McMillan, W.J.**
1996: Nechako Project Overview, central British Columbia; in Current Research 1996-A; Geological Survey of Canada.

**Tipper, H.W.**
1961: Prince George map area, British Columbia; Geological Survey of Canada, Preliminary Map 49-1961.
1963: Nechako River map area, British Columbia; Geological Survey of Canada, Map 1131A.

**Tipper, H.W., Campbell, R.B., Taylor, G.C., and Stott, D.F.**
1979: Parsnip River, British Columbia, Sheet 93; Geological Survey of Canada, Map 1424A.

**Wheeler, J.O. and McFeely, P.**
1991: Tectonic assemblage map of the Canadian Cordillera and adjacent parts of the United States of America; Geological Survey of Canada, Map 1712A.

Geological Survey of Canada Project 950036

# Geology near Fort St. James, central British Columbia[1,2]

L.C. Struik, C. Floriet[3], and F. Cordey[4]
GSC Victoria, Vancouver

*Struik, L.C., Floriet, C., and Cordey, F., 1996: Geology near Fort St. James, central British Columbia; in Current Research 1996-A; Geological Survey of Canada, p. 71-76.*

**Abstract:** The Cache Creek Group rocks of the Fort St. James area (93K) have been differentiated into Upper Paleozoic and Mesozoic suites. The Mesozoic rocks include greywacke, siltstone, argillite, limestone, and basalt tuff previously mapped as part of the Takla Group. Fine grained clastic rocks west of Stuart Lake may also be mainly of Triassic and possibly Early Jurassic age. The Cache Creek limestone (here called Mount Pope sequence limestone) is probably thrust onto Triassic ribbon cherts.

**Résumé :** Les roches du Groupe de Cache Creek de la région de Fort St. James (93K) ont été divisées en suites du Paléozoïque supérieur et du Mésozoïque. Les roches mésozoïques incluent du grauwacke, du siltstone, de l'argilite, du calcaire et du tuf basaltique, antérieurement assignés au Groupe de Takla. Les clastites à grain fin observées à l'ouest du lac Stuart pourraient également être des roches datant principalement du Trias et peut-être du Jurassique précoce. Le calcaire de Cache Creek (appelé, dans le cas présent, calcaire de la séquence de Mount Pope) chevauche probablement des cherts rubanés du Trias.

[1] Contribution to the Nechako NATMAP project
[2] This is a joint mapping project of the Geological Survey of Canada and British Columbia Geological Survey Branch.
[3] Department of Geological Sciences, University of British Columbia, 6339 Stores Road, Vancouver, British Columbia V6T 2B4
[4] #311-1080 Pacific Street, Vancouver, British Columbia V6E 4C2

## INTRODUCTION

As part of the Nechako NATMAP project new bedrock geological mapping has begun in the Fort Fraser map area in British Columbia (NTS 93K, Fig. 1; Struik and McMillan, 1996). The work will result in a revised and more detailed 1:250 000 scale map. The area was first regionally mapped by Armstrong (1949), and subsequently has had a thorough remapping of its surficial deposits (Plouffe, 1994 and maps in progress). Several localities have been studied by the British Columbia Geological Survey Branch, university graduate students, and mineral exploration industry.

The following descriptions and preliminary interpretations are from examinations in the vicinity of Fort St. James.

## GEOLOGY

Rocks examined during this first phase of mapping have been included in the Cache Creek, and Takla groups, and some younger intrusions (Fig. 2, 3). They consist of limestone, basalt (flows, breccias, tuffs), chert, ultramafic rocks, serpentinite, greywacke, siltstone, and slate. Feldspar porphyry and diorite intrude these rocks as dykes and plutons.

These rocks are part of assemblages that outcrop along the length of the Cordillera (Wheeler and McFeely, 1991). They represent oceanic and island arc suites obducted onto the North American margin during the Mesozoic (Paterson, 1973) and are included in the Cache Creek and Stikine terranes.

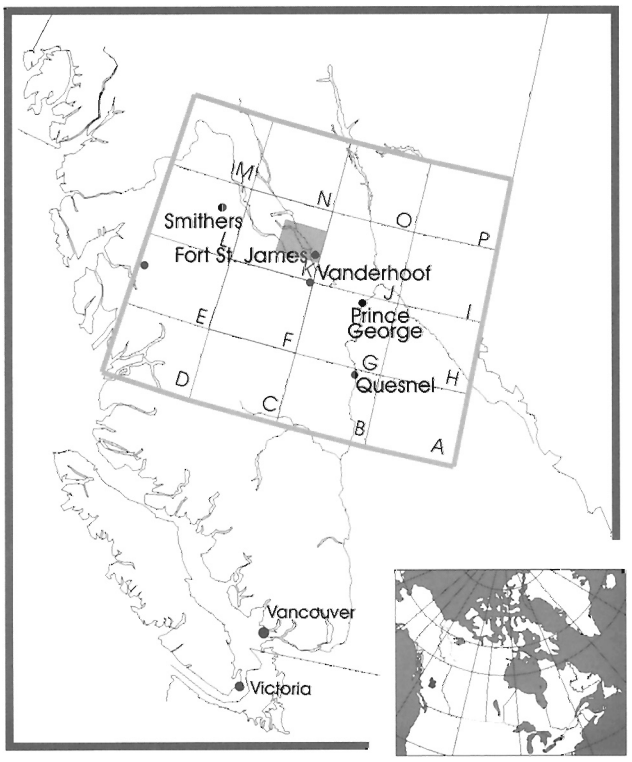


*Figure 1. Location of the study area in relation to surrounding NTS maps of the Parsnip River (93) 1:1 000 000 scale map.*

This work builds on the regional mapping of Armstrong (1949) and the detailed mapping of Paterson (1973) and Ash et al. (1993). Those works should be referred to for more complete descriptions and distributions of some of the rock units described here.

For this publication, rocks mapped as Takla Group along the south side of Pinchi Lake will be included in the Cache Creek Group. Cache Creek Group of the Fort St. James area will be divided into six units, most of which are informal designations. They include: Mount Pope sequence undifferentiated basalts, Trembleur ultramafics, Railway gabbro, Sowchea sequence, and Pinchi sequence. These rocks will not be described in detail here. An overview of their characteristics and age will be given for a background to the two new features determined for these rocks.

### *Upper Paleozoic*

#### Mount Pope sequence (PTCCl)

Mount Pope sequence consists mainly of light grey weathering, light brown-grey and grey micrite and bioclastic limestone. Interlayered with the limestone in a few places are thin basalt breccia and ribbon chert units. The best exposures are at Mount Pope where a nearly continuous section can be mapped from the shore of Stuart Lake to the top of the mountain (Fig. 2). Locally the limestone shows bedding generally defined by accumulations of bioclasts (crinoids and fusulinids). Mostly the limestone is massive except where it is partly silicified and the silica follows compositional layers (Fig. 4). The unit is more than 800 m thick.

The age of the limestone has been previously determined as Pennsylvanian and Permian from fusulinids and conodonts (Dawson, 1878; Armstrong, 1942, 1949; Thompson, 1965; Paterson, 1973; M.J. Orchard in Struik, 1994). Orchard and Struik (1996) describe new conodont fauna from the unit in this same map area.

#### Undifferentiated basalt

Cache Creek Group basalt near Fort St. James is mainly olive, aphanitic to finely crystalline, massive to breccia. Some of the breccia fragments are tinged with maroon and the matrix can be olive or maroon. In places the basalts are altered by hydrothermal influxes of carbonate. The fine crystals are plagioclase and some pyroxene.

A single layer of basalt breccia (10-40 m thick) is interlayered with the Mount Pope limestone near its base on the southwest side of Mount Pope. At the old bridge over the Stuart River, at Highway 27, basalt is interlayered with thin limestone beds rich in crinoidal debris. Basalt breccia, perhaps the same unit as southwest of Mount Pope, occurs interbedded with Mount Pope sequence limestone to the north of Mount Pope at the junction of the Tachie road and the forest service road heading north to Pinchi Lake just east of the

Pinchi Creek. An easily accessible exposure of typical massive aphanitic basalt underlies the observation platform at the golf course west of Fort St. James.

### Trembleur ultramafic

Armstrong (1942, 1949) and Paterson (1973) mapped these rocks as harzburgites and peridotites. Locally they are layered cumulates, and invariably have been partly altered to serpentinite. They occur as fault bounded blocks surrounded by other units of the Cache Creek Group. Ash et al. (1993) divided these rocks into crustal and mantle representatives.

### Railway gabbro (PTCCv)

Gabbro underlies a narrow belt along the south side of Pinchi Lake. The gabbro is intimately mixed with basalt and microgabbro, and all those rocks are crosscut by numerous veins and veinlets of plagioclase and cryptocrystalline quartz. The best exposures are found on the ridge just south of the B.C. Rail line, south of Pinchi Lake and east of Pinchi Creek. These rocks were mapped as "Basic rocks south of Pinchi Lake" by Paterson (1973). Paterson suggested the gabbro basalt sequence was unconformably overlain by upper Triassic limestone and volcaniclastics to the north, and possibly underlain by ultramafic rocks to the south.

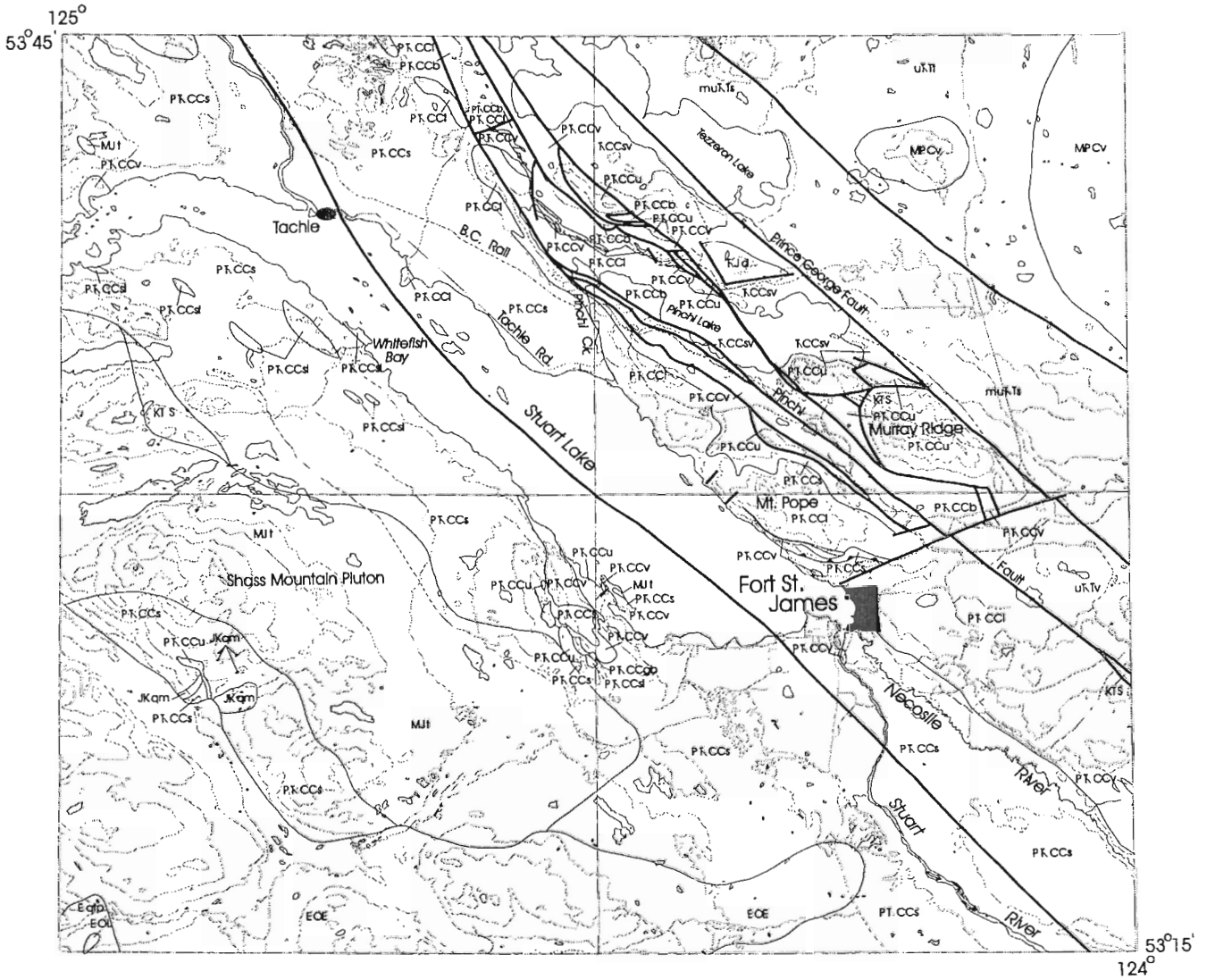


***Figure 2.*** *Geological reference map of the area near Fort St. James modified from Bellefontaine et al. (1995) to include some of the geological interpretations from this project. Solid thin lines are approximate and assumed bedrock geological contacts, and thick lines are approximate and assumed faults. For legend see Figure 3.*

The gabbro and basalt are locally crosscutting although individual rocks in the area exhibit a complete spectrum of textural variation between them. The gabbro is dark green and has medium to fine crystals of nearly equal proportions of plagioclase and hornblende (0.5-2 mm). The hornblende is an alteration product of augite, and epidote and chlorite are locally abundant. Some of the rock is very magnetic.

The basalt is dark olive and weathers rusty brown, and generally aphanitic to felted with sub-millimetre size plagioclase. In most places it is massive, and in the northeastern most exposures near the railway line is a breccia (5-25 mm clasts). In places the basalt is highly altered, having cavity fillings and veins rich in chlorite and epidote.

**Miocene and Pliocene**

MPCv *Chilcotin Group:* olivine basalt

**Eocene**

EOE *Endako Group:* basalt, andesite, minor gabbro

EOL *Ootsa Lake Group:* rhyolite, dacite, andesite

Eqfp rhyolite porphyry dykes

**Cretaceous and Tertiary**

KTS *Sifton Formation:* conglomerate, sandstone siltstone, shale, coal (10)

**Jurassic and Cretaceous**

*Francois Intrusions* (JKqm - JKg)

JKqm hornblende-biotite quartz monzonite

JKg granite, granodiorite

**Jurassic**

MJt tonalite, diorite (11)

**Triassic and Jurassic**

TRJd diorite (11)

**Triassic**

*Takla Group* (uTRTt, muTRTs)

uTRTt tuff, cherty tuff, siliceous argillite

uTRTv basalt

muTRTs argillite, greywacke, siltstone, shale, minor limestone, tuff, basalt

*Cache Creek Group* (TRCCsv - PT CCvs)

TRCCsv *Pinchi Sequence:* greywacke, siltstone, slate, basalt tuff, minor limestone, siliceous argillite (8)

**upper Carboniferous to Triassic**

*Sowchea Sequence* (PTRCCs - P TRCCsl)

PTRCCs argillite, chert, siltstone, phyllite, sandstone, limestone, basalt (5,6)

PTRCCsl limestone, greenstone, chert (7)

PTRCCl *Pope formation:* limestone, greenstone, chert (7)

PTRCCv basalt, minor limestone, argillite, chert (4)

PTRCCgb *Railway Gabbro:* grabbro, diorite, peridotite, hornblendite, pyroxenite (3)

PTRCCu *Trembleur Ultramafics:* serpentinite, harzburgite, dunite, peridotite, carbonatized equivalents (1,2)

PTRCCb blueschist (chert, schist, greywacke, metabasalt, limestone)

***Figure 3.*** *Legend to the geological map of Figure 2.*

### *Mesozoic (mainly Middle and Upper Triassic)*

#### Sowchea sequence (PTRCCs and PTRCCsl)

This unit underlies a large area mainly to the southwest of Stuart Lake. The rocks consist of siltstone, slate, chert, limestone, and lesser amounts of greywacke. Locally these rocks are interbedded with intraformational conglomerates and breccias. Most of the fine grained sediments are very siliceous, ranging from cherty argillites and slates to muddy cherts. Rocks of the unit are grey to dark grey and thinly bedded, and are commonly disrupted by bedding parallel and nearly bedding parallel slip. Typical of these clastic rocks are the easily accessible outcrops at the west end of the Sowchea Bay Provincial Park on Stuart Lake.

Ribbon cherts form lenses within the mainly finely clastic units. In most places to the south of Stuart Lake these chert beds are recrystallized. Better preserved, yet highly disrupted beds of ribbon chert are exposed along the shore of Stuart Lake and roadcuts just to the northwest of Fort St. James. At the Stuart Lake Sailing Club they are interbedded with siltstone and intraformational siltstone conglomerates (Cordey and Struik, 1996). A roadcut on the road along the north shore of Stuart Lake leading from Fort St. James to the Stuart Lake Lodge exposes highly disrupted cherts in fault contact to the west with Mount Pope sequence limestone.

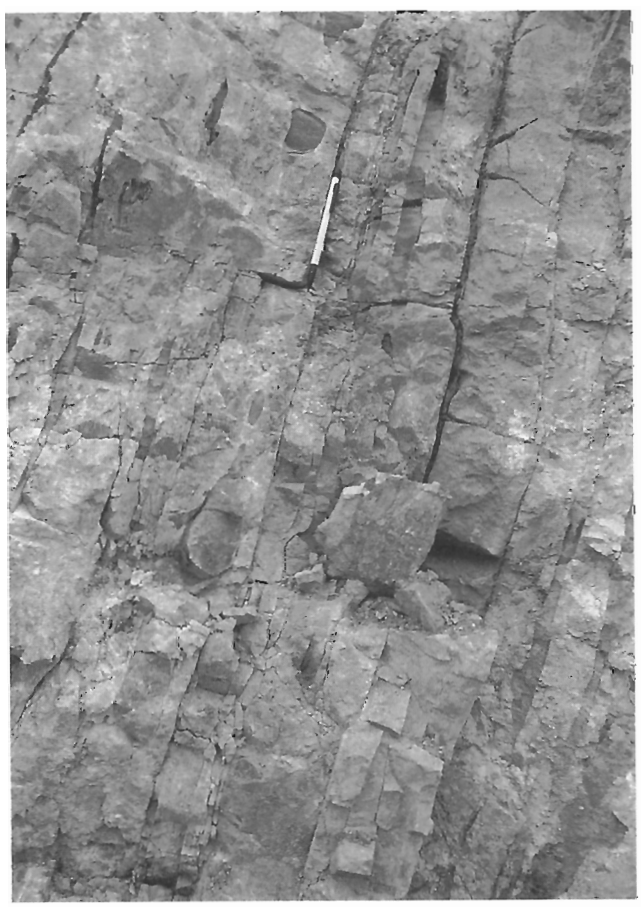

***Figure 4.*** *Silification layering in the Mount Pope sequence limestone to the east of Fort St. James.*

In the north near White Fish Bay the unit contains limestone and limestone conglomerate beds. Flattened pebble and granule size clasts in the limestone matrix consist of slate and cherty slate. The limestone and conglomerate are interbedded with 1-4 m beds of siltstone and intraformational conglomerate.

The age of the Sowchea sequence is in part Triassic as it includes ribbon cherts near the Stuart Lake Sailing Club that have yielded Triassic radiolaria (Cordey and Struik, 1996), and ribbon chert on the Stuart Lodge road that contain Triassic (Norian) conodonts (Orchard and Struik, 1996). Poorly preserved radiolaria extracted from siliceous argillites of the sequence west of Stuart Lake appear to form a Triassic faunal assemblage (Cordey and Struik, 1996).

### Pinchi sequence (ŦCCsv)

These rocks are exposed on either side of Pinchi Lake. They consist of greywacke, chert sandstone, siltstone, slate, basalt tuff, and minor limestone. Good exposures of this sequence are found west of Murray Ridge and between the B.C. Rail line and Pinchi Lake (Fig. 2). This sequence was mapped by Armstrong (1949) and Paterson (1973) as Takla Group, and by Bellefontaine et al. (1995) as Cache Creek Group. Paterson interpreted the unit to unconformably overlie the Railway gabbro.

The greywacke is composed of plagioclase, augite, chert, and rounded volcanic rock fragments (0.2-2 mm) and is gradational with the chert sandstone. Locally the finer grained beds are graded. Beds are generally thin (2-70 mm), and have even contacts.

The basalt tuff is brown-weathering, dark olive and consists of finely crystalline plagioclase and augite (1-2.5 mm), and at the top of the sequence is an augite porphyry agglomerate. The tuff also contains some rounded chert and minor granitic clasts of sand and granule size, and rare wood twig fragments. The chert granules have visible radiolaria.

The limestone is light grey-weathering, grey and dark grey, occurs as thin units and locally contains colonial corals, crinoid fragments, and pelecypods (Paterson, 1973). In places it weathers brown where it forms thin interbeds with greywacke and limestone matrix conglomerate. The limy conglomerate contains fragments of basalt. Paterson (1973) lists a point count of the fragments from this conglomerate as basalt (50%), chert (45%), and gabbro (5%). He describes intraformational limestone conglomerate from this unit that is very similar to limestone conglomerate found to the west of Whitefish Bay on western Stuart Lake (Fig. 2). Those conglomerates are included in the Sowchea sequence.

These rocks are very similar to clastic assemblages of the upper part of the Cache Creek Group in Yukon Territory (Cache Creek Group assemblage 3 of Gordey and Stevens, 1994) and in southern British Columbia (Shannon, 1982; Monger, 1985). This similarity and the absence of chert clast-bearing volcaniclastics in the Takla Group is why we include these rocks with the Cache Creek Group.

The age of the Pinchi sequence is determined from *Monotis* and coral fossils indicative of an Upper Triassic age (Armstrong, 1949; Paterson, 1973). These rocks are here correlated with the Sowchea sequence and other Triassic Cache Creek Group sedimentary sequences in the Cordillera.

### Shass Mountain Pluton

Quartz diorite and tonalite underlies a large area around Shass Mountain and occurs as smaller bodies throughout the area west of Stuart Lake. These rocks contain biotite and hornblende and have been dated at 165 +2/-1 Ma (Ash et al., 1993).

## *Mesozoic or Tertiary*

### Sailing Club dyke

Biotite plagioclase-porphyry felsite intrudes the Sowchea sequence at the Stuart Lake Sailing Club. The dyke is approximately 1-3 m thick and forms a tight curve. The rock may be of Tertiary age. It is definitely post-Triassic – the age of the cherts that it intrudes.

## STRUCTURES AND METAMORPHISM

The Sowchea sequence is tightly folded and occurs in overturned folds asymmetric to the northeast. This style of deformation is typical of much of the sedimentary sequences throughout the Cache Creek Group in the area. Disruption of bedding by irregular boudinage and dismembering of folds is common in interbedded sequences of ribbon chert and muddy and silty clastics (Fig. 5). Where sequences of chert are preserved they show tight chevron style folds, with well developed cleavage in the slate interbeds (Fig. 6).

***Figure 5.*** *Disrupted ribbon chert in siltstone and argillite matrix, from the Sowchea sequence at the Stuart Lake Sailing Club marina near Fort St. James.*

*Figure 6. Fold and cleavage style of interbedded chert and slate from Cache Creek Group rocks northwest of Vanderhoof, British Columbia. Chert beds are the resistant and poorly cleaved ones.*

The Mount Pope Limestone forms broad open folds and is in shallow fault contact with underlying ribbon cherts in a roadcut along the Stuart Lodge road. The cherts have been dated as Triassic to the southeast (Cordey and Struik, 1996; Orchard and Struik, 1996). This relationship would place the older (Pennsylvanian and Permian) Mount Pope sequence limestone onto younger ribbon cherts, and therefore the fault is interpreted as a thrust (Fig. 2).

Most of the rocks have been regionally metamorphosed to low greenschist and locally to greenschist facies. Contact metamorphic recrystallization and hornfels are typical of rocks surrounding the Shass Mountain Pluton and its equivalents. To the north along the Pinchi Fault, blueschist facies are exposed (Paterson, 1973): they have not been re-examined during this study.

## CONCLUSIONS

Rocks in the Fort St. James area have been included in the Cache Creek Group and divided into Upper Paleozoic and Mesozoic units. Rocks formerly included in the Triassic Takla Group are here assigned to the Cache Creek Group. Most of the sedimentary rocks of the area appear to be of Triassic and possibly early Jurassic age whereas the Mount Pope limestone, much of the basalt, gabbro, and ultramafic rocks are late Paleozoic. The ribbon chert sequences may be either Paleozoic or Mesozoic age. The dated cherts are Triassic. The Mount Pope Limestone is probably thrust onto the Sowchea sequence near Fort St. James.

## ACKNOWLEDGMENTS

Discussions with Jim Monger, Mike Orchard, and a field trip with Steve Gordey to the Cache Creek Group in Teslin map area (Struik) and one with Ian Paterson to the Cache Creek Group north of Pinchi Lake have been very useful in guiding the mapping project and deciphering the intricacies of the Cache Creek Group.

## REFERENCES

**Armstrong, J.E.**
1942: The Pinchi Mercury Belt; Geological Survey of Canada, Paper 42-11.
1949: Fort St. James map-area, Cassiar and Coast districts, British Columbia; Geological Survey of Canada, Memoir 252.

**Ash, C., MacDonald, R.W.J., and Paterson, I.A.**
1993: Geology of the Stuart and Pinchi Lakes area, central British Columbia (93K); British Columbia Ministry of Energy Mines and Petroleum Resources, Open File 1993-9.

**Bellefontaine, K.A., Legun, A., Massey, N., and Desjardins, P.**
1995: Digital geological compilation of northeast B.C. – southern half (NTS 83D, E, 93F, G, H, I, J, K, N, O, P); British Columbia Ministry of Energy Mines and Petroleum Resources, Open File 1995-24.

**Cordey, F. and Struik, L.C.**
1996: Scope and preliminary results of radiolarian biostratigraphic studies, Fort Fraser and Prince George map areas, central British Columbia; in Current Research 1996-A; Geological Survey of Canada.

**Dawson, G.M.**
1878: Report on explorations in British Columbia, chiefly in the basins of the Blackwater, Salmon, and Nechako Rivers, and on Francois lake; Geological Survey of Canada, Report of Progress 1876-1877, pt. III, p. 17-54.

**Gordey, S.P. and Stevens, R.A.**
1994: Tectonic framework of the Teslin region, southern Yukon Territory; in Current Research 1994-A; Geological Survey of Canada, p. 11-18.

**Monger, J.W.H.**
1985: Structural evolution of the southwestern Intermontane Belt, Ashcroft and Hope map areas, British Columbia; in Current Research, Part A; Geological Survey of Canada, Paper 85-1A, p. 349-358.

**Orchard, M.J. and Struik, L.C.**
1996: Conodont biostratigraphy, lithostratigraphy, and correlation of the Cache Creek Group near Fort St. James, British Columbia; in Current Research 1996-A; Geological Survey of Canada.

**Paterson, I.A.**
1973: The geology of the Pinchi Lake area, central British Columbia; PhD. thesis, University of British Columbia, Vancouver, British Columbia, 263 p.

**Plouffe, A.**
1994: Surficial geology of the Tezzeron Lake; Geological Survey of Canada, Open File 2846.

**Shannon, K.R.**
1982: Cache Creek Group and contiguous rocks,, near Cache Creek, British Columbia; MSc. thesis, University of British Columbia, Vancouver, British Columbia, 72 p.

**Struik, L.C.**
1994: Geology of the McLeod Lake map area, central British Columbia; Geological Survey of Canada, Open File 2439.

**Struik, L.C. and McMillan, W.J.**
1996: Nechako Project Overview, central British Columbia; in Current Research 1996-A; Geological Survey of Canada.

**Thompson, M.L.**
1965: Pennsylvanian and Early Permian fusulinids from Fort St. James area, British Columbia, Canada; Journal of Paleontology, v. 39.

**Wheeler, J.O. and McFeely, P.**
1991: Tectonic assemblage map of the Canadian Cordillera and adjacent parts of the United States of America; Geological Survey of Canada, Map 1712A.

Geological Survey of Canada Project 950036

# Conodont biostratigraphy, lithostratigraphy, and correlation of the Cache Creek Group near Fort St. James, British Columbia[1, 2]

M.J. Orchard and L.C. Struik
GSC Victoria, Vancouver

*Orchard, M.J. and Struik, L.C., 1996: Conodont biostratigraphy, lithostratigraphy, and correlation of the Cache Creek Group near Fort St. James, British Columbia; in Current Research 1996-A; Geological Survey of Canada, p. 77-82.*

**Abstract:** An extensive north-northwestward trending belt of Cache Creek Group limestone in the central Canadian Cordillera has been re-examined near Fort St. James. These carbonates are informally referred to the Mount Pope sequence. New conodont fauna extracted from these rocks are largely Upper Carboniferous (Bashkirian and Moscovian) with some Triassic (Norian) fauna recovered from chert. The youngest conodonts recovered to date from the massive limestones are very similar to those from the northern Cache Creek Group, but are slightly older than the oldest known conodonts from the type area in southern B.C. Although much of the fauna from the limestones of Mount Pope sequence is shallow water in origin, conodont biofacies and lithological features suggest that much of the macroscopic bioclastic material has been transported into the basin and deposited in laminar beds that accumulated in deeper water adjacent to the carbonate buildup.

**Résumé :** Une vaste bande d'orientation nord-nord-ouest, composée de calcaires du Groupe de Cache Creek et se trouvant dans le centre de la Cordillère canadienne, a fait l'objet d'une nouvelle analyse près de Fort St. James. Ces roches carbonatées sont désignées informellement «séquence de Mount Pope». De nouvelles faunes de conodontes extraites de ces roches datent principalement du Carbonifère supérieur (Bashkirien et Moscovien) et certaines faunes provenant de cherts remontent au Trias (Norien). À ce jour, les conodontes les plus jeunes récupérés des calcaires massifs sont très semblables à ceux observés dans la partie septentrionale du Groupe de Cache Creek; ils sont cependant légèrement plus anciens que les conodontes les plus vieux connus, provenant de la région type dans le sud de la Colombie-Britannique. Même si le plus gros de la faune des calcaires de la séquence de Mount Pope est d'origine épicontinentale, les biofaciès des conodontes et les caractéristiques lithologiques indiquent qu'une grande partie du matériau bioclastique macroscopique a été transportée vers le bassin et déposée dans des couches laminaires qui se sont accumulées en eau plus profonde, dans les zones adjacentes aux édifices carbonatés.

[1] Contribution to the Nechako NATMAP Project
[2] This is a joint mapping project of the Geological Survey of Canada and British Columbia Geological Survey Branch.

## INTRODUCTION

Thick bioclastic limestone units characterize the Cache Creek Terrane in central and southern Canadian Cordillera (Fig. 1). In central British Columbia, Cache Creek Group limestone forms a narrow, nearly continuous belt extending from near Vanderhoof, north-northwestward to the north end of Takla Lake. Previous macrofossil and fusulinid collections from the limestone have dated it as Late Carboniferous and Permian (Dawson, 1878; Armstrong, 1942, 1949; Thompson, 1965; Paterson, 1973; Struik, 1994). Some of the fusulinid fauna have Tethyan affinity and hence constrain the paleogeography of the unit (Monger and Ross, 1971). The lithological association of the limestone with oceanic basalts and ribbon cherts, and its characteristic fauna, suggest the limestone originated as a shallow water carbonate atoll in an oceanic setting. A similar setting is envisaged for correlative massive limestones of the Cache Creek Group in southern British Columbia (Marble Canyon Formation) (Dawson, 1878; Armstrong, 1942; Monger and Ross, 1971; Paterson, 1973), and northern British Columbia (Monger and Ross, 1971).

Conodont samples were first collected from the Fort St. James area on a reconnaissance basis by Orchard in 1985. Additional material was collected by Struik in 1988 during regional mapping of the McLeod Lake (93J) and Fort Fraser (93K) map areas. These faunas and the general character of the limestone unit from which they were extracted are here described, and the age of the suite discussed.

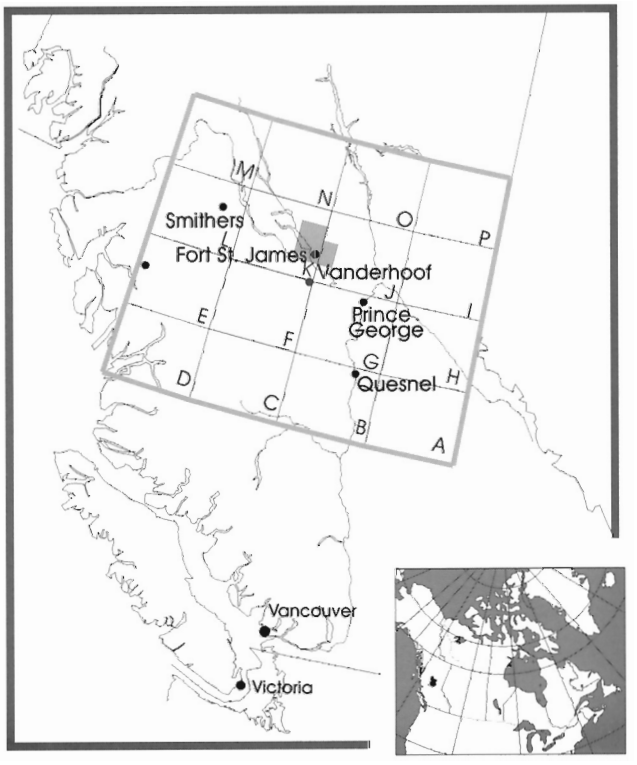


***Figure 1.*** *Regional geographic setting of the Fort St. James area. The grid represents 1:1 000 000 map of Parsnip River (NTS 93). The shaded area is shown enlarged in Figure 2.*

## GEOLOGY

### *Mount Pope sequence*

The Mount Pope sequence consists mainly of limestone with minor amounts of undifferentiated basalt, chert, and phyllite. Its type area is on Mount Pope northwest of the southern end of Stuart Lake, near Fort St. James (Fig. 2, 3). These rocks have been referred to by previous workers as the limestone of Mount Pope. The thickness of the sequence is unknown, but is estimated from interpretation of the regional structure to be approximately 1 km. It has been previously mapped by Dawson (1878), Armstrong (1942, 1949), and Paterson

**Miocene and Pliocene**

MPCv — *Chilcotin Group:* olivine basalt

**Eocene**

EOE — *Endako Group:* basalt, andesite, minor gabbro

EOL — *Ootsa Lake Group:* rhyolite, dacite, andesite

Eqfp — rhyolite porphyry dykes

**Cretaceous and Tertiary**

KTS — *Sifton Formation:* conglomerate, sandstone siltstone, shale, coal (10)

**Jurassic and Cretaceous**

*Francois Intrusions* ( JKqm - JKg )

JKqm — hornblende-biotite quartz monzonite

JKg — granite, granodiorite

**Jurassic**

MJt — tonalite, diorite (11)

**Triassic and Jurassic**

TRJd — diorite (11)

**Triassic**

*Takla Group* ( uTRTt , muTRTs )

uTRTt — tuff, cherty tuff, siliceous argillite

uTRTv — basalt

muTRTs — argillite, greywacke, siltstone, shale, minor limestone, tuff, basalt

*Cache Creek Group* ( TRCCsv - PTRCCvs )

TRCCsv — *Pinchi Sequence:* greywacke, siltstone, slate, basalt tuff, minor limestone, siliceous argillite (8)

**upper Carboniferous to Triassic**

*Sowchea Sequence* ( PTRCCs - PTRCCsl )

PTRCCs — argillite, chert, siltstone, phyllite, sandstone, limestone, basalt (5,6)

PTRCCsl — limestone, greenstone, chert (7)

PTRCCl — *Pope formation:* limestone, greenstone, chert (7)

PTRCCv — basalt, minor limestone, argillite, chert (4)

PTRCCgb — *Railway Gabbro:* grabbro, diorite, peridotite, hornblendite, pyroxenite (3)

PTRCCu — *Trembleur Ultramafics:* serpentinite, harzburgite, dunite, peridotite, carbonatized equivalents (1,2)

PTRCCb — blueschist (chert, schist, greywacke, metabasalt, limestone)

***Figure 2.*** *Legend.*

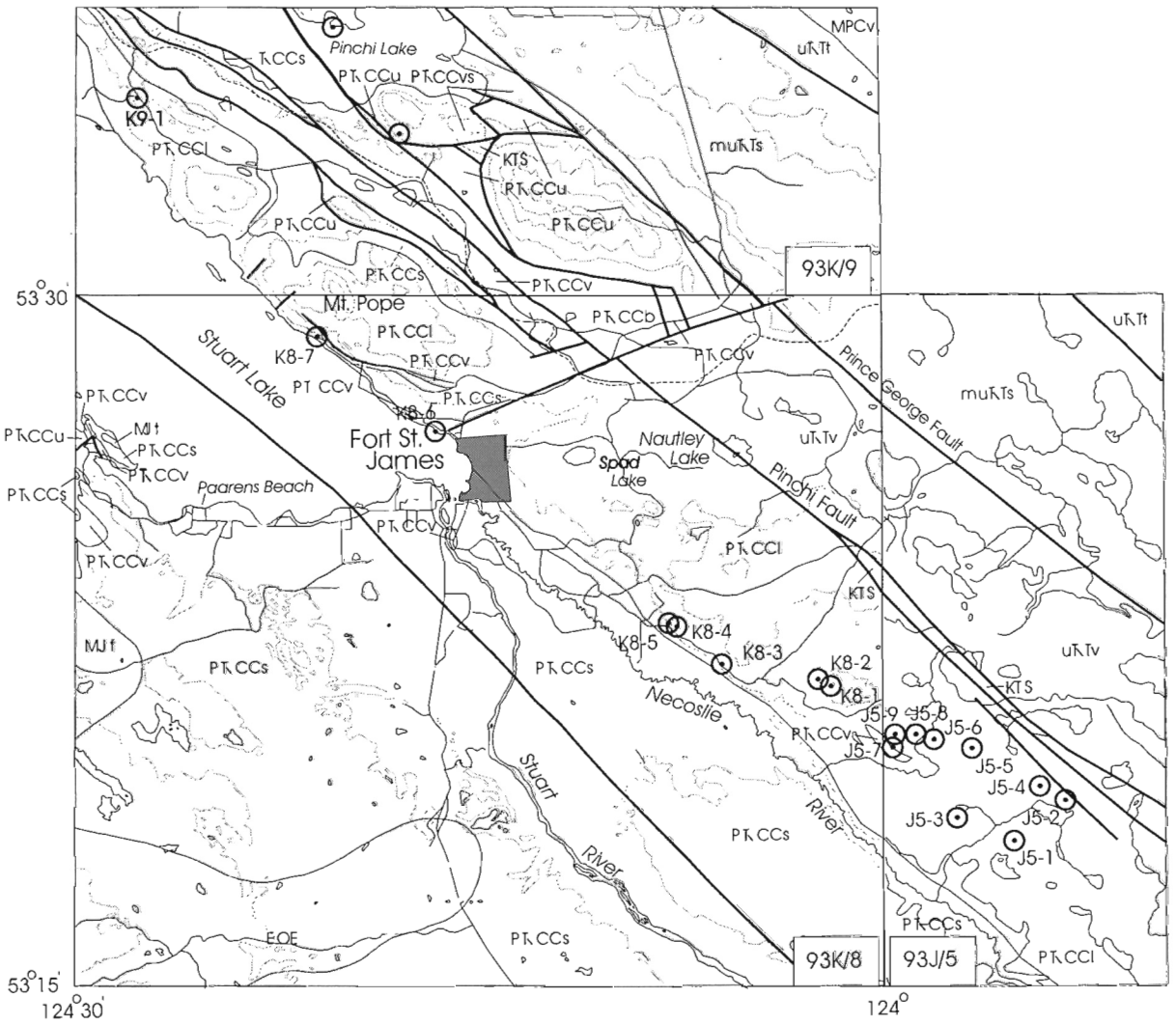


***Figure 2.*** *Geological setting of the Mount Pope sequence near Fort St. James and the location of conodont faunas shown by circled dots. Quadrangle 93K/8 is part of the Fort Fraser map area, 93J/5 is of McLeod Lake map area. The numbers in the legend refer to the unit designations of Ash et al. (1993), and the base map is modified from Bellefontaine et al. (1995).*

(1973) as part of the Cache Creek Group. It can be differentiated from other limestones in the area by its association with ribbon chert and basalt, and by its massive nature and common occurrence of medium- to small-sized crinoid fragments and lesser fusulinids.

The limestone weathers light grey and varies from grey to light grey and light brownish-grey on fresh surfaces. It consists mainly of zones of cryptocrystalline calcite with massive areas of bioclastic and clastic limestone. The bioclasts (1-25 mm, 4-30%) consist of crinoid stem fragments and lesser amounts of fusulinid, coral, bryozoan, and brachiopod fragments, together with laminar algal structures. The fusulinids are invariably found in the clastic and bioclastic carbonate rather than the micrite. Limestone clasts (5-30 mm, 5-10%) with fine grained ooids and bioclasts are found intermixed with the bioclasts in some locations

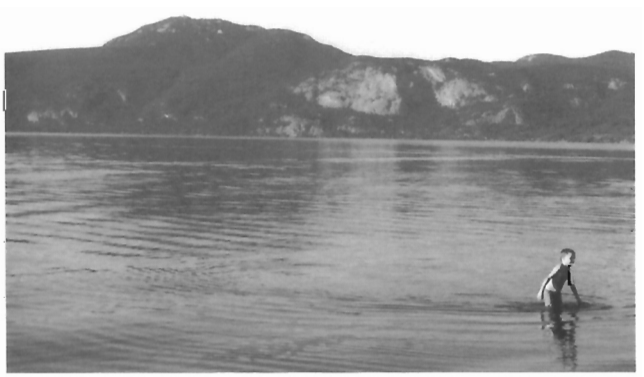

***Figure 3.*** *Mount Pope looking to the north across Stuart Lake from the Paarens Beach Provincial Park.*

(see also Paterson, 1973; for an extended description of this limestone). Layering is very obscure and could not be detected in many exposures.

The limestones of the Mount Pope sequence are locally dolomitized and silicified with dolomite crystals (0.5-1 mm) replacing the cryptocrystalline calcite matrix. In places the crinoid debris remains as calcite and the matrix is completely replaced by dolomite. In such places moulds of the crinoids are preserved by the dolomite matrix. Silicification occurs parallel to original bedding and as irregular lenses. It commonly is associated with dolomitization. The silica is cryptocrystalline and light grey to grey. In places the limestone is invaded by veins of varying proportions of calcite, limonite, quartz, and chlorite. Brecciated limestone is common within some of the larger vein systems such as displayed in the quarry south of Spad Lake (Fig. 2).

The limestone is interpreted as having formed mainly from debris flows, based on the presence of unsorted massive bioclasts and clasts, and the absence of well defined beds and in situ fossils. The flows may have occurred in shallow water just below wave base. The algal laminae, which support a shallow water interpretation, may have formed during periods of calm weather, low water, and little to no clastic input.

Dark grey to black ribbon chert and phyllite sequences are found within some of the limestone. Where the contacts of these units with the limestone are seen, they are sharp and locally associated with fault gouge. The chert beds (3-6 cm thick) are separated by thin partings of phyllite. Many of the sequences are disrupted and little of the original bedding structure is preserved as continuous layers.

Basalt breccia occurs in beds apparently deposited within the limestone sequence underlying Mount Pope. These beds are thin and locally discontinuous. The breccia consists of purple and green, aphanitic and plagioclase-felted, angular to subangular basalt fragments with common calcareous, and locally quartzose interstitial filling. The fragments are from 0.5-4 cm across. In some places the basalt contains numerous small irregularly shaped amygdules filled with silica and carbonate. The basalt layers, which are from 10-30 m thick, are interpreted to have been deposited within a carbonate mud sequence because of the abundance of calcite matrix. Similar, though coarser grained basalt breccia and agglomerate underlies limestone of the Mount Pope sequence at site J5-7 (Fig. 2).

## CONODONT FAUNA

To date, 22 conodont collections have been recovered from the Cache Creek Group in the Fort Fraser-McLeod Lake area of central B.C. This summary provides a preliminary overview of these conodont collections. All but one collection originate in the belt of limestones southwest of the Pinchi Fault (Fig. 2), with 13 from within Fort Fraser map area (93K), and 9 within McLeod Lake map area (93J). Preservation of the conodonts is poor to good, with CAI (Colour Alteration Index) values typically in the range 3.5-4.5, implying postdepositional temperatures in the range of 150-300°C. Over half of the collections are insufficient to provide high resolution dating. Of the remainder, most are of Late Carboniferous age, and a few are Triassic.

The oldest conodont fauna recovered to date comes from Mount Pope (Fig. 2, K8-7). This fauna, which was not collected in place, is dominated by *Idiognathodus* sp(p)., which outnumbers co-occurring *Adetognathus lautus* (Gunnell 1931) by about 3:1. The latter species is about twice as abundant as *Idiognathoides convexus* (Ellison and Graves 1941), and the remainder of the fauna consists of fewer *Streptognathodus expansus* Igo and Koike 1964 and *Hindeodus* sp. The age of this collection is Bashkirian (Morrowan). Other collections made from near the exposed base of the limestone at Mount Pope, and from isolated outcrops further to the northwest (K9-1), contain relatively few specimens of *Adetognathus* and *Hindeodus*, and may be either contemporaneous with the first collection, or as young as Early Permian. Both these latter taxa are indicative of relatively shallow water environments.

A collection (K8-2) from near the eastern edge of Fort Fraser map area differs from the Mount Pope fauna in containing *Idiognathoides sinuatus* (Harris and Hollingsworth 1933) and *Neognathodus* sp. in a ratio of about 5:1. This fauna is also judged to be Bashkirian in age, but is both slightly younger (?Atokan) than the Mount Pope fauna, and representative of less restricted environment. *Adetognathus* does not occur in any of the collections from the Necoslie River area of Fort Fraser, and *Hindeodus* is rare. The smaller collections from this area (Fig. 2, K8-1, -3, -5) also contain *Idiognathoides* and *Idiognathodus*, but can only be dated at present as Bashkirian-Moscovian.

Along strike in McLeod Lake map area, several relatively large and diverse conodont collections have been recovered. As at Mount Pope, *Idiognathodus* is the dominant genus, and similar to those collections from immediately to the west, *Neognathodus* is well represented. *Idiognathoides*, common in Fort Fraser, occurs only in the two southernmost collections. The notable feature of the McLeod Lake collections is the occurrence of species of *Gondolella* and *Neogondolella*, taxa that are regarded as indicative of a relatively deep and/or offshore marine setting. This contrasts with the *Adetognathus*-bearing faunas further northwest. In McLeod Lake, *Neogondolella clarki* (Koike 1967), occurs in two collections (J5-3, -6), *Gondolella laevis* Kosenko & Kozitskaya 1975 occurs in three collections (J5-1, -6, -7), and *Gondolella* ex gr. *magna* Stauffer & Plummer 1932 occurs in two collections (J5-1, -8). The first two species appear in the Atokan in North America, whereas the third species is no older than Desmoinesian. In Eurasian terms, the suite of conodont collections from the Mount Pope sequence in McLeod Lake map area includes both Bashkirian and Moscovian faunas.

Although Permian strata are well documented on the basis of fusulinaceans in the Cache Creek limestones of Fort Fraser (see below), these strata have yet to produce conodont fauna. The youngest conodonts recovered from the Cache Creek Group in the Fort Fraser region come from ribbon chert outcropping on the shores of Stuart Lake (K8-6). The collection

includes *Epigondolella* and *Neogondolella*, and is dated as Norian in age. To the north, a collection from carbonate on the south side of Pinchi Lake (Paterson, 1973) contains the same conodont genera, and is also Norian.

## OTHER FAUNA

In the past, fossil control on the Cache Creek Group in Fort Fraser map area has been largely based on fusulinids. Armstrong (1949) described several localities for these fossils, and Thompson (1965) described many new fusulinid taxa. In the area of Mount Pope, Thompson (1965) described both Late Carboniferous and Early Permian (Wolfcampian) fusulinids, and Armstrong (1949, p. 45) noted a Carboniferous coral. According to these authors, the Upper Carboniferous fauna in the area of Figure 2 consists of species of *Akiyoshiella, Eoschubertella, Fusulina, Fusulinella, Millerella, Nankinella, Paramillerella, Profusilinella?, Pseudostaffella, Schuburtella,* and *Staffella*, whereas the Lower Permian faunas include species of *Oketaella, Pseudoschwagerina, Quasifusulina, Schubertella,* and *Triticites*. The only published account of Upper Permian fusulinids from Fort Fraser describes material from near Trembleur Lake, where *Cancellina, Misellina, Neoschwagerina, Parafusulina,* and *Verbeekina* are recorded from a succession of limestones (Armstrong, 1949, p. 45). Modern study and reappraisal of the fusulinid faunas has been undertaken in a preliminary way by Ross and Ross (in Carter et al., 1991, Table 2.1, column 9).

Most of the fossils recorded from the Cache Creek Group within the area of Figure 2 are Upper Carboniferous fusulinids, but in adjoining Manson River map area (NTS 93N), Armstrong (1949, p. 46) also recorded (Late) Carboniferous brachiopods, bryozoans, corals, and gastropods, and Permian brachiopods. None of these are well studied. In siliceous strata of the Cache Creek Group, Permian and Triassic radiolarian faunas are also known (Cordey and Struik, 1996).

## FAUNAL COMPARISONS

As summarized by Ross and Ross (in Carter et al., 1991), the fusulinid fauna of the Cache Creek Group has a distinctive Tethyan aspect, suggesting that it originated in the tropical part of the Panthalassa ocean. Biogeographic differentiation of the faunas increased through the late Paleozoic as plate motions modified migration routes. At the present time, it is not obvious that any of the Carboniferous conodont faunas are biogeographically restricted, although this might be anticipated more at the species level, and is likely to be more pronounced in Permian collections.

In terms of stratigraphic range, it is noteworthy that all the conodonts from the Cache Creek Group in Fort Fraser-McLeod Lake, with the exception of the Triassic ones, are older than those described from the Marble Canyon Formation of the southern Cache Creek Group (Orchard, 1984; Beyers and Orchard, 1991). The only Paleozoic faunal comparison that is currently possible with the Cache Creek Group in its type area is with the conodonts of the carbonate olistoliths that occur within the eastern belt of the southern area, that is the Melange Unit. Two conodont faunas are recognized in that belt: one with *Idiognathodus* and *Gondolella* ex gr. *magna* of Late Carboniferous age, and a Lower Permian association (Orchard, 1984; Orchard and Danner, 1991). The late Carboniferous fauna has elements in common with the youngest of the McLeod Lake conodont faunas, but lacks the older species of *Gondolella* and *Neogondolella*, and is therefore probably slightly younger. There is no indication at present that thick Lower Triassic (Spathian) limestone, such as occurs in the Marble Canyon Formation, is developed in the Fort St. James area. In common with Fort Fraser, ribbon cherts in southern Cache Creek basin are also Norian.

Comparisons are more readily made with the northern Cache Creek Group near Atlin-Teslin. The oldest conodont faunas recovered from that region are Early Carboniferous (Serpukovian) in age and predate all those recovered to date from Fort Fraser. However, in common with the latter, most recovered conodont faunas from the northern Cache Creek Group are Late Carboniferous in age. They include representatives of *Idiognathodus, Idiognathoides, Neognathodus,* and *Diplognathodus*. Many of these taxa are conspecific with those in the Fort Fraser area. As in central British Columbia, the Permian conodont faunas of the north are not yet known. Upper Triassic, including Rhaetian, conodonts are known from chert (Orchard, 1986, 1991; Cordey et al., 1991).

## CONCLUSIONS

Conodont collections so far recovered from the Mount Pope sequence and correlative thick limestones of the Cache Creek Group in Fort Fraser-McLeod Lake represent several levels within the Bashkirian-Moscovian stages of the Late Carboniferous. The youngest correlate broadly with the oldest conodont faunas known from the southern Cache Creek Group, although the latter are only known from olistoliths. Permian comparisons between the two areas are not yet possible. No Lower Triassic carbonates such as those that occur in the Marble Canyon Formation in the south are yet identified. In common with the entire Cache Creek Terrane, Upper Triassic ribbon cherts occur within the Cache Creek Group.

Many of the Upper Carboniferous conodont faunas are diverse and probably represent deeper water environments than the other faunal elements. This supports the notion that much of the limestone of the Mount Pope sequence accumulated after downslope transportation.

## ACKNOWLEDGMENTS

We thank Pete Forster and Clare Floriet for assistance in the field. Sue Walsh helped in the compilation of archival fossil data from Fort St. James. Jim Haggart provided a useful review of the manuscript.

## REFERENCES

**Armstrong, J.E.**
1942: The Pinchi Mercury Belt; Geological Survey of Canada, Paper 42-11.
1949: Fort St. James map-area, Cassiar and Coast districts, British Columbia; Geological Survey of Canada, Memoir 252.

**Ash, C., MacDonald, R.W.J., and Paterson, I.A.**
1993: Geology of the Stuart and Pinchi Lakes area, central British Columbia (93K); British Columbia Ministry of Energy Mines and Petroleum Resources, Open File 1993-9.

**Bellefontaine, K.A., Legun, A., Massey, N., and Desjardins, P.**
1995: Digital geological compilation of northeast B.C. – southern half (NTS 83D, E, 93F, G, H, I, J, K, N, O, P); British columbia Ministry of Energy Mines and Petroleum Resources, Open File 1995-24.

**Beyers, J.M. and Orchard, M.J.**
1991: Upper Permian and Triassic conodont faunas from the type area of the Cache Creek Complex, south-central British Columbia; in Ordovician to Triassic Conodont Paleontology of the Canadian Cordillera, (ed.) M.J. Orchard and A.D. McCracken; Geological Survey of Canada, Bulletin 417, p. 269-298.

**Carter, E.S., Orchard, M.J., Ross, C.A., Ross, J.R.P., Smith, P.L., and Tipper, H.W.**
1991: Part B, Paleontological Signatures of Terranes; in Chapter 2 of Geology of the Cordilleran Orogen in Canada, (ed.) H. Gabrielse and C.J. Yorath; Geological Survey of Canada, Geology of Canada, no. 4 (also Geological Society of America, The Geology of North America, v. G-2).

**Cordey, F. and Struik, L.C.**
1996: Scope and preliminary results of radiolarian biostratigraphic studies, Fort Fraser and Prince George map areas, central British Columbia; in Current Research 1996-A; Geological Survey of Canada.

**Cordey, F., Gordey, S.P., and Orchard, M.J.**
1991: New biostratigraphic data for the northern Cache Creek Terrane, Teslin map-area, southern Yukon; in Current Research, Part E; Geological Survey of Canada, Paper 91-1E, p. 67-76.

**Dawson, G.M.**
1878: Report on explorations in British Columbia, chiefly in the basins of the Blackwater, Salmon, and Nechacco rivers, and on Francois Lake; Geological Survey of Canada, Report of Progress 1876-1877, pt. III, p. 17-94.

**Monger, J.W.H. and Ross, C.A.**
1971: Distribution of the Fusulinaceans in the western Canadian Cordillera; Canadian Journal of Earth Sciences, v. 8, p. 259-278.

**Orchard, M.J.**
1984: Pennsylvanian, Permian and Triassic conodonts from the Cache Creek Group, Cache Creek, Southern British Columbia; in Current Research, Part B; Geological Survey of Canada, Paper 84-1B, p. 197-206.
1986: Conodonts from Western Canadian chert: their nature, distribution and stratigraphic application; in Conodonts, Investigative Techniques and Applications, (ed.) R.L. Austin; Proceedings of the Fourth European Conodont Symposium (ECOS IV), Chapter 5, p. 96-121. Ellis-Horwood, Chichester, England.
1991: Conodonts, time and terranes: an overview of the biostratigraphic record in the western Canadian Cordillera; in Ordovician to Triassic Conodont Paleontology of the Canadian Cordillera, (ed.) M.J. Orchard and A.D. McCracken; Geological Survey of Canada, Bulletin 417, p. 1-26.

**Orchard, M.J. and Danner, W.R.**
1991: The paleontology of the Cache Creek Terrane; in A Field Guide to the Paleontology of Southwestern Canada, (ed.) P.L. Smith; Canadian Paleontology Conference I, Vancouver, British Columbia, p. 169-202.

**Paterson, I.A.**
1973: The geology of the Pinchi Lake area, central British Columbia; PhD. thesis, University of British Columbia, Vancouver, British Columbia, 263 p.

**Struik, L.C.**
1994: Geology of the McLeod Lake map-area (93J), British Columbia; Geological Survey of Canada, Open File 2439.

**Thompson, M.L.**
1965: Pennsylvanian and Early Permian fusulinids from Fort St. James area, British Columbia, Canada; Journal of Paleontology, v. 39, p. 224-234.

Geological Survey of Canada Project 950036

# Scope and preliminary results of radiolarian biostratigraphic studies, Fort Fraser and Prince George map areas, central British Columbia[1,2]

F. Cordey[3] and L.C. Struik
GSC Victoria, Vancouver

*Cordey, F. and Struik, L.C., 1996: Scope and preliminary results of radiolarian biostratigraphic studies, Fort Fraser and Prince George map areas, central British Columbia; in Current Research 1996-A; Geological Survey of Canada, p. 83-90.*

**Abstract:** As part of the new Nechako NATMAP project, radiolarian biostratigraphic investigations started in the Fort Fraser (93K) and Prince George (93G) map areas in central British Columbia. Their scope is to provide control on the age and structures of the Cache Creek Group and related units. Eighty samples of radiolarian chert, siliceous mudstone, and chert clasts have been collected. Preliminary chemical processing confirms radiolarians from ribbon chert strata near Fort St. James, and undated siliceous mudstone of the Sowchea sequence. Six chert pebbles from a Cretaceous conglomerate near Pinchi Lake released well preserved associations ranging in age from Middle Triassic (late Anisian-Ladinian) to Late Triassic (late Carnian, early-middle Norian, late Norian/Rhaetian). Similar associations are known within the Cache Creek Group in southern British Columbia and Yukon Territory.

**Résumé :** Des travaux sur la biostratigraphie des radiolaires ont été entrepris dans le cadre du nouveau projet du CARTNAT dans la région de Nechako (feuillets de Fort Fraser, 93K, et de Prince George, 93G). Leur but est de circonscrire l'âge et établir la structure du Groupe de Cache Creek et des autres unités de la région. Quatre-vingts échantillons de chert à radiolaires, de mudstone siliceux et de clastite cherteuse ont été prélevés. Une phase préliminaire de traitement chimique confirme la présence de radiolaires au sein des cherts rubanés de la région de Fort St. James ainsi que des mudstones silicieux de la séquence de Sowchea. L'analyse de six galets de chert extraits d'un conglomérat crétacé, près du lac Pinchi, a permis de dégager des associations variant en âge du Trias moyen (Anisien tardif-Ladinien) au Trias tardif (Carnien tardif-Rhétien). Des associations semblables sont connues au sein du Groupe de Cache Creek, dans le sud de la Colombie-Britannique et au Yukon.

[1] Contribution to the Nechako NATMAP Project
[2] This is a joing mapping project of the Geological Survey of Canada and British Columbia Geological Survey Branch
[3] 311-1080 Pacific Street, Vancouver, British Columbia V6E 4C2; e-mail: fabrice_cordey@mindlink.bc.ca

## SCOPE OF WORK

As part of the Nechako NATMAP mapping project, new bedrock geological mapping has started in the Fort Fraser map area (93K) (Struik et al., 1996), one of the least known areas of the Cache Creek terrane. In conjunction with this new project, radiolarian biostratigraphic investigations have been undertaken in the area, and to a minor extent in Prince George map area (93G) (Fig. 1).

We hope to improve the stratigraphy of the Cache Creek Group and related units in the region, as well as the understanding of structural relationships within and between these units. Dating of chert clasts from local breccia and conglomerates is expected to yield information on origin of source rocks and potential tracking of missing stratigraphic record. This research utilizes radiolarian techniques applied to oceanic terranes in other regions of the Canadian Cordillera.

The segment of the Cache Creek terrane exposed in Fort Fraser and Prince George map areas is midway between the southern and northern parts of the terrane in southern British Columbia and northern British Columbia/southern Yukon, where radiolarian biostratigraphy has been applied on Paleozoic and Mesozoic oceanic strata (Cordey et al., 1987, 1991; Cordey and Read, 1992). Data from those areas will serve for comparisons with Fort Fraser and Prince George areas. In addition, biostratigraphic results from central British Columbia are expected to provide new information on paleogeographic and paleoenvironmental settings within the Cache Creek belt as a whole.

A further aspect of the radiolarian study is to date chert clasts found in several units of the area. In the Canadian Cordillera, clasts contain radiolarian associations that are commonly better preserved than those found in situ within correlative units (Cordey, in press). In addition to providing information on potential source rocks, some of these chert-bearing clastics locally contain fragments of chert strata no longer exposed. In Fort Fraser map area, Late Jurassic and Middle Cretaceous plutonism have affected large areas of the Cache Creek Group whose local equivalents may be found within clastic units.

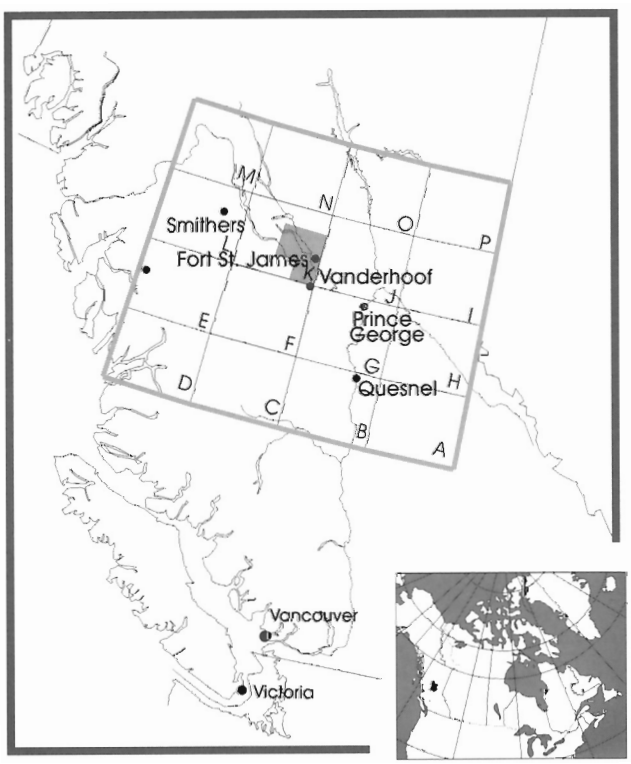


***Figure 1.*** *Location of the field area. The letters define the NTS maps within the 1:1 000 000 Parsnip River map area (93A-P). Fort Fraser map area is 93K.*

## PREVIOUS WORK

The Cache Creek Group in Fort St. James region is exposed along a zone that has been called the Stuart Lake belt by Armstrong (1949). In the belt, three main lithological divisions were identified: (1) limestone, (2) ribbon chert, and (3) greenstone. Within the ribbon chert division, Armstrong (1949) recognized occurrences of ribbon chert, slate, and argillaceous quartzite, in places interstratified with schistose greywacke and conglomerate, as well as intercalated bodies of greenstone. Ribbon chert strata was estimated at a minimum total thickness of 1500 m.

The age of the Cache Creek Group in Fort Fraser has been determined by dating the limestone division with fusulinids and conodonts (Orchard and Struik, 1996, and references therein), but until recently, no age control was known from the ribbon chert division, interpreted as Paleozoic in age based on spatial associations with the limestone (Armstrong, 1949). Only three chert localities dated by Late Triassic conodonts and radiolarians were previously established (Cordey, 1990; Orchard and Struik, 1996). We expect a more complete outcome from the present study, as radiolarian-bearing strata from other areas of the Cache Creek terrane range in age from Pennsylvanian to Early Jurassic (Cordey, in press, and references therein). In Ashcroft (92I) map area (southern British Columbia), chert is Early Permian to Late Triassic in age, along with Early or Middle Jurassic siliceous argillite (Cordey et al., 1987). In Taseko Lakes (92O) area, chert of Early Permian to Early Jurassic age is conformably overlain by Early Jurassic siliceous mudstone (Cordey and Read, 1992). In Atlin (104N) and Teslin (105C) map areas of northern British Columbia and southern Yukon, radiolarian cherts range in age from Pennsylvanian to Early Jurassic, including a wide area of exposure of Middle and Late Triassic ribbon chert interbedded with fine- and coarse-grained siliceous clastic rocks of Late Triassic and Early Jurassic age (Orchard, 1986; Cordey et al., 1991; Gordey and Stevens, 1994).

Following Davies' (1918) hypothesis, Armstrong (1949) interpreted the depositional origin of Cache Creek cherts in Fort St. James area as related to volcanic activity, due to spatial association of ribbon chert with greenstone. Recent models derive the ribbon chert from the accumulation of

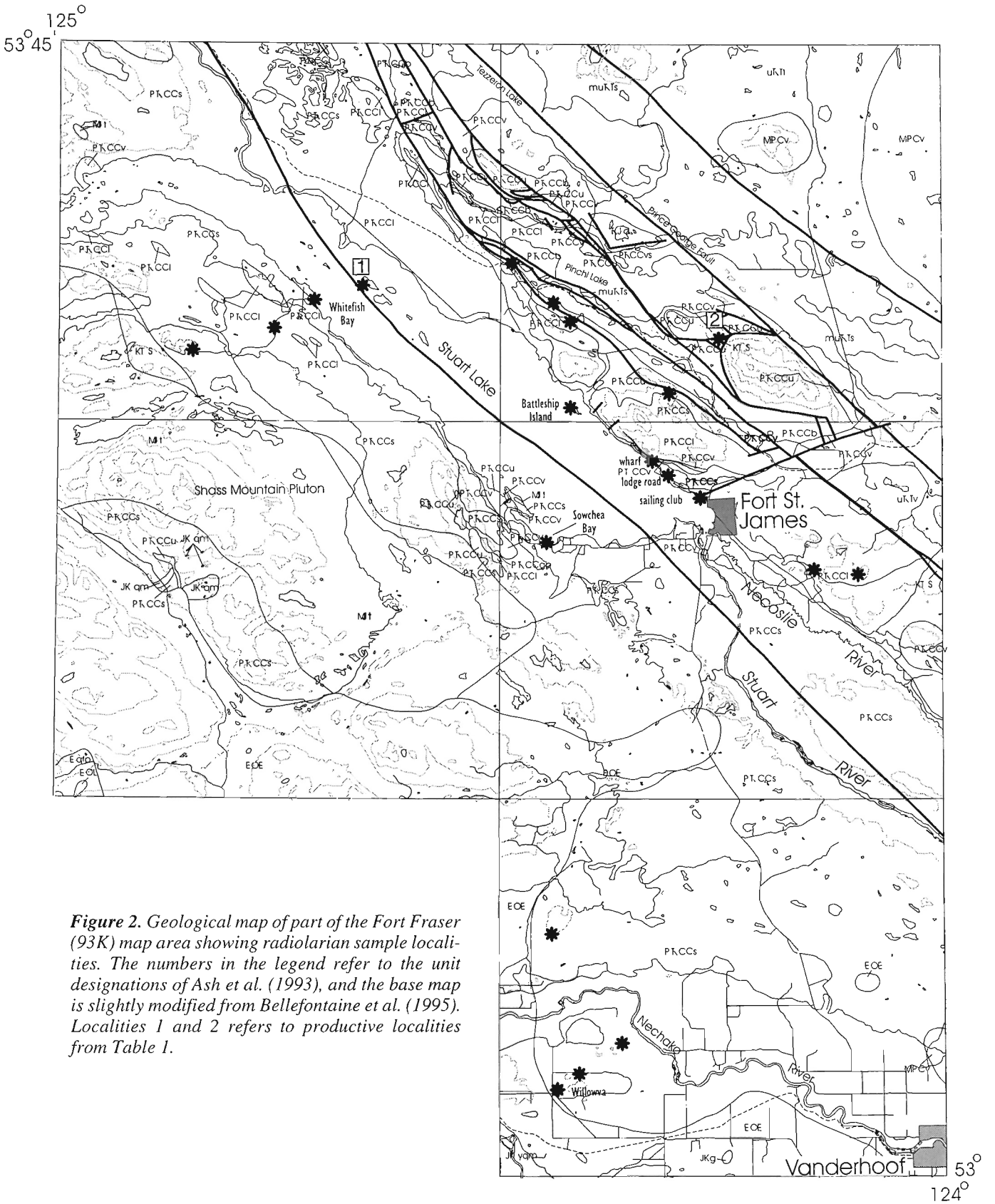


***Figure 2.*** *Geological map of part of the Fort Fraser (93K) map area showing radiolarian sample localities. The numbers in the legend refer to the unit designations of Ash et al. (1993), and the base map is slightly modified from Bellefontaine et al. (1995). Localities 1 and 2 refers to productive localities from Table 1.*

radiolarian shells directly related to oceanic surficial planktonic productivity, independent from volcanic input (Cordey, in press, and references therein).

## METHOD AND TECHNIQUES

Eighty samples of chert, siliceous mudstone, and chert clasts were collected during the 1995 field season. Main areas of sampling are located in Figure 2. Rocks at these localities were examined using field techniques of radiolarian detection and selection. Within ribbon chert sequences, radiolarians are visible when present but their preservation varies significantly from bed to bed. Shells are commonly harder to detect within dark-coloured clastic sedimentary rocks such as siliceous mudstone or slate, but their occurrence was confirmed locally in fine grained or cherty layers.

Following fieldwork, a first phase of chemical processing was undertaken and preliminary results are presented herein. Samples were processed with 4 to 8% hydrofluoric acid (HF) solutions during variable amount of time ranging from 12 to 48 hours.

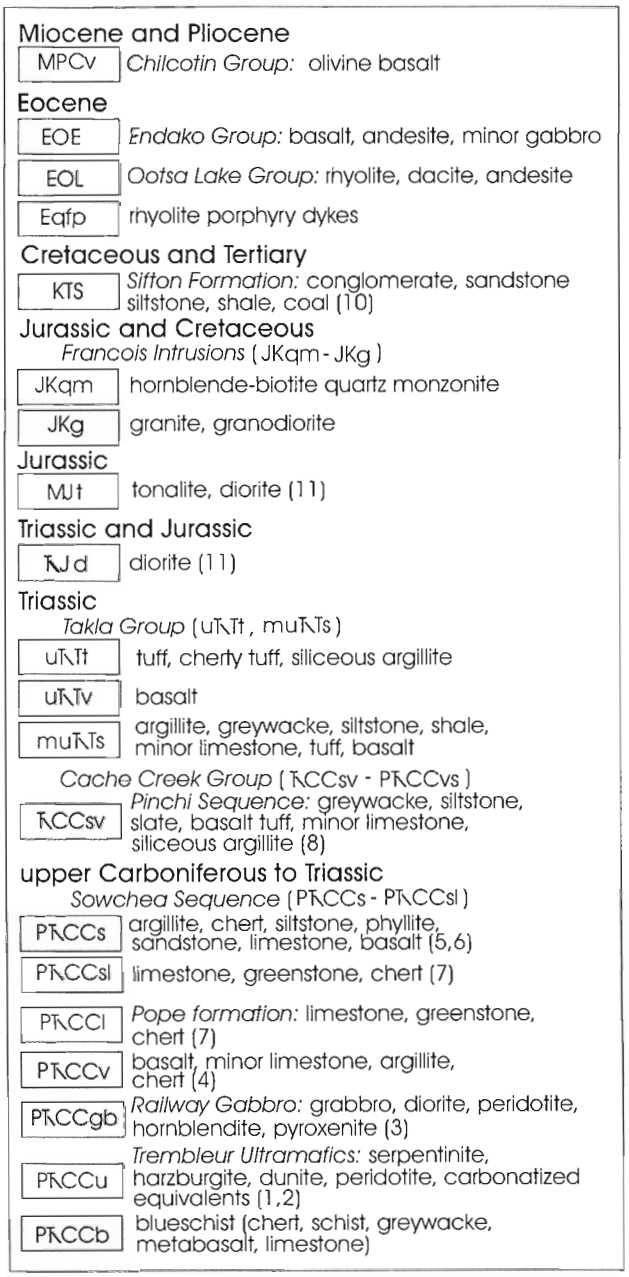


***Figure 2.*** *Legend*

## SAMPLED UNITS AND PRELIMINARY RESULTS

In Fort St. James area, radiolarian-bearing rocks consist of three types: 1) ribbon chert, 2) siliceous mudstone, and 3) chert clasts. These rocks were sampled from various units within the Cache Creek Group, although they are primarily from units 5, and 6 of Ash et al. (1993) (Fig. 2). The chert clasts were mainly from unit 8 (Ash et al., 1993).

### *Ribbon chert*

Ribbon chert is the dominant rock type within the Stuart Lake belt of the Cache Creek Group (Armstrong, 1949). More recently, it has been established as characteristic of unit 5 of Ash et al. (1993). Consistent with these previous surveys, the principal areas of exposure of ribbon chert are: 1) Fort St. James area, 2) south-central side of Stuart Lake, and 3) north shore of the North Arm of Stuart Lake. Chert exposures near Fort St. James are referred to as the Stuart Lodge cherts (Struik et al., 1996). In southern Fort Fraser map area, Cache Creek Group ribbon chert has been sampled on both sides of the Nechako River (Fig. 2).

***Figure 3.*** *Exposure of the Stuart Lodge cherts on the Stuart Lodge road near Fort St. James. Disruption shown by faulting and folding is characteristic of Cordilleran ribbon chert units.*

Ribbon chert of the map area is dominantly grey or blue-grey, with local variations to light green, light grey, or black. Chert layers vary from 1 to 10 cm thick, with an average of 3 or 4 cm. They are separated by shale or schist partings of 0.2 to 5 cm thick. Locally, the chert layers are uneven in thickness, differentiating themselves into egg-shaped nodules, a feature of uncertain diagenetic or tectonic origin; similar shapes are observed within chert pebbles from local conglomerates.

As is common elsewhere in the accreted terranes of the Canadian Cordillera, the ribbon chert sequences are folded and faulted (Fig. 3). Locally, "flat" chevron folds duplicate the beds (Fig. 4). Cleavage bedding relationships within the chert and interlayers of schist are locally sufficiently developed to determine the orientation of fold asymmetries. Chert is typically more highly folded and faulted than adjacent lithologies, but it is unclear if it is due to stratigraphic unconformities and/or tectonic juxtaposition, or a distinct tectonic behaviour related to the incompetent, thinly-bedded sedimentary structure of ribbon chert.

A framework of thick quartz joints and thin veinlets are common. In certain zones of the map area, particularly near major plutonic bodies like Shass Mountain pluton (Fig. 2), the

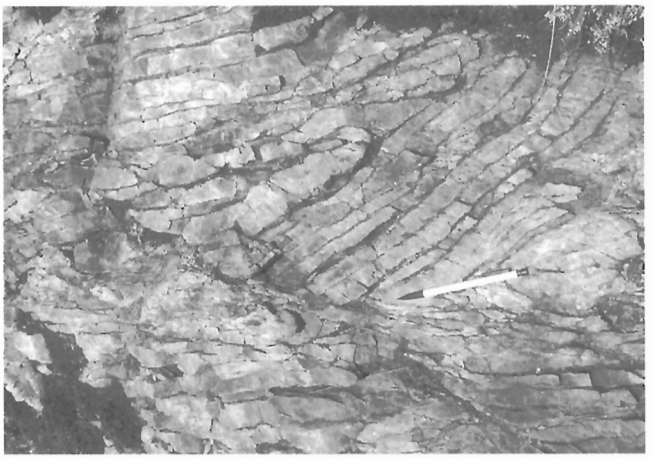

***Figure 4.*** *Close-up of chevron folds within the Stuart Lodge cherts.*

***Figure 5.*** *Outcrop on the northwest shore of Battleship Island showing interbedded chert (black) and limestone (white).*

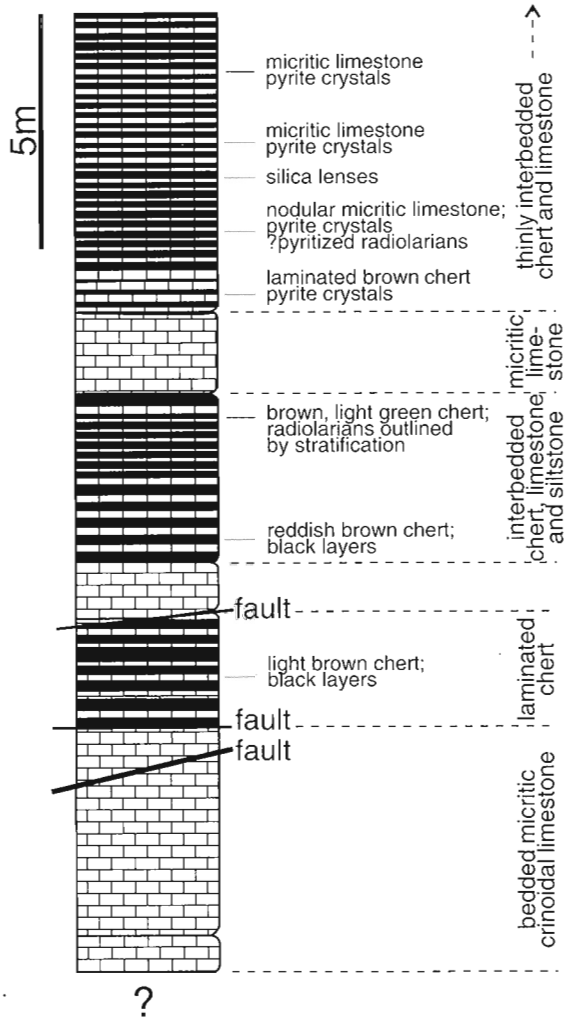


***Figure 6.*** *Stratigraphic section illustrating interbedding of chert and limestone on the northwest shore of Battleship Island (long. 124°25′05″W; lat. 54°30′38″N).*

chert beds are recrystallized and display a white, granular, "quartzitic" aspect, while the schist interlayers have a well developed cleavage.

Ribbon chert is locally interbedded with siliceous siltstone and chert breccias, as for example at the sailing club locality in Fort St. James (Fig. 2), a locality where Late Triassic conodonts (Orchard and Struik, 1996) and radiolarians (Cordey, 1990) were previously found. These clastic layers are characteristic of the Sowchea sequence (Struik et al., 1996). Ribbon chert sequences are locally found interlayered with basalt breccia and limestone, although stratigraphic relationships are unclear in many places.

On Battleship Island, the most southwest extension of the Mount Pope limestone unit (Fig. 2), thinly bedded micritic limestone is interbedded with black and light brown chert (2 mm-5 cm thick) (Fig. 5, 6). Locally, radiolarians and laminations are visible within the chert, and the interbeds of limestone and chert appear depositional. However, some of the chert beds may be of chemical origin, resulting from a dissolution of radiolarian shells within calcareous and siliceous strata and a remobilization and concentration of silica into layers. Local occurrences of black cherty nodules and pyritized radiolarians within the limestone may support this interpretation.

As a complement to investigations in Fort Fraser map area, radiolarian work began on Cache Creek Group rocks within Prince George (93G) map area. Initial sampling was done based on geological mapping of Prince George east half (Struik et al., 1990). Sampled localities comprise a section of grey radiolarian chert overlain by siliceous mudstone along the Blackwater River near the crossing of the Blackwater road (Punchaw Lake 93G/6), and scattered chert and siliceous mudstone localities near Buchan Creek (Cottonwood Canyon 93G/2). Preliminary chemical processing shows that selected samples from these localities contain identifiable radiolarians.

### *Siliceous mudstone*

This rock strata is characteristic of the Sowchea sequence (Struik et al., 1996) which consists of siltstone and slate with minor amounts of chert, limestone, and greywacke. This unit, partly referred to as unit 6 by Ash et al. (1993), underlies a large area to the southwest of Stuart Lake (PTCCs, Fig. 2). No fossils have been reported from the unit, and its age was based on association with the Mt. Pope limestone (Armstrong, 1949). It may be in part Triassic as it is locally interlayered with Late Triassic ribbon cherts near the Fort St. James sailing club (Struik et al., 1996). Chemical processing of cherty mudstone from Whitefish Bay (Loc. 1, Fig. 2) confirms the occurrence of radiolarians within this unit. Preliminary

**Table 1.** Radiolarian associations and ages from siliceous mudstone and chert pebbles from Fort Fraser (93K) map area. See Figure 2 for position of localities 1 and 2.

| Field No. | Locality (Fig. 2) | Unit (Fig. 2) | Lithology | Radiolarian association | Age |
|---|---|---|---|---|---|
| 95FC-08-2 | 1 | PTCCl | siliceous mudstone | ?*Capnuchosphaera* sp. | possibly Late Triassic |
| 95FC-17-1 | 2 | KTS | black mudstone | Abundant sponge spicules<br>fragment of ?Latentifistulidae | possibly Paleozoic |
| 95FC-17-2 | 2 | KTS | black chert pebble | *Plafkerium* sp.<br>*Pseudoeucyrtis*(?) sp.<br>*Pseudostylosphaera magnispinosa* Yeh<br>*Ps.* aff. *tenuis* (Nakaseko and Nishimura)<br>*Triassocampe* sp. | Middle Triassic; Ladinian |
| 95FC-17-3 | 2 | KTS | black chert pebble | *Capnodoce* sp.<br>*Capnuchosphaera* sp.<br>*Pseudostylosphaera* sp. | Late Triassic; late Carnian |
| 95FC-18-1 | 2 | KTS | light green chert pebble | *Livarella* sp.<br>*Paratriassoastrum* sp. | Late Triassic; late Norian / Rhaetian |
| 95FC-19-3 | 2 | KTS | green chert pebble | *Canesium lentum* Blome<br>*Capnodoce fragilis* Blome<br>*C. traversi* Blome<br>*Latium* sp.<br>*Palaeosaturnalis vigrassi* (Blome)<br>*Sarla* sp.<br>*Syringocapsa* sp. | Late Triassic; early-middle Norian |
| 95FC-19-4 | 2 | KTS | green chert pebble | *Plafkerium cochleatum* (Nakaseko and Nishimura)<br>*Poulpus* sp.<br>*Praesarla* sp. cf. *integrita* Cordey et al.<br>*Pseudoeucyrtis*(?) sp.<br>*Silicarmiger* aff. *costatus* Dumitrica, Kozur and Mostler<br>*Yeharaia elegans* Nakaseko and Nishimura | Middle Triassic; late Anisian-Ladinian |

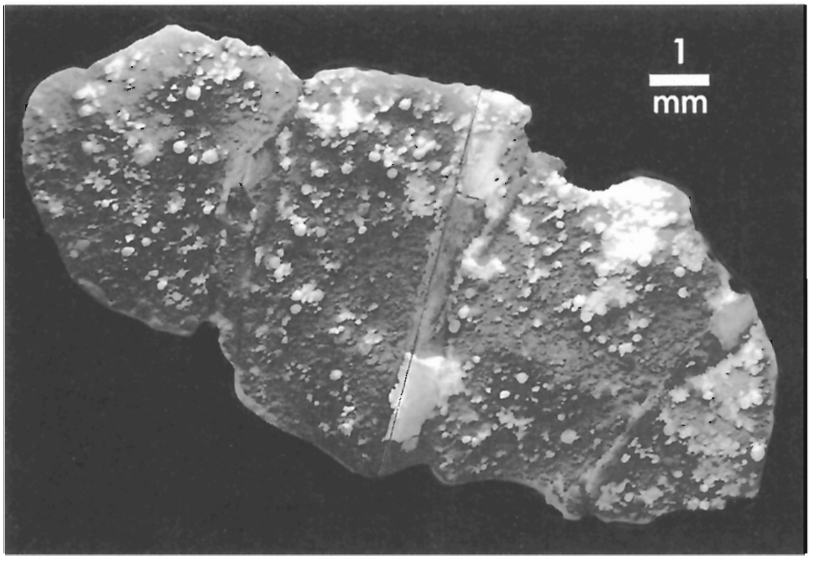


***Figure 7.***

*Scanning Electron Microscope (SEM) picture of a radiolarian chert pebble from Sifton Formation (KTS) near Pinchi Lake (sample 95FC-18-1, loc. 2, Fig. 2). This pebble was etched with a 5% solution of hydrofluoric acid (HF) for 24 hours, releasing radiolarians of Late Triassic age (late Norian/Rhaetian; Table 1). Spherical radiolarian shells, some of which bear visible spines, are partly released from the matrix. Three thin quartz joints are also outlined by the chemical processing.*

assessment of the radiolarian fauna suggests a Late Triassic age for this locality (Loc. 1, Table 1). Several other localities are under investigation.

### *Chert clasts*

Chert clasts are found in three main units of the region: (1) intra-sedimentary layers of chert breccia interbedded with Stuart Lodge ribbon cherts, (2) chert clasts of various sizes within sandstone and greywacke layers of Pinchi Sediments and Basalts (Struik et al., 1996) (PTCCs between Stuart and Pinchi lakes, Fig. 2), and (3) chert pebbles within Cretaceous breccia and conglomerate (Sifton Formation KTS, Fig. 2) located to the southeast of Pinchi Lake (Fig. 2).

Within the Sifton Formation, clastic layers grade from breccia to conglomerate facies in a broad northwest to southeast direction. Chert clasts are dominantly grey or green, locally brown or black. Occurrence of small angular chert chips from breccia beds and large round pebbles from conglomerate favour the interpretation of a local origin for the clasts. They could have been derived from the chert units of the Cache Creek Group visible to the southwest near Fort St. James. Six chert clasts removed from this unit (Loc. 2, Fig. 2) have been processed and released radiolarian associations of moderate to excellent preservation. They range in age from Middle Triassic (late Anisian-Ladinian) to Late Triassic (late Norian/Rhaetian), including Ladinian, late Carnian and early-middle Norian ages (Table 1). The smallest diagnostic pebble (95FC-18-1) of the batch is illustrated in Figure 7. These ages are consistent with known age ranges of chert strata from the Cache Creek Group in southern and northern British Columbia where Middle and Late Triassic chert localities are common (Cordey and Read, 1992; Cordey et al., 1991). Another chert pebble is a spiculite (95FC-17-1), an uncommon feature in chert strata of the Cache Creek Group indicating a chert deposition in shallow water; its age is tentatively assigned to the late Paleozoic (Table 1).

## CONCLUSIONS

The Cache Creek Group in central British Columbia, previously considered confined to the Pennsylvanian and Permian in age has yielded Triassic radiolaria from its ribbon chert strata. In addition, chert pebbles from Sifton Formation conglomerate and breccia in the same area, possibly derived from the Cache Creek Group, have yielded a wide range of Triassic ages. The youngest age is near the Triassic/Jurassic boundary. Preliminary examination of poorly preserved radiolaria from the siliceous argillites on the west side of Stuart Lake indicates those argillites may in part be of Triassic age.

## ACKNOWLEDGMENTS

In an earlier phase of the study, Mike Orchard provided support and biostratigraphic information on the region of Fort St. James. Claire Floriet (University of British Columbia) gave enthusiastic assistance in the field. Mike Orchard and Bev Vanlier are thanked for respectively reviewing and editing the manuscript.

## REFERENCES

**Armstrong, J.E.**
1949: Fort St. James map-area, Cassiar and Coast Districts, British Columbia; Geological Survey of Canada, Memoir 252.

**Ash, C., MacDonald, R.W.J., and Paterson, I.A.**
1993: Geology of the Stuart and Pinchi Lakes area, central British Columbia (93K); British Columbia Ministry of Energy Mines and Petroleum Resources, Open File 1993-9.

**Bellefontaine, K.A., Legun, A., Massey, N., and Desjardins, P.**
1995: Digital Geological Compilation of Northeast B.C. - Southern Half (NTS 83D, E, 93F, G, H, I, J, K, N, O, P); British Columbia Ministry of Energy Mines and Petroleum Resources, Open File 1995- 24.

**Cordey, F.**
1990: Comparative study of radiolarian faunas from the sedimentary basins of the Insular, Coast, and Intermontane belts; unpublished manuscript, 57 p.

**Cordey, F.** (cont.)
in press: Radiolaires des complexes d'accrétion cordillerains; Geological Survey of Canada, Bulletin.
**Cordey, F. and Read, P.B.**
1992: Permian and Triassic radiolarian ages from the Cache Creek Complex, Dog Creek and Alkali Lake, southwestern British Columbia; in Current Research, Part E; Geological Survey of Canada, Paper 92-1E, p. 41-51.
**Cordey, F., Gordey, S.P., and Orchard, M.J.**
1991: New biostratigraphic data for the northern Cache Creek Terrane, Teslin map area, southern Yukon; in Current Research, Part E; Geological Survey of Canada, Paper 91-1E, p. 67-76.
**Cordey, F., Mortimer, N., DeWever, P., and Monger, J.W.H.**
1987: Significance of Jurassic radiolarians from the Cache Creek terrane, British Columbia; Geology, v. 15, p. 1151-1154.
**Davies, E.F.**
1918: The radiolarian cherts of the Franciscan Group; University of California, Bulletin of the Department of Geology, v. 11, p. 235-432.
**Gordey, S.P. and Stevens, R.A.**
1994: Tectonic framework of the Teslin region, southern Yukon Territory; in Current Research 1995-A; Geological Survey of Canada, p. 11-18.
**Orchard, M.J.**
1986: Conodonts from western Canadian chert: their nature, distribution and stratigraphic application; in Investigative Techniques and Applications, (ed.) R.H. Austin; Ellis Horwood Limited, Chichester, p. 94-119.
**Orchard, M.J. and Struik, L.C.**
1996: Conodont biostratigraphy, lithostratigraphy, and correlation of the Cache Creek Group near Fort St. James, British Columbia; in Current Research 1996-A; Geological Survey of Canada.
**Struik, L.C., Floriet, C., and Cordey, F.**
1996: Geology near Fort St. James, central British Columbia; in Current Research 1996-A; Geological Survey of Canada.
**Struik, L.C., Fuller, E.A., and Lunch, T.**
1990: Geology of Prince George (east half), British Columbia (93G East); Geological Survey of Canada, Open File 2172.

Geological Survey of Canada Project 950036

# Time-domain electromagnetic surveys in drift covered regions of the Fawnie Creek map area, British Columbia[1]

M.E. Best, V.M. Levson[2], and L. Diakow[2]
GSC Victoria, Sidney

*Best, M.E., Levson, V.M., and Diakow, L., 1996: Time-domain electromagnetic surveys in drift covered regions of the Fawnie Creek map area, British Columbia; in Current Research 1996-A; Geological Survey of Canada, p. 91-100.*

**Abstract:** Time-domain electromagnetic surveys were carried out at 3 sites in the Nechako Plateau of British Columbia to investigate the use of electromagnetic methods for mapping the contact between granitic and basaltic rocks in drift-covered areas. This is difficult because resistive environments have a low EM signal-to-noise (S/N) ratio.

The results indicate that electromagnetic methods can map changes in bedrock resistivity, even with drift thickness in excess of 100 m. Resistivity effects associated with the contact, e.g., alteration and/or fracturing, were observed at site 1. Changes in bedrock resistivity at site 2 may be associated with the contact as well. In addition, a bedrock conductor was located near this contact.

The EM results at these sites are consistent with the interpretation of a high mineral potential for the area, based on bedrock mapping as well as till, lake sediment, and rock geochemistry results.

**Résumé :** Des levés électromagnétiques dans le domaine temporel ont été réalisés à trois sites répartis sur le plateau Nechako (Colombie-Britannique), dans le but d'analyser l'utilisation des méthodes électromagnétiques pour cartographier les contacts entre les roches granitiques et basaltiques dans des zones recouvertes de débris glaciaires. La difficulté de ces levés réside dans le fait que les milieux à forte résistivité présentent un faible rapport signal-bruit électromagnétique.

Les résultats indiquent que les méthodes électromagnétiques peuvent servir à déceler les variations dans la résistivité du socle, même si la puissance des débris glaciaires dépasse 100 mètres. Les effets de la résistivité au niveau d'un contact entre ces deux types de roches, p. ex. l'altération ou la fracturation, ont été observés au site 1. Les changements de résistivité dans le socle du site 2 peuvent aussi être associés au contact en question. De plus, un conducteur dans le socle a été localisé près de ce contact.

Les résultats électromagnétiques à ces sites corroborent l'interprétation, basée sur la cartographie du socle ainsi que les données géochimiques du till, des sédiments lacustres et de la pétrologie, selon laquelle il existe un potentiel minéral élevé dans cette région.

[1] Contribution to Canada-British Columbia Agreement on Mineral Development (1991-1995), a subsidiary agreement under the Canada-British Columbia Economic and Regional Development Agreement.
[2] British Columbia Geological Survey Branch, 5th floor, 1810 Blanshard Street, Victoria, British Columbia V8V 1X4

## INTRODUCTION

The southern Nechako Plateau of British Columbia (Fig. 1a) is a region of low relief covered with glacial drift of variable thickness and composition. The drift limits bedrock mapping to regions of outcrop or to specific areas where bedrock can be inferred indirectly from topographic features and other indirect indicators. Geological mapping must therefore be supplemented by geochemical and geophysical surveys.

With this in mind a Geonics EM-47 time-domain electromagnetic (TDEM) survey was carried out to investigate whether EM could map bedrock lithology and structure, as well as thickness and lithology of the drift (Best, 1995; Best et al., 1995). As the contact between the Capoose batholith and the surrounding volcanic rocks is associated with known mineralization (Lane and Schroeter, 1995) a major objective of the surveys was to locate this contact beneath the drift cover.


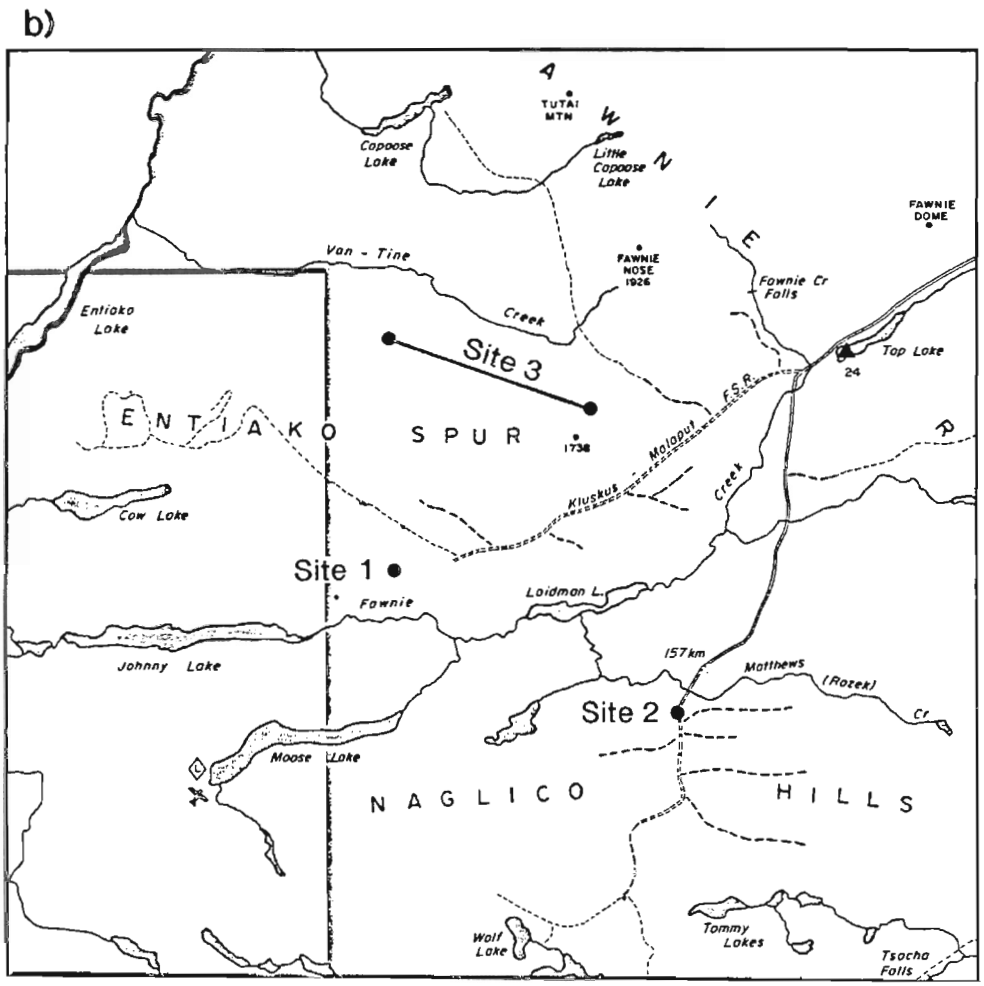


***Figure 1. a)*** *Location map of the Interior Plateau electromagnetic survey.* ***b)*** *Forestry Recreational map (Vanderhoof Forest District) showing the three EM-47 survey sites.*

Bedrock consists of resistive intrusive and volcanic rocks. The eddy current generated within these resistive bodies decays quickly, thus generating a low S/N ratio at long times (greater than 0.5 ms). Resistive drift also overlies the resistive bedrock. Such environments are a challenge for EM methods.

Two sites were selected close to the expected contact and EM surveys were conducted across the proposed contact. Soundings in a third site investigated the ability of the time-domain electromagnetic survey to map variations in drift thickness and lithology.

## DESCRIPTION OF STUDY AREA

### *Bedrock geology and mineral potential*

The bedrock geology of the Fawnie Creek map area was first mapped by Tipper (1954, 1963) and recently by Diakow et al. (1994). The area is part of a broad, structurally uplifted zone that includes the Fawnie Range and the Nechako Range to the east. The oldest strata, of probable Early Jurassic age, consist mainly of felsic volcanoclastic rocks. These in turn are conformable with stratigraphically overlying basaltic flows with interlayered fossil-bearing sediments of Middle Jurassic age. The Jura-Cretaceous Capoose batholith, composed of quartz monzonite and granodiorite, projects southwest beneath the Entiako Spur and a relatively thin cap of Jurassic rocks that are variably altered to a propylitic assemblage. Eocene volcanic rocks of the Ootsa Lake Group form scattered, relatively thin outliers that rest unconformably on the Jurassic rocks. Miocene and younger basalts of the Chilcotin Group underlie mainly topographically subdued areas south and northwest of the Naglico Hills.

Anticipated mineral potential of the Fawnie Creek map area is high, based on the recent discovery of new precious metal prospects (Diakow and Webster, 1994), encouraging till and lake sediment geochemical results (Levson et al., 1994; Cook and Jackaman, 1994) and geological mapping that shows a close spatial and possible genetic association between the Capoose batholith and a variety of known mineralization (Lane and Schroeter, 1995). Mineralization in the Fawnie Creek and adjoining areas consists mainly of deposits found within or along the margin of subvolcanic and larger epizonal calc-alkaline plutons. Three magmatic-mineralizing events are inferred from recent 1:50 000 scale geological mapping and new radiometric dates. The oldest event, represented by the Jura-Cretaceous Capoose batholith, is genetically associated with skarn, base metal veins, and precious metal epithermal prospects. Latest Cretaceous felsic hypabyssal plutons at the Capoose prospect, contain either porphyry copper or disseminated silver mineralization, and Eocene rhyolitic volcanic rocks host epithermal precious metal stockwork veins at the Wolf prospect (Andrew, 1988).

### *Quaternary geology*

During the late Wisconsian Fraser glaciation, ice moved into this part of the Nechako Plateau from the Coast Mountains (Tipper, 1971). Ice-flow studies indicate one dominant flow-direction towards the east-northeast, modified by topographic control during both early and late stages of glaciation (Giles and Levson, 1994; Levson and Giles, 1994). At the last glacial maximum, ice covered the highest peaks in the region suggesting an ice thickness in excess of 1000 m. Glacial deposits in the region are of variable thickness and include: compact, matrix-supported, silty diamictons interpreted as basal melt-out and lodgement tills (Fig. 2), and loose, massive to stratified, sandy diamictons of inferred debris-flow origin, Typically, basal tills unconformably overlie bedrock and are overlain by glacigenic debris-flow deposits, glaciofluvial sediments or colluvium. Thick (10 m or more) sequences of till occur both in main valleys and smaller valleys oriented oblique to the regional ice-flow direction, such as the Van Tine Creek Valley.

During deglaciation, glaciofluvial and glaciolacustrine sediments were deposited in many parts of the region on or near the ablating glaciers. Glaciofluvial sediments consist mainly of poor to well sorted, stratified, gravels and sands and commonly occur as eskers, kames, terraces, fans, and outwash plains in valley bottoms and along valley flanks. Several small eskers formed under downwasting ice in Van Tine Creek (Fig. 3) and Fawnie Creek valleys. Gravelly outwash plains

***Figure 2.***

*Till and glacigenic debris flow deposits overlying bedrock exposed in a trench at the Wolf epithermal gold prospect.*

covered the main valley bottoms as large volumes of sediment and water were removed from the ice margin. Glacial lakes formed locally along the margins of the retreating ice. One such lake on the south side of the Entiako Spur (near site 1) probably was dammed by stagnant ice in Fawnie Valley. A coarsening-upward sequence of well sorted, ripple-bedded, sands (Fig. 4; see also section 9.5 in Levson and Giles, 1994) at this site is interpreted as a prograding fan-delta (Fig. 5) that formed along the margin of the lake. Glacial lake sediments have also been mapped in the northern part of the region and may extend into the Van Tine Creek valley in the vicinity of EM survey site 3.

During postglacial times, the surficial geology of the area was modified mainly by fluvial activity and the local development of alluvial fans in valley bottoms (Fig. 5), as well as by colluvial reworking of glacial deposits along the valley sides. Holocene fluvial sediments in the map area are dominated by floodplain silts, fine sands, and organic material. Low areas in valleys are characterized by marshes and shallow lakes filled with organic sediments (Fig. 5).

## SITE DESCRIPTIONS

Figure 1b shows the location of the EM sites. Sites 1 and 3 are situated well down on the south and north sides of the Entiako Spur respectively, in areas where outcrop is generally poorly exposed. Site 2 is situated at a low elevation on the gentle north slope of the Naglico Hills, in an area where glacial deposits, presumed to be thick, mantle bedrock. The sites are located approximately 150 to 160 km southwest of Vanderhoof in the Fawnie Creek map sheet (NTS 93F/3).

### *Site 1 (CAP)*

Regionally anomalous concentrations of gold, silver, arsenic, and antimony in tills (Levson et al., 1994) and gold and arsenic in sediments (Cook and Jackaman, 1994) occur at site 1 and, although the surficial sediment cover is extensive, silicified and mineralized country rock has been observed nearby along the margin of the Capoose batholith (Diakow et al., 1994). These data point to an area of potentially significant mineralization, along the west-central margin of the Capoose batholith. Due to the thick overburden in this area,

***Figure 3.***

*Exposure of glaciofluvial gravels and sands in a small esker in the Van Tine Creek valley near site 3. Measuring rod is 4 m long.*

***Figure 4.***

*Exposure at site 1, of well-sorted, ripple-bedded, fine to coarse sand in a coarsening upward sequence interpreted as a glaciofluvial fan-delta deposit. Measuring rod is 3 m long.*

Levson et al. (1994) suggested that geophysical prospecting was required to locate the sources of the gold anomalies. The EM survey reported here was initiated in part to investigate the thickness of the overburden and to help identify the western margin of the Capoose batholith in this area of high mineral potential.

Site 1 (Fig. 1b) consists of nine 80 x 80 m loop soundings situated along the Kluskus-Malaput Forestry Road in the Vanderhoof Forestry District, approximately 160 km southwest of Vanderhoof. Sounding 0W was located on the north side of the road with the centre of the loop about 25 m east of kilometre 19 (Best, 1995).

### *Site 2 (CAP2)*

The main purposes of the EM survey at this site were to better locate the buried southern boundary of the Capoose batholith and to determine the drift thickness in the area. Results of lithological analyses of pebbles from tills in this area show a consistent northward increase in the percentage of quartz monzonite clasts derived from the Capoose batholith. Percentages of quartz monzonites range from 0% a few kilometres south of the inferred contact of the batholith, to 5% near the contact, and 10-23% north of the contact. Conversely, Jurassic andesite percentages decrease from a high of 45%, a few kilometres south of the inferred contact, to 17-24% north of the contact.

Site 2 consists of seven 40 x 40 m loop soundings and one 80 x 80 m loop sounding (OS) situated along the Kluskus-Ootsa Forestry Road in the Vanderhoof Forestry District, approximately 150 km southwest of Vanderhoof (Fig. 1b). Sounding 0S was located on the west side of the road about 1.4 km south of the bridge crossing Matthews (Rozek) Creek (Best, 1995).

### *Site 3 (CLVAN)*

Anomalous gold concentrations in tills throughout this area (soundings CLVAN-1 to CLVAN-5 inclusive) were documented by Levson et al., 1994 and are associated with a belt of thermally altered Hazelton rocks (Diakow et al., 1994). This area is believed to be near the edge of the northern part of the Capoose batholith. Anomalously high copper values also occur in till near soundings CLVAN-2 (64 ppm) and CLVAN-5 (43 ppm) (Levson et al., 1994). Mineral occurrences known in the area southeast of sounding CLVAN-5 include a magnetite skarn and epithermal-style mineralization (Lane and Schroeter, 1995). The main purposes of the EM

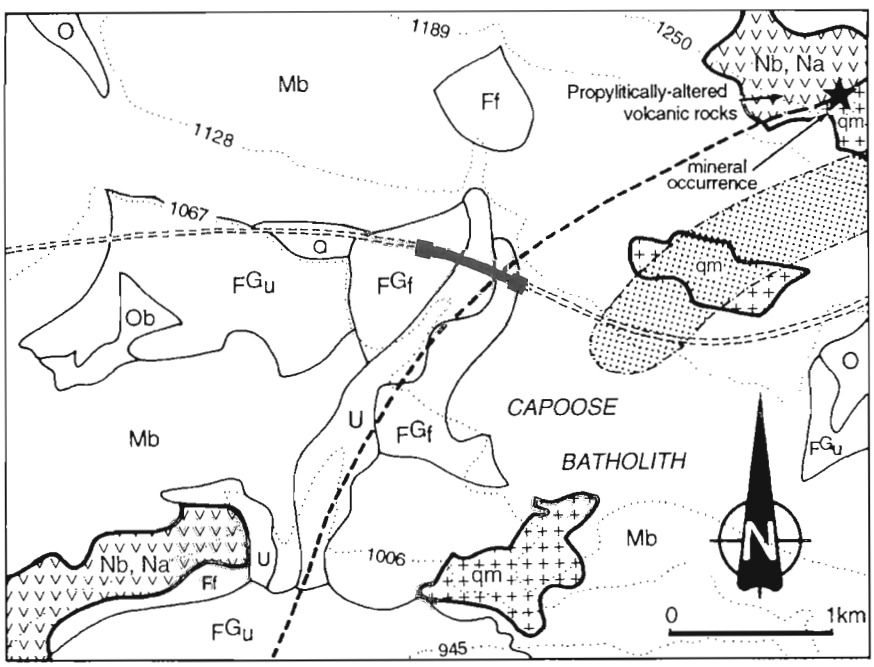


***Figure 5.*** *Bedrock and surficial geology of the region around EM survey site 1. The location of the EM survey (thick bar) along the Kluskus-Malaput forestry road (double dashed line), the inferred contact of the Capoose batholith with volcanic country rocks (thick dashed line) and an area of anomalous (10-80 ppb) gold in tills (shaded) are shown. qm – quartz monzonite; Nb, Na – basalt and andesite; $F^Gf$ – glaciofluvial fan-delta; $F^Gu$ – glaciofluvial outwash; Ff – alluvial fan; Mb – morrained blanket; O, Ob – organics; U – undifferentiated (steep gullies).*

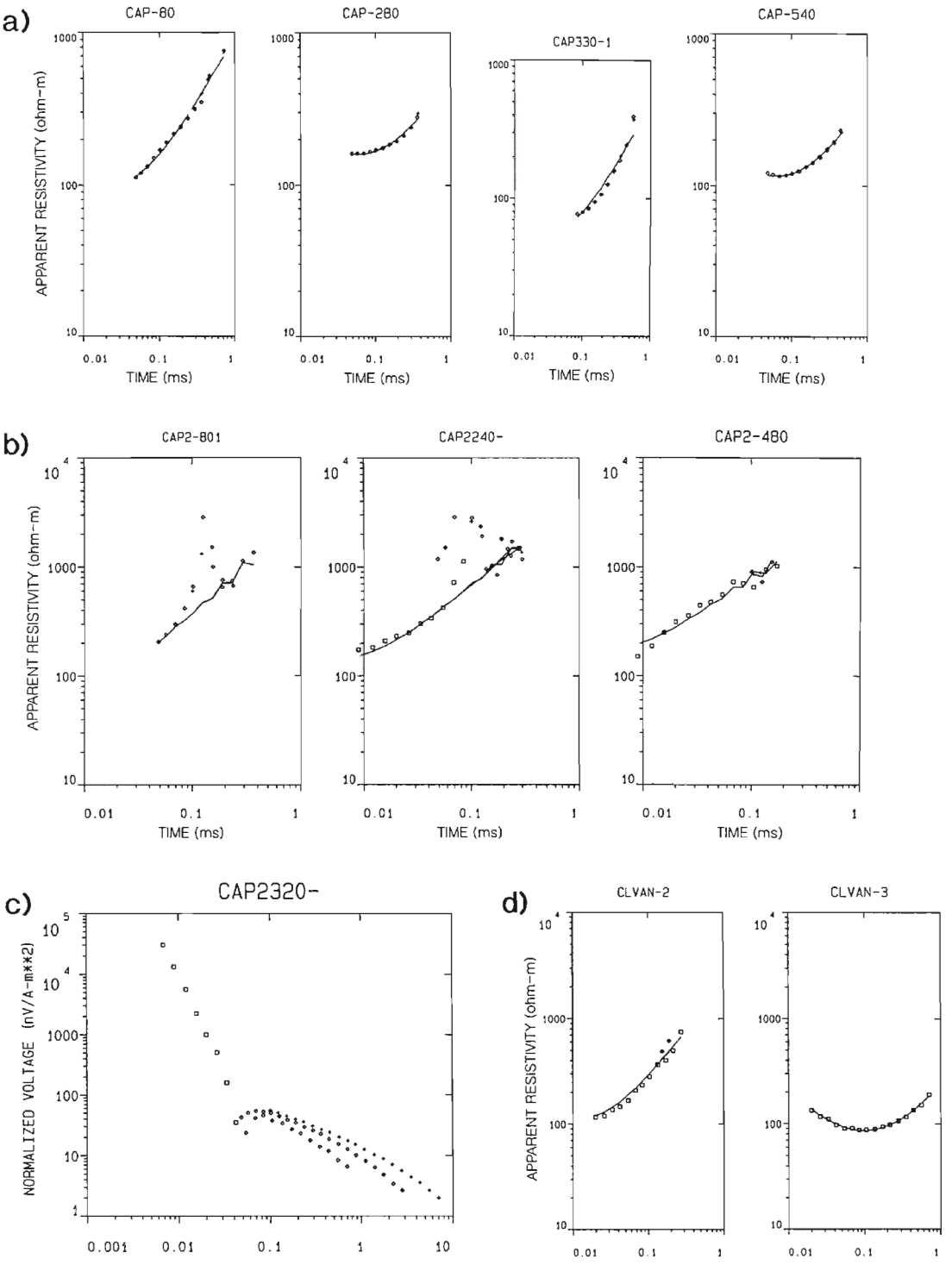


***Figure 6. a)*** *Edited apparent resistivity versus time (log-log) plots for several soundings at site 1.* ***b)*** *Edited apparent resistivity versus time (log-log) plots for several soundings at site 2.* ***c)*** *Example of cross over time for one of the soundings at site 2 (the squares are positive voltages and the pluses are negative voltages).* ***d)*** *Edited apparent resistivity versus time (log-log) plots for several soundings at site 3.*

survey at this site were to determine the depth to the top of the Capoose batholith, in other words drift thickness, and drift lithology in the area.

Site 3 consists of five 80 x 80 m loop soundings situated along the Van-Tine Road, approximately 150 km southwest of Vanderhoof (Fig. 1b). The five soundings were spaced about 1.5 km apart (Best, 1995).

## ELECTROMAGNETIC METHODS

The time-domain electromagnetic survey used a Geonics EM-47 (Geonics, 1991) leased from the Ontario Geological Survey. Best (1995), Best et al. (1995), and the references therein contain a description of this system and a summary on electromagnetic methods.

The central sounding mode was used for all soundings. The period T of the transmitter current consists of a positive square wave of duration T/4, followed by an off-time of duration T/4 (receiver measurement time). These are then reversed to give a total period equal to T. The frequency of the transmitted square wave is the reciprocal of the period T. Three frequencies are available with the EM-47 system (UH = Ultra High frequency = 285 Hz, VH = Very High frequency = 75 Hz and H = High frequency = 30 Hz).

The receiver voltage in the EM-47 unit is measured in millivolts and then converted to the time derivative of the vertical magnetic field. This derivative, also called the normalized voltage, is measured in $nV/m^2$. The TEMIXGL software (Interpex Limited, 1994) can plot this voltage as a function of time.

The voltages can also be converted to apparent resistivity values ($\rho_a$) using the late time normalized voltage (Kaufmann and Keller, 1983; Fitterman and Stewart, 1986; Spies and Eggers, 1986). The apparent resistivity is defined as the ratio of the measured voltage to the voltage that would be measured over a half-space of constant resistivity.

Once the apparent resistivity versus time curves are computed, the data can be interpreted in terms of multi-layered earth models using standard forward and inverse mathematical modelling programs. A number of assumptions are required to ensure the data can be meaningfully represented by a layered earth model. We used the TEMIXGL software package for modelling the data from the Fawnie Creek map area.

## FIELD PROCEDURES

Three data sets were collected at the high and very high frequency ranges at each sounding. A single data set was collected for the ultra high range at most soundings.

Two transmitter loop sizes were used: 80 m by 80 m (area = 6400 $m^2$) and 40 m by 40 m (1600 $m^2$). The current in the wire was approximately 2.3 A.

There were no cultural noise problems in the area, such as those caused by grounded pipes, electric transmission lines, and electric fences. Several electrical storms occurred during the survey but did not interfere with the EM measurements.

The EM 47 system turned out to be very reliable and robust in the field. There was no down time due to instrument problems.

The data for each site and/or sounding were transferred to a PC using software provided by Geonics. The files created by this software were subsequently translated into a form compatible with the Interpex software package TEMIXGL.

## EDITING THE DATA

The data were first edited to remove noisy or bad data from the files. Examples of the noise encountered are given in Best (1995). The TEMIXGL software permitted the rapid removal of this noise using an interactive mouse. The results can quickly be displayed to ensure that all the noise is removed.

## INTERPRETATION OF THE DATA

The edited apparent resistivity data formed the basis of the interpretation. Details on interpretation procedures can be found in Best (1995) and Best et al. (1995).

When an apparent resistivity curve does not fit a layered-earth model the voltage data can only be interpreted by forward modelling. In this case type curves and other available models are compared with the data (McNeill et al., 1984; Spies and Parker, 1984; West et al., 1984). Fortunately all the data from this survey, with the exception of five soundings from site 2, fit a one-dimensional earth model.

### *Site 1*

Examples of apparent resistivity versus time plots for site 1 are illustrated in Figure 6a. The data fit a model consisting of a layer of drift overlying resistive bedrock (Fig. 7a). The overburden resistivity is relatively constant (68 to 157 Ω-m), but its thickness varies from 30 m to 120 m. The bedrock resistivity changes from about 8400 Ω-m on the east end of the traverse to about 10 000 Ω-m on the west end. The overburden was thickest about 80 m to the east of the gully. Sounding 330 in the gully is difficult to fit to a one-dimensional model because the gully completely distorts any layering.

The interpretation of the EM results for this site, that is a generally thick overburden section, is supported by results of geology mapping (Levson and Giles, 1994). A large Late Pleistocene glaciofluvial fan delta (Fig. 5) occurs at this site and it is an obvious feature on air photos and on the ground. Exposures of the fan delta sediments in the area reveal up to several metres of ripple bedded and trough crossbedded sands (Fig. 4; see Section 93-5, Levson and Giles, 1994). The fan delta sediments overlie till which is exposed in a modern gully that has incised the fan delta. Several tens of metres of till are

exposed in cuts along the gully below the fan delta, further supporting the interpretation for thick overburden in this area. The EM results, however, provide the best estimate of the variations in drift thickness.

The bedrock depression between soundings 80W and 330W, and the lower bedrock resistivities associated with the depression, occur at the inferred location of the contact between granite to the east and volcanic rocks to the west. The contact is extrapolated through this area from rock exposures to the north and south (Fig. 5; see Diakow et al., 1994). The lower resistivities across the contact could be a result of increased porosity (more water) due to fracturing or alteration of minerals in the contact zone to clay. The bedrock resistivity at the two ends of the line (≈ 8400 Ω-m to the east and ≈ 10 000 Ω-m to the west) are consistent with unaltered granite and basalt respectively. Considering the high resistivity of overburden and bedrock (low signal-to-noise ratio at large times) the information gleaned from the TDEM data is quite impressive.

A linear gold anomaly extending eastward for over 5 km from the vicinity of site 1 (Fig. 5) is documented by Levson et al. (1994). The anomaly contains the highest gold concentration recovered from regional till samples in the map area (77 ppb). Anomalous gold values occur at sample sites throughout this zone which is about 1 km wide and several kilometres long. The shape of this anomalous zone is suggestive of a well developed, glacial dispersal train, comparable with or even larger than other dispersal trains in the region, including for example that developed down-ice of the Wolf property (Levson and Giles, 1995). This interpretation is further supported by the orientation of the anomalous zone which is parallel to the glacial paleoflow direction in the area. The up-ice end of the gold anomaly (Fig. 5) also coincides

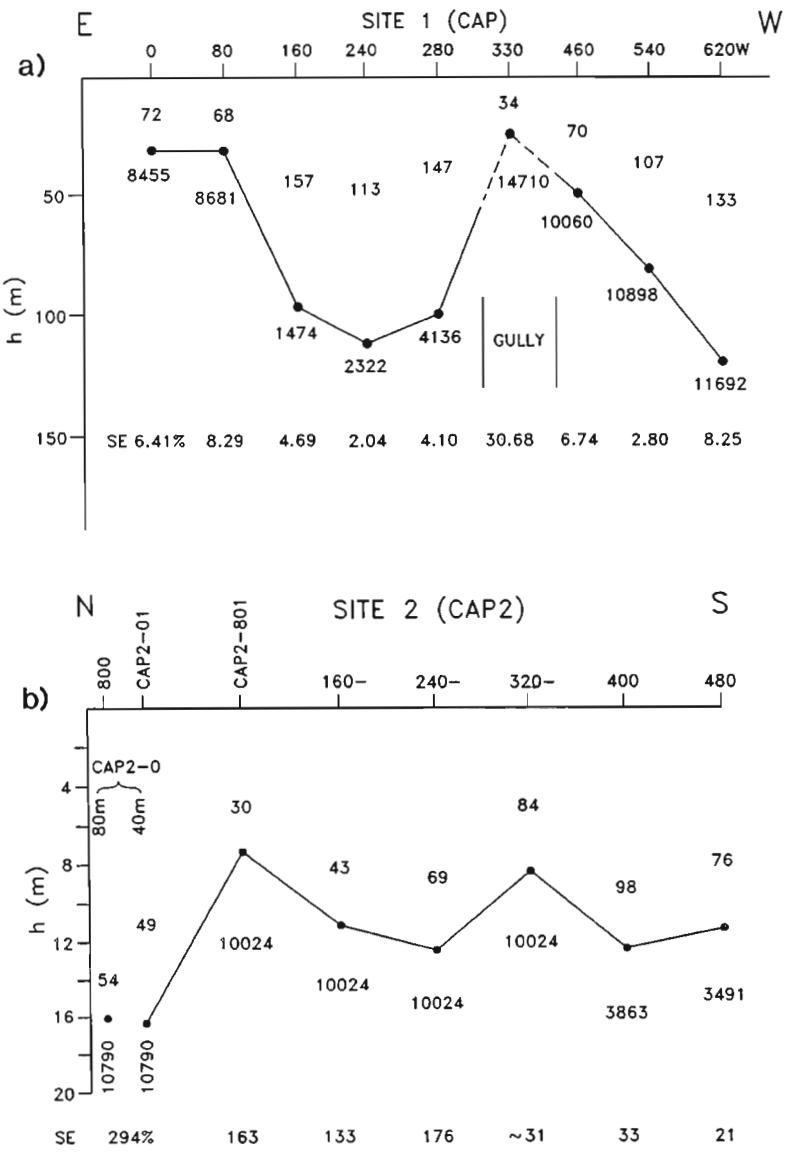


***Figure 7.***

***a)*** *Resistivity section based on the layered earth interpretation of the apparent resistivity plots for site 1.* ***b)*** *Resistivity section based on the layered earth interpretation of the apparent resistivity plots for site 2. The values of standard error of fit from the inversion (labelled SE in the diagrams) are shown along the bottom of the two sections. The high SE values for CAP2-01 to CAP2-240 are caused by the finite conductor superimposed on the layered earth responses.*

with an area of regionally anomalous arsenic (25 to 46 ppm), antimony (2.2 to 2.8 ppm), and silver (0.4 ppm) concentrations in till (Levson et al., 1994) and with anomalous gold and arsenic concentrations in lake sediments (Cook and Jackaman, 1994). Pervasively silicified and veined country rock adjacent to the intrusion, chip-sampled directly north of this area (asterisk in Fig. 5), yield gold, arsenic, and antimony concentrations of 101 ppb, 12 730 ppm and 79 ppm, respectively, as well as anomalous silver (6 ppm), copper (186 ppm), lead (321 ppm), zinc (675 ppm), and molybdenum (14 ppm) concentrations (Diakow et al., 1994) These data further suggest that the area west of the anomalous zone, along the western edge of the Capoose batholith, is a prime target for exploration.

### *Site 2*

Three of the seven apparent resistivity versus time plots for Site 2 are illustrated in Figure 6b. The five northern soundings (CAP2-0 to CAP2-320) have approximately the same shape as the two southern soundings (CAP2-400 and CAP2-480) but have a finite conductor response superimposed on them (see CAP-801 and CAP2240). Finite conductors have a cross over time, the time when the voltage changes sign, that is related to the depth to the top of the conductor.

The character of the voltage versus time curves changes going from north (CAP2-0) to south (CAP2-480). For example, the cross over time decreases going north to south indicating the conductor axis (top of the conductor) is shallower at the southern end. Sounding CAP2-320 is unique (Fig. 6c) since the voltage decays very slowly at times greater than 0.4 ms. Indeed, the conductor axis must be very shallow at this sounding as the cross over time is between 42 and 69 μs. There is the possibility that the conductor may be a culvert, although none was obvious in the area. Further field investigation is warranted to define the nature of this conductor.

The conductor is not present on the two southern soundings. Indeed, a one-layer model fit to the data indicates that the drift is around 10 to 12 m thick and that the bedrock has a resistivity of 3500 Ω-m. An overburden thickness in the order of 10 m is compatible with estimates from surficial and bedrock geology mapping. A similar drift thickness is obtained from the five northern soundings when the finite conductor response is ignored (Fig. 7b). The depth to the finite conductor current axis is consistent with the drift thickness.

The bedrock resistivity beneath the northern soundings is about 3 times larger than beneath the southern values. This change may be related to the granite-volcanic contact. An inferred contact between granitic and volcanic rocks has been mapped in the vicinity of this EM survey site (Diakow et al., 1994) but no bedrock exposures are present. However, tills immediately south of this area contain abundant basaltic boulders whereas those to the north contain numerous granitic clasts. This supports the EM interpretation of a bedrock contact between the Capoose batholith and volcanic rocks at site 2. More field work is needed to verify this and explain the nature of the conductor.

### *Site 3*

Two of the five apparent resistivity versus time plots for site 3 are illustrated in Figure 6d. The voltage (apparent resistivity) for CLVAN-1 is very noisy but nevertheless fits a homogeneous half space model that is very resistive. See Best (1995) for further details.

The other four soundings along the Van Tine Road are quite different and suggest the drift consists of two layers: one resistive and the other is more (Fig. 6d). The one-dimensional models for soundings CLVAN-3 to CLVAN-5, at the east end of the site 3 traverse (Fig. 1b), have the conductive layer overlying bedrock whereas CLVAN-2, near the west end of the traverse, has the resistive layer overlying bedrock (Best, 1995). The drift resistivities are greater than 60 Ω-m, and bedrock resistivities are several thousand ohm-metres. No drillholes or other information on the depth to bedrock are available. However, glaciolacustrine sediments have been mapped northwest of this region. These clay-rich sediments generally have a lower resistivity than sands and gravels. Regional stratigraphic studies indicate that ice damming prior to the last glaciation was common (Levson and Giles, 1995) and it is quite plausible that a glaciolacustrine unit may be present in the subsurface of this region. Tills in the area contain an unusually high proportion of clay further suggesting that they may overlie a clay-rich unit. The till near site CLVAN-3 is especially clay rich, has an unusual yellow-brown colour (possibly indicating a high iron content), and is overlain by a spruce bog (see site 93114, Levson et al., 1994). The conductive layer at the surface at CLVAN-2 may therefore represent a small late-glacial clay unit.

## SUMMARY AND OUTLOOK

The results of this survey indicate that useful electromagnetic data can be obtained in drift covered areas in the Nechako Plateau. The signal-to-noise (S/N) ratio is low at measurement times greater than 0.5 ms; thus little information is gleaned from the data at long times. Differences in bedrock resistivity of 2 or more can be resolved however and the drift thickness can easily be measured.

The contact between the granitic pluton and the volcanic host rock at site 1 appears to be associated with thicker drift and more conductive bedrock, perhaps a result of (clay?) alteration or fracturing along the contact. One of the most pronounced multi-element till geochemical anomalies in the Fawnie Creek map area occurs directly east of EM survey site 1, adjacent to the western margin of the Capoose batholith. Here anomalous gold values occur in an east-trending zone that is about a kilometre wide and several kilometres long which parallels the local ice-flow direction. Till samples at several sites in this zone also contain anomalous arsenic, antimony, and silver values. The geochemical anomaly indicates an up-ice source in the vicinity of the EM survey, along the western margin of the batholith. Elsewhere, along the batholith margin, variably silicified country rock sometimes associated with barite (see Malaput prospect in Diakow and Webster, 1994) suggests that near-surface hydrothermal

activity locally accompanied the emplacement of the Capoose batholith. Further research, including drilling, is required to verify this concept.

A finite bedrock(?) conductor was located at site 2. The drift here is quite thin (less than 15 m) with resistivity values similar to those at site 1. The bedrock resistivity near the conductor differs from the resistivity farther south, but it is not clear if it is associated with the granite-volcanic contact. Further field examination of the area is needed to verify that the conductor is real and not associated with a buried object such as a culvert.

The resistivity character of the drift at site 3, soundings CLVAN-2 to CLVAN-4, is different than the drift at the other two sites and is most likely underlain by glaciolacustrine sediments. Further investigations are needed to verify these results since there are no drillholes in this area.

In conclusion, the results of the EM-47 survey in this region of the Interior Plateau are encouraging, in that the method successfully resolved till thickness, multiple Quaternary stratigraphic units, bedrock contacts, possible alteration zones as well as bedrock conductors. The potential contribution of electromagnetic techniques to regional geoscience programs is significant and we recommend and encourage their use.

## ACKNOWLEDGMENTS

We thank Bill Hill for electronic support and for providing computers and other electronic field equipment. Participation in the field program by Aaron Best, Erin O'Brian, and Gordon Weary is appreciated. We thank the Ontario Geological Survey for providing the Geological Survey of Canada with access to the Geonics EM-47 system used in the field program.

## REFERENCES

**Andrew, K.P.E.**
1988: Geology and genesis of the Wolf precious metal epithermal prospect and the Capoose base and precious metal porphyry-style prospect, Capoose Lake area, central British Columbia; MSc. thesis, The University of British Columbia, Vancouver, British Columbia, 334 p.

**Best, M.E.**
1995: Time-domain electromagnetic surveys near the Capoose batholith, Fawnie Creek map sheet (NTS 93F/3); Geological Survey of Canada, Open File 3126.

**Best, M.E., Todd, B.J., and O'Leary, D.**
1995: Fraser Valley hydrogeology project: time-domain EM surveys, June 20 to July 8, 1994; Geological Survey of Canada, Open File 3095.

**Cook, S.J. and Jackaman, W.**
1994: Regional lake-sediment and water geochemistry of part of the Nechako River area (NTS 93 F2/3: parts of 93 F2/6, 11, 12, 13, 14); British Columbia Ministry of Energy, Mines and Petroleum Resources, Open File 1994-19.

**Diakow, L. and Webster, I.C.L.**
1994: Geology of the Fawnie map area (93F/3); in Geological Fieldwork 1993, (ed.) B. Grant and J.M. Newell; British Columbia Ministry of Energy, Mines and Petroleum Resources, Paper 1994-1, p. 15-26.

**Diakow, L., Webster, I.C.L., Levsen, V.M., and Giles, T.R.**
1994: Bedrock and surficial geology of Fawnie Creek map area, NTS 93F/3; British Columbia Ministry of Energy, Mines and Petroleum Resources, Open File 1994-2.

**Fitterman, D.V. and Stewart, M.T.**
1986: Transient electromagnetic soundings for ground water; Geophysics, v. 51, p. 995-1005.

**Geonics**
1991: Geonics Protem 47 operating manual; Geonics Limited, 8-1745 Meyerside Drive, Mississauga, Ontario, L5T 1C6.

**Giles, T.R. and Levson, V.M.**
1994: Surficial geology and drift exploration studies in the Fawnie Creek region (93 F/3); in Geological Fieldwork 1993, (ed.) B. Grant and J.M. Newell; British Columbia Ministry of Energy, Mines and Petroleum Resources, Paper 1994-1, p. 27-38.

**Interpex Limited**
1994: TEMIXGL user manual, transient electromagnetic data interpretation software; Interpex Limited, P.O. Box 839, Golden, Colorado 80402.

**Kaufmann, A.A. and Keller, G.V.**
1983: Frequency and transient soundings; Elsevier Scientific Publishing Company.

**Lane, R.A. and Schroeter, T.G.**
1995: Mineral occurrence investigations and exploration monitoring in the Nechako Plateau (93 F/2, 3, 7, 10, 11, 12, 14, 15); British Columbia Ministry of Energy, Mines and Petroleum Resources, Paper 1995-1, p. 177-191.

**Levson, V.M. and Giles, T.R.**
1994: Surficial geology and Quaternary stratigraphy of the Fawnie Creek Area (NTS 93F/3); British Columbia Ministry of Energy, Mines and Petroleum Resources, Open File 1994-9.
1995: Glacial dispersal patterns of mineralized bedrock with examples from the Nechako Plateau, central British Columbia; in Drift Exploration, (ed.) P.T. Bobrowsky, S.J. Sibbick, and J.M. Newell; British Columbia Ministry of Energy, Mines and Petroleum Resources, Paper 1995-2.

**Levson, V.M., Giles, T.R., Cook, S.J., and Jackaman, W.**
1994: Till geochemistry of the Fawnie Creek Area (NTS 93F/3); British Columbia Ministry of Energy, Mines and Petroleum Resources, Open File 1994-18, 34 p.

**McNeill, J.D., Edwards, R.N., and Levy, G.M.**
1984: Approximate calculation of the transient electromagnetic response from buried conductors in a half-space; Geophysics, v. 49, p. 918-924.

**Spies, B.R. and Eggers, D.E.**
1986: The use and misuse of apparent resistivity in electromagnetic methods; Geophysics, v. 51, p. 1462-1471.

**Spies, B.R. and Parker, P.D.**
1984: Limitations of large-loop transient electromagnetic surveys in conductive terrain; Geophysics, v. 49, p. 902-912.

**Tipper, H.W.**
1954: Geology of Nechako River British Columbia (93F); Geological Survey of Canada, Map 1131A.
1963: Nechako River map area, British Columbia; Geological Survey of Canada, Memoir 324, 59 p.
1971: Glacial morphology and Pleistocene history of central British Columbia; Geological Survey of Canada, Bulletin 196, 89 p.

**West, G.F., Macnae, J.C., and Lamontagne, Y.**
1984: A time-domain electromagnetic system measuring the step response of the ground; Geophysics, v. 49, p. 1010-1026.

Geological Survey of Canada Project 940010

# Albian-Cenomanian conglomerates along the Intermontane/Insular superterrane boundary, Canadian Cordillera, British Columbia: a critical test for large-scale terrane translation?

J. Brian Mahoney[1], J.W.H. Monger, and C.J. Hickson
GSC Victoria, Vancouver

*Mahoney, J.B., Monger, J.W.H., and Hickson, C.J., 1996: Albian-Cenomanian conglomerates along the Intermontane/Insular superterrane boundary, Canadian Cordillera, British Columbia: a critical test for large-scale terrane translation?; in Current Research 1996-A; Geological Survey of Canada, p. 101-109.*

**Abstract:** The mid-Cretaceous-early Tertiary paleogeography of the Canadian Cordillera generates intense debate among geoscientists forced to evaluate two contradictory data sets: 1) paleomagnetic data suggest large-scale northward translation of the Insular and Intermontane superterranes between 80-60 Ma; 2) geological data indicate significantly smaller displacements. This paper outlines a critical stratigraphic test of a prediction of the large-scale translation hypothesis. Nonmarine, chert and volcanic conglomerates of Albian-Cenomanian age (ca. 100-90 Ma) occur on both the Intermontane superterrane and within the mid-Cretaceous collisional orogen (amalgamated Methow, Bridge River, and Cadwallader terranes) associated with the Insular superterrane. Different magnitudes of displacement of each superterrane require that the conglomerate units were deposited in entirely different sedimentary systems and are not correlative. This paper outlines a multidisciplinary investigation, including lithostratigraphy, clast geochemistry and isotopic signature, detrital zircon studies, palynology, and paleomagnetic studies, that will examine potential correlations among Albian-Cenomanian strata.

**Résumé :** La paléogéographie du Crétacé moyen au Tertiaire précoce dans la Cordillère canadienne suscite un débat houleux entre les géoscientifiques obligés d'évaluer deux ensembles de données contradictoires : 1) les données paléomagnétiques permettent de supposer une translation à grande échelle vers le nord des superterranes insulaire et intermontagneux entre 80 et 60 Ma; 2) les données géologiques indiquent des déplacements significativement moins importants. Le présent texte donne les grandes lignes d'une vérification stratigraphique critique d'une prédiction rattachée à l'hypothèse de translation à grande échelle. Les cherts et les conglomérats volcaniques non marins de l'Albien-Cénomanien (vers 100-90 Ma) sont présents à la fois dans le superterrane intermontagneux et dans l'orogène de collision du Crétacé moyen (terranes de Methow, de Bridge River et de Cadwallader amalgamés) associé au superterrane insulaire. Pour expliquer les variations d'amplitude de déplacement de chaque superterrane, il faut que les conglomérats aient été déposés dans des systèmes sédimentaires tout à fait différents et qu'ils ne soient pas en corrélation. Le présent document porte sur une étude multdisciplinaire (lithostratigraphie, géochimie des clastes et signature isotopique, analyse des zircons détritiques, palynologie et paléomagnétisme), qui permettra d'identifier les corrélations possibles au sein des strates albiennes-cénomaniennes.

[1] Department of Geology, University of Wisconsin-Eau Claire, Eau Claire, Wisconsin 54702;
e-mail: mahonej@uwec.edu

## INTRODUCTION

One of the most fundamental controversies in Cordilleran tectonics today concerns the paleogeographic setting and accretion history of allochthonous terranes of the Canadian Cordillera between mid-Cretaceous and Eocene time. Paleomagnetic data from stratified and unstratified rocks from both the Coast and Intermontane belts suggest large-scale northward translation of these rocks during this time interval (ca. 90-55 Ma) (Irving, 1985; Umhoefer, 1987; Irving and Wynne, 1990; Ague and Brandon, 1992; Wynne et al., 1995; Irving et al., 1995). Paleomagnetic data from the Intermontane belt indicate northward translation of 1100 ± 600 km between ca. 95-55 Ma (Marquis and Globerman, 1988; Irving and Thorkelson, 1990; Irving et al., 1995); data from the eastern and central Coast Belt indicate northward translation of 3000 ± 500 km during a similar time interval (ca. 80-55 Ma) (Ague and Brandon, 1992; Wynne et al., 1995). Geological data, on the other hand, suggest allochthonous terranes of the Canadian Cordillera were largely amalgamated by mid-Cretaceous time, and have been subject to <1000 km of margin-parallel translation since that time (Monger et al., 1982; Rusmore et al., 1988; Rubin et al., 1990; Garver, 1992; van der Heyden, 1992; Monger and Journeay, 1992; Mahoney and Journeay, 1993; Mahoney, 1994; Monger et al., 1994; Monger and Price, in press). Recent publication of new and revised paleomagnetic data (Irving et al., 1995; Wynne et al., 1995), together with both recent Geological Society of America symposia (Cowan et al., 1994) and a review of the debate (Cowan, 1994) have renewed interest in resolving this controversy. Cowan (1994) argued that the only way to resolve the debate was to utilize tests specifically designed to rule out predications put forth by either of the proposed tectonic models. This report describes stratigraphic and structural studies initiated during the 1995 field season specifically designed to test predictions of the large-scale displacement hypothesis.

### *The problem*

The two conflicting models of tectonic evolution of the Canadian Cordillera are both working hypotheses, and each of the models makes very specific predictions. Critical testing of a hypothesis' predictions is fundamental to assessing the validity of that hypothesis. In its most basic sense, the investigation described herein is a very straightforward test of a specific prediction of the large-scale translation hypothesis. The large-scale translation hypothesis postulates major dextral translation between ca. 80-60 Ma (Cowan, 1994), including approximately 2000 km of relative displacement between the Intermontane and Insular superterranes. If there has been 2000 km of relative displacement between the Intermontane and Insular superterranes, then the Albian-Cenomanian (ca. 100-90 Ma) conglomerate units exposed on each superterrane cannot be correlative. Assessing the correlative or noncorrelative nature of the strata exposed on each superterrane is therefore of utmost importance. Correlation (or noncorrelation) of the strata must be proven via multiple lines of evidence. Stratigraphic sequences that will be examined during this investigation will be compared using multidisciplinary techniques including:

1. lithostratigraphy, 2. vertical and lateral variations in clast composition, 3. geochemistry/isotopic analysis of volcanic clasts, 4. micropaleontology and geochemistry of chert clasts, 5. palynology, 6. detrital zircon studies, 7. paleocurrent analysis, and 8. paleomagnetic signatures.

The primary goal of these analyses is proving or disproving stratigraphic linkages between the various Albian-Cenomanian conglomeratic sequences. Preliminary data and previous investigations (Garver, 1989, 1992; Mahoney et al., 1992) indicate these Albian to Cenomanian conglomerate units are nonmarine assemblages, probably deposited in fault-bounded (piggyback?) basins. In such systems, localized episodic tectonism produces a number of individual depocentres characterized by abrupt lateral facies changes, precluding system-wide stratigraphic correlations. The emphasis in a correlation study must therefore be placed on identifying unique provenance indicators suggesting derivation from a common source. Particular attention is being paid to quartzite clasts found in strata of the Intermontane Belt, identification of the provenance of muscovite in strata of the eastern Coast Belt, and the paleontology and geochemistry of chert clasts found in all sequences. In addition, the structural setting of each sequence is being examined to determine similarities in structural trend, fault and fold vergence, or other features that may suggest derivation within a single structural system.

## GEOLOGICAL SETTING

### *Terrane distribution*

A central tenet of the paleomagnetic tectonic model is that northward displacement of allochthonous terranes has been differentially distributed. Paleomagnetic studies from the Cretaceous Spences Bridge Group (104-90 Ma; Thorkelson and Rouse, 1989) of the *Intermontane superterrane* (amalgamated Stikine, Quesnellia, Cache Creek terranes) suggest these rocks have been translated ~1100 km north along a dextral fault that lay within the eastern third of Quesnellia, west of the Omineca belt (Fig. 1) (Irving and Thorkelson, 1990; Irving et al., 1995). Data from the *Insular superterrane* to the west of the Intermontane superterrane indicate substantially greater displacement. Paleomagnetic data from the Upper Cretaceous Silverquick conglomerate and overlying Powell Creek volcanic rocks (ca. 100-80 Ma; Garver, 1989; Wynne et al., 1995) of the Eastern Coast Belt require ~3000 km of dextral displacement along a fault between westernmost Intermontane strata and easternmost Coast Belt (i.e. Methow terrane) strata. This translation estimate is in good agreement with data from the Mt. Stuart batholith to the southwest (Ague and Brandon, 1992). Both the Silverquick conglomerate and Mt. Stuart batholith are within the 'mid-Cretaceous collisional orogen' of Cowan (1994). As defined by Cowan (1994), this orogen encompasses a number of small terranes, including the Methow, Bridge River, and Cadwallader terranes, that were amalgamated to the Insular superterrane between 100-90 Ma (Journeay and Friedman, 1993; Cowan, 1994), and thus were part of the Insular superterrane during any subsequent dextral translation (Fig. 1). The Methow, Bridge River, and Cadwallader terranes of Cowan's

'mid-Cretaceous collisional orogen' are part of the eastern Coast Belt, and were subject to contractional and translation deformation from mid-Cretaceous to early Tertiary time (Journeay and Friedman, 1993).

Differences in the magnitude of estimated displacement of the Intermontane and Insular superterranes requires up to 2000 km of relative motion between the two entities. The locus of this displacement must be a fault east of the Insular superterrane and associated mid-Cretaceous collisional orogen (Methow, Bridge River, Cadwallader terranes) and west of the Intermontane superterrane (Fig. 1). In the southern Canadian Cordillera, east of the Fraser fault system, the western boundary of the Intermontane superterrane is the Pasayten fault (Fig. 2). However, fabrics along the Pasayten fault record mid-Cretaceous sinistral and Eocene brittle reverse motion (Greig, 1992; Hurlow and Nelson, 1993; Monger and Price, in press), indicating that the Pasayten fault was not the locus of large-scale dextral translation. West of the Fraser fault system, the trace of the Pasayten fault is lost beneath a cover of Tertiary volcanic strata, and the locus of relative displacement must be constrained by the distribution

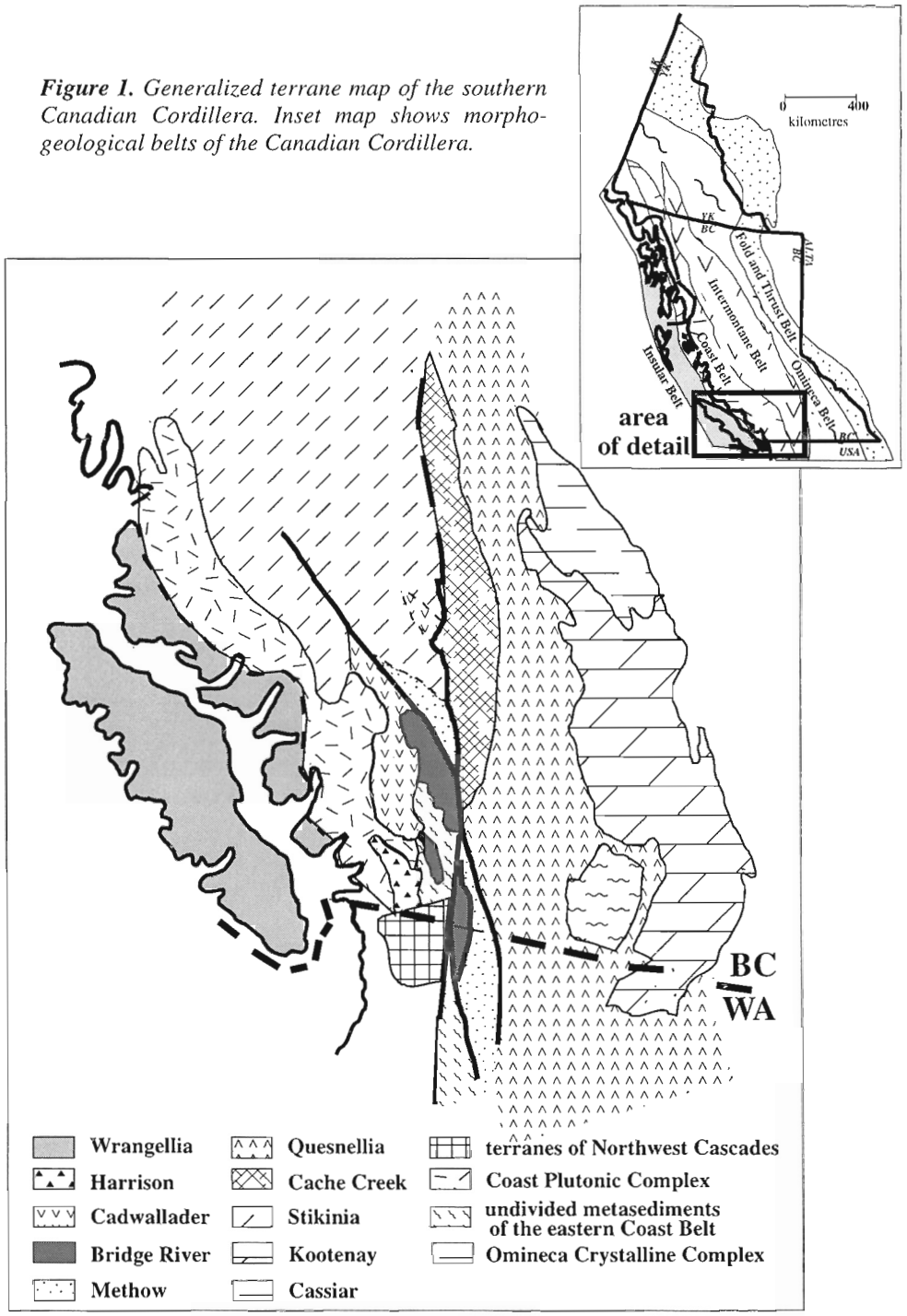


***Figure 1.*** *Generalized terrane map of the southern Canadian Cordillera. Inset map shows morpho-geological belts of the Canadian Cordillera.*

of rocks of the Intermontane superterrane versus those of the mid-Cretaceous collisional orogen. Westernmost Intermontane strata form a northwest-trending outcrop belt between the Fraser fault system and Churn Creek; younger rocks obscure all older strata to the north (Fig. 3). Rocks in this belt consist of Lower Cretaceous volcanic units and associated granitoid intrusions, and are correlated with coeval rocks of the Spences Bridge Group of the Intermontane Belt on the basis of stratigraphic, lithological, and geochronological similarities (Hickson et al., 1991). In Churn Creek, chert and volcanic pebble conglomerate correlated with the Albian-Cenomanian Silverquick conglomerate of the Methow terrane unconformably(?) overlie andesite of the Spences Bridge Group (Hickson et al., 1991; Mahoney et al., 1992). Southwest of Churn Creek, strata of the Methow terrane (part of mid-Cretaceous collisional orogen) form a northwest-trending outcrop belt that parallels the Intermontane belt (Fig. 2, 3). Methow strata are exposed between the Yalakom fault to the southwest and a cover of Tertiary volcanic rocks to the northeast (Fig. 2, 3). The maximum cross-strike distance between the two belts is 15-20 km, and the belts are directly adjacent across a splay of the Fraser fault system (Slok Creek fault), north of the Yalakom/Fraser fault juncture. Following the 'large-scale displacement' axiom, this zone between Intermontane and Insular/mid-Cretaceous collisional orogen strata must contain a fault that has accommodated at least 2000 km dextral translation, and pre-55 Ma strata on either side of that structure cannot be correlative. This investigation is designed to test that assertion.

### *Albian-Cenomanian conglomerate units*

Upper Cretaceous conglomeratic strata occur within rocks associated with both the Intermontane and the Insular superterranes in the southern Canadian Cordillera. The Insular superterrane is flanked on both its east and west margins by Upper Cretaceous clastic strata (Wheeler and McFeely, 1991). On the west, the Turonian to Maastrichtian (ca. 90-65 Ma) Nanaimo Group forms a westward thinning clastic wedge that received detritus from the mid-Cretaceous collisional orogen to the east (Mustard, 1994; Mustard et al., 1995). On the east, thick sequences of Upper Cretaceous strata were deposited in the Methow-Tyaughton basin, which developed on top of the previously amalgamated Methow, Bridge River, and Cadwallader terranes (now part of the mid-Cretaceous collisional orogen) (Garver, 1989, 1992; Mahoney and Journeay, 1993; Mahoney, 1994). The Albian-Cenomanian (100-90 Ma) Silverquick conglomerate and overlying Powell Creek volcanic rocks constitute the youngest strata within the mid-Cretaceous collisional orogen. The Silverquick conglomerate and correlative strata are widely exposed in the Methow terrane on both sides of the Fraser fault system, along the eastern margin of the collisional orogen

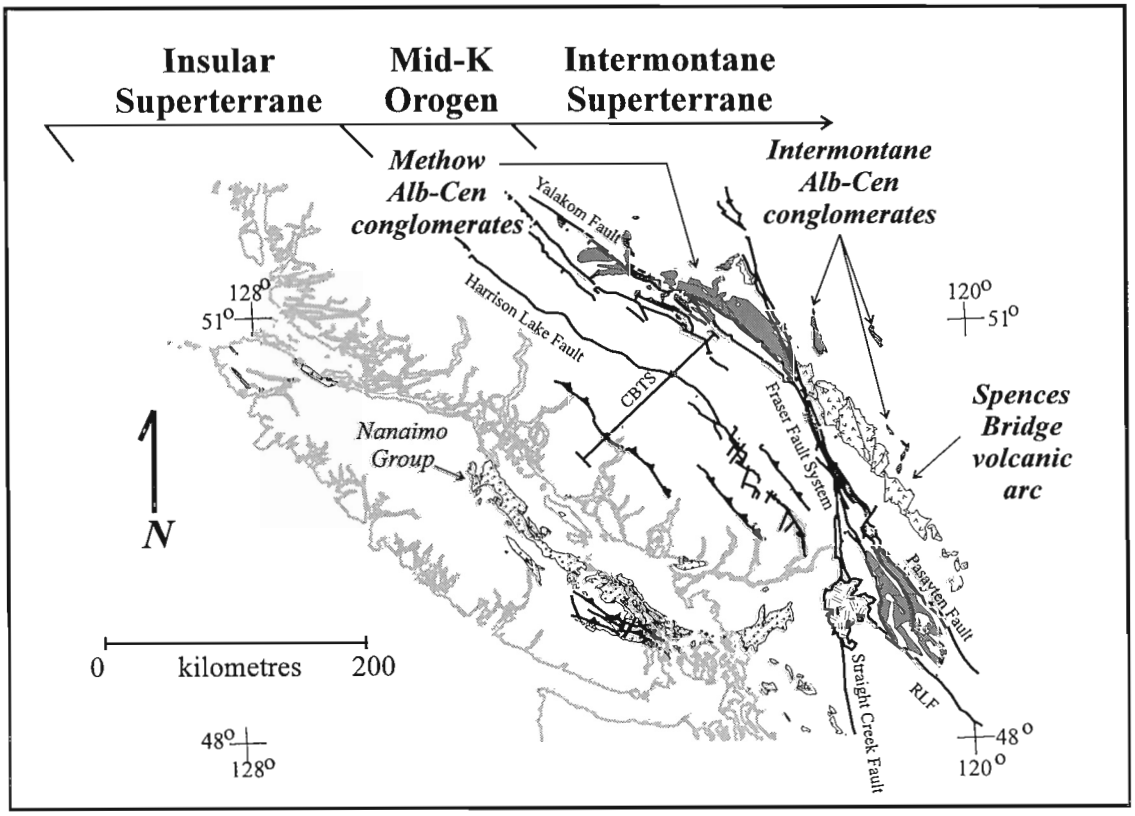


***Figure 2.*** *Schematic geological map of the eastern Coast Belt and western Intermontane Belt showing distribution of Albian-Cenomanian conglomerate units and major faults. CBTS=Coast Belt Thrust System of Journeay and Friedman (1993)*

(Monger and Journeay, 1992). These strata are interpreted to be nonmarine sediments derived from an intrabasinal uplifted block of Bridge River terrane (Garver, 1989, 1992).

Although Albian-Cenomanian strata are uncommon in the southern Intermontane superterrane, isolated remnants of conglomeratic strata are found along the western margin of the superterrane in widely scattered exposures flanking the north end of the main outcrop belt of the Spences Bridge Group (Fig. 2). The Spences Bridge Group is at the north end of a northwest-trending late Early Cretaceous volcanoplutonic complex referred to as the Okanagan-Spences Bridge Arc (Thorkelson and Rouse, 1989; Hurlow and Nelson, 1993). This volcanoplutonic complex occupies a north-plunging elongate structural depression that results in increasingly deeper levels of erosion to the south, and any post-late Early Cretaceous supracrustal rocks have been removed. The scattered remnants that remain at the north end of the outcrop belt consist of volcanic and chert pebble to boulder conglomerate deposited in nonmarine environments. East of the Fraser fault system, these strata unconformably overlie rocks of the Mississippian-Jurassic Cache Creek Complex and Triassic Nicola Group. West of the Fraser fault system and north of the Yalakom fault, coeval strata apparently unconformably overlie the Spences Bridge Group (Hickson et al., 1991; Mahoney et al., 1992).

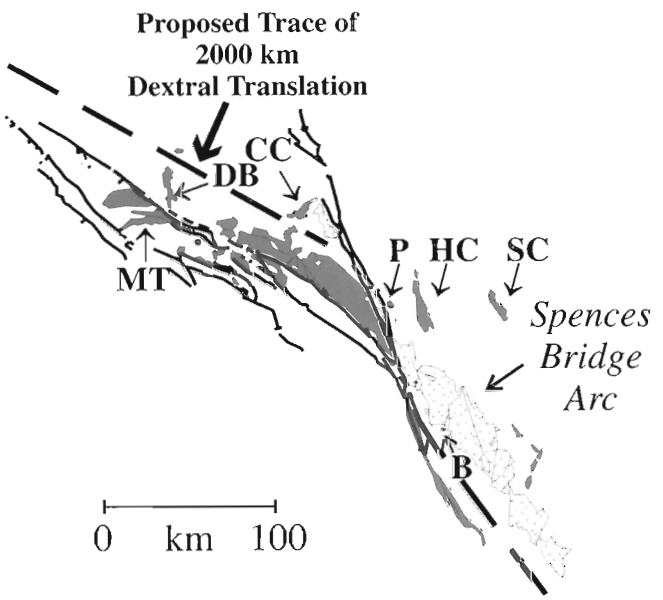


***Figure 3.*** *Schematic geological map of the study area. Note outcrop belts of Spences Bridge Group of the Intermontane superterrane and Methow terrane strata of the mid-Cretaceous collisional orogen. Dashed fault is inferred location of dextral translation fault required by paleomagnetic data. Exposures being examined include, from east to west: SC=Sabiston Creek, HC=Hat Creek, P=Pavillion, B=Bontanie Creek, CC=Churn Creek; DB=Davidson Bridge, MT=Mt. Tatlow. CC=Churn Creek exposures of Silverquick conglomerate; DB=Davidson Bridge paleomagnetic site within strata of the mid-Cretaceous collisional orogen.*

## *Stratigraphic sections*

Stratigraphic analysis begun during the 1995 field season concentrated on reconnaissance of all sections and collection of representative samples of both conglomerate clasts and country rock for initial laboratory analysis. Sections examined are described from east to west.

### 1. Conglomerate of Sabiston Creek

Pebble to cobble polymict conglomerate unconformably overlies Triassic Nicola Group strata east of Sabiston Creek, at the northwestern end of Kamloops Lake (SC in Fig. 3). The conglomerate is primarily clast supported, matrix supported in part, and locally displays strong clast imbrication. Clasts are predominantly andesite and dacite volcanic rock, andesite to dacite porphyries, rhyolite, rhyolite tuff, volcaniclastic sandstones, with subordinate black chert and quartzite. Grain size is strongly bimodal, characterized by pebble to cobble-sized volcanic clasts intermixed with pebble-sized black chert clasts. Pebble- to boulder-sized light grey quartzite clasts are a conspicuous component of the conglomerate, and have been sampled for detrital zircon analysis. Monger (1982) suggested the only known source for such clasts is Proterozoic to Lower Paleozoic strata exposed east of the area in the Omineca Crystalline Belt (Fig. 1). These rocks were previously mapped as the Jurassic Ashcroft Formation (Monger, 1982), but recent palynological data indicate these rocks are of Late Cretaceous age (P. Reid and G. Rouse, pers. comm., 1994).

### 2. Conglomerate of Hat Creek

Polymict chert-pebble conglomerate is contained within a 25-30 km long, north-trending fault block centred on the lower reaches of Hat Creek (HC in Fig. 3). The conglomerate is well exposed along both sides of Hat Creek, which provides an excellent cross-section through a broad anticline within the unit. The base of the unit is exposed in the core of the anticline, where it is interpreted to unconformably overlie both the Triassic Nicola Group and the Mississippian-Jurassic Cache Creek Group. Although the contact is not exposed, the occurrence of angular granule- to pebble-sized clasts of green, siliceous metavolcanic rocks and black phyllite near the contact with the underlying Nicola Group suggests derivation from the immediately subjacent units. Shearing is evident in the Nicola Group, and is localized near the contact; deformation is not pervasive, and is believed to represent interstratal slip along an unconformable contact. The conglomerate of Hat Creek consists of approximately 425 m of intercalated pebble to cobble conglomerate and medium- to coarse-grained sandstone with subordinate siltstone and shale (Fig. 4). Conglomerate clasts are predominantly black, grey, and red chert, green metavolcanic rocks, black phyllite, and vein quartz in a chert lithic sandstone matrix. The conglomerate is laterally discontinuous and appears to contain abundant channels with crude internal bedding. Channels amalgamate to form 25-50 m thick massive-appearing conglomerate. Clast composition varies strongly, from monomict chert pebble conglomerate to polymict chert, volcanic, and black phyllite pebble to cobble conglomerate.

Intercalated sandstone locally contains abundant feldspar and quartz, indicative of a plutonic source. Preliminary paleocurrent measurements suggest paleoflow was dominantly to the east (77-92°). There are strong east to west lateral lithologic variations within the unit, exhibited by a dramatic increase in the amount and size of angular to subrounded limestone clasts along the western side of the outcrop belt. These limestone clasts contain the Late Paleozoic fusulinid *Yabeina*, indicating derivation from the Marble Canyon Formation of the Cache Creek Group directly to the west. The conglomerate of Hat Creek contains palynomorphs of Late Albian to Cenomanian age (Shannon, 1981).

### 3. Pavilion conglomerate

Isolated remnants of polymict conglomerate are exposed on the cliffs above the settlement of Pavilion, directly east of the Fraser River (P in Fig. 3). The unit is also exposed in small outcrops east of Pavilion, and at the head of a large landslide complex south of Pavilion. North of Pavilion, the unit is only exposed directly on the cliff face, where approximately 50-60 m of conglomerate unconformably overlies chert-rich strata of the Cache Creek Group along a well-exposed contact. The unit consists of 0.5-3 m beds of crudely stratified, unsorted angular chert granule to boulder conglomerate/breccia intercalated with thin beds of pebbly sandstone to mudstone. Heavy iron oxidation and concretions in the fine grained interbeds may indicate paleosol horizons. Conglomerate beds are lenticular, have erosive bases, and appear to be channelized in part. Channel axis orientations suggest the dominant paleoflow was to the east. The unsorted, angular nature of the conglomerate and crude channel organization suggest this unit may represent a proximal fanglomerate.

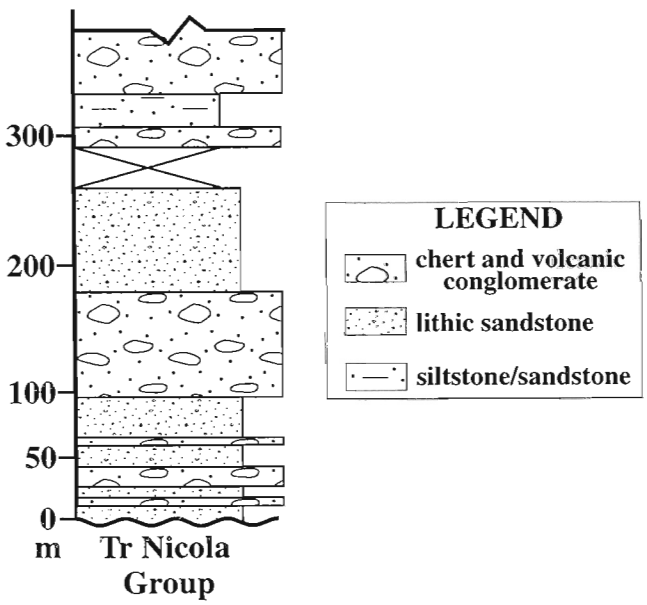


***Figure 4.*** *Measured stratigraphic section of Albian-Cenomanian conglomerate along Hat Creek.*

These conglomerates are Albian-Cenomanian in age, based on microflora from intercalated siltstone beds (Monger and McMillan, 1989).

### 4. Conglomerate of Botanie Creek

Red-stained polymict chert-pebble conglomerate is exposed in fault slivers along the western and eastern sides of the Permian Mt. Lytton Complex (B in Fig. 3). Along the eastern side of the complex, conglomerate is exposed along Botanie Creek, north of the Thompson River. The unit is poorly exposed, but apparently lies unconformably above the Mt. Lytton Complex. A distinct reddish horizon at the base of the unit is interpreted by Monger and Journeay (1992) to represent a paleosol developed on deeply eroded Mt. Lytton Complex in the mid-Cretaceous. Along the western side of the complex, the conglomerate is caught up in strands of the Fraser fault system and is chaotically deformed. However, the occurrence of large, angular clasts of Mt. Lytton Complex within the conglomerate adjacent to a sheared contact between the complex and the conglomerate strongly suggests this contact is a sheared unconformity. The conglomerate of Botanie Creek consists of intercalated pebble to boulder conglomerate, medium- to coarse-grained well sorted sandstone, red siltstone and argillite. Deformation and lack of continuous exposure makes compilation of a stratigraphic section difficult. Clast composition varies widely within the conglomerate, from monomict chert pebble conglomerate to mixed volcanic and chert conglomerate; subordinate angular tuffaceous clasts may indicate contemporaneous volcanism. Pebble-sized clasts of light grey quartzite form a distinct component of the unit, and will be examined for detrital zircons. Palynomorphs indicate the conglomerate of Botanie Creek is mid-Albian to Cenomanian (Monger and McMillan, 1989; Monger and Journeay, 1992).

### 5. Conglomerate of Churn Creek

Well-exposed sections of chert pebble and volcanic clast conglomerate occur in Churn Creek, west of the Fraser fault system and northeast of the Yalakom fault (CC in Fig. 3). These rocks are described in detail by Mahoney et al. (1992), and are only briefly summarized here. The conglomerate of Churn Creek was correlated by Mahoney et al. (1992) with the Silverquick conglomerate, whose type area is exposed approximately 30 km to the south (Garver, 1989). The conglomerate (Fig. 5) of Churn Creek comprises over 1100 m of strata that may be subdivided into three distinct units based on clast composition and grain size: 1) a lower unit composed of coarse sand to pebble chert-rich sediment; 2) a middle unit containing cobble to boulder volcanic clast conglomerate intercalated with coarse grained feldspathic lithic sandstone; and 3) an upper unit containing cobble to boulder volcanic clast conglomerate with a significant proportion of pink quartz monzonite clasts. Excellent exposures of a fault juxtaposing pink monzonite against boulder conglomerate demonstrate that the pink monzonite in the upper unit was derived from a pluton uplifted along a syndepositional, northwest-trending, northeast-vergent thrust fault (Mahoney et al., 1992). The conglomerate is channelized, lenticular in

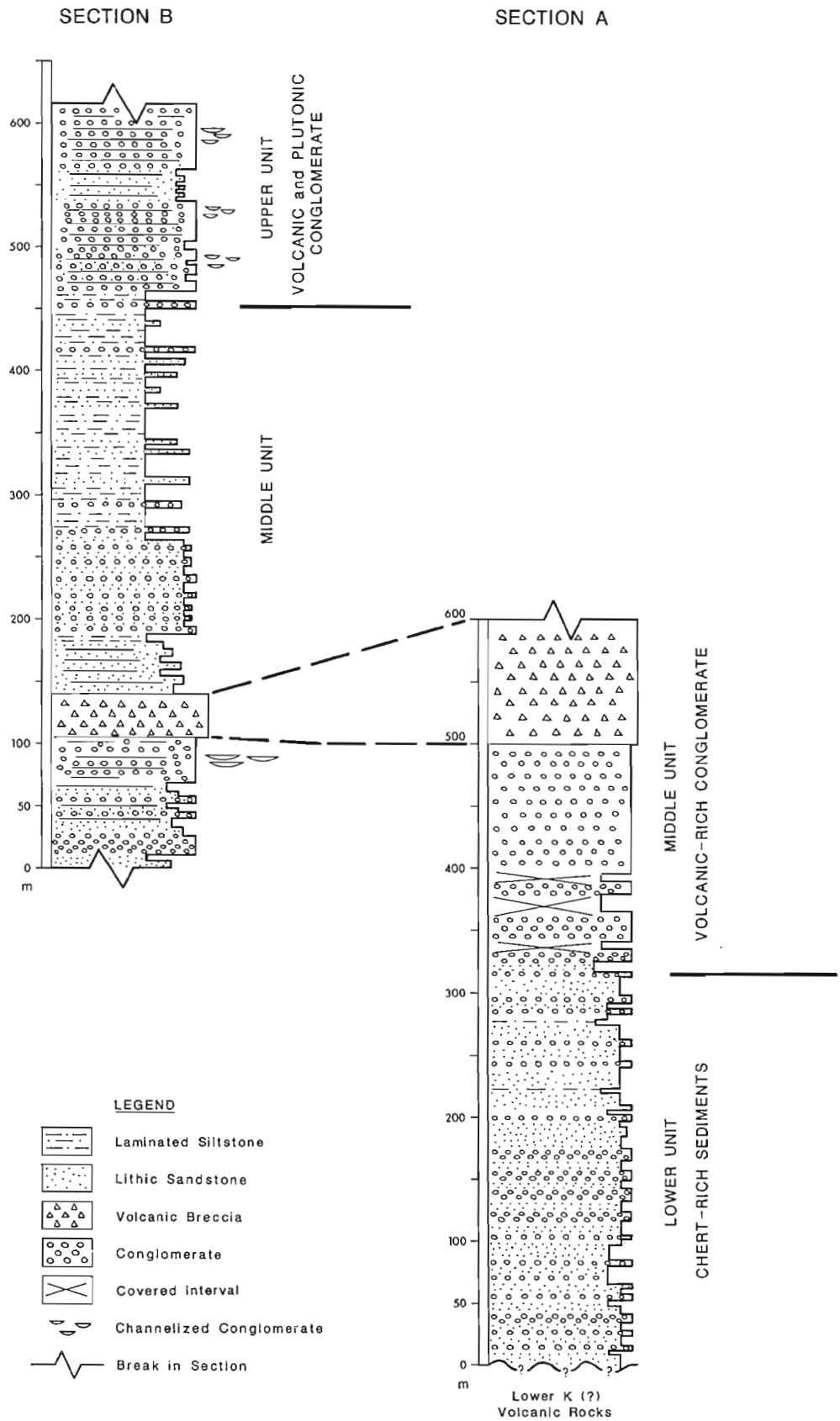


***Figure 5.*** *Stratigraphic sections of Silverquick conglomerate on Churn Creek. From Mahoney et al., 1992.*

cross-section, and contains erosive bases. The entire section is characterized by rapid lateral and vertical facies changes. The conglomerate in Churn Creek yields a late Albian to early Cenomanian palynomorph assemblage (Hickson et al., 1991).

Similarities in age, lithology, clast composition, stratigraphy, association with overlying volcanic rocks (Powell Creek volcanics), and depositional environment led Mahoney et al. (1992) to correlate rocks along Churn Creek with the Silverquick conglomerate of Garver (1989, 1992). The base of the conglomerate in Churn Creek occurs in the core of an anticline, where chert-rich conglomerate appears to unconformably overlie amygdaloidal, zeolite-rich, andesitic lava. The underlying volcanic succession yields a 101.0 ± 3 Ma K-Ar date. Similarities in age, lithology, alteration, and stratigraphy indicate these volcaniclastic rocks are correlative with the Spences Bridge Group to the southeast (Green, 1989, 1990; Hickson et al., 1991; Mahoney et al., 1992). The contact between the conglomerate and underlying volcanic rocks is critical, as are the correlations just described. If the contact is indeed disconformable, then rocks believed to be correlative with the youngest unit of the mid-Cretaceous collisional orogen unconformably overlie the Spences Bridge Group of the Intermontane superterrane. This relationship would rule out the possibility of the large-scale displacement between the Intermontane superterrane and rocks associated with the Insular superterrane suggested by paleomagnetic studies. The rocks exposed in Churn Creek will be extensively re-examined during the 1996 field season.

### 6. Silverquick strata of Mt. Tatlow

In their paleomagnetic study, Wynne et al. (1995) sampled strata from the Mt. Tatlow area southwest of the Yalakom fault and the Davidson Bridge area northeast of the fault (MT and DB in Fig. 3). These rocks have not yet been examined by the authors. The following summary is based on descriptions in Wynne et al. (1995). They correlated the rocks near Mt. Tatlow with the Silverquick conglomerate based on stratigraphic position and age constraints. The Upper Cretaceous conglomerate in the Mt. Tatlow area is significantly finer grained than rocks of the Silverquick conglomerate in the type area of Garver (1989, 1992). The unit consists of channelized sandstone and conglomerate, with a high proportion of thinly bedded, planar laminated fine grained sandstone, siltstone, and mudstone. The fine grained beds are interpreted as fluvial overbank and crevasse splay deposits. The base of the unit is interpreted to be disconformable with underlying rocks of the Taylor Creek Group of the Tyaughton basin (P. Schiarizza, pers. comm., 1995). The strata are conformably overlain by the Powell Creek volcanic rocks, which yield a $^{40}Ar$-$^{39}Ar$ date of 92 ± 1.3 Ma. Wynne et al. (1995) regarded the Silverquick conglomerate as entirely Cenomanian in age, based on microflora and age constraints from overlying and underlying units.

The rocks sampled by Wynne et al. (1995) on both sides of the Yalakom fault are lithologically and stratigraphically similar and give similar paleomagnetic signatures, indicating that the Yalakom fault is not the locus of major translation. If the Yalakom fault is not the locus of major translation, then the locus must be located between the rocks Wynne et al. (1995) sampled on the eastern side of the Yalakom fault and the exposures correlated with the Spences Bridge Group in Churn Creek. Strata of the Mt. Tatlow and Davidson Bridge areas will be examined in detail by the authors during the course of this study.

## SUMMARY

Cowan (1994) very correctly pointed out neither of the two data sets regarding large-scale terrane translation are conclusive, and that available evidence is compatible with more than one paleogeographic interpretation. The investigation described herein is designed to critically evaluate a direct prediction of the paleomagnetic hypothesis: the correlation or non-correlation of Albian-Cenomanian strata between the Insular and Intermontane superterranes. This investigation is truly an interdisciplinary effort involving scientists from both sides of the debate.

## ACKNOWLEDGMENTS

This investigation represents a co-operative effort among geologists and geophysicists from both sides of the debate to solve the fundamental conflict of terrane translation. The problem being addressed has concerned the authors for some time, and the focus of the problem was precisely defined during a 1995 reconnaissance field trip with two of the authors (J.B. Mahoney, J.W.H. Monger), and Ted Irving, Jane Wynne, Randy Enkin, Paul Schiarizza and Darrel Cowan. We wish to thank those people for their insight and scientific assistance, past, present, and future. We particularly wish to commend Darrel Cowan for bringing the conflicting data sets more sharply into focus. Comments by Murray Journeay improved the manuscript, and Bev Vanlier is once again thanked for her technical assistance and patience.

## REFERENCES

**Ague, J.J. and Brandon, M.T.**
1992: Tilt and northward offset of Cordilleran batholiths resolved using igneous barometry; Nature, v. 360, p. 146-149.

**Cowan, D.S.**
1994: Alternative hypotheses for the Mid-Cretaceous paleogeography of the Western Cordillera; GSA Today, v. 4, no. 7, p. 181-186.

**Cowan, D.S., Brandon, M.T., and Garver, J.I.**
1994: Potential geologic refutations of the Baja B.C. hypothesis; Geological Society of America, Abstracts with Programs, v. 26, no. 7, p. 461.

**Garver, J.I.**
1989: Basin evolution and source terranes of Albian-Cenomanian rocks in the Tyaughton basin, southern British Columbia: implications for mid-Cretaceous tectonics in the Canadian Cordillera; PhD. thesis, University of Washington, Seattle, Washington, 228 p.
1992: Provenance of Albian-Cenomanian rocks of the Methow and Tyaughton basins, southern British Columbia: a mid-Cretaceous link between North America and Insular terranes; Canadian Journal of Earth Sciences, v. 29, p. 1274-1295.

**Green, K.C.**
1989: Geology and industrial minerals of the Gang Ranch area; British Columbia Ministry of Energy, Mines, and Petroleum Resources, Open File 1989-27
1990: Structure, stratigraphy, and alteration of Cretaceous and Tertiary strata in the Gang Ranch area, British Columbia; MSc. thesis, Univerisity of Calgary, Calgary, Alberta, 118 p.

**Greig, C.J.**
1992: Jurassic and Cretaceous plutonic and structural styles of the Eagle Plutonic Complex, southwestern British Columbia, and their regional significance; Canadian Journal of Earth Sciences, v. 29, p. 793-811.

**Hickson, C.J., Read, P., Mathews, W.H., Hunt, J.A., Johansson, G., and Rouse, G.E.**
1991: Revised geological mapping of northeastern Taseko Lakes map area, British Columbia; in Current Research, Part A; Geological Survey of Canada, Paper 91-1A, p. 207-217.

**Hurlow, H.A. and Nelson, B.K.**
1993: U-Pb zircon and monazite ages for the Okanogan Range batholith, Washington: Implications for the magmatic and tectonic evolution of the southern Canadian and northern United States Cordillera; Geological Society of America Bulletin, v. 105, p. 231-240.

**Irving, E.**
1985: Whence British Columbia?; Nature, v. 314, p. 673-674.

**Irving, E. and Thorkelson, D.J.**
1990: On determining paleohorizontal and latitudinal shifts: Paleomagnetism of Spences Bridge Group, British Columbia; Journal of Geophysical Research, v. 95, p. 19,213-19,234.

**Irving, E. and Wynne, P.J.**
1990: Palaeomagnetic evidence bearing on the evolution of the Canadian Cordillera; Philosophical Transactions of the Royal Society of London, v. 331A, p. 487-509.

**Irving, E., Thorkelson, D.J., Wheadon, P.M., and Enkin, R.J.**
1995: Paleomagnetism of the Spences Bridge Group and northward displacement of the Intermontane Belt, British Columbia: a second look; Journal Geophysical Research, v. 100, no. B4, p. 6057-6071.

**Journeay, J.M. and Friedman, R.M.**
1993: The Coast Belt Thrust System: Evidence of Late Cretaceous shortening in southwest British Columbia; Tectonics, v. 3, p. 756-775.

**Mahoney, J.B.**
1994: Nd isotopic signatures and stratigraphic correlations: examples from western Pacific marginal basins and Middle Jurassic rocks of the southern Canadian Cordillera; PhD. thesis, University of British Columbia, Vancouver, British Columbia, 328 p.

**Mahoney, J.B. and Journeay, J.M.**
1993: The Cayoosh assemblage, southwestern British Columbia: last vestige of the Bridge River ocean; in Current Research, Part A; Geological Survey of Canada, Paper 93-1A, p. 235-244.

**Mahoney, J.B., Hickson, C.J., van der Heyden, P., and Hunt, J.A.**
1992: The Late Albian-Early Cenomanian Silverquick conglomerate, Gang Ranch area: evidence for active basin tectonism; in Current Research, Part A; Geological Survey of Canada, Paper 92-1A, p. 249-260.

**Marquis, G. and Globerman, B.R.**
1988: Northward motion of the Whitehorse Trough: paleomagnetic evidence from the Upper Cretaceous Carmacks Group; Canadian Journal of Earth Sciences, v. 25, p. 2005-2016.

**Monger, J.W.H.**
1982: Geology of Ashcroft map area, southwestern British Columbia; in Current Research, Part A; Geological Survey of Canada, Paper 82-1A, p. 293-297.

**Monger, J.W.H. and Journeay, J.M.**
1992: Guide to the geology and tectonic evolution of the southern Coast Belt: Proceedings to Penrose Conference on the "Tectonic Evolution of the Coast Mountains Orogen", p. 97.

**Monger, J.W.H. and McMillan, W.J.**
1989: Geology, Ashcroft, British Columbia; Geological Survey of Canada, Map 42-1989, sheet 1, scale 1:250 000.

**Monger, J.W.H. and Price, R.A.**
in press: Geological constraints on Late Cretaceous large-scale northward displacement in the southwestern Canadian Cordillera inferred from paleomagnetic data by Wynne et al., 1995; Journal of Geophysical Research.

**Monger, J.W.H., Price, R.A., and Tempelman-Kluit, D.J.**
1982: Tectonic accretion and the origin of the two major metamorphic welts in the Canadian Cordillera; Geology, v. 10, p. 70-75.

**Monger, J.W.H., van der Heyden, P., Journeay, J.M., Evenchick, C.A., and Mahoney, J.B.**
1994: Jurassic-Cretaceous basins along the Canadian Coast Belt: their bearing on pre-mid-Cretaceous sinistral displacements; Geology, v. 22, p. 175-178.

**Mustard, P.S.**
1994: The Upper Cretaceous Nanaimo Group, Georgia Basin; in Geology and Geological Hazards of the Vancouver Region, Southwestern British Columbia, (ed.) J.W.H Monger; Geological Survey of Canada, Bulletin 481, p. 27-95.

**Mustard, P.S., Parrish, R.R., and McNicoll, V.**
1995: Provenance of the Upper Cretaceous Nanaimo Group, British Columbia: evidence from U-Pb analyses of detrital zircons; in Stratigraphic Evolution of Foreland Basins; Society of Economic Paleontologists and Mineralogists, Special Publication No. 52, p. 65-75.

**Rubin, C.M., Saleeby, J.B., Cowan, D.S., Brandon, M.T., and McGroder, M.F.**
1990: Regionally extensive mid-Cretaceous west-vergent thrust system in the northwestern Cordillera: Implications for continent-margin tectonism; Geology, v. 18, p. 276-280.

**Rusmore, M.E., Potter, C.J., and Umhoefer, P.J.**
1988: Middle Jurassic terrane accretion along the western edge of the Intermontane Superterrane, southwestern British Columbia; Geology, v. 16, p. 891-894.

**Shannon, K.R.**
1981: The Cache Creek Group and contiguous rocks near Cache Creek, British Columbia; in Current Research, Part A; Geological Survey of Canada, Paper 81-1A, p. 217-221.

**Thorkelson, D.J. and Rouse, G.E.**
1989: Revised stratigraphic nomenclature and age determinations for mid-Cretaceous volcanic rocks in southwestern British Columbia; Canadian Journal of Earth Sciences, v. 26, p. 2016-2031.

**Umhoefer, P.J.**
1987: Northward translation of "Baja British Columbia" along the Late Cretaceous to Paleocene margin of western North America; Tectonics, v. 6, p. 377-394.

**van der Heyden, P.**
1992: A Middle Jurassic to Early Tertiary Andean-Sierran arc model for the Coast Belt of British Columbia; Tectonics, v. 11, p. 82-97.

**Wheeler, J.O. and McFeeley, P.**
1991: Tectonic assemblage map of the Canadian Cordillera and adjacent parts of the United States of America; Geological Survey of Canada, Map 1712A, scale 1:2 000 000.

**Wynne, P.J., Irving, E., Maxson, J.A., and Kleinspehn, K.L.**
1995: Paleomagnetism of the Upper Cretaceous strata of Mount Tatlow: evidence for 3000 km of northward displacement of the eastern Coast Belt, British Columbia; Journal of Geophysical Research, v. 100, no. B4, p. 6073-6091.

Geological Survey of Canada Project 890039

# U-Pb zircon ages of the Island Copper deposit intrusions, northern Vancouver Island, British Columbia

K.V. Ross, R.M. Friedman[1], K.M. Dawson, and C.H.B. Leitch[2]
Mineral Resources Division, Vancouver

*Ross, K.V., Friedman, R.M., Dawson, K.M., and Leitch, C.H.B., 1996: U-Pb zircon ages of the Island Copper deposit intrusions, northern Vancouver Island, British Columbia; in Current Research 1996-A; Geological Survey of Canada, p. 111-117.*

**Abstract:** A rhyodacite quartz-feldspar porphyry dyke complex, comprising three phases, hosts the Island Copper mine, a Cu-Mo-Au island arc-type porphyry deposit. New zircon U-Pb age dates for the phases, bracket the timing of mineralization to ca. 169-166 Ma and include: 168.5 + 0.3/-1.7 Ma for the earliest, generally premineral phase; 168.5 ± 0.6 Ma for the second Cu-Mo-Au mineralizing phase; and 166.2 ± 0.7 Ma for the third, generally barren phase. The older mineralized dykes are coeval with the adjacent Rupert stock to the east, and the dates are permissive of previously proposed cogenesis. These ages are also nearly coeval with the youngest intrusions of the Island Intrusions and with arc volcanic rocks of the upper Bonanza Group on northern Vancouver Island. These and other Middle Jurassic magmatic rocks define an arc that extends eastward across the southern Coast Belt and northward through the northern Insular and Coast belts to Alaska.

**Résumé :** Un complexe de dykes de rhyodacite porphyrique à quartz-feldspaths, divisé en trois phases, renferme le gisement porphyrique de Cu-Mo-Au de type arc insulaire de la mine Island Copper. Les nouvelles datations U-Pb sur zircon des différentes phases permettent de limiter la minéralisation à un intervalle approximatif s'échelonnant de 169 Ma à 166 Ma. Les âges obtenus sont les suivants : 168,5 + 0,3/- 1,7 Ma pour la phase initiale généralement antérieure à la minéralisation; 168,5 ± 0,6 Ma pour la deuxième phase de minéralisation en Cu-Mo-Au; 166,2 ± 0,7 Ma pour la troisième phase généralement stérile. Les dykes minéralisés les plus anciens sont contemporains du stock de Rupert, immédiatement à l'est, et les datations permettent de confirmer la cogenèse antérieurement proposée. Ces âges sont en outre quasi contemporains des intrusions les plus récentes de la suite plutonique d'Island et des roches d'arc volcanique de la partie supérieure du Groupe de Bonanza, observées dans la partie nord de l'île de Vancouver. Ces unités et d'autres roches magmatiques du Jurassique moyen définissent un arc qui traverse, vers l'est, le sud de la chaîne Côtière et, vers le nord, les chaînes Insulaire et Côtière jusqu'en Alaska.

[1] Geochronology Laboratory, University of British Columbia, 6339 Stores Road, Vancouver, British Columbia V6T 1Z4
[2] 492 Isabella Point Road, Salt Spring Island, British Columbia V8K 1V4

## INTRODUCTION

The Island Copper mine, operated by BHP Minerals Ltd., encompasses an island-arc-type porphyry Cu-Mo-Au deposit (Perello et al., 1989, in press; Arancibia and Clark, 1990; Leitch et al., 1995) on northern Vancouver Island, near Port Hardy, British Columbia (Fig. 1). The deposit is hosted by a series of rhyodacite quartz-feldspar porphyry dykes of the Island Intrusions and comagmatic high-alumina basalts, basaltic andesites, minor rhyolite, and pyroclastic rocks of the Lower to Middle Jurassic Bonanza Group (Northcote and Robinson, 1973; Muller et al., 1974; Nixon et al., 1994). The copper-bearing dykes are likely lateral offshoots of the Rupert Stock (Northcote and Robinson, 1973), which outcrops to the east of the deposit. Crosscutting relationships and variation in intensity of alteration among the dykes, visible in drill core and the open pit, support three main stages of intrusion. Three samples of rhyodacite quartz-feldspar porphyries representative of the three episodes of intrusion (Fig. 2) were collected during 1994 field season for U-Pb age determinations.

The new ages reported here contribute to a joint project which involves the Mineral Resources Division of the Geological Survey of Canada, the British Columbia Geological Survey Branch (BCGSB), BHP Minerals Ltd., and Auckland University (New Zealand). The project was initiated to study the Island Copper deposit prior to mine closure and pit flooding, anticipated in 1995, and complements ongoing regional work by the BCGSB in the northern Vancouver Island area.

## TECTONIC SETTING AND REGIONAL GEOLOGY

Northern Vancouver Island is part of Wrangellia which is bounded to the east by the Coast Plutonic Complex, and on the west by the Pacific Rim and Ozette accretionary complexes (Wheeler and McFeely, 1991). The area is underlain by fault-bounded blocks of Upper Triassic to Middle Jurassic Vancouver and Bonanza group sedimentary and volcanic strata, intruded by Jurassic plutons of the Island Intrusions (Muller et al., 1974), and unconformably overlain by Cretaceous sedimentary rocks (Nixon et al., 1994). The Upper Triassic Vancouver Group comprises Karmutsen, Quatsino, and Parson Bay formations. The Karmutsen Formation consists of basaltic lava flows, subvolcanic intrusions, and minor intercalated limestone horizons (Nixon et al., 1994). The Quatsino Formation conformably overlies the Karmutsen Formation and consists of thickly bedded to massive, generally unfossiliferous, limy mudstone, which is recrystallized

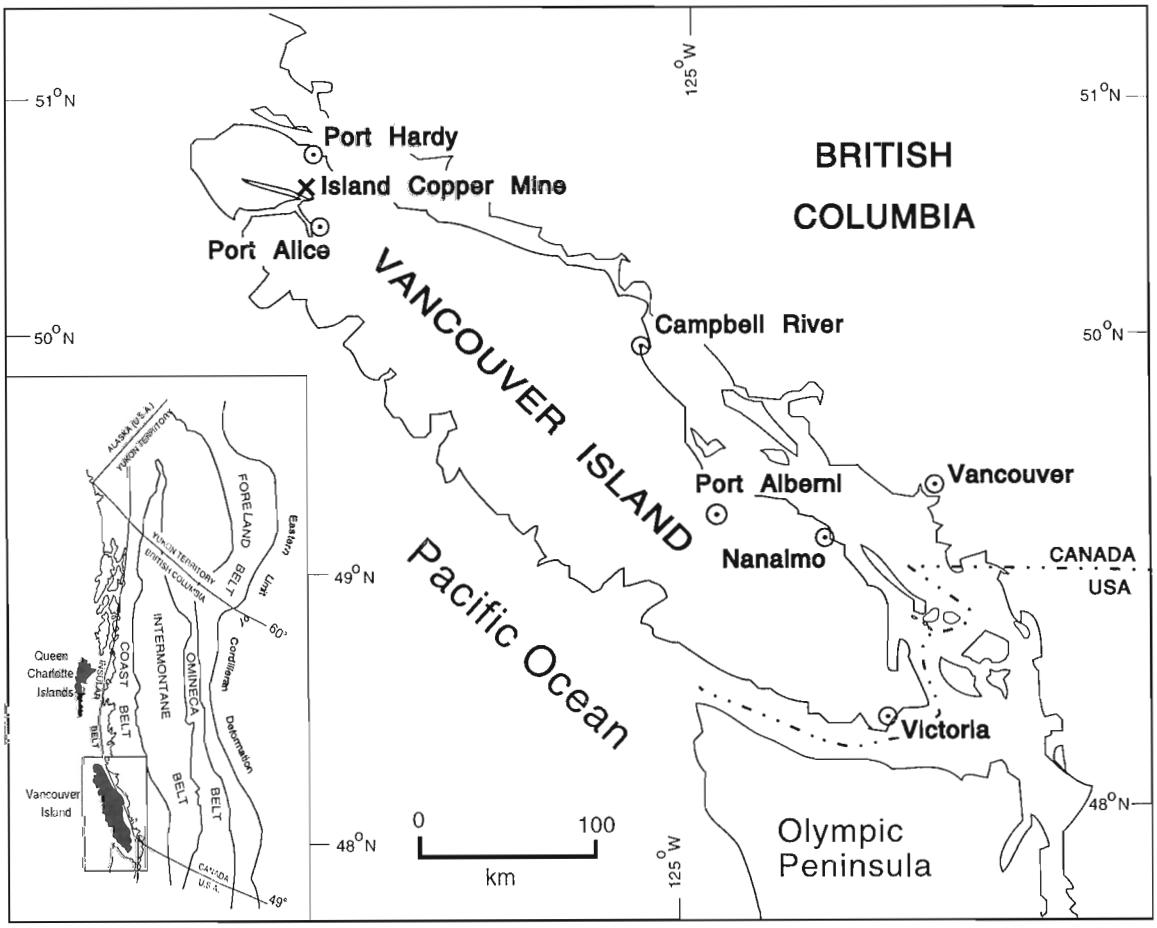


***Figure 1.*** *Location of the Island Copper mine, Port Hardy, British Columbia.*

adjacent to plutons and faults. It grades upwards into the Parsons Bay Formation, which consists of a calcareous western facies and a weakly to noncalcareous eastern and northern facies. The conformably overlying Lower to Middle Jurassic Bonanza Group is a succession of pyroclastic-epiclastic subaqueously deposited basaltic andesite and minor rhyolite, that is overlain by a thick succession of subaerial lavas and pyroclastic rocks with minor sedimentary horizons. In the area of the Island Copper mine, the pyroclastic-epiclastic sequences are over 1000 m thick (Fahey, 1979). The granitoids of the Jurassic Island Intrusions intrude, and are in part, coeval with the Bonanza Group (Northcote and Muller, 1972). They range from diorite, monzodiorite, quartz diorite to granodiorite in composition. The Cretaceous strata comprise sandstones, siltstones, pebble conglomerate, and coal beds. The Island Copper intrusion is a N70°W trending, 60°N dipping composite dyke, 200 m wide, that is probably an offshoot of the Rupert Stock (Northcote and Robinson, 1973), a medium- to coarse-grained, equigranular to porphyritic granodiorite that occurs approximately 1 km to the east of the deposit.

## PREVIOUS AGE CONSTRAINTS FOR THE ISLAND INTRUSIONS AND BONANZA GROUP ON NORTHERN VANCOUVER ISLAND

Fossil data from marine strata of the Bonanza Group indicate an early Sinemurian to late Pliensbachian age (cf. Muller et al., 1974). Early Sinemurian (time scale of Harland et al., 1990) fossils have been found in Bonanza Group sediments in the vicinity of the Island Copper mine (Haggart and Tipper, 1994). The presence of the bivalve *Myophorella taylori* in water-laid tuff and volcaniclastic sediments in the open pit suggests that the age of these beds is Aalenian, or earliest Middle Jurassic (Poulton and Tipper, 1991, p. 24).

Previous K-Ar geochronological data for rocks of the Bonanza Group and Island Intrusions have been reviewed by Archibald and Nixon (1995). Data for Bonanza Group rocks were derived from whole rock samples, and those for the Island Intrusions from altered or impure mineral separates

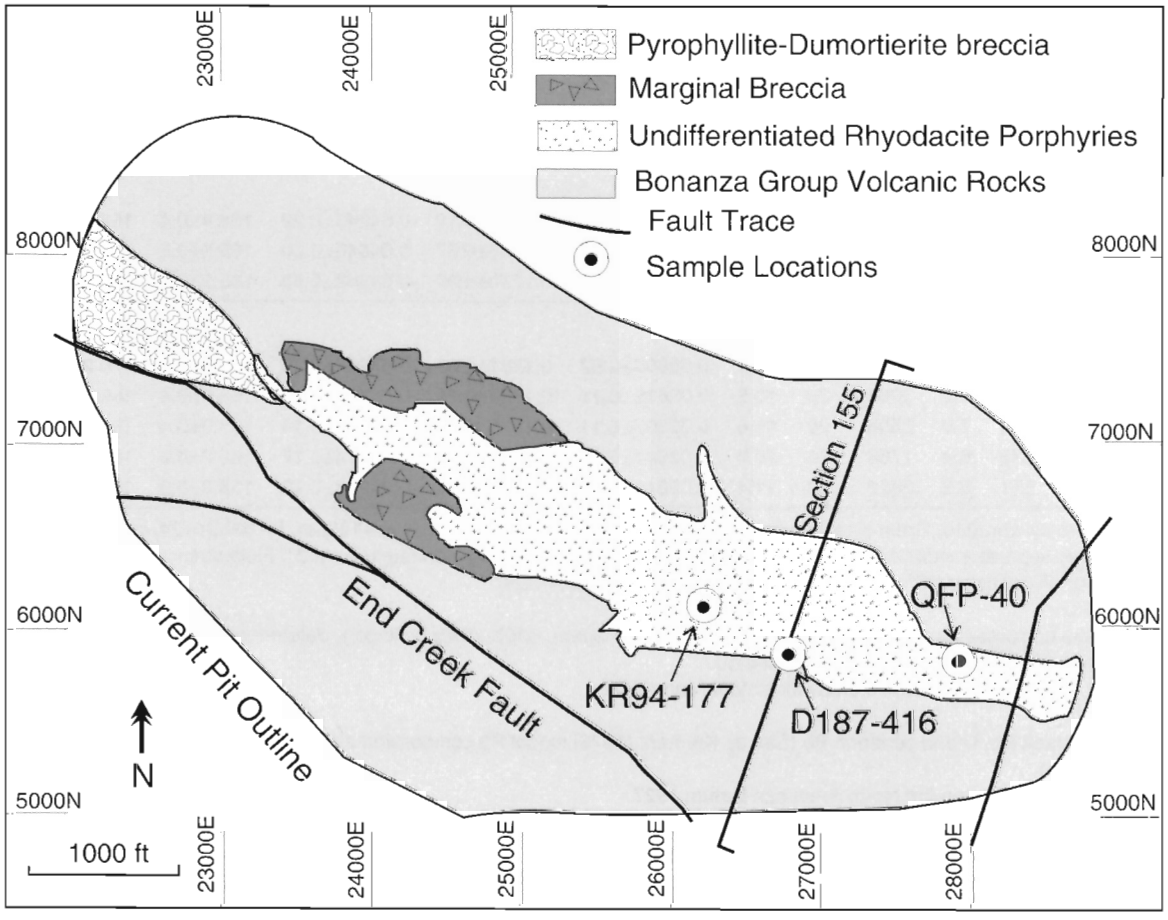


***Figure 2.*** *Location of samples in the open pit, Island Copper mine, Port Hardy, British Columbia. Mine grid is in feet. The pit is located at latitude 50°37′ north, longitude 127°28′ west.*

(Muller et al., 1974). The wide range of apparent ages, 184-105 Ma, is difficult to interpret. $^{40}Ar/^{39}Ar$ dating of primary biotite and hornblende from rocks of the Island Intrusions has given an age range of 177-165 Ma for the cooling ages of these rocks (Archibald and Nixon, 1995). $^{40}Ar/^{39}Ar$ dating of hypogene secondary alunite and sericite from mineralized and/or altered rocks of the Bonanza Group and Island Intrusions yielded an age range of 170-160 Ma (Panteleyev et al., 1995). Preliminary U-Pb ages of 170-165 Ma for rhyolitic units of the Bonanza Group in the Pemberton Hills-Mount McIntosh region, several Island Intrusions, and acid sulphate-altered volcanic rocks from the upper Bonanza Group are concordant with the $^{40}Ar/^{39}Ar$ ages and suggest similar timing for plutonism, volcanism, and mineralization on northern Vancouver Island (Friedman and Nixon, 1995). The Rupert stock yielded a U-Pb age of 168 +8/-2 Ma (Friedman and Nixon, 1995), which is concordant with our reported U-Pb dates for the porphyry samples and supports the model that the stock and dykes were coeval and cogenetic.

## SAMPLE DESCRIPTIONS AND U-Pb RESULTS

Sample preparation and analytical techniques employed at the University of British Columbia Geochronology Laboratory are presented in Journeay and Friedman (1993). New U-Pb data listed in Table 1 are plotted on concordia diagrams in Figure 3.

The oldest phase of the rhyodacitic quartz-feldspar porphyry (KR94-177) is characterized by intense magnetite alteration. A sample was collected from the 160 bench (840

**Table 1.** U-Pb analytical data for samples from the Island Copper pit.

| Fraction[1] | Wt. | U | Pb[2] | $^{206}Pb$[3] | Pb[4] | $^{208}Pb$[5] | Isotopic ratios(±1σ,%)[6] | | | Isotopic dates(Ma,±2σ)[6] | | |
|---|---|---|---|---|---|---|---|---|---|---|---|---|
| | mg | ppm | ppm | $^{204}Pb$ | pg | % | $^{206}Pb/^{238}U$ | $^{207}Pb/^{235}U$ | $^{207}Pb/^{206}Pb$ | $^{206}Pb/^{238}U$ | $^{207}Pb/^{235}U$ | $^{207}Pb/^{206}Pb$ |
| KR94-177: Early Porphyry (5560580, 590800)[7] | | | | | | | | | | | | |
| B,m,N2,p | 0.090 | 285 | 7.7 | 1494 | 27 | 11.5 | 0.02641±0.12 | 0.1800±0.30 | 0.04944±0.23 | 168.1±0.4 | 168.1±0.9 | 168.6±10.7 |
| C,f,N2,p | 0.093 | 281 | 7.5 | 1439 | 29 | 11.4 | 0.02631±0.18 | 0.1793±0.34 | 0.04943±0.24 | 167.4±0.6 | 167.5±1.0 | 168.4±11.1 |
| D,m,N2,p | 0.205 | 245 | 6.6 | 959 | 87 | 11.2 | 0.02640±0.12 | 0.1800±0.28 | 0.04945±0.24 | 168.0±0.4 | 168.1±0.9 | 169.3±11.2 |
| E,f,N2,p | 0.156 | 282 | 7.6 | 1761 | 42 | 11.7 | 0.02649±0.10 | 0.1806±0.26 | 0.04943±0.19 | 168.5±0.3 | 168.5±0.8 | 168.5±8.7 |
| QFP- 40: Intramineral Porphyry (5560580, 590800)[7] | | | | | | | | | | | | |
| A,c,N2,p | 0.142 | 191 | 5.1 | 1763 | 24 | 10.8 | 0.02647±0.12 | 0.1804±0.29 | 0.04943±0.22 | 168.4±0.4 | 168.4±0.9 | 168.1±10.4 |
| B,c,N2,p,ti | 0.128 | 178 | 4.8 | 1334 | 27 | 11.3 | 0.02648±0.17 | 0.1806±0.37 | 0.04945±0.30 | 168.5±0.6 | 168.5±1.2 | 169.4±14.0 |
| C,c,N2,p | 0.157 | 200 | 5.3 | 646 | 76 | 10.7 | 0.02597±0.18 | 0.1770±0.60 | 0.04942±0.53 | 165.3±0.6 | 165.4±1.8 | 167.9±24.7 |
| D187-416: Late Porphyry (5560580, 590800)[7] | | | | | | | | | | | | |
| A,c,N2,p | 0.161 | 184 | 5.0 | 2201 | 22 | 11.1 | 0.02600±0.52 | 0.1831±0.56 | 0.04994±0.17 | 169.2±1.7 | 170.8±1.8 | 192.1±8.0 |
| B,c,N2,p | 0.123 | 247 | 6.5 | 2084 | 24 | 10.8 | 0.02616±0.11 | 0.1781±0.24 | 0.04939±0.16 | 166.4±0.4 | 166.4±0.7 | 166.4±7.4 |
| C,m,N2,p | 0.115 | 264 | 7.0 | 2506 | 20 | 11.6 | 0.02607±0.11 | 0.1775±0.23 | 0.04939±0.14 | 165.9±0.4 | 165.9±0.7 | 166.5±6.5 |
| D,c,N2,p | 0.166 | 238 | 6.4 | 1766 | 36 | 10.9 | 0.02644±0.10 | 0.1806±0.25 | 0.04954±0.17 | 168.2±0.3 | 168.6±0.8 | 173.6±7.9 |
| E,f,N2,p | 0.160 | 251 | 6.8 | 2822 | 23 | 11.4 | 0.02640±0.10 | 0.1805±0.21 | 0.04958±0.13 | 168.0±0.3 | 168.5±0.7 | 175.1±6.0 |

[1] All fractions are air abraded; Grain size, intermediate dimension: c= +134μm, m=-134μm+100μm, f=-100μm+74μm; Magnetic codes: Franz magnetic separator sideslope at which grains are nonmagnetic; e.g., N2=nonmagnetic at 2°; Field strength for all fractions =1.8A; Front slope for all fractions=20°; Grain character codes: p=prismatic, ti=tips;

[2] Radiogenic Pb

[3] Measured ratio corrected for spike and Pb fractionation of 0.0043/amu ±20% (Daly collector), determined by repeated analysis of National Bureau of Standards SRM981 Pb standard.

[4] Total common Pb in analysis based on blank isotopic composition

[5] Radiogenic Pb

[6] Corrected for blank Pb, U and common Pb (Stacey-Kramers (1975) model Pb composition at the $^{207}Pb/^{206}Pb$ date of fraction, or age of sample).

[7] UTM coordinates, based on the North American Datum 1927.

Additional notes: Laboratory blank amount and isotopic compositions were determined by analysing procedural blanks with each batch of unknowns. During the course of this study Pb and U blanks were 9-12 pg and 0.5-1.7 pg, respectively. Decay constants are those recommended by the IUGS Subcommission on Geochronology (Steiger and Jäger, 1977). Ages and associated errors were calculated using the methods of Parrish (1987), Parrish et al. (1987), and Roddick (1987). Isotopic ratios are reported at the 1σ (%) level, isotopic data errors are reported at the 2σ level and error elipses are plotted at the 2σ level (Figure 3). Sample preparation and analytical techniques are listed in Journeay and Friedman (1993).

feet below sea level) on the south wall of the pit (Fig. 2). The rock consists of approximately 50% fine grained purplish-grey groundmass, 20% quartz phenocrysts (0.1-1.0 cm in size), 25% greenish plagioclase phenocrysts (1-5 mm), and 5% chloritized biotite (1-2 mm). Magnetite is finely disseminated in the groundmass, former biotite sites, and hairline fractures. Quartz phenocrysts have embayments and are strained. Primary plagioclase is replaced by a secondary plagioclase-sericite-chlorite-calcite assemblage. Biotite is replaced by chlorite-calcite-rutile-magnetite-pyrite-chalcopyrite. The groundmass is strongly altered by a secondary quartz-plagioclase-magnetite-calcite-sericite-chlorite assemblage. The rock is only weakly mineralized with chalcopyrite. Clasts of this porphyry are found in the margins of weakly magnetite altered, copper-mineralized porphyry intrusions.

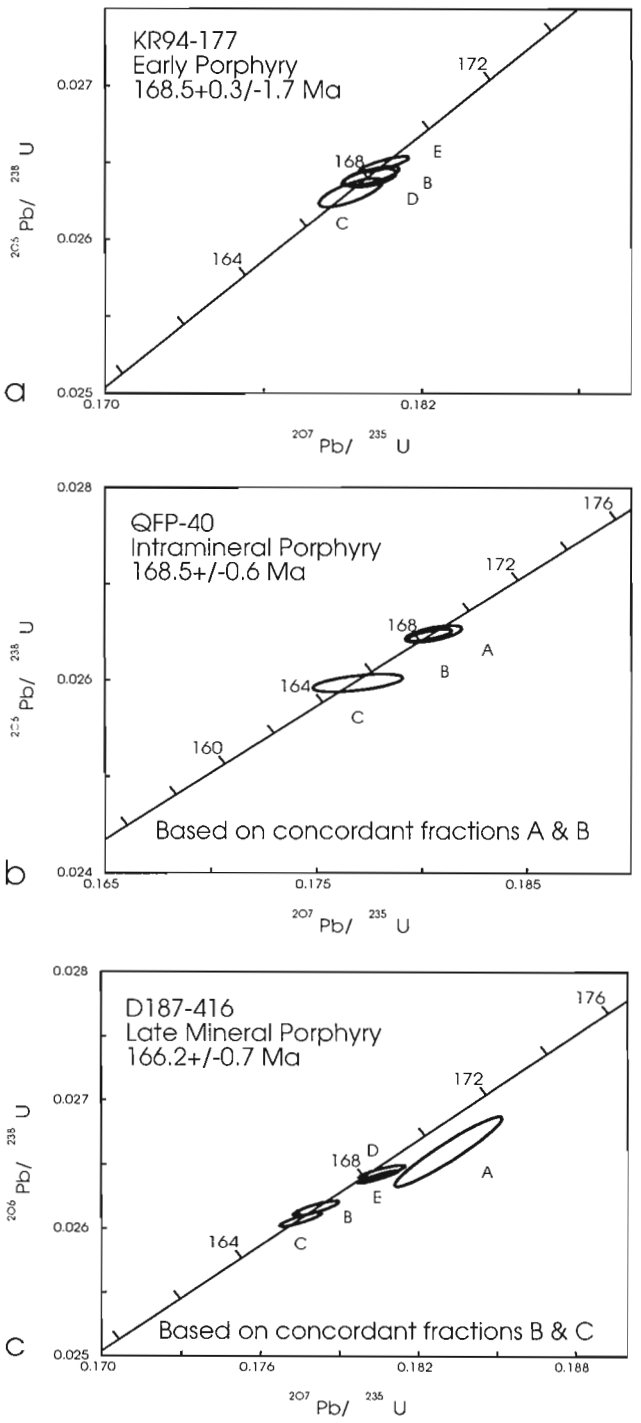


***Figure 3.*** *Concordia diagrams for samples from the Island Copper pit. See text for discussions of age interpretations.* ***a)*** *Early Porphyry, KR94-177.* ***b)*** *Intramineral Porphyry, QFP-40.* ***c)*** *Late Porphyry, D187-416.*

Zircon recovered from this sample is characterized by high quality, clear, pale pink, euhedral, stubby prismatic grains (l/w=2-3) with subrounded cross-sections. No cores were observed during sample selection. Four analyzed zircon fractions plot with some mutual overlap, on concordia at ca. 168 Ma, that is broadly indicative of the age of this rock (Fig. 3a). We regard fraction E, which yielded a $^{206}Pb/^{238}U$ age of 168.5 ± 0.3 Ma, as the best estimate of the age of this sample, and attribute the restricted spread of data for fractions C, B, and D to minor Pb loss. However, we cannot preclude the possibility that this spread is due to inheritance of zircons, or inheritance plus Pb loss, which would lead to slightly younger age estimates for this sample. To account for this uncertainty we report an age of 168.5 +0.3/-1.7 Ma, which reflects the preferred Pb loss interpretation and has an expanded error envelope that includes younger age estimates based on inheritance interpretations.

The intra-mineral quartz feldspar porphyry (QFP-40) was collected from the -40 bench (1040 feet below sea level) in the deepest portion of the east end of the pit (Fig. 2). It is characterized by a pink primary K-feldspar-quartz groundmass which comprises 60% of the rock with 15% quartz phenocrysts (1-7 mm), 20% plagioclase phenocrysts (1-6 mm) and 5% biotite (1-2 mm). There is only a trace of magnetite as disseminations and rare hairline fractures. The rock is weakly to well mineralized with finely disseminated and fracture controlled chalcopyrite-minor pyrite. Plagioclase phenocrysts have some calcite in their cores. Biotite is only partially chloritized and may contain chalcopyrite.

Zircon recovered from this rock is indistinguishable from that of the previous sample, KR94-177. Two of the three analyzed zircon fractions (A and B) lie superimposed on concordia at about 168 Ma (Fig. 3b). The third analysis, (fraction C) composed of slightly lower quality grains, yields younger $^{206}Pb/^{238}U$ dates and is interpreted to have lost Pb. The average $^{206}Pb/^{238}U$ age for fractions A and B, 168.5 ± 0.6 Ma, is interpreted as the best estimate of the age of this rock.

The late quartz feldspar porphyry (D187-416) is characterized by a pale pink to white groundmass, lack of magnetite, and weak Cu-Mo mineralization. The sample was taken from drill hole D187 on the 155W section (eastern half of the pit, Fig. 2), from approximately the 0 bench (1000 feet below sea level). The rock is comprised of 70% pale pink K-feldspar-quartz groundmass, with 10% quartz phenocrysts (1-5 mm), 15% plagioclase phenocrysts, and 5% biotite. The groundmass has been moderately to intensely albitized. The plagioclase phenocrysts

are altered to albite-sericite-calcite-chlorite and the biotite is chloritized. Traces of pyrite and chalcopyrite are present in biotite sites and in fractures.

Zircons are generally pale pink, clear to very clear, euhedral, stubby prisms with subrounded cross-sections. Five analyzed zircon fractions are plotted on Figure 3c. Fractions B and C are concordant at about 166 Ma while A, D, and E are discordant, with older $^{206}Pb/^{238}U$ and $^{207}Pb/^{206}Pb$ ages (Table 1). The former two fractions are interpreted to provide the best estimate of the age of this sample, based on their strong concordance and agreement at the $2\sigma$ level, while the latter three are likely to contain inherited zircon. An age of $166.2 \pm 0.7$ Ma, the average of $^{206}Pb/^{238}U$ ages for fractions B and C with the error derived from their combined precisions, is the best estimate for the age of the rock.

## DISCUSSION

The interpreted ages for the early porphyry (168.5+0.3/-1.7 Ma) and intramineral porphyry ($168.5 \pm 0.6$ Ma) samples are identical within the reported precisions. Strong similarities in the physical nature and geochemical characteristics of zircon from these two dykes support their cogenesis. These ages are also coeval with the U-Pb age of the Rupert Stock (168.5 +8/-2 Ma), and support the origin of the dykes as offshoots of this stock (Northcote and Robinson, 1973). The slightly younger U-Pb age data obtained for sample D187-416 ($166.2 \pm 0.7$ Ma) is within the quoted $2\sigma$ error for sample KR94-177, but is consistent with crosscutting field relationships and its relatively unmineralized character. The ages of the rhyodacite porphyry dykes brackets the timing of mineralization at the Island Copper deposit to between ca. 169 and 166 Ma. Fossil data suggest that the age of the host volcanic rocks is Aalenian (178-173.5 Ma, time scale of Harland et al., 1990).

Our new U-Pb data and previously published U-Pb and Ar-Ar data indicate that crystallization and cooling of the youngest intrusions of the Island Intrusions and some flows of the upper Bonanza Group on Northern Vancouver Island occurred between about 165 and 170 Ma. Furthermore, mineralization and associated acid sulphate alteration were coeval or only slightly younger (minimum age of about 160 Ma; Panteleyev et al., 1995) and are cospatial with the intrusions. This Middle Jurassic episode represents the youngest phase of Bonanza-Island Intrusion magmatism that was initiated in the Early Jurassic. On the Queen Charlotte Islands, to the north, coeval Middle Jurassic plutons of the Burnaby Island suite and volcanic rocks of the Yakoun Group occur within a stratigraphic section that is correlative with the northern Vancouver Island section (Anderson and McNicoll, 1995), and are likely to have been generated within the same arc. Middle Jurassic rocks on Vancouver Island and the Queen Charlotte Islands presently define the western margin of this arc, some 100 to 200 km west of the Middle to Late Jurassic magmatic front defined by Monger and Journeay (1994), between Vancouver Island and mainland British Columbia. The regional distribution of Middle Jurassic magmatic rocks suggest that this arc extended eastward across the southern Coast Belt to Harrison Lake (Friedman and Armstrong, 1995), and northward from southern Vancouver Island through the northern Insular and Coast belts to Alaska (Anderson and Reichenbach, 1991; van der Heyden, 1992; Wheeler and McFeely, 1991; Dodds and Campbell, 1988).

## ACKNOWLEDGMENTS

We are grateful to Island Copper Mines for access to the pit and core library, assistance in the field, and permission to publish this report. Financial assistance from BHP International, for the U-Pb analyses made this study possible. Thanks to R. Anderson for critical review of the manuscript.

## REFERENCES

**Anderson, R.G. and McNicoll, V.J.**
1995: A note on U-Pb dating of Middle Jurassic plutonic suites: Cumshewa Head pluton, southeastern Moresby Island, Queen Charlotte Islands, British Columbia; in Current Research 1995-A; Geological Survey of Canada, p. 91-96.

**Anderson, R.G. and Reichenbach, I.**
1991: U-Pb and K-Ar framework for Middle to Late Jurassic (172-≥158 Ma) and Tertiary (46-27 Ma) plutons in Queen Charlotte Islands, British Columbia; in Evolution and Hydrocarbon Potential of the Queen Charlotte Basin, British Columbia, (ed.) G.J. Woodsworth; Geological Survey of Canada, Paper 90-10, p. 59-87.

**Arancibia, O.N. and Clark, A.H.**
1990: Early magnetite-rich alteration/mineralization in the Island Copper porphyry copper-molybdenum-gold deposit, British Columbia; Geological Association of Canada-Mineralogical Association of Canada, Program with Abstracts, v. 15, p. A4.

**Archibald, D.A. and Nixon, G.T.**
1995: $^{40}Ar/^{39}Ar$ geochronometry of igneous rocks in the Quatsino-Port McNeill map area, northern Vancouver Island (92L/12,11); in Geological Fieldwork 1994; British Columbia Ministry of Energy, Mines and Petroleum Resources, Paper 1995-1, p. 49-59.

**Dodds, C.J. and Campbell, R.B.**
1988: Potassium-argon ages of mainly intrusive rocks in the Saint Elias Mountains, Yukon and British Columbia; Geological Survey of Canada, Paper 87-16, 43 p.

**Fahey, P.L.**
1979: The geology of Island Copper Mine, Vancouver Island, British Columbia; MSc. thesis, University of Washington, Seattle, Washington, 52 p.

**Friedman, R.M. and Armstrong, R.L.**
1995: Jurassic and Cretaceous geochronology of the southern Coast Belt, British Columbia, 49°-51°N; in Jurassic Magmatism and Tectonics of the North American Cordillera, (ed.) D.M. Miller and C. Busby; Geological Society of America Special Paper 299, Boulder, Colorado, p. 95-139.

**Friedman, R.M. and Nixon, G.T.**
1995: U-Pb zircon dating of Jurassic porphyry Cu (-Au) and associated acid sulphate systems, northern Vancouver Island, British Columbia; in Program and Abstracts volume, Geological Association of Canada/Mineralogical Association of Canada Annual Meeting, Victoria '95, p. A-34.

**Haggart, J.W. and Tipper, H.W.**
1994: New results in Jura-Cretaceous stratigraphy, northern Vancouver Island, British Columbia; in Current Research 1994-E; Geological Survey of Canada, p. 59-66.

**Harland, W.B., Armstrong, R.L., Cox, A.V., Craig, L.E., Smith, A.G., and Smith, D.G.**
1990: A Geologic Time Scale: 1989; Cambridge, England, Cambridge University Press, 263 p.

**Journeay, J.M. and Friedman, R.M.**
1993: The Coast Belt Thrust System: Evidence of Late Cretaceous shortening in the Coast Belt of southwestern British Columbia; Tectonics, v. 12, p. 756-775.

**Leitch, C.H.B., Ross, K.V., Fleming, J.A., and Dawson, K.M.**
1995: Preliminary studies of hydrothermal alteration events at the Island Copper deposit, northern Vancouver Island, British Columbia; in Current Research 1995-A; Geological Survey of Canada, p. 51-59.

**Monger, J.W.H. and Journeay, J.M.**
1994: Basement geology and tectonic evolution of the Vancouver region; in Geology and Geological Hazards of the Vancouver Region, Southwestern British Columbia, (ed.) J.W.H. Monger; Geological Survey of Canada, Bulletin 481, p. 3-25.

**Muller, J.E., Northcote, K.E., and Carlisle, D.**
1974: Geology and mineral deposits of Alert-Cape Scott map-area, British Columbia; Geological Survey of Canada, Paper 74-8, 77 p.

**Nixon, G.T., Hammack, J.L., Koyanagi, V.M., Payie, G.J., Panteleyev, A., Massey, N.W.D., Hamilton, J.V., and Haggart, J.W.**
1994: Preliminary geology of the Quatsino-Port McNeill map areas, northern Vancouver Island (92L/12,11); in Geological Fieldwork 1993; British Columbia Ministry of Energy, Mines and Petroleum Resources, Paper 1994-1, p. 63-85.

**Northcote, K.E. and Muller, J.E.**
1972: Volcanism, plutonism and mineralization: Vancouver Island; Canadian Institute of Mining and Metallurgy Bulletin, v. 65, p. 49-57.

**Northcote, K.E. and Robinson, W.C.**
1973: Island Copper Mine; in Geology, Exploration and Mining in British Columbia-1972; British Columbia Ministry of Energy, Mines and Petroleum Resources, p. 293-303.

**Panteleyev, A., Reynolds, P.H., and Koyanagi, V.M.**
1995: $^{40}Ar/^{39}Ar$ ages of hydrothermal minerals in acid sulphate-altered Bonanza volcanics, northern Vancouver Island (92L/12); in Geological Fieldwork 1994; British Columbia Ministry of Energy, Mines and Petroleum Resources, Paper 1995-1, p. 61-65.

**Parrish, R.R., Roddick, J.C., Loveridge, W.D., and Sullivan, R.W.**
1987: Uranium-Lead analytical techniques at the geochronology laboratory; Geological Survey of Canada, Paper 87-2, p. 3-7.

**Perello, J.A., Arancibia, O.N., Burt, P.D., Clark, A.H., Clarke, G.A., Fleming, J.A., Himes, M.D., Leitch, C.H.B., and Reeves, A.T.**
1989: Porphyry Cu-Mo-Au mineralization at Island Copper, Vancouver Island, B.C.; Paper presented at Geological Association of Canada-Mineral Deposits Division Workshop on Porphyry Cu-Au Deposits, Vancouver, British Columbia, April 1989, 22 p.

**Perello, J.A. Fleming, J.A., O'Kane, K.P., Burt, P.D., Clarke, G.A., Himes, M.D., and Reeves, A.T.**
in press: Porphyry copper-gold-molybdenum mineralization in the Island Copper cluster, Vancouver Island; Canadian Institute of Mining and Metallurgy, Special Volume 46.

**Poulton, T.P. and Tipper, H.W.**
1991: Aalenian ammonite and strata of western Canada; Geological Survey of Canada, Bulletin 411, 71 p.

**Roddick, J.C.**
1987: Generalized numerical error analysis with application to geochronology and thermodynamics; Geochimica et Cosmochimica Acta, v. 51, p. 2129-2135.

**Stacey, J.S. and Kramers, J.D.**
1975: Approximation of terrestrial lead isotope evolution by a two-stage model; Earth and Planetary Science Letters, v. 26, p. 207-221.

**Steiger, R.H. and Jäger, E.**
1977: Subcommission on geochronology: convention on the use of decay constants in geo- and cosmochronology; Earth and Planetary Science Letters, v. 36, p. 359-362.

**van der Heyden, P.**
1992: A Middle Jurassic to Early Tertiary Andean-Sierran arc model for the Coast Belt of British Columbia; Tectonics, v. 11, p. 82-97.

**Wheeler, J.O. and McFeely, P.** (comp.)
1991: Tectonic assemblage map of the Canadian Cordilleran and adjacent parts of the United States of America; Geological Survey of Canada, Map 1712A, scale 1:2 000 000.

Geological Survey of Canada Project 740098-IC

# Diachronous low-temperature Paleogene cooling of the Alberni Inlet area, southern Vancouver Island, British Columbia: evidence from apatite fission track analyses

Lisel D. Currie and A. (Sandy) M. Grist[1]
GSC Victoria, Vancouver

*Currie, L.D. and Grist, A.M., 1996: Diachronous low-temperature Paleogene cooling of the Alberni Inlet area, southern Vancouver Island, British Columbia: evidence from apatite fission track analyses; in Current Research 1996-A; Geological Survey of Canada, p. 119-128.*

**Abstract:** Apatite fission track ages and track length distributions are used to constrain the timing of low-temperature cooling across western- and central-southern Vancouver Island. Relatively slow cooling (roughly 1°C/Ma) of the western Alberni Inlet area between 70 and 20 Ma is attributed to a decrease in heat flow following igneous activity associated with the Flores volcanics and the Clayoquot intrusive suite, and possibly continued post-Jurassic erosion. More rapid cooling (roughly 5°C/Ma) of central-southern Vancouver Island from 45 to 35 Ma is coeval with the development of the Cowichan Fold and Thrust Belt, and underplating by the Crescent terrane and oceanic crust along east-dipping faults below western Vancouver Island. The change in the locus of greatest cooling, and perhaps denudation and uplift, from the west coast of southern Vancouver Island to central-southern Vancouver Island is correlated with the change in Pacific/North American relative plate motions at ~41 Ma.

**Résumé :** Les datations par trace de fission de l'apatite et les distributions des longueurs de trace servent à établir la chronologie du refroidissement à basse température dans tout l'ouest et le centre de la partie sud de l'île de Vancouver. Le refroidissement relativement lent (env. 1 °C/Ma) dans la partie ouest de la région de l'inlet d'Alberni, entre 70 et 20 Ma, est attribué à une diminution du flux de chaleur après un épisode d'activité ignée associée aux volcanites de Flores et à la suite intrusive de Clayoquot, mais aussi peut-être à une érosion post-jurassique continue. Le refroidissement plus rapide (env. 5 °C/Ma) dans le centre sud de l'île de Vancouver, entre 45 et 35 Ma, est contemporain de la formation du pli et de la nappe de charriage de Cowichan, mais aussi du sous-placage, par le terrane de Crescent et la croûte océanique, le long des failles à pendage est au-dessous de la partie ouest de l'île de Vancouver. Le déplacement du lieu de refroidissement maximal et peut-être de la dénudation et du soulèvement qui, dans la partie sud de l'île de Vancouver, va de son extrémité ouest à sa portion centrale, est corrélé au changement de mouvement relatif des plaques pacifique et nord-américaine à env. 41 Ma.

[1] Fission track laboratory, Department of Geology, Dalhousie University, Halifax, Nova Scotia B3H 3J5

## INTRODUCTION

For the past 40 million years, southwestern British Columbia has been part of the Cascade magmatic arc, which formed above the subducting oceanic Juan de Fuca Plate (Fig. 1). During this time interval, most of Vancouver Island apparently lay in the forearc region between the arc and the subducting plate. This study was undertaken to determine the Cenozoic to Holocene cooling history of the forearc, which reflects the thermal, surface uplift, and denudation histories of the region. Herein, we present model cooling histories determined from apatite fission track length analyses and cooling ages to document changes in Cenozoic cooling rates across southern Vancouver Island (Fig. 2). This study is part of a larger project investigating the age and origin of Georgia Depression, between Vancouver Island and the Coast Mountains (Fig. 2).

Although the Tertiary cooling, denudation, and surface uplift histories of Vancouver Island have not been studied in detail, a number of different methods used in earlier studies provide some insight into the uplift and denudation history of Vancouver Island. They include geodetic, paleomagnetic, sedimentological, metamorphic, and fission track studies, and the analysis of inferred erosion surfaces. Geodetic studies indicate that Vancouver Island and the Coast Mountains are rising at rates of about 2 mm/a (Vanicek and Nagy, 1981; Riddihough, 1982) and more than 3 mm/a north of Campbell River on Vancouver Island (Holdahl et al., 1989), while the intervening Georgia Strait area is subsiding at 1-2 mm/a (Vanicek and Nagy, 1981; Holdahl et al., 1989). Parrish (1983) inferred more than 2 km of post-10 Ma surface uplift for central Vancouver Island on the basis of the altitudes of summits which may represent a former erosion surface of Miocene age, the presence of Late Miocene to Pliocene volcanic rocks and sediments around the perimeter of Vancouver Island, and the assumption that most of Vancouver Island was near sea level at 10 Ma. Paleomagnetic data for two small Early Eocene (50 to 52 Ma) stocks exposed on the west coast of Vancouver Island, just north of Alberni Inlet, are indicative of about 30° postemplacement tilts toward the west (Irving and Brandon, 1990).

Metamorphic facies assemblages suggest that Vancouver Island has experienced the greatest denudation along its west side (e.g., Greenwood et al., 1991). High pressure metamorphic assemblages preserved in the Pacific Rim terrane (Fig. 3), and amphibolite facies metamorphic mineral assemblages exposed on western Vancouver Island contrast with prehnite-pumpellyite facies assemblages preserved along its eastern margin (see Read et al., 1991). Paleocurrent indicators and evidence for Late Cretaceous uplift in the Coast Mountains indicate that the denudation of Vancouver Island was not a major source of the Late Cretaceous Nanaimo basin

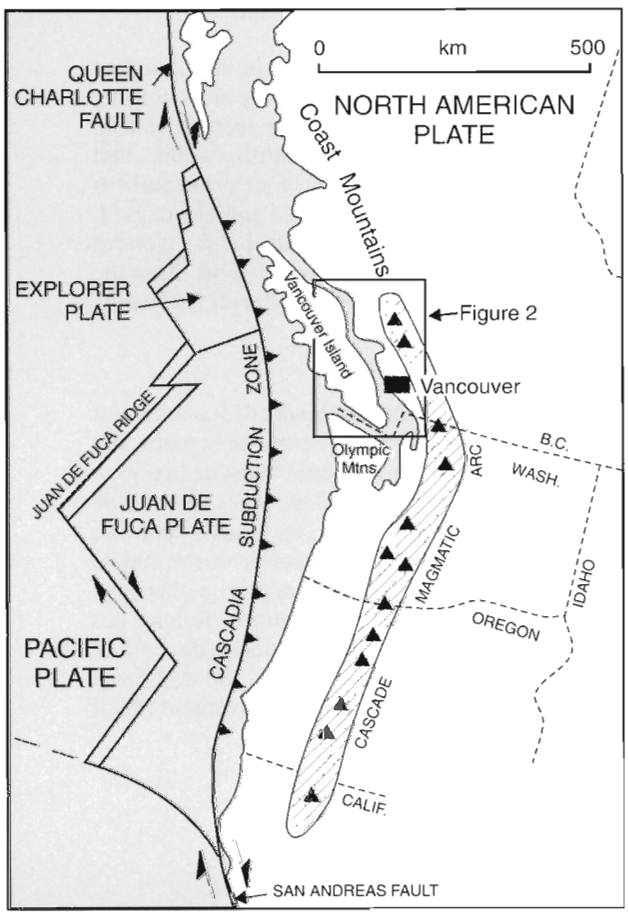


***Figure 1.*** *Map of the Cascadia subduction zone and related tectonic elements (modified from Monger and Journeay, 1994).*

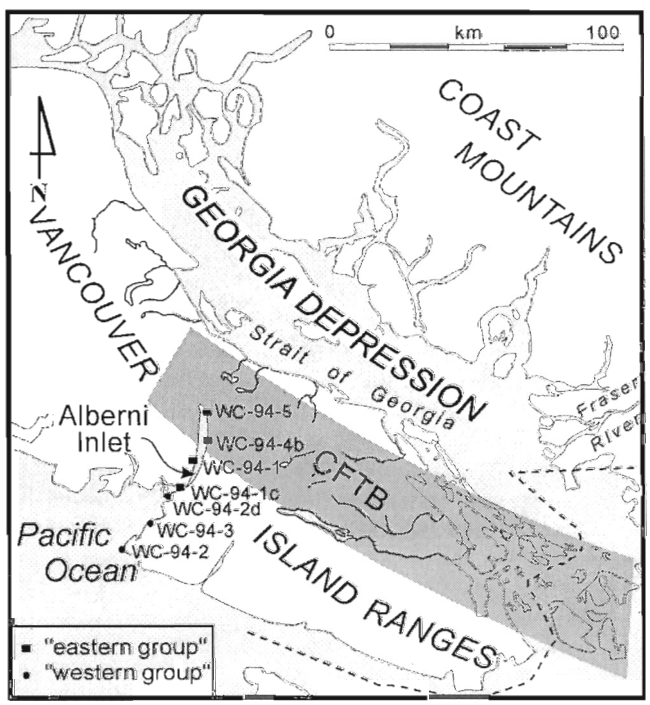


***Figure 2.*** *Map of southwestern British Columbia showing physiographic elements and sample locations. CFTB = Cowichan Fold and Thrust Belt (modified from Mustard, 1994).*

sediments; instead, the southern Coast Mountains and the San Juan Islands are considered the primary sources for Nanaimo Group detritus (Mustard, 1994; Mustard et al., 1995). This interpretation is supported by apatite fission track cooling ages for igneous rocks from the San Juan Islands, immediately south of the Haro Fault, that range from about 84 Ma to 94 Ma (Johnson et al., 1986); resetting of these apatite fission track dates has been attributed to denudation resulting from uplift due to Late Cretaceous thrusting, implying that the Haro Fault accommodated much of the Late Cretaceous uplift of the southern San Juan Islands block (Fig. 3; Johnson et al., 1986). Apatite fission track cooling ages from north of the Haro Fault are from 35.6 ± 13.9 Ma to 69.3 ± 9.5 Ma (most ages are between 60 and 70 Ma, excluding error; Johnson et al., 1986). The cause of this Tertiary low-temperature cooling is not clear. Apatite fission track ages from about 30 km south of Alberni Inlet have also been used to determine the low temperature cooling histories for rocks in the Cowichan Fold and Thrust belt of southern Vancouver Island (unpub. data of T.J. England and M.K. Roden-Tice, pers. comm., 1994; discussed below; Fig. 2, 4), and the southern Coast Mountains (Parrish, 1983; Currie et al., 1995).

This paper discusses the low-temperature cooling history of samples collected from a transect across western- and central-southern Vancouver Island. The samples are from Alberni Inlet, which crosses approximately two-thirds of the island, and provides an opportunity to collect samples from a single elevation (near sea level) for a distance of about 60 km across regional strike (Fig. 2). The samples collected for fission track analysis were chosen on the basis of their perceived likelihood of containing apatite. They are from the Early Jurassic West Coast Complex and granodioritic to dioritic rocks of the Jurassic Island Suite (also referred to as Island Intrusions; Muller, 1977).

## FISSION TRACK THERMOCHRONOLOGY OF VANCOUVER ISLAND

### *Scientific basis*

Fission tracks are cylindrical zones of structural damage in a crystal lattice that are produced by the movement of highly charged particles created during the spontaneous fission of $^{238}U$. They are initially about 17 μm long and a few angstroms wide. Because $^{238}U$ decay proceeds at a constant rate, the number of tracks per unit area provides a measure of the time elapsed since track accumulation began; this is referred to as the fission track age (e.g., Wagner and Van den Haute, 1992).

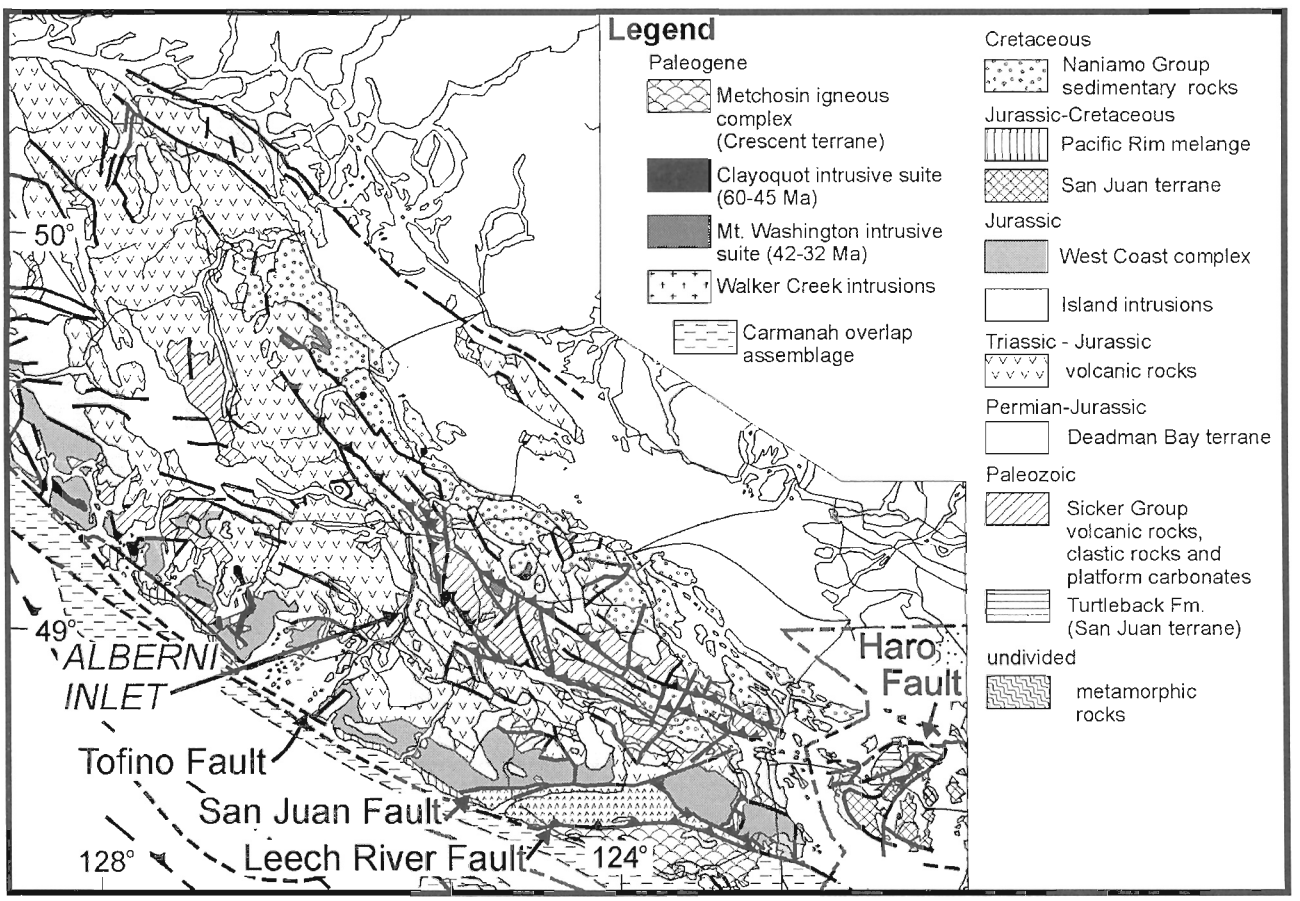


***Figure 3.*** *Geological map of southern and central Vancouver Island (modified from Wheeler et al., 1991).*

Fission tracks can be annealed by progressively heating the host lattice, which causes the tracks to shorten until they disappear completely. Within mineral grains, the maximum temperature at which 50% of a fission track is retained over geological periods of time is referred to as the closure temperature for fission track retention in that mineral. At typical geological cooling rates of 1-10°C/Ma fission tracks in apatite are preserved only at temperatures below about 100 ± 20°C, "the closure temperature for fission track retention in apatite" (Wagner and Van den Haute, 1992, and references therein).

Because the decrease in track length by annealing of fission track damage is a thermally activated process, track length distributions contain valuable information about the thermal history of the mineral. Apatite fission tracks that have been kept at temperatures above about 130°C for geologically significant periods of time will anneal and disappear completely, whereas tracks that experience temperatures within 20°C to 40°C of apatite's approximate 100°C closure temperature for limited lengths of time will experience partial annealing. The portion of the crust within which partial annealing of apatite fission tracks occurs (i.e. that part that is at temperatures between ~120°C and ~60°C) is referred to as the "partial annealing zone" for fission tracks in apatite.

After an apatite grain cools below partial annealing zone temperatures, all new tracks will be retained and will experience only minor annealing. Mean confined track length measurements between 14 and 15 μm with standard deviations >0.8-1.3 μm are characteristic of apatites that cooled rapidly between ~120°C and 60°C. Shorter mean confined track length measurements with larger standard deviations are associated with apatites that have cooled relatively slowly through the same temperatures. Thus, a combination of the

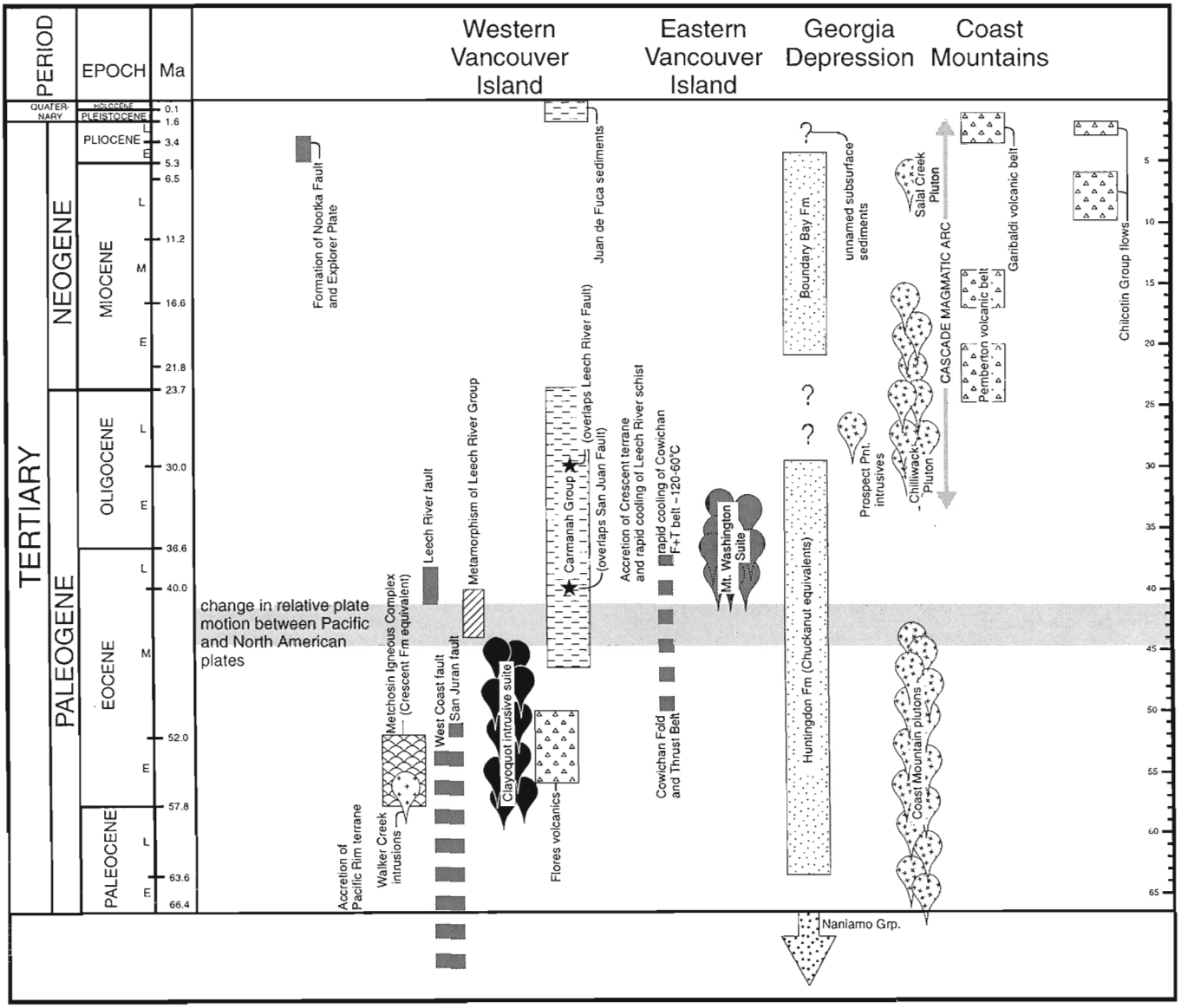


***Figure 4.*** *Time-space diagram of sedimentation, magmatic and tectonic episodes, and relative plate motions, for southwestern British Columbia.*

fission track age and the confined track length distribution can be used to reveal the time-temperature path since the time of the formation of the oldest retained fission track (below ~120°C; e.g., Green et al., 1989; Corrigan, 1991).

### *Geological interpretation of fission track results from Vancouver Island*

Low-temperature cooling histories recorded by apatite fission tracks may reflect three processes, whose relative contributions may be difficult or impossible to determine. They are: (1) erosional or tectonic denudation; (2) underthrusting of relatively cool material; and (3) changes in the location of the magmatic front. Although tectonic denudation has not been recognized in southern Vancouver Island, there is strong evidence for erosion. For example, a nonconformity exposed southeast of Port Alberni that has basal (?) Nanaimo Group granitoid-bearing conglomerate or siltstone/greywacke overlying plutonic rocks of the Island Suite shows that erosion took place between Late Jurassic mid-Cretaceous time (R.G. Anderson, pers. comm., 1995), and an unconformity between the Eocene to Oligocene Carmanah Group and Jurassic rocks of the Nootka Sound area demonstrates that at least the west side of the island was exhumed sometime between Jurassic and Eocene time.

If erosion could be directly related to uplift, about 2-3 km of denudation would be required to exhume a rock that has cooled through the closure temperature for track retention in apatite (assuming a geothermal gradient of 25°C/km). However, apatite fission track age data cannot be directly translated into exhumation rates because isotherms will be compressed during rapid denudation, precluding the possibility of maintaining a constant geothermal gradient throughout exhumation and resulting in an overestimation of the exhumation rate. In addition, the geothermal gradient may be perturbed by the juxtaposition of hot or cold crust, migration of hot fluids, or intrusion of magma during denudation. Low heat flow observed west of the Coast Mountains today has been attributed to the subducting Juan de Fuca Plate acting as a heat-sink, and the dramatic increase in heat flow along the western flank of the Coast Mountains has been considered the result of convective upwelling above the down-going slab (Riddihough and Hyndman, 1991).

Subduction of oceanic material beneath western Vancouver Island has probably been going on for at least the last 40 Ma, and this, together with underthrusting of the Crescent terrane, may have contributed to Eocene cooling on Vancouver Island. In the Tertiary, there appears to have been an eastward migration of magmatism across southwestern British Columbia, from the west side of Vancouver Island (~51 Ma Flores Volcanics and the ~60-45 Ma Clayoquot

**Table 1.** Fission track analytical results for samples from Alberni Inlet, southern Vancouver Island.

| Sample Number | Location | UTM | Elevation (metres) | Grains Counted | $N_s$ | $N_i$ | $Rho_s$ | $Rho_i$ | Chi-Square probability (%) | $N_d$ | Age (Ma) | U concentration (ppm) |
|---|---|---|---|---|---|---|---|---|---|---|---|---|
| CENTRAL GROUP | | | | | | | | | | | | |
| WC-94-1* | Southwest of Hocking Point | 365600E 5438000N | 0 | 26 | 126 | 582 | 1.78 | 8.21 | 26 | 8000 | 39 ± 8 | 5 |
| WC 94-1c* | Pocahontas Point | 360300E 5427400N | 0 | 25 | 40 | 223 | 0.67 | 3.75 | 98 | 8000 | 33 ± 11 | 2 |
| WC-94-4b* | South of China Creek | 369125E 5444050N | 0 | 26 | 69 | 353 | 0.61 | 3.14 | 99 | 8000 | 36 ± 10 | 2 |
| WC-94-5* | Port Alberni | 368350E 5433250N | 200 | 25 | 127 | 659 | 1.43 | 7.44 | 93 | 8000 | 36 ± 7 | 4 |
| WESTERN GROUP | | | | | | | | | | | | |
| WC-94-2* | Hissin Point | 354875E 5424725N | 0 | 24 | 52 | 151 | 1.06 | 3.07 | 74 | 8000 | 63 ± 21 | 2 |
| WC-94-2d | Point south of Mud Cove | 337400E 5406350N | 0 | 26 | 844 | 2920 | 9.14 | 31.6 | 21 | 8000 | 53 ± 6 | 18 |
| WC-94-3* | North of Bamfield | 343400E 5411600N | 0 | 6 | 22 | 72 | 1.35 | 4.42 | 96 | 8000 | 56 ± 28 | 2 |

All ages are calculated using pooled statistics. Abbreviations are as follows: $N_s$ and $N_i$ are the number of spontaneous (fossil) and induced tracks, respectively; $Rho_s$ and $Rho_i$ are the density of spontaneous and induced tracks, respectively ($x10^5/cm^2$); $N_d$ is the number of flux dosimeter (CN-5) tracks counted. A value of 345.3 ± 12 (CN-5 glass) was used for the zeta factor. Age error estimates are at the 95% (2-σ) confidence level. Samples marked * were sent to Rensselaer Polytechnic Institute, for irradiation with $^{252}Cf$. All samples passed the chi-squared test at the 95% confidence level (ie. all have a chi-squared probability >5%), indicating that individual-grain ages from each sample are consistent with a single population (Galbraith, 1982). This test provides an indication of the quality of the data, which may be affected by anisotropy effects, poor contact between mica and grain, inclusions or dislocations in the grains, and/or differing chemistry among the grains. Apatite chemistry, particularly to the ratio of chlorine to fluorine, is of concern because it affects the annealing behaviour of fission tracks (e.g., Green et al. 1985, 1986; O'Sullivan and Parrish, 1995). A qualitative assessment of the etching behavior of the grains suggests that the Cl/F ratio of the grains from within each sample dated in this study, was reasonably constant. Analyses by A.M. Grist.

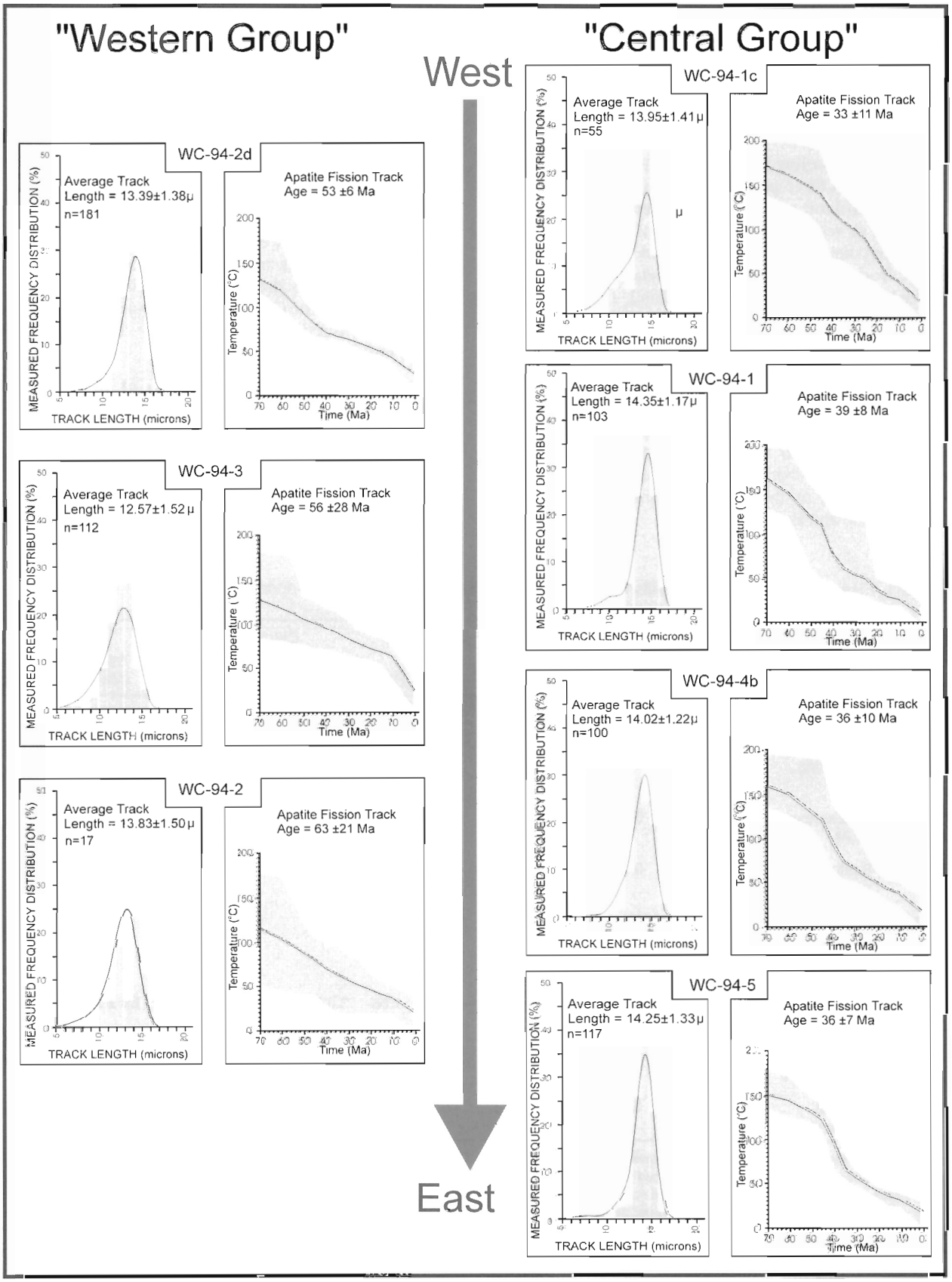
"Western Group"
"Central Group"
West
East
WC-94-2d
Average Track Length = 13.39±1.38µ
n=181
Apatite Fission Track Age = 53 ±6 Ma
WC-94-3
Average Track Length = 12.57±1.52µ
n=112
Apatite Fission Track Age = 56 ±28 Ma
WC-94-2
Average Track Length = 13.83±1.50µ
n=17
Apatite Fission Track Age = 63 ±21 Ma
WC-94-1c
Average Track Length = 13.95±1.41µ
n=55
Apatite Fission Track Age = 33 ±11 Ma
WC-94-1
Average Track Length = 14.35±1.17µ
n=103
Apatite Fission Track Age = 39 ±8 Ma
WC-94-4b
Average Track Length = 14.02±1.22µ
n=100
Apatite Fission Track Age = 36 ±10 Ma
WC-94-5
Average Track Length = 14.25±1.33µ
n=117
Apatite Fission Track Age = 36 ±7 Ma
MEASURED FREQUENCY DISTRIBUTION (%)
TRACK LENGTH (microns)
Temperature (°C)
Time (Ma)

intrusive suite), to the east side of the island (42-32 Ma Mt. Washington intrusive suite), and then to the east side of Georgia Depression where 35 Ma and younger Cascade volcanism was initiated (Fig. 1, 3, 4).

### *Results*

The analytical procedures used for fission track analyses presented here are discussed in Appendix 1, fission track ages are presented in Table 1, and a confined track length histogram and model cooling history for each sample are shown in Figure 5. Uncertainties presented in the text and figures are $\pm 2\sigma$. The ages are considered cooling ages because they are significantly less than the inferred Jurassic emplacement ages of the samples, which are based on their correlation with dated samples of Island Intrusions and West Coast Complex rocks (J.K. Mortensen, unpub. U-Pb zircon ages).

The dated samples are divided into two populations on the basis of their fission track ages: the four samples from central Vancouver Island have ages that range from 33 to 39 Ma (excluding error) and are referred to as the "central group"; and the three samples from western Vancouver Island have ages from 53 to 63 Ma (excluding error), and are referred to as the "western group". Three of the four "central group" samples have average fission track lengths greater than 14 μm with standard deviations between 1.17 μm and 1.33 μm, whereas the southwest-most "central group" sample has an average track length slightly less than 14 μm and a standard deviation of 1.41 μm. All of the "western group" samples have average fission track lengths less than 14 μm. Standard deviations of average fission track lengths from this group decrease toward the northeast, from 1.38 μm to 1.52 μm. Only 17 tracks were counted from the northeasternmost sample due to small sample size.

### *Interpretation*

The westernmost sample of the "western group"(WC-95-2d), has a narrow track length distribution and the smallest fission track age error, suggesting that it cooled rapidly and spent less time in the partial annealing zone than the samples to the northeast. The shorter average track lengths of the "western group" are indicative of slow cooling during the Paleogene, whereas the long average track lengths of the "central group" reflect rapid cooling during Late Eocene to Early Oligocene time. Thus, the "central group" was still at temperatures greater than about 120°C when the "western group" began to cool through the partial annealing zone. This interpretation is supported by the less than 14 μm average track length and skewed track length distribution of the southwesternmost sample from the "central group" (WC-95-1c), which is thought to have spent more time in the partial annealing zone than "central group" samples from the northeast.

***Figure 5.*** *Horizontal confined apatite fission track length histograms, and model time-temperature paths derived from inversion of the confined fission track length data for samples from Alberni Inlet. The curves shown on the track length histograms are the probability distribution function for the weighted average thermal history illustrated in the time-temperature diagram for each sample. The shaded areas shown in the time-temperature diagrams are defined by 250 cooling histories that adequately fit the track length data (note that the limits of the shaded area cannot be considered acceptable thermal histories), and the line within the shaded area represents the weighted average of this model set.*

### *Thermal models*

Thermal models may be used to quantify the results that can be inferred from the track length histograms. Model time-temperature paths for each sample shown Figure 5 are derived from fission track ages and the inversion of confined fission track length data, using a program developed by S.D. Willett and D.R. Issler that is based on data from an empirical laboratory study of annealing in Durango apatite by Laslett et al. (1987; Issler et al., 1990; Ravenhurst et al., 1994; Issler and Stockmal, 1995). The program uses a constrained random-search algorithm, which finds a set of 250 forward models which statistically fit the observed fission track age and track length distribution. All models presented here assume that the samples have experienced simple cooling histories, with no significant reheating after they cooled through about 200°C.

Thermal models for the "western group" indicate that these samples cooled relatively slowly (roughly 1°C/Ma) from about 120°C to 60°C, between 70 Ma and 20 Ma, although the westernmost sample may have cooled more quickly (the cooling history of sample WC-94-2 is poorly constrained because of its small sample size). In contrast, thermal models for the "central group" imply that this group cooled rapidly (roughly 5°C/Ma) from about 120°C to 60°C between about 44 and 34 Ma ago (Fig. 5). The southwesternmost sample from this group may have been hotter than 60°C after 34 Ma.

#### Low-temperature cooling of the "western group" (~53-63 Ma apatite cooling ages)

The narrow track length distribution of the westernmost sample suggest that a distinct cooling event occurred about $53 \pm 6$ Ma ago. This age interpretation is supported by the similar cooling ages of the other two "western group" samples. The proximity of the westernmost sample to the Tofino fault suggests that cooling may be related to displacement on this fault. Although Eocene sediments exist on the island, indicating that some erosion took place during that time, it is not clear that cooling was primarily due to erosion.

It seems most likely that rocks exposed along the western reaches of Alberni Inlet experienced significant reheating after they cooled through about 200°C, making the simple cooling history assumed for the thermal models incorrect. The presence of the Early Eocene Flores Volcanics (~52-50 Ma U-Pb zircon ages; Irving and Brandon, 1990) and the 60-45 Ma Clayoquot intrusive suite (Massey, 1994) along the west coast of southern Vancouver Island suggests that heat flow increased at this time, resetting the apatite fission track

ages. These apatite fission track cooling ages closely resemble those from north of the Haro Fault, in the San Juan Islands (Johnson et al., 1986).

### Low-temperature cooling of the "central group" (~36-39 Ma apatite cooling ages)

Apatite fission track results from this area are similar to cooling ages from southeast of Alberni Inlet that are interpreted to reflect unroofing due to the development of the Cowichan Fold and Thrust Belt, and range in age from 31 ± 6 Ma to 55 ± 14 Ma (unpub. T.J. England and M.K. Roden-Tice, pers. comm., 1994). It seems likely that deformation and denudation associated with the development the Cowichan Fold and Thrust Belt extended farther north and west than previously recognized, and cooling ages for the "central group" reflect the same contractional event. Sediments produced during denudation may have contributed to the Carmanah Group, which is preserved on the north side of Juan de Fuca Strait and in the Nootka Sound area, and/or could have been subducted on the Juan de Fuca Plate, or transported northward on the Pacific Plate.

Late Eocene cooling may not be solely related to denudation reflecting uplift and erosion. Post-Eocene and pre-Late Miocene cooling may also be related to refrigeration caused by underplating of oceanic material and the Crescent terrane along east-dipping faults that have been inferred from deep seismic reflection profiles across Vancouver Island (e.g., Yorath et al., 1985; Hyndman et al., 1989). Also coeval with the Eocene low-temperature cooling of eastern Alberni Inlet is the eastward migration of magmatism from the east side of Vancouver Island (42-32 Ma Mt. Washington intrusive suite), to the east of Georgia Depression (35 Ma and younger Cascade volcanism). These changes followed the dramatic approximately 41 Ma change in the motion of the Pacific Plate, relative to North America (Fig. 4).

## CONCLUSIONS

The Cenozoic cooling history of southern Vancouver Island is characterized by at least two periods of low-temperature cooling. Sometime between the Middle Jurassic and Late Eocene time erosion, and therefore cooling must have been most pronounced along Vancouver Island's west coast to create the observed eastward decrease in metamorphic grade across the island. An approximately 53 Ma low-temperature cooling event recorded by samples from western Alberni Inlet was most likely dominated by cooling related to Early Tertiary intrusions. The approximately 33-39 Ma cooling event recorded by apatite in rocks exposed along eastern Alberni Inlet, was probably related to uplift and erosion associated with Cowichan Fold and Thrust Belt deformation, and reflects a change in the locus of maximum denudation from the west coast of Vancouver Island to its axis.

## ACKNOWLEDGMENTS

We wish to thank Chris Huggins, who provided cheerful assistance in the field, the geochronology laboratory at the University of British Columbia for generously allowing us to use their Wifley table, and Jim Monger and Dennis Arne for reviews that significantly improved an earlier version of this paper.

## REFERENCES

**Corrigan, J.**
1991: Inversion of apatite fission track data for thermal history information; Journal of Geophysical Research, v. 96, p. 10,347-10,360.

**Currie, L.D., Arne, D.C., and Grist, A.M.**
1995: Tertiary surface uplift and fault movement in southwestern British Columbia: a progress report; Geological Association of Canada-Mineralogical Association of Canada Annual Meeting, Program with Abstracts, v. 20, p. A22.

**Donelick, R.A., Bergman, S.C., and Talbot, J.**
1992: $^{252}Cf$ irradiation of apatite fission track samples improves spontaneous, confined, track-in-track (TINT) densities; 7th International Workshop on Fission-Track Thermochronology, Philadelphia, U.S.A., p. 80.

**Fleischer, R.L., Price, P.B., and Walker, R.M.**
1964: Fission track ages of zircons; Journal of Geophysical Research, v. 69, p. 4885.
1975: Nuclear Tracks in Solids: Principles and Applications; University of California Press, Berkeley, California, 605 p.

**Galbraith, R.G.**
1982: Statistical analysis of some fission track counts and neutron fluence measurements; Nuclear Tracks, v. 6, p. 99-107.

**Green, P.F., Duddy, I.R., Gleadow, A.J.W., Tingate, P.R., and Laslett, G.M.**
1985: Fission track annealing in apatite: track length measurements and the form of the Arrhenius plot; Nuclear Tracks, v. 10, p. 323-328.
1986: Thermal annealing of fission tracks in apatite, 1, A qualitative analysis; Chemical Geology (Isotope Geoscience Section), v. 59, p. 237-253.

**Green, P.F., Duddy, I.R., Laslett, G.M., Hegarty, K.A., Gleadow, A.J.W., and Lovering, J.F.**
1989: Thermal annealing of fission tracks in apatite 4. Quantitative modelling techniques and extension to geological timescales; Chemical Geology (Isotope Geoscience Section), v. 79, p. 155-182.

**Greenwood, H.J., Woodsworth, G.J., Read, P.B., Ghent, E.D., and Evenchick, C.A.**
1991: Metamorphism; in Geology of the Cordilleran Orogen in Canada, (ed.) H. Gabrielse and C.J. Yorath; Geological Survey of Canada, Geology of Canada, no. 4, p. 533-570 (also Geological Society of America, The Geology of North America, v. G-2).

**Grist, A.M. and Ravenhurst, C.E. (comp.)**
1992: A step-by-step laboratory guide to fission track thermochronology at Dalhousie University; in Low Temperature Thermochronology; Mineralogical Association of Canada Short Course Handbook, v. 20, Appendix 1, p. 189-201.

**Holdahl, S.R., Faucher, F., and Dragert, H.**
1989: Contemporary vertical crustal motion in the Pacific northwest; in Slow Deformation and Transmission of Stress in the Earth, (ed.) S.C. Cohen and P. Vanicek; American Geophysical Union IUGG Geophysical Monograph 49, v. 4, p. 17-29.

**Hurford, A.J. and Green, P.F.**
1982: The zeta age calibration of fission track dating; Chemical Geology (Isotope Geoscience Section), v. 1, p. 285-317.

**Hyndman, R.D., Yorath, C.J., Clowes, R.M., and Davis, E.E.**
1989: The northern Cascadia subduction zone at Vancouver Island: seismic structure and tectonic history; Canadian Journal of Earth Sciences, v. 27, p. 313-329.

**Irving, E. and Brandon, M.T.**
1990: Paleomagnetism of the Flores volcanics, Vancouver Island, in place by Eocene time; Canadian Journal of Earth Sciences, v. 27, p. 811-817.

**Issler, D.R. and Stockmal, G.S.**
1995: Pitfalls of apatite fission track modelling and interpretation: examples using forward and inverse techniques; in Proceedings of the Oil and Gas Forum '95, (ed.) J.S. Bell, T.S. Bird, T.L. Hillier, and P.L. Greener; Geological Survey of Canada, Open File 3058, p. 519-523.

**Issler, D.R., Beaumont, C., Willett, S.D., Donelick, R.A., Mooers, J., and Grist, A.M.**
1990: Preliminary evidence from apatite fission-track data concerning the thermal history of the Peace River Arch region, Western Canada Sedimentary Basin; Bulletin of Canadian Petroleum Geology, v. 38A, p. 250-269.

**Johnson, S.Y., Zimmerman, R.A., Naeser, C.W., and Whetten, J.T.**
1986: Fission track dating of the tectonic development of the San Juan Islands, Washington; Canadian Journal of Earth Sciences, v. 23, p. 1318-1330.

**Laslett, G.M., Green, P.F., Duddy, I.R., and Gleadow, A.J.W.**
1987: Thermal annealing of fission tracks in apatite: 2. A quantitative analysis; Chemical Geology (Isotope Geoscience Section), v. 65, p. 1-13.

**Massey, N.W.D.**
1994: Geological Compilation, Vancouver Island, British Columbia (NTS 92 B, C, E, F, G, K, L, 102 I); British Columbia Ministry of Energy, Mines and Petroleum Resources, Open File 1994-6; 5 digital files, legend, scale 1:250 000.

**Monger, J.W.H. and Journeay, J.M.**
1994: Basement geology and tectonic evolution of the Vancouver region; in Geology and Geologic Hazards of the Vancouver Region, Southwestern British Columbia, (ed.) J.W.H. Monger; Geological Survey of Canada, Bulletin 481, p. 3-25.

**Muller, J.E.**
1977: Geology of Vancouver Island; Geological Survey of Canada, Open File Map OF-463.

**Mustard, P.S.**
1994: The Upper Cretaceous Nanaimo Group, Georgia Basin; in Geology and Geological Hazards of the Vancouver Region, Southwestern British Columbia, (ed.) J.W.H. Monger; Geological Survey of Canada, Bulletin 481, p. 27-95.

**Mustard, P.S., Parrish, R.R., and McNicoll, V.**
1995: Provenance of the Upper Cretaceous Nanaimo Group, British Columbia: evidence from U-Pb analyses of detrital zircons; in Stratigraphic Evolution of Foreland Basins, Society of Economic Paleontologists and Mineralogists, Special Publication No. 52, p. 59-76.

**O'Sullivan, P.B. and Parrish, R.R.**
1995: The importance of apatite composition and single-grain ages when interpreting fission track data from plutonic rocks: a case study from the Coast Ranges, British Columbia; Earth and Planetary Science Letters, v. 132, p. 213-224.

**Parrish, R.R.**
1983: Cenozoic thermal evolution and tectonics of the Coast Mountains of British Columbia 1. Fission track dating, apparent uplift rates, and patterns of uplift; Tectonics, v. 2, p. 601-631.

**Ravenhurst, C.E., Willett, S.D., Donelick, R.A., and Beaumont, C.**
1994: Apatite fission track thermochronometry from central Alberta: implications for the thermal history of the Western Canada Sedimentary Basin; Journal of Geophysical Research, v. 99, p. 20,023-20,041.

**Read, P.B., Woodsworth, G.J., Greenwood, H.J., Ghent, E.D., and Evenchick, C.A.**
1991: Metamorphic Map of the Canadian Cordillera; Geological Survey of Canada, Map 1714A, scale 1:2 000 000.

**Riddihough, R.P.**
1982: Contemporary movements and tectonics on Canada's west coast: a discussion; Tectonophysics, v. 86, p. 319-341.

**Riddihough, R.P. and Hyndman, R.D.**
1991: Modern plate tectonic regime of the continental margin of western Canada; in Geology of the Cordilleran Orogen in Canada, (ed.) H. Gabrielse and C.J. Yorath; Geological Survey of Canada, Geology of Canada, no. 4, p. 435-455 (also Geological Society of America, The Geology of North America, v. G-2).

**Vanicek, P. and Nagy, D.**
1981: On the compilation of the map of vertical crustal movements in Canada; Tectonophysics, v. 71, p. 75-86.

**Wagner, G.A. and Van den Haute, P.**
1992: Fission Track Dating; Kluwer Academic Publishers, Dordrecht, The Netherlands, 285 p.

**Wheeler, J.O., Brookfield, A.J., Gabrielse, H., Monger, J.W.H., Tipper, H.W., and Woodsworth, G.J.**
1991: Terrane map of the Canadian Cordillera; Geological Survey of Canada Map 1713, scale 1:2 000 000.

**Yorath, C.J., Green, A.G., Clowes, R.M., Sutherland Brown, A., Brandon, M.T., Kanasewich, E.R., Hyndman, R.D., and Spencer, C.**
1985: Lithoprobe-southern Vancouver Island: seismic reflection sees through Wrangellia to the Juan de Fuca Plate; Geology, v. 13, p. 759-762.

Geological Survey of Canada Project 930038

# Appendix I

## Analytical procedure for apatite fission track analyses

Mineral concentrates from the Alberni Inlet samples were separated using conventional magnetic and heavy liquid techniques (see Grist and Ravenhurst, 1992). Apatite separates (consisting of a few to more than one thousand apatite grains) were mounted in Araldite epoxy and polished to expose internal grain surfaces. Spontaneous tracks were revealed by etching in 5M $HNO_3$ for 20 seconds at 24°C. For samples that had relatively few fossil fission tracks, duplicate grainmounts were made and sent to the Irradiation Laboratory at Rensselaer Polytechnic Institute, Troy, New York, for irradiation (under vacuum for 5 days at a distance of 9 cm) with $^{252}Cf$ fission fragments to increase the number of confined tracks revealed by etching (Donelick et al., 1992). These samples are indicated in Table 1.

Fission track ages were determined using the external detector method (Fleischer et al., 1964; Hurford and Green, 1982). A thin sheet of low-uranium muscovite was placed in contact with the polished surface of each grain mount to serve as a detector of neutron-induced fission. Samples were irradiated at the Dalhousie University Slowpoke reactor in the presence of a glass neutron dosimeter (CN5) of known characteristics. The thermal-neutron fluence obtained was approximately $9 \times 10^{15}$ neutrons/cm$^2$. The cadmium ratio for Au is 4.3 at this site. Micas were etched at room temperature in 48% HF for 30 minutes.

Track densities (tracks/cm$^2$) for both spontaneous and induced fission track populations were measured with a Zeiss Axioplan microscope at 1000X magnification (100X dry objective, 10X oculars). Fission track ages were calculated using a weighted mean zeta calibration factor (Fleischer et al., 1975; Hurford and Green, 1982), determined using the Fish Canyon Tuff apatite (obtained from C.W. Naeser), and Durango apatite (obtained commercially) age calibration standards.

Horizontal confined tracks are internal fission tracks that are subparallel to the mineral surface. Etchable length distributions of horizontal, confined tracks (in crystallographic planes parallel to the c-axis) were also measured on a Zeiss Axioplan microscope at 1000X magnification (100X dry objective, 10X oculars) using a digitizing pad interfaced with a personal computer. Positioning of the mouse (with an attached LED) on the digitizing surface was made possible by attaching a projection tube to the microscope. The precision of each individual track length measured is approximately $\pm 0.2$ μm.

# Quaternary stratigraphy of Taseko valley, south-central British Columbia[1]

A. Plouffe, V. Levson[2], and T. Giles[3]
Terrain Sciences Division, Ottawa

*Plouffe, A., Levson, V., and Giles, T., 1996: Quaternary stratigraphy of Taseko valley, south-central British Columbia; in Current Research 1996-A; Geological Survey of Canada, p. 129-134.*

**Abstract:** The Quaternary succession in Taseko valley, near the confluence of Taseko River and Tête Angela Creek, includes three major units (in decreasing age): (1) advance phase sediments, (2) till and (3) glaciofluvial and fluvial sand and gravel. It is suggested that at the onset of the last (Fraser) glaciation, as ice advanced down Taseko valley, there was a lake at the ice front, impounded by an ice or sediment dam located farther downstream. The dam may have formed when prograding outwash or valley glaciers, derived from mountainous areas that flank Fraser and Chilcotin valleys, blocked the drainage. The Taseko valley stratigraphy is correlated with stratigraphies at other sites in Chilcotin and Fraser River valleys where advance phase glaciolacustrine sediments have been reported.

**Résumé :** La stratigraphie du Quaternaire dans la vallée Taseko, près de la confluence de la rivière Taseko et du ruisseau Tête Angela, comprend trois unités principales qui sont, en âge décroissant, les suivantes : (1) des sédiments d'avancée glaciaire, (2) un till, (3) du sable et du gravier fluvio-glaciaires et fluviatiles. Il est suggéré qu'au début de la dernière glaciation (Fraser), lorsque la glace avançait dans la vallée Taseko, un lac était retenu au front du glacier par un barrage de glace ou de sédiments situé plus loin en aval. Ce barrage aurait pu avoir été formé lorsque des plaines d'épandage ou des glaciers de vallée, provenant des régions montagneuses avoisinantes aux vallées Fraser et Chilcotin, bloquaient le drainage. La stratigraphie de la vallée Taseko est mise en corrélation avec celle d'autres sites dans les vallées Chilcotin et Fraser, où des sédiments glaciolacustres d'avancée glaciaire ont été observés.

[1] Contribution to Canada-British Columbia Agreement on Mineral Development 1991-1995, a subsidiary agreement under the Canada-British Columbia Economic and Regional Development Agreement.
[2] Geological Survey Branch, Ministry of Energy, Mines and Petroleum Resources, Victoria, British Columbia
[3] Kamloops Forest Region, British Columbia Minsitry of Forests, Kamloops, British Columbia

## INTRODUCTION

At the onset of the late Wisconsinan Fraser Glaciation in central British Columbia, glaciers advanced from cirques in mountainous areas into valleys and onto surrounding plateaus. Prograding outwash and advancing ice tongues locally blocked the regional drainage, forming advance-phase glacial lakes. Advance-phase glaciolacustrine sedimentation is well documented in the Fraser and Chilcotin river valleys (Clague, 1987, 1988; Eyles and Clague, 1987, 1991; Eyles et al., 1987; Ryder et al., 1991; Huntley and Broster, 1993, 1994; Levson and Giles, 1993; Levson et al., 1995). Huntley and Broster (1994) formally named the proglacial lake that invaded Fraser valley south of Chilcotin River at the beginning of the Fraser Glaciation "Glacial Lake Camelsfoot". Advance-phase proglacial lakes occupied major valleys in central British Columbia; their presence and extent in smaller tributary valleys of the area is not documented. The purpose of this paper is to report on the stratigraphy of the Taseko River valley and to present evidence of glaciolacustrine sedimentation there at the onset of the Fraser Glaciation.

### *Physiography and bedrock geology*

The study area is located at the boundary of the Fraser Plateau and Coast Mountains physiographic regions, as defined by Holland (1976) (Fig. 1). The Fraser Plateau is a rolling to relatively flat landscape with an average elevation of 1360-1515 m (4500-5000 ft.) a.s.l. It includes a few mountainous areas such as the Camelsfoot and Marble ranges with cirques and arêtes; only a few peaks rise above 1970 m (6500 ft.) a.s.l. The Coast Mountains also contain several major cirques, but peaks commonly are higher than 2400 m (8000 ft.) a.s.l. Taseko River flows north from the Coast Mountains into Chilko River, a tributary of Chilcotin River (Fig. 1).

The Fraser Plateau in Taseko valley is underlain by Mesozoic and Tertiary sedimentary and volcanic rocks (basalt, dacite, andesite, and rhyolite) (Tipper, 1963; Hickson, 1993; Riddell et al., 1993). The Coast Mountains to the south consist of Upper Cretaceous volcanic (andesite) and intrusive rocks (mostly granodiorite and quartz diorite) of the Coast Plutonic Complex (Roddick et al., 1979).

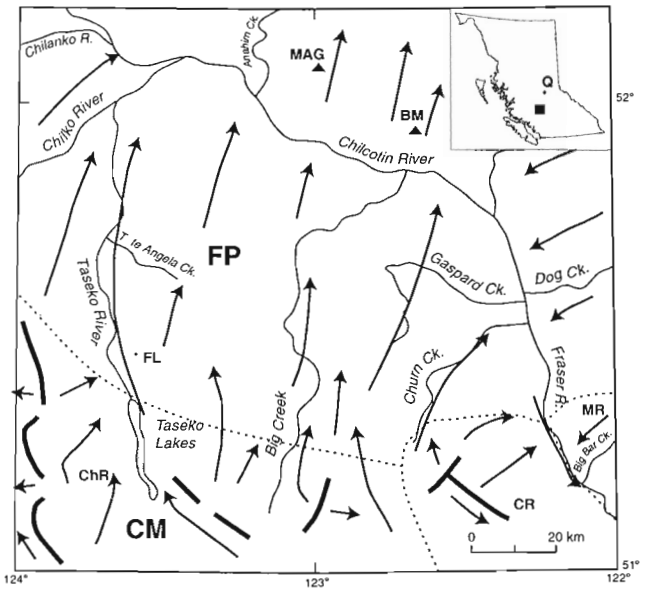


*Figure 1. Location map, showing physiographic units and generalized ice flow directions; modified from Huntley and Broster (1993). Thicker lines represent ice divides. BM – Bald Mountain, ChR – Chilcotin Ranges, CR – Camelsfoot Ranges, CM – Coast Mountains, FL – Fish Lake mineral deposit, FP – Fraser Plateau, MAG – Mount Alex Graham, MR – Marble Ranges, and Q – Quesnel (inset map only).*

### *Glacial geology*

Alpine glaciers developed in the Coast Mountains and in the Camelsfoot and Marble ranges at the beginning of the Fraser Glaciation (Huntley and Broster, 1993). From these accumulation areas, ice generally flowed north and north-northeast (Fig. 1), deflected in places by topography (Heginbottom, 1972; Huntley and Broster, 1993; Plouffe and Ballantyne, 1994). Early during the Fraser Glaciation, ice from the Camelsfoot and Marble ranges blocked Fraser River, ponding Glacial Lake Camelsfoot in Fraser valley (Huntley and Broster, 1993, 1994). This proglacial lake reached an elevation of at least 710 m (2343 ft.) a.s.l. as determined by the highest occurrence of glaciolacustrine sediments in the valley of Churn Creek (Huntley and Broster, 1994).

### *Methodology*

Sections along Taseko River and Tête Angela Creek were logged in 1994. Each stratigraphic unit was described with respect to its thickness, texture, sedimentary structures, colour, clast composition, paleocurrent data, contact relationships, and lateral continuity. Locations of measured sections are shown in Figure 2a.

## STRATIGRAPHY

Till deposited during Fraser Glaciation is the most abundant surficial sediment on the Fraser Plateau. Older sediments were only found in Taseko valley which is incised approximately 180 m (595 ft.) into the plateau. The valley fill near Tête Angela Creek (Fig. 3) includes a glaciolacustrine advance sequence (unit 1) overlain by till (unit 2). Glaciofluvial and fluvial sand and gravel (unit 3), deposited during ice retreat, unconformably overlie the glaciolacustrine sequence at lower elevation in the valley.

### *Unit 1 – advance phase complex*

The oldest unit in the valley comprises three interbedded lithofacies (1a, 1b, 1c) (Fig. 2).

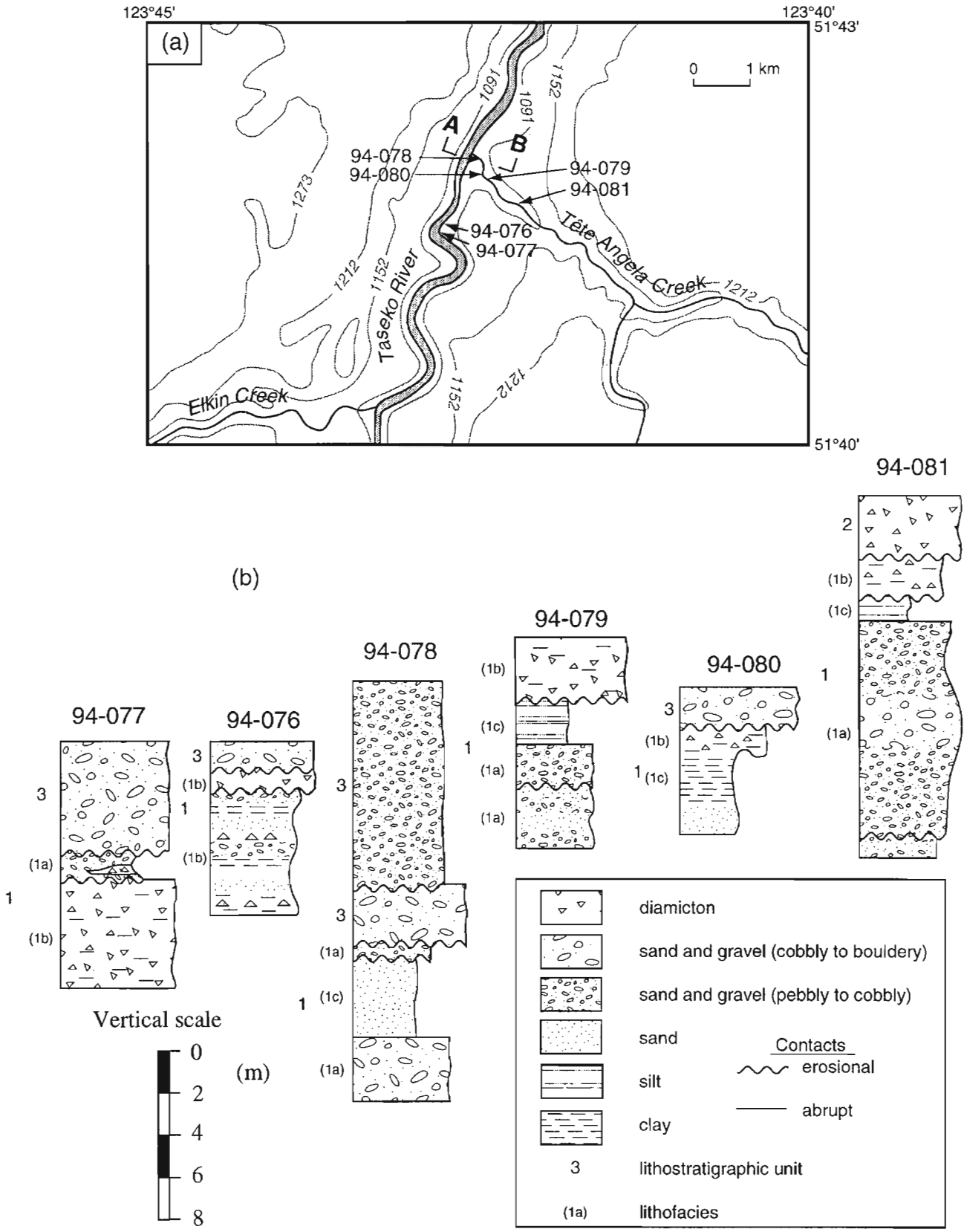


***Figure 2. a)*** *Section locations. Contours in metres (converted from feet).* ***b)*** *Lithostratigraphic columns.*

*Lithofacies 1a – crudely stratified gravel.* Crudely stratified gravel is best exposed along Tête Angela Creek at section 94-081 (Fig. 2, 4) where it has a maximum thickness of 11 m. The gravel is clast-supported but contains rare beds of matrix-supported diamicton. At section 94-081, it contains scattered boulders up to 2 m across (Fig. 4). Gravel beds locally exhibit crude trough crossbedding, fine upwards, and have scoured lower contacts. They are dominated by stones of local volcanic and sedimentary bedrock, but include minor granodiorite (probably derived from the Coast Mountains) and rounded silt clasts ('rip-ups'). Paleoflow, indicated by cross-stratification in sand lenses at section 94-079 (Fig. 2), is to the northeast.

Unit 1a is interpreted to be ice-proximal glaciofluvial sediments deposited during the onset of glaciation in the valley. Part of this lithofacies may have been deposited by tributary streams. Gravel beds represent longitudinal bar and channel-fill deposits. Diamicton beds are probably debris flows of glaciogenic origin.

*Lithofacies 1b – crudely stratified to massive diamicton.* A 5 m thick diamicton unit is exposed at the base of sections 94-076 and 94-077 (Fig. 2). It is massive to crudely stratified and contains several continuous clayey interbeds as well as gravel, sand, and silt lenses. The matrix of the diamicton is silty to clayey. Clasts range from pebble- to boulder-size. Large boulders of local volcanic bedrock are abundant, and intrusive clasts are also present.

The diamicton is interpreted to be subaqueous debris flow deposits, similar to those described elsewhere in the region by Eyles and Clague (1987), Eyles et al. (1987), Clague (1988), Eyles and Clague (1991), and Huntley and Broster (1994). Multiple beds probably represent several flow events at a site. Debris flows likely occurred in response to drowning of the Taseko valley and slumping of unstable bedrock and unconsolidated sediments on the surrounding steep slopes (see Eyles and Clague, 1987).

*Lithofacies 1c – stratified sand, silt, and clay.* Horizontally-laminated sand, silt, and clay and trough cross-bedded sand are found within unit 1. This lithofacies varies greatly in thickness from site to site but is a maximum of 5 m thick at section 94-080 (Fig. 2). Penecontemporaneous deformation structures (folds and fluid escape structures) and slickensided surfaces were observed in this lithofacies at one site (section 94-080).

Sand, silt, and clay of lithofacies 1c are interpreted to be low-energy glaciolacustrine sediments. The association of these sediments with coarse gravel and diamicton suggests that they were deposited in a lake near the ice margin.

### *Unit 2 – Fraser Glaciation till*

A dense massive, matrix-supported diamicton with a sandy to silty matrix covers the upper slopes of Taseko valley (Fig. 3) and the surface of Fraser Plateau. In Taseko valley, it unconformably overlies unit 1. It contains abundant striated clasts of local and distant (Coast Mountains) origin. Discontinuous sand lenses, generally less than 2 m long, have been observed in this unit on the Fraser Plateau. The diamicton range in thickness from 1 m to more than 5 m. Unit 2 differs from lithofacies 1b because it is not crudely stratified and does not contain continuous clayey interbeds.

This diamicton is interpreted as Fraser Glaciation till. The presence of sand lenses in this till suggest that it might have been deposited by melt-out.

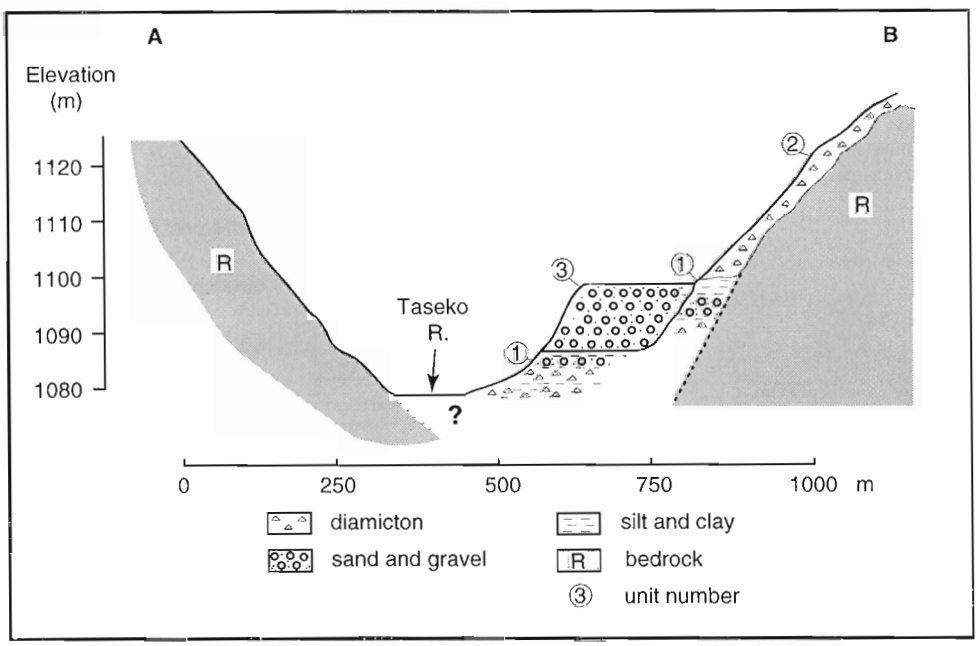


***Figure 3.*** *Schematic cross-section of Taseko valley showing distribution of unconsolidated sediments described in this paper. See text for description of units.*

### *Unit 3 – Glaciofluvial and fluvial sand and gravel*

Terraces within Taseko valley are underlain by well stratified sand and gravel. These sediments unconformably overlie unit 1. The gravel is loose, clast-supported, has a sandy matrix and contains rounded to subrounded clasts of pebble- to cobble-size. Tertiary volcanic and sedimentary rocks are the dominant lithologies, but there are approximately 5-10% intrusive clasts.

This unit records glaciofluvial deposition at the end of the Fraser Glaciation, probably followed by fluvial sedimentation during the Holocene. The distinction between glaciofluvial and fluvial terraces is arbitrary and in this portion of the valley, it is solely based on terrace elevation; highest terraces are thought to be underlain by glaciofluvial deposits and the lowest ones, closer to the river level, more likely consist of fluvial sediments. The unconformity at the base of unit 3 and the absence of till in the lower portion of Taseko valley (Fig. 3) suggest that glaciofluvial aggradation was preceded by incision.

## INFERRED GLACIAL HISTORY

At the beginning of the Fraser Glaciation, ice advanced down the Taseko River valley from accumulation areas in the Coast Mountains. A sediment or ice dam downstream of the confluence of Tête Angela Creek and Taseko River blocked the drainage and impounded a lake in Taseko valley. Sediments of unit 1 were deposited in this lake.

Huntley and Broster (1994) suggest that Glacial Lake Camelsfoot inundated Fraser valley to a minimum elevation of 710 m (2343 ft.) a.s.l. at least as far north as the mouth of Chilcotin River. Unit 1 is present to at least 1100 m (3630 ft.) a.s.l. which thus is the minimum elevation reached by the lake in Taseko valley. It is unlikely that Glacial Lake Camelsfoot and the lake in Taseko valley were a single water body, since it would require a thick ice accumulation in Fraser valley, at a time when Taseko valley was free of ice. A more likely scenario is that the lake in Taseko valley was independent of that in Fraser valley. It may have been dammed by glaciers flowing from mountainous area north of Gaspard Creek or from Alex Graham or Bald mountains (Fig. 1). Valley glaciers flowing from these areas or prograding outwash fans associated with these glaciers may have filled the Chilcotin River and thus inundated Taseko valley. Following the flooding of the valley, unstable sediments and bedrock on steep slopes were probably remobilized as debris flows (see Eyles and Clague, 1987; Eyles et al., 1987).

No evidence of glacial lake impoundment during ice retreat was found in the Taseko valley. Drainage apparently was open, and glaciofluvial sediments that aggraded in the valley were incised by Taseko River after deglaciation.

## CORRELATION WITH OTHER AREAS

The Quaternary stratigraphy of the Taseko River valley is similar to that to the east and northeast, in the Fraser and Chilcotin valleys and their tributaries (Table 1). Taseko valley and valleys to the east were blocked at the onset of the Fraser Glaciation which resulted in deposition of advance-phase glaciolacustrine sediments. The glaciolacustrine sediments were overridden by the glaciers that deposited Fraser till. However, during ice retreat, conditions were different in the two areas. Glacial lakes formed in the Fraser and Chilcotin valleys (Eyles and Clague, 1991), whereas in Taseko valley, ice retreated up-slope and the drainage was open at the ice front.

## IMPLICATION FOR MINERAL EXPLORATION

Several mineral exploration programs have been conducted in the Taseko valley area in the late 1980s and early 1990s, since the discovery of the porphyry Cu-Au deposit at Fish Lake (Fig. 1). Following a reconnaissance till sampling program, till geochemistry has been found to be effective to


***Figure 4.***

*Photograph of section 94-081. Note the large boulder in the glaciofluvial gravel (unit 1a). Person (arrow) provides scale. See Figure 2b and text for description of units.*

**Table 1.** Correlation of lithostratigraphic units (modified from Huntley and Broster, 1994).

| Sediment type | Gang Ranch (Huntley and Broster, 1994) | Chilcotin and Fraser valley (Eyles and Clague, 1991) | Williams Lake (Clague, 1987) | Quesnel (Clague, 1988) | Taseko valley (this paper) |
|---|---|---|---|---|---|
| Glaciofluvial and fluvial sediments | 5a | E | 8 | 13 | 3 |
| Retreat glaciolacustrine sediments | 5b | E | 7 | 12 | None |
| Fraser till | 4 | D | 6 | 11 | 2 |
| Advance glaciolacustrine sediments | 3b | D | 4,5 | 10 | 1a,b and c |

detect bedrock mineralization, even in areas where outcrops are rare and unconsolidated sediment cover is thick (Plouffe and Ballantyne, 1994).

The stratigraphy presented in this paper has two major implications for mineral exploration: (1) till, the most suitable sampling medium for mineral exploration (Shilts, 1993; Plouffe and Ballantyne, 1994), is not easily accessible in the Taseko valley, and (2) till geochemical anomalies located in the valley are not necessarily directly derived from bedrock but could originate from the reworking of older sediments by the glacier. Consequently, the use of till geochemistry to ascertain the bedrock mineralization potential within Taseko valley (at least in the Tête Angela Creek area) is limited.

## ACKNOWLEDGMENTS

Fieldwork was funded by the Canada-British Columbia Agreement on Mineral Development. The authors were capably assisted in the field by C. McPhee. J.J. Clague greatly improved an earlier version of the manuscript.

## REFERENCES

**Clague, J.J.**
1987: Quaternary stratigraphy and history, Williams Lake, British Columbia; Canadian Journal of Earth Sciences, v. 24, p. 147-158.
1988: Quaternary stratigraphy and history, Quesnel, British Columbia; Géographie physique et Quaternaire, v. 42, p. 279-288.

**Eyles, N. and Clague, J.J.**
1987: Landsliding caused by Pleistocene glacial lake ponding - an example from central British Columbia; Canadian Geotechnical Journal, v. 24, p. 656-663.
1991: Glaciolacustrine sedimentation during advance and retreat of the Cordilleran Ice Sheet in central British Columbia; Géographie physique et Quaternaire, v. 45, p. 317-331.

**Eyles, N., Clark, B.M., and Clague, J.J.**
1987: Coarse-grained sediment gravity flow facies in a large supraglacial lake; Sedimentology, v. 34, p. 193-216.

**Heginbottom, J.A.**
1972: Surficial geology of Taseko Lakes map-area British Columbia; Geological Survey of Canada, Paper 72-14, 9 p.

**Hickson, C.J.**
1993: Geology of the northwest quadrant Taseko Lake map area (92O), west central British Columbia; Geological Survey of Canada, Open File 2695, scale 1:50 000 scale maps.

**Holland, S.S.**
1976: Landforms of British Columbia, a physiographic outline; British Columbia Department of Mines and Petroleum Resources, Bulletin 48, 138 p.

**Huntley, D.H. and Broster, B.E.**
1993: Glacier flow patterns of the Cordilleran Ice Sheet during the Fraser Glaciation, Taseko Lakes map area, British Columbia; Current Research, Part A; Geological Survey of Canada, Paper 93-1A, p. 167-172.
1994: Glacial Lake Camelsfoot: a Late Wisconsinan advance stage proglacial lake in the Fraser River valley, Gang Ranch area, British Columbia; Canadian Journal of Earth Sciences, v. 31, p. 798-807.

**Levson, V.M. and Giles, T.R.**
1993: Geology of Tertiary and Quaternary gold-bearing placers in the Cariboo region, British Columbia; British Columbia Ministry of Energy, Mines and Petroleum Resources, Bulletin 89, 202 p.

**Levson, V.M., Clague, J.J., and Fulton, R.J.**
1995: Quaternary geology and placer gold deposits of central British Columbia; Geological Association of Canada, Fieldtrip Guidebook A4, 67p.

**Plouffe, A. and Ballantyne, S.B.**
1994: Regional till geochemistry, Mount Tatlow and Elkin Creek area, British Columbia (92-O/5 and O/12); Geological Survey of Canada, Open File 2909, 62 p.

**Riddell, J., Schiarizza, P., Gaba, R., McLaren, G., and Gouse, J.**
1993: Geology of the Mt. Tatlow map area, British Columbia; British Columbia Ministry of Energy Mines and Petroleum Resources, Open File 1993-8, 2 sheets, scale 1:50 000.

**Roddick, J.A., Muller, J.E., and Okulitch, A.V.**
1979: Fraser River, Sheet 92; Geological Survey of Canada Map 1386A, scale 1: 1 000 000.

**Ryder, J.M., Fulton, R.J., and Clague, J.J.**
1991: The Cordilleran Ice Sheet and the glacial geomorphology of southern and central British Columbia; Géographie physique et Quaternaire, v. 45, p. 365-377.

**Shilts, W.W.**
1993: Geological Survey of Canada' s contributions to understanding the composition of glacial sediments; Canadian Journal of Earth Sciences, v. 30, p. 333-353.

**Tipper, H. W.**
1963: Nechako River map-area, British Columbia; Geological Survey of Canada, Memoir 324, 59 p.

Geological Survey of Canada Project 900004

# New stratigraphic and tectonic interpretations, north Okanagan Valley, British Columbia

Robert I. Thompson and Kenneth L. Daughtry[1]
GSC Victoria, Vancouver

*Thompson, R.I. and Daughtry, K.L., 1996: New stratigraphic and tectonic interpretations, north Okanagan Valley, British Columbia; in Current Research 1996-A; Geological Survey of Canada, p. 135-141.*

**Abstract:** Palaeozoic stratigraphic markers on both sides of the north Okanagan Valley (82L) suggest the valley is a graben that underwent relatively little extension. Interpretation of a shallow west-dipping extension fault along the valley trace cannot be supported by the local geology.

Radiometric dates from an undeformed pluton and pegmatite mapped across the inferred trace of the Okanagan Fault, south of Wood Lake, cut the regional foliation and constrain the fabric as older than latest Jurassic.

Schist and gneiss that comprise the Shuswap Metamorphic Complex (formerly Monashee Group) extend northwest across the north Okanagan Valley to Little Shuswap Lake, implying stratigraphic equivalence between the Monashee Group and the Silver Creek Formation.

The Tsalkom, Mara, and Sicamous formations may outcrop at Keefer Gulch, 10 km east of Vernon. The Sicamous Formation may be Permian. Lithologically, the Mara Formation strongly resembles parts of the Eagle Bay Formation.

**Résumé :** Des repères stratigraphiques paléozoïques des deux côtés de la partie nord de la vallée de l'Okanagan (82L) portent à croire qu'il s'agit d'un graben qui résulte d'une extension relativement faible. Les données géologiques à l'échelle locale ne corroborent pas l'interprétation selon laquelle il existe une faille d'extension peu profonde à pendage ouest longeant la vallée.

Des datations radiométriques d'un pluton et d'une pegmatite non déformés qui recoupent la foliation régionale, cartographiés transversalement à la trace inférée de la faille d'Okanagan, au sud du lac Wood, permettent d'assigner un âge antérieur au Jurassique terminal à la fabrique.

Les schistes et les gneiss qui comprennent le complexe métamorphique de Shuswap (auparavant le Groupe de Monashee) s'étendent vers le nord-ouest à travers la partie nord de la vallée de l'Okanagan jusqu'au lac Little Shuswap, appuyant une équivalence stratigraphique entre le Groupe de Monashee et la Formation de Silver Creek.

Les formations de Tsalkom, de Mara et de Sicamous affleurent peut-être au ravin Keefer, 10 km à l'est de Vernon. La Formation de Sicamous pourrait dater du Permien. Du point de vue lithologique, la Formation de Mara s'apparente fortement à certaines parties de la Formation d'Eagle Bay.

[1] Discovery Consultants, P.O. Box 933, Vernon, British Columbia V1T 6M8

## INTRODUCTION

Field work in 1995 focused on the Okanagan Valley and Salmon River Valley area between the towns of Vernon and Salmon Arm (Fig. 1) in the north-central Vernon map area (82L). The purpose was threefold: to assess the magnitude and style of Eocene extension; to explore possible stratigraphic correlations between strata in the Salmon Arm and Vernon areas; and to investigate current tectonostratigraphic interpretation that Quesnel Terrane is separate, distinct, and exotic with respect to Kootenay Terrane (e.g., Monger et al., 1991).

Between Armstrong and Mara Lake, the north Okanagan Valley narrows to a few kilometres, providing ideal spacial constraints to establish the geometric configuration and amount of Eocene extension across the north Okanagan Valley. This work follows from studies farther south between Vernon and Wood Lake. There, high grade metamorphic rocks are juxtaposed across either side of the inferred trace of the Okanagan Fault; the geological characteristics normally associated with significant displacement across a crustal scale extension fault could not be documented (Thompson and Daughtry, 1994). These observations have since been corroborated by preliminary results from radiometric dating (U-Pb) of an undeformed pluton and an undeformed pegmatite that cut foliated rocks within the fault zone; both dates are Jurassic. The evidence presented below is best explained by steep-dipping faults with relatively little displacement that define the trace of the northern Okanagan Valley north of Enderby. Johnson (1989) presented evidence for the Eagle River Fault, a crustal scale extension fault mapped from Sicamous northward along the trace of the Eagle River; he inferred the fault continues southward as far a Grindrod. We cannot comment on the nature of the Eagle River Fault but we suggest it must plunge southward, into the subsurface, before the south end of Mara Lake.

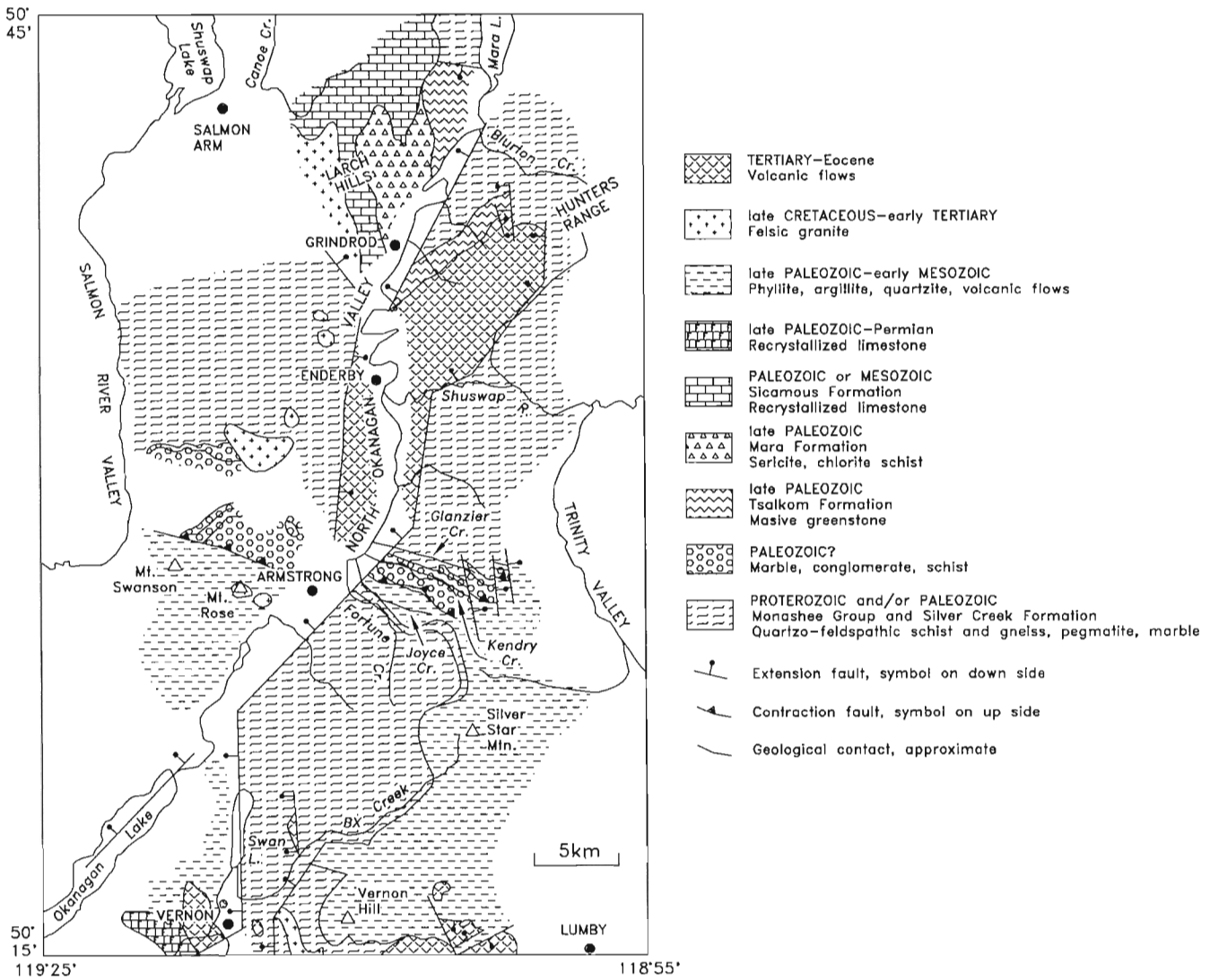


***Figure 1.*** *Generalized geological map of the north Okanagan region between Vernon and Sicamous.*

At Enderby and along Mara Lake, one can compare and contrast the lithologies, style of deformation, and metamorphic grade of schist and gneiss flanking both margins of the Okanagan Valley. The evidence presented below suggests there is little reason to discriminate one from the other, as Jones (1959) did on his map; it is more reasonable that his Monashee Group and part of his Mount Ida Group – specifically Silver Creek Formation and some of what he termed Mara Formation – are the same lithostratigraphic succession. This was Nielsen's (1982) conclusion as well; he was able to correlate units within the Monashee and Mt. Ida groups across the south end of Mara Lake.

We discuss the possible correlation of strata between Shuswap Lakes and the Vernon area, in particular the Tsalkom, Eagle Bay, and Sicamous formations in the north with some of the unnamed units that form Jones' (1959) Cache Creek Group farther south. Other correlations mapped by Jones (1959) cannot be substantiated; strata west of Armstrong and greenstone belonging to the Tsalkom Formation at the south end of Mara Lake, are not equivalent.

We are still looking for the tectonic boundary between Quesnel Terrane and underlying Kootenay Terrane. Distinction between the two terranes becomes increasingly blurred as details of the stratigraphy are examined. We present some of our observations.

## THE OKANAGAN FAULT

There is ample evidence along that segment of the Okanagan Fault extending from Armstrong to the south end of Mara Lake to suggest the Okanagan Valley is a graben floor, probably tilted to the east, and bounded by relatively steep-dipping faults having unequal displacements. Vertical separation along the eastern flank is approximately 1 km; along the west flank it is less, perhaps no more than a few hundred metres. Horizontal separation is in the same range.

These conclusions stem from a comparison of geology, including stratigraphy, metamorphic grade, and style of deformation, along either flank of the Okanagan Valley (Fig. 1).

### *The succession near Armstrong*

East of the town of Armstrong, in the upper reaches of Glanzier, Kendry, and Joyce creeks, is a distinctive stratigraphic succession consisting of a coarse-crystalline light grey marble couplet separated by black, biotite-hornblende schist, and overlain by quartzite containing stretched pebble conglomerate. Northwest of Armstrong, along the northern flank of Mount Swanson, are two marble units, separated by graphitic, biotite-hornblende schist and overlain by quartzite containing stretched pebble conglomerate. The succession dips gently westward.

The quartzite succession is the most distinctive and comparable unit. It is approximately 15 m thick, medium to fine crystalline with occasional argillaceous bands in an otherwise pure quartz assemblage. Quartzite pebble outlines are moderately distinct with long to short axis ratios of about 5 to 1.

The marble units are medium to coarse crystalline, void of internal structure save complex flowing fold patterns outlined by colour bands. The schists are typically black, graphitic, and fine to medium grained with porphyroblasts of biotite, hornblende, and less commonly garnet and (staurolite?).

The succession has the same lithostratigraphic signature, one side of the valley to the other, the same tectonite fabric and comparable metamorphic grade.

Maximum horizontal separation is 8 km, the horizontal distance separating the most westerly outcrop of marble on the east side of the valley from the most easterly outcrop of marble on the west side of the valley. Maximum vertical displacement is about 1 km, the maximum difference in elevation between outcrops on either side of the valley.

### *The succession near Grindrod*

North of the town of Grindrod, on the west side of the Okanagan Valley is a distinctive stratigraphic succession; it consists of the Tsalkom Formation (greenstone) overlain by sericite-chlorite schist belonging to the Mara Formation, capped by crystalline limestone belonging to the Sicamous Formation. The succession forms a south-dipping homocline.

East of Grindrod, on the steep western flank of the Hunters Range, Tsalkom Formation, including a distinctive grey chert near its base, forms a south-dipping homocline traceable from near the valley floor at 500 m to an elevation of 1400 m. It is overlain unconformably by Eocene volcanic breccia and flows. Sericite-chlorite schist typical of the Mara Formation is present but we have not, as yet, demonstrated that it overlies the Tsalkom greenstone.

The only comparable unit across the valley is the Tsalkom greenstone. A notable comparison is the occurrence of a light-grey weathering chert succession, a few metres thick (at least), occurring near the base of the greenstone on either side of the valley.

On the west flank of the valley, Jones (1959) showed the Tsalkom Formation overlying quartz-biotite schist belonging to the Mara Formation. Along the east flank of the valley Jones (1959) mapped Monashee Group only, no Tsalkom. We present evidence in the following section suggesting the Mara Formation mapped at the south end of Mara Lake belongs to the Monashee Group. In other words, Tsalkom Formation overlies the Monashee Group.

Using the stratigraphic interpretation at Grindrod, the maximum horizontal component of fault displacement across the valley is approximately 2 km – the horizontal distance

between outcrops of greenstone; the maximum vertical component of fault displacement is, if any, a few hundred metres. This suggests to us that this segment of the Okanagan Valley is a two-sided graben.

The data presented above do not support the notion that the northern segment of the Okanagan Valley contains a gently west-dipping extension fault having tens of kilometres of displacement across it. The displacements quoted above are small, typical of simple half graben or full graben structures, and they presume displacement occurred prior to eruption of Eocene volcanic rocks. If displacement occurred during or after emplacement of Eocene volcanic strata, estimates decrease.

### *Constraints provided by radiometric dates*

Field relationships reported from the Vernon-Kalamalka Lake area by Thompson and Daughtry (1994) suggested the Okanagan Fault there had little displacement on it. Biotite-feldspar-quartz schist belonging to the biotite/hornblende feldspar quartz assemblage on both east and west sides of Wood Lake, near water level, suggests the fault has minor importance there.

This hypothesis has been further tested using U-Pb dating techniques. At the south end of Wood Lake, in the valley bottom, a fine- to medium-grained granite cuts foliated biotite-feldspar-quartz schist within the Okanagan Valley fault zone – rocks that occur in both footwall and hanging wall of the fault. An undeformed pegmatite, mapped as an apophyses from the granite, also cuts the schist. Both rock types were sampled and dated. Preliminary results of 162.8 ± 8 Ma for the granite, and 161.7 ± 2.9 Ma (weighted mean of two determinations) for the pegmatite demonstrate that the schistosity at this location is Jurassic or older.

We interpret these results to mean that the schistose (flattening) fabric at Wood Lake is not associated with a crustal scale extensional shear of Eocene age; furthermore, lack of penetrative deformation within the granite and the pegmatite suggest this was not an area of penetrative shear or reheating after the Jurassic.

Carr (1990) suggested that strata belonging to the Upper Crustal Zone – Middle Jurassic rocks which preserve the Middle Jurassic compressional history of the orogen and have Mesozoic plutonic and cooling histories – cooled during the Mesozoic whereas as the Middle Crustal Zone – Proterozoic to Mesozoic amphibolite-facies rocks that were polydeformed during Mesozoic-early Tertiary compression, intruded by Late Palaeocene-Eocene leucogranite and penetratively deformed by Eocene extension – cooled during the Eocene. In other words, the graphitic schist-phyllite package mapped from Vernon to Salmon Arm should give Jurassic radiometric ages whereas the underlying feldspar- and quartz-rich assemblage of schists and gneiss should yield Eocene ages.

In the Enderby area Mathews (1981) demonstrated Early Cenozoic resetting of potassium-argon dates within higher metamorphic grade schist and gneiss – Carr's Middle Crustal Zone – but not within overlying lower grade phyllite and greenstone – Carr's Upper Crustal Zone. However, two samples from near the summit of Silver Stat Mountain (Fig. 1), one a graphitic phyllite, the other a biotite schist – both samples from the Upper Crustal Zone – give ages of 53.1 ± 1.9 Ma (K-Ar in whole rock) and 52.8 ± 1.8 Ma (K-Ar in biotite) respectively (W.H. Mathews, pers. comm., 1994). There are no nearby Tertiary plutons. A systematic analysis of radiometric dates within the region is in progress.

## LITHOSTRATIGRAPHIC CORRELATION

### *The Silver Creek/Monashee successions*

Field work in 1993 and 1994 revealed that the thick succession of biotite and/or hornblende feldspar-quartz semi-schist that outcrops on the east side of Wood and Kalamalka lakes, continues north, across Coldstream Valley to include the western flanks of Vernon Hill and Silver Star Mountain (Thompson and Daughtry, 1994). We also reported occurrences of the semi-schist on the east side of Wood Lake in the hanging wall of the Okanagan Fault. In other words, Coldstream Valley was not the locus of a terrane boundary, between Kootenay and an "unassigned" metamorphic complex and the Okanagan Fault did not necessarily coincide with a terrane boundary separating Kootenay Terrane from Quesnel Terrane.

Jones (1959) showed a belt of strata he called the Silver Creek Formation, extending from Enderby northwest to and beyond Little Shuswap Lake. It is a succession of quartz-feldspar-biotite and/or muscovite schist cut by granitoid and pegmatitic sills and dykes. Included in these schists are calcareous quartzite, siliceous marble, and micaceous marble. This succession also occurs along the southwest margin of Mara Lake in what Jones (1959) mapped as Mara and Sicamous formations.

Identical lithologies occur both north and south of the Shuswap River, on the northern flank of the Silver Star Range and the southern flank of the Hunters Range, and along the western flank of the Hunters Range at least as far as Mara Lake (Fig. 1). As with the Silver Creek Formation, these rocks are quartz and feldspar rich, they contain calcareous quartzite and marble marker units; pegmatite and/or granitoid dykes and sills are ubiquitous.

To date, none of the strata containing graphitic schist and phyllite has been observed cut by pegmatite or coarse-grained felsic dykes and sills. Those strata cut by these intrusions are the quartz- and feldspar-rich schist and gneiss successions – Monashee Group and Silver Creek Formation. It appears that bulk composition of the host is an important influence on presence or absence of pegmatite.

In our discussion of the succession at Grindrod, above, we pointed out that the Tsalkom greenstone succession has been mapped on either side of the Okanagan Valley overlying the Silver Creek/Monashee successions. We contend that the Silver Creek Formation is, in fact, a westward extension of

Jones' (1959) Monashee Group thereby taking the northern Okanagan valley "out of play" as a major tectonic or terrane boundary.

### *The Tsalkom, Mara, and Sicamous formations*

Good exposures of Tsalkom (chloritic greenstone), Mara (chlorite-sericite schist and phyllite), and Sicamous formations (recrystallized limestone) occur northwest of Grindrod (Fig. 1). We do not agree with the distribution as portrayed by Jones (1959) on his map. From our observations we interpret the Tsalkom, Mara, and Sicamous to form a south-dipping homocline; we found no evidence to support existence of an east-west trending anticline whose northern limb brings these units down to the shoreline of Mara Lake.

In this region, between Grindrod and the Larch Hills (Fig. 1) 12 km farther north, Jones (1959) mapped three separate and partially fault-bound occurrences of limestone; two he mapped as Sicamous (Archean or later) and the third he mapped as an unnamed unit within the Cache Creek Group (late Palaeozoic). Our data suggest the three occurrences are essentially continuous. The "Palaeozoic" limestone is identical, lithologically, with the Sicamous limestone which caps the Larch Hills; evidence for a fault contact separating different limestones is lacking. We suspect Jones' (1959) interpretation was strongly influenced by the collection of crinoid debris found near Canoe Creek. Having placed Tsalkom, Mara, and Sicamous formations with the Archean and later Monashee Group, he had to explain the presence of Paleozoic limestone typical of his "unit 15" mapped to the south and west hence the fault bound block of "Permian" limestone adjacent to Sicamous limestone at Canoe Creek. Since that time speculation on the age of the Sicamous Formations has ranged from Cambro-Ordovician to Triassic (e.g., Okulitch, 1975, 1979, 1989; Okulitch and Cameron, 1976), but no one, to our knowledge, has speculated a Permian age for the Sicamous Formation. We think this is a possibility for the following reason.

The Tsalkom, Mara, and Sicamous formations may occur at Keefer Gulch, 10 km east of Vernon on the south flank of Vernon Hill. Here a chloritized succession of massive brecciated greenstone containing some epidote, is overlain by a conglomerate consisting of angular cobbles and pebbles of pale green chlorite-sericite schist; this is overlain, in turn, by Permian limestone (Jones' unit 15). Previously, Thompson and Daughtry (1994) suggested the volcanic rocks might be a dip slope of Eocene breccia, however the presence of chlorite and epidote argues against an Eocene age for these volcanic rocks. The lithostratigraphic sequence at Keefer Gulch is the same as at Grindrod and at Keefer Gulch we know the limestone is Permian. Though tenuous, we're suggesting that the Tsalkom, Mara, Sicamous succession extends as far south as Vernon. Additional fossil control is essential. Okulitch (1975) made brief reference to Sicamous Formation occurring east of Vernon: "...the Nicola Group and the Sicamous Formation unconformably overlie limestone of the Cache Creek Group." (p. 27). He was referring to Triassic limestone that outcrops east of the town of Lumby (Okulitch and Cameron, 1976); this is not the correlation we infer for the Sicamous.

A lithostratigraphic correlation we do not support is the tie, shown by Jones (1959), between rocks west of Armstrong and the Tsalkom Formation farther north. The succession west of Armstrong – marble couplet, biotite-hornblende schist, quartzite with stretched pebble conglomerate – described in a previous section, is not typical of Tsalkom greenstone.

One of the working hypotheses to be tested in future is correlation of chlorite and sericite schist belonging to the Mara Formation with chlorite and sericite schist belonging to the Eagle Bay Formation; establishing this stratigraphic link would have profound implications with respect to regional correlation of map units.

### *Distribution of strata of Triassic age*

Conodonts of Late Triassic age have been recovered from calcareous argillite, and argillaceous limestone within the succession of graphitic rocks that cover much of Vernon Hill and the eastern flank of Silver Star Mountain (Fig. 1; M.J. Orchard, pers. comm., 1995). These data support the interpretation by Okulitch (1979) that most of the black phyllite, siliceous argillite, calcareous argillite, and argillaceous limestone that dominate this succession is Late Triassic.

## FUNDAMENTAL TECTONOSTRATIGRAPHIC BUILDING BLOCKS

Stratigraphy described above can be divided into three fundamental lithostratigraphic assemblages (Fig. 1). At the base is the quartz- and feldspar-rich schist and gneiss assemblage belonging to the Monashee Group and Silver Creek Formation – what Carr (1990) called the Middle Crustal Zone. It is overlain by a more diverse assemblage including unnamed marble, mafic schist, and quartzite (near the town of Armstrong); greenstone, phyllite, and limestone belonging to the Tsalkom, Mara, and Sicamous formations respectively; and graphitic rocks including siliceous argillite, phyllite, schist and carbonaceous limestone (on Vernon Hill and much of Silver Star Mountain). The third assemblage, which overlaps the other two with profound erosional unconformably, is the Eocene and younger volcanic and volcano-sedimentary assemblage (Jones, 1959; Okulitch, 1979; Thompson and Daughtry, 1994).

The two most pervasive and obvious distinguishing characteristics between the quartz- and feldspar-rich assemblage and the succeeding assemblage is bulk composition, and the presence of pegmatite and granitoid sills and dykes in the former but not the latter. Other distinguishing characteristics include a marked upward decrease in metamorphic grade at the assemblage boundary accompanied by a decrease in

overall grain size (crystallinity), and a less penetrative style of deformation. This distinction is similar to that on the east margin of the Shuswap Metamorphic Complex where the same change in bulk composition and metamorphic grade occurs between Eocambrian and older strata, and Paleozoic strata belonging to the overlying Lardeau Group.

In recent analyses (e.g., Monger et al., 1991), the lithostratigraphy has been subdivided into two separate terranes – Kootenay and Quesnel – but not using the lithological criteria described above. Kootenay is said to contain the quartz- and feldspar-rich succession together with the Tsalkom, Mara, Sicamous, and Eagle Bay formations; the latter are tentatively correlated with strata making up the Lardeau Group farther east. Quesnel Terrane is said to contain the remaining pre-Eocene strata including the Permian limestone succession near Vernon which is placed in the Harper Ranch subterrane of Quesnel Terrane.

We've suggested that Tsalkom, Mara, and Sicamous formations may occur east of Vernon, at Keefer Gulch; this implies that remnants of younger strata within Kootenay Terrane extend farther south and east than previously thought. At the same time it removes the need for Harper Ranch subterrane in the Vernon area. In this interpretation Quesnel Terrane rocks are restricted to the Triassic carbonaceous succession.

The unnamed marble, mafic schist, quartzite succession found near Armstrong is higher metamorphic grade and more penetratively deformed than is the Tsalkom, Mara, Sicamous succession; on this basis we think it stratigraphically older. So, tentatively, it becomes part of Kootenay Terrane.

Interpretations of deep seismic reflection profiles that cross the Vernon map area (Cook et al., 1993 and references therein) suggest North American-like basement extends westward beneath Quesnel Terrane. This interpretation requires a crustal scale thrust fault separating Kootenay from overlying Quesnel Terrane.

Quesnel Terrane is most closely associated with the Nicola Group, an extensive belt of Upper Triassic-Lower Jurassic potassic igneous rocks (Mortimer, 1986, 1987). Nicola Group volcanism has been interpreted as a consequence of amalgamation of the Intermontane Superterrane when subduction of the Cache Creek basin brought component terranes together (e.g., Souther, 1991; Monger et al., 1991 and references therein). Nicola Group volcanic rocks are rare in the Vernon area; the Upper Triassic carbonaceous phyllite, schist, siliceous argillite, and carbonaceous limestone succession is interpreted as a back-arc, distal sedimentary facies of Nicola volcanic rocks (e.g., Monger et al., 1991).

However, it is not clear to us that the graphitic succession is allochthonous with respect to older (underlying) strata and there is no obvious tectonic boundary (thrust fault?) at the base of the graphitic succession.

For example, on Silver Star Mountain one can observe graphitic schist and phyllite overlying granitoid sills and biotite-quartz-feldspar schist. The contact is sharp, has relief in the order of centimetres, and looks depositional. On Fortune Creek (due east of the town of Armstrong), the transition from pegmatite-rich schist to phyllite is more gradual, occupying a stratigraphic interval of 200 to 300 m in which a variety of lithologies including muscovite schist without pegmatite, micaceous quartzite, and mica schist with minor quartz and feldspar are present. Again, the transition looks stratigraphic rather than tectonic.

Northward along the ridge from Silver Star Mountain toward Shuswap River, there is a reversal in metamorphic grade. Phyllite and siliceous argillite at the head of Alderson Creek pass northward into micaceous schist with staurolite and eventually to biotite-quartz-feldspar schist with abundant pegmatite belonging to the Monashee Group. If there is a terrane boundary at any of these localities, we have not observed it.

## CONCLUSIONS

The northern Okanagan Valley, from Vernon to Mara Lake, has been interpreted as the topographic expression of a crustal scale extension fault with 40 km or more of west-side-down extension across it (e.g., Carr, 1990). Our mapping shows corresponding stratigraphic units having the same metamorphic grade and style of deformation on either flank of the valley. This suggests the valley is the geomorphic expression of a simple half graben and or graben. Jurassic ages from an undeformed pluton and pegmatite that crosscut the regional foliation within schist and gneiss in the Okanagan Fault zone south of Wood Lake support our revised interpretation.

We suggest that the Sicamous Formation crystalline limestone may be Permian; that portions of the Mara Formation bear strong lithological resemblance to part of the Eagle Bay Formation; and that the Tsalkom, Mara, and Sicamous formations may outcrop east of Vernon at Keefer Gulch.

Evidence for a crustal scale thrust fault separating rocks ascribed to Quesnel Terrane from those ascribed to Kootenay Terrane has yet to be observed. If Permian crystalline limestone in the Vernon area belongs to the Sicamous Formation, then Harper Ranch subterrane would not exist in the Vernon area.

## REFERENCES

**Carr, S.D.**
1990: Late Cretaceous-Early Tertiary tectonic evolution of the southern Omineca Belt, Canadian Cordillera; Ph.D. thesis, Carleton University, Ottawa, Ontario, 223 p.

**Cook, F.S., Varsek, J.L., Clowes, R.M., Kanasewich, E.R., Spencer, C.S., Parrish, R.R., Brown, R.L., Carr, S.D., Johnson, B.J., and Price, R.A.**
1993: Lithoprobe crustal reflection cross-section of the southern Canadian Cordillera, 1, Foreland thrust and fold belt to Fraser River fault; Tectonics, v. 11, p. 12-35.

**Johnson, B.J.**
1989: Geology of the west margin of the Shuswap Terrane near Sicamous implications for Tertiary extension tectonics; in Geological Fieldwork 1988; British Columbia Ministry of Energy, Mines and Petroleum Resources, Paper 1989-1, p. 49-54.

**Jones, A.G.**
1959: Vernon map-area, British Columbia; Geological Survey of Canada, Memoir 296, 186 p.

**Mathews, W.H.**
1981: Early Cenozoic resetting of potassium-argon dates and geothermal history of north Okanagan area, British Columbia; Canadian Journal of Earth Science, v. 18, p. 1310-1319.

**Monger, J.W.H., Wheeler, J.O., Tipper, H.W., Gabrielse, H., Harms, T., Struik, L.C., Campbell, R.B., Dodds, C.J., Gehrels, G.E., and O'Brien, J.**
1991: Part B. Cordilleran terranes; in Upper Devonian to Middle Jurassic assemblages, Chapter 8 of Geology of the Cordilleran Orogen in Canada, (ed.) H. Gabrielse and C.J. Yorath; Geological Survey of Canada, Geology of Canada, no. 4, p. 281-327 (also Geological Society of America, The Geology of North America, v. G-2).

**Mortimer, N.**
1986: Late Triassic, arc-related, potassic igneous rocks in the North American Cordillera; Geology, v. 14, p. 1035-1038.
1987: The Nicola Group: Late Triassic and Early Jurassic subduction-related volcanism in British Columbia; Canadian Journal of Earth Sciences, v. 24, p. 2521-2536.

**Nielsen, K.C.**
1982: Structural and metamorphic relationships between the Mount Ida and Monashee Groups at Mara Lake, British Columbia; Canadian Journal of Earth Sciences, v. 19, p. 288-307.

**Okulitch, A.V.**
1975: Stratigraphy and structure of the Mount Ida Group, Vernon (82L), Seymour Arm (82M), Bonaparte Lake (92P) and Kettle River (82E) map-areas, British Columbia; in Report of Activities, Part A; Geological Survey of Canada, Paper 74-1A, p. 25-30.

**Okulitch, A.V.** (cont.)
1979: Lithology, stratigraphy, structure and mineral occurrences of the Thompson-Shuswap-Okanagan area, British Columbia; Geological Survey of Canada, Open File 637.
1989: Revised stratigraphy and structure in the Thompson-Shuswap-Okanagan map area, southern British Columbia; in Current Research, Part E; Geological Survey of Canada, Paper 89-1E, p. 51-60.

**Okulitch, A.V. and Cameron, B.E.B.**
1976: Stratigraphic revisions of the Nicola, Cache Creek, and Mount Ida groups, based on conodont collections for the western margin of the Shuswap Metamorphic Complex, south-central British Columbia; Canadian Journal of Earth Sciences, v. 13, p. 44-53.

**Souther, J.G.**
1991: Volcanic regimes; in Geology of the Cordilleran Orogen in Canada, (ed.) H. Gabrielse and C.J. Yorath; Geological Survey of Canada, Geology of Canada, No. 4, p. 459-490 (also Geological Society of America, The Geology of North America, Volume G-2).

**Thompson, R.I. and Daughtry, K.L.**
1994: A new regional mapping project in Vernon map area, British Columbia; in Current Research 1994-A; Geological Survey of Canada, p. 117-122.

Geological Survey of Canada Project 930036

# Neotectonic stress orientation indicators in southwestern British Columbia

J.S. Bell and G.H. Eisbacher[1]
GSC Calgary, Calgary

*Bell, J.S. and Eisbacher, G.H., 1996: Neotectonic stress orientation indicators in southwestern British Columbia; in Current Research 1996-A; Geological Survey of Canada, p. 143-154.*

**Abstract:** Possible indicators for in situ rock stress orientation were identified and analyzed in roadcuts and on glacier forefields in southwestern British Columbia as part of the Geological Survey of Canada's Cordilleran Neotectonic Map Project. A particular effort was made to obtain readings from plutonic and high-grade metamorphic rocks of the Southern Coast Belt and the Omineca Belt. At all sites, great care had to be taken in order to avoid measuring features that could have been influenced by rock fabric, pre-Pleistocene structures, or local topography. Data were gathered from offset preshear boreholes, axial fractures propagated from preshear boreholes, and stress-controlled breakage fractures in artificial roadcuts, and from neotectonic faults, hairline fractures, and glacial neotectonic plucking fractures on glacier forefields.

**Résumé :** Dans le cadre du Projet de cartographie néotectonique de la Cordillère entrepris par la Commission géologique du Canada, on a relevé et analysé des indicateurs possibles d'orientation des contraintes in situ associées à des roches de tranchées routières et d'avant-zones glaciaires de la partie sud-ouest de la Colombie-Britannique. On a mis l'accent sur les roches plutoniques et fortement métamorphisées du sud de la chaîne Côtière et du domaine d'Omenica. À tous les sites, on a pris soin d'éviter de mesurer les éléments qui auraient pu être influés par la fabrique pétrologique, les structures antérieurs au Pléistocène ou la topographie locale. Dans les tranchées routières artificielles, les données recueillies proviennent de trous de sondage décalés antérieurs au cisaillement, de fractures axiales propagées à partir de trous de sondage antérieurs au cisaillement et de fractures de rupture contrôlés par des contraintes. Dans les avant-zones glaciaires, elles proviennent aussi de failles néotectoniques, de fractures infimes et de fractures d'arrachement glaciaire néotectoniques.

[1] Geologisches Institut, Universität Karlsruhe, Kaiserstrasse 12, D-7500 Karlsruhe, Germany

## METHODS

Fieldwork focused on identifying stress relief features in natural or artificial outcrops from which loads were recently removed, with the ultimate aim of obtaining indicators for contemporary principal stress orientations. Because the main mechanism of stress release at or very near the Earth's surface is the natural or induced propagation of extension fractures, we carefully selected potential outcrops which had not been previously fractured and thus destressed prior to the formation of the youngest fractures. Also, the fabric of the rock needed to be sufficiently homogenous and isotropic so that the identified stress relief fractures were unambiguous and directionally diagnostic. In this respect, massive unfractured rocks with a relatively isotropic granular fabric were found to be the most suitable. Our efforts were concentrated on two types of geological settings: artificial roadcuts and recently exposed glacier forefields. The roadcuts from which we obtained relevant data are in massive crystalline rock that has been excavated by controlled blasting in presheared boreholes. Ideally, such roadcuts are located in low relief areas a reasonable distance from any steep slopes that could generate topographically-induced lateral stresses. The glacier forefields were selected by helicopter inspection on the basis of their flatness, limited topographic relief, clean exposure of massive rocks, and distance from steep mountain slopes. These criteria had been established previously in sedimentary rocks of the southeastern Canadian Cordillera (Bell and Eisbacher, 1995).

Offset of preshear boreholes can be diagnostic of stress release if the displacement is updip along an inclined surface although, in detail, movement may be partly determined by pre-existing structures and may therefore not precisely reflect the azimuth of the largest principal stress. Boreholes that are offset downdip on inclined surfaces need not be diagnostic of anything other than the effect of overburden weight. Downdip displacements of boreholes therefore were ignored.

On glacier forefields, we tried to identify structural features which either formed during recent glacial unloading or developed soon after glacial retreat. Fractures which existed prior to glacial unloading cannot be used to diagnose the contemporary stress regime. In our case we had to spend several hours at each site examining the glacially striated bedrock before making any measurements, since the most recent fractures and related stress relief features were not always obvious at first glance.

## LOCATION DESCRIPTIONS

### *1. Roadcut on Highway 99, 24 km south-southwest of Whistler Village, B.C. (latitude 49.870°N, longitude 123.159°W)*

This roadcut is in granodiorite of the Late Jurassic Cloudburst Pluton of the Coast Plutonic Complex and is locally intruded by diabase dykes (Monger and Journeay, 1994). It is located along the west side of Highway 99, some 500 m south of the bridge crossing Culliton Creek (Fig. 1). The roadcut is approximately vertical, its mean strike ranges from 166° to 204° and single rock faces range from 3 to 6 m in height. They are excavated in the central part of a low relief bench (Fig. 1), approximately 400 m from the steep slopes of Brohm Ridge to the southeast. Thus there is no significant load above or beside them. The granodiorite is massive and cut by widely spaced, subhorizontal exfoliation fractures. It exhibits an

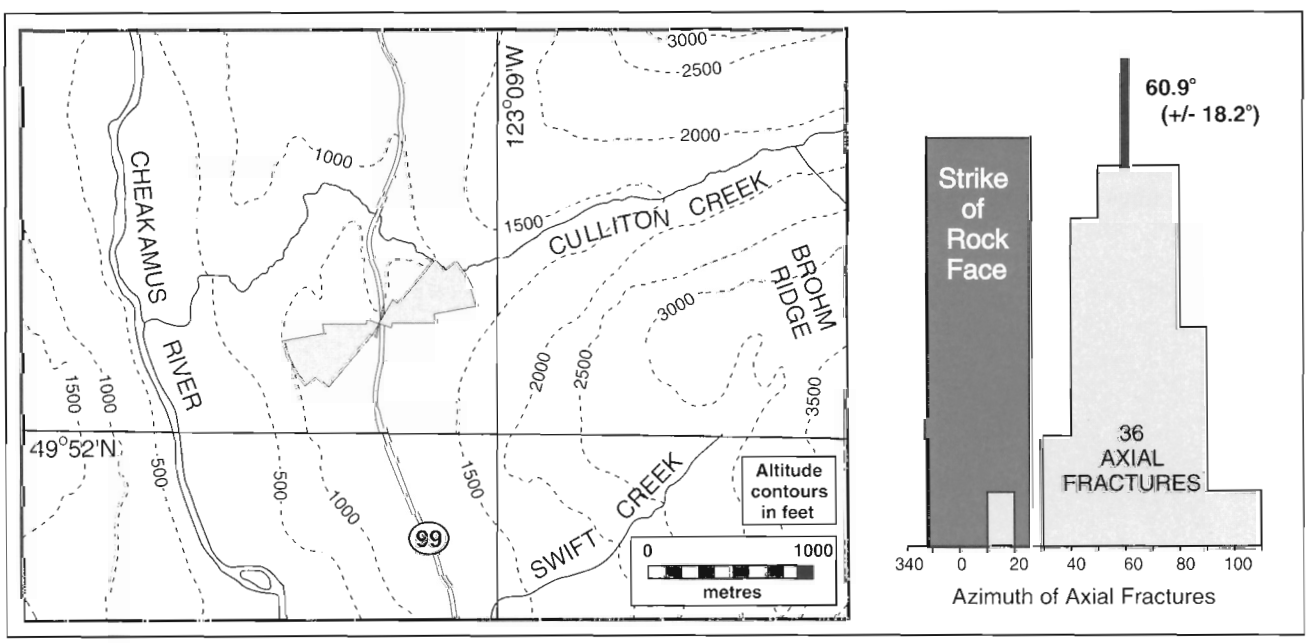


***Figure 1.*** *Map showing the location of the roadcut at Location 1 on Highway 99, south of Culliton Creek, British Columbia.*

isotropic fabric. Locally, vertical and inclined fractures of presumed pre-Pleistocene age are present, but these are not abundant.

The roadcut was excavated by dynamite charges set at the bottom of vertical holes drilled into the rock mass. The rear halves of these preshear boreholes thus remain on the rock faces. Five of these borehole halves are offset outward, toward the highway (Fig. 2). The displacment is in an updip direction on two west-dipping surfaces 40 to 50 cm apart and the displaced block is laterally confined by two strongly mineralized fracture surfaces (Fig. 2). It appears that these pre-existing high-angle fractures, in combination with the basal slip surfaces, controlled the subhorizontal displacement recorded by the offset boreholes. We interpret the updip slip as an extensional stress relief event within the granodiorite outcrop. However, the slip vector need not be precisely diagnostic of the regional $S_{Hmax}$, because the displacment probably also was guided by the pre-existing high-angle planes of weakness.

Many of the borehole walls contain fractures with rough low-relief surfaces that extend into the rock face but generally follow the axis of the hole. They are here described as axial fractures. Typically, axial fractures occur within the lowermost 2 m of the roadcuts and are observed only rarely near the tops of the excavated rock faces. Many axial fractures are discontinuous and anastomosing (Fig. 3a); some are associated with distinct clusters of downward-facing horsetail cracks (Fig 3b) that extend into the surrounding rockmass. The fresh nature of the axial fracture surfaces and their parallelism with the boreholes indicates that they are genetically related to the boreholes and most probably coeval with them. We interpret them as extension fractures that formed when the dynamite charges in the boreholes were fired. As such they would have propagated parallel to $S_{Hmax}$ in the plane of the two largest principal stresses, as indicated in Figure 4.

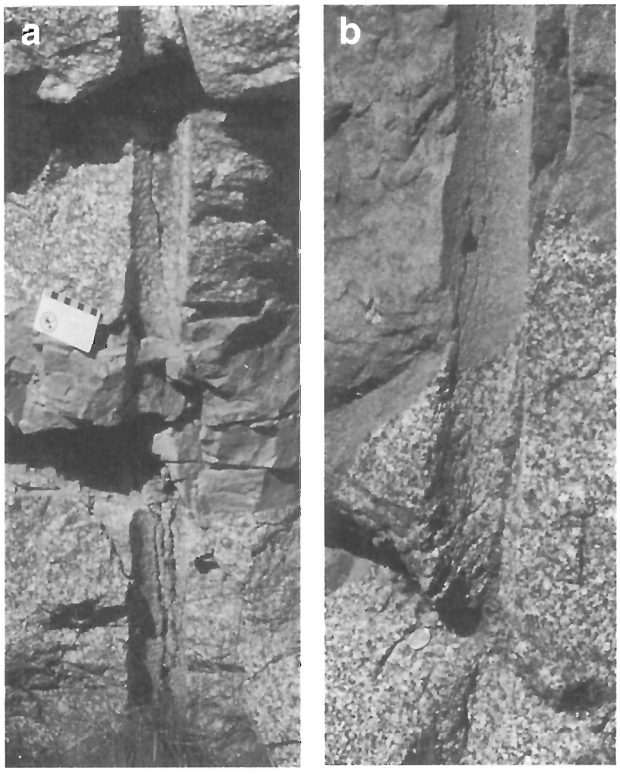


***Figure 3.*** *a) Axial fractures in a preshear borehole at Location 1.* ***b***) *Downward-facing horesetail cracks associated with an axial fracture at Location 1.*

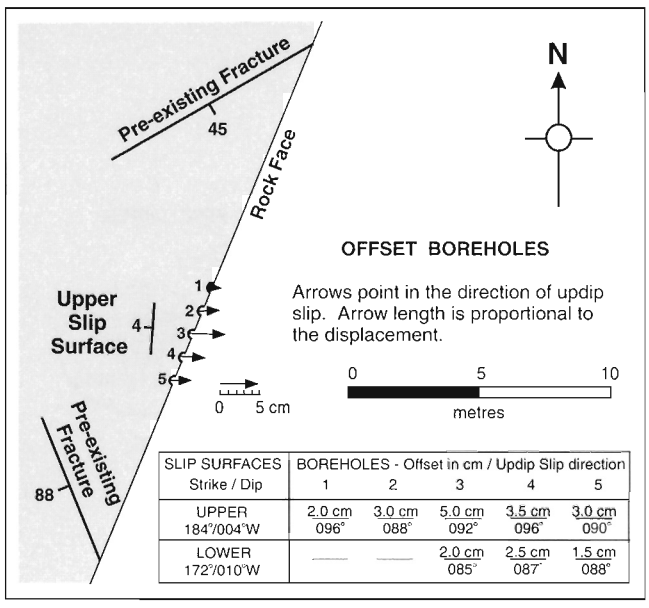


***Figure 2.*** *Offset boreholes at Location 1 in the roadcut on Highway 99, south of Culliton Creek. Note that the updip slip direction is probably controlled by pre-existing fractures at either end of the stress-relieved rock mass.*

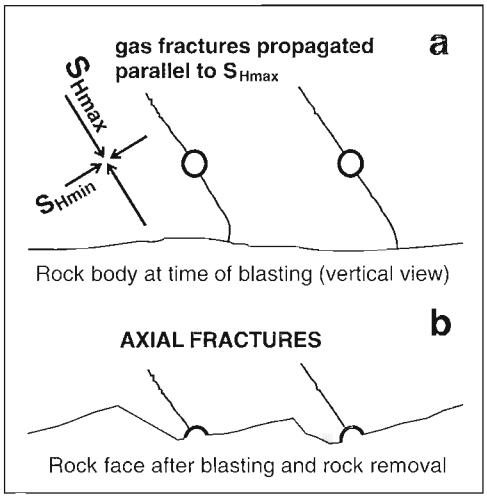


***Figure 4.*** *Schematic diagram showing the proposed origin of axial fractures in the wall of vertical boreholes during blasting. They are thought to originate as gas pressure-induced fractures.*

In the roadcut, the axial fractures measured exhibit a well-clustered mean strike orientation of 60.6° (±18.2°), and therefore are oblique to the mean strike of the outcrop surface (Fig. 1). Thus any free surface that might have existed prior to excavation did not influence the propagation direction of the axial fractures, nor is this mean orientation related to any nearby slope (Fig. 1). We interpret the axial fractures as paralleling the ambient $S_{Hmax}$ orientation for this location.

Locally, the rock faces broke away on two sets of ribbed surfaces that were approximately perpendicular to each other. We describe these ribbed fracture sets as breakage fractures (Fig. 5). One of the ribbed surfaces approximately parallels the axial fracture set, so that we suspect the breakage fractures to be in situ stress-related features.

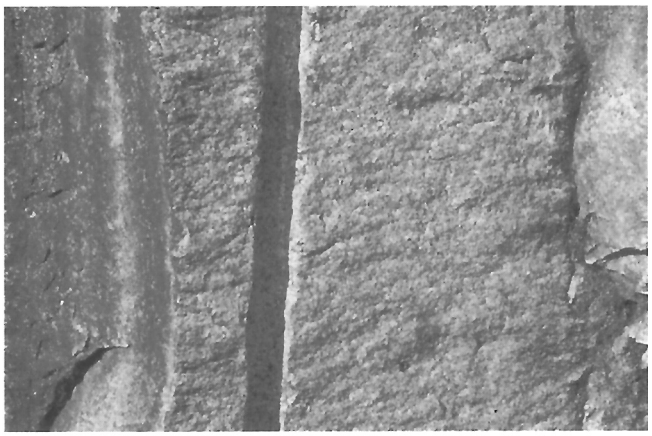

***Figure 5.*** *Horizontally-ribbed breakage fractures in granodiorite at Cheam View at Location 2.*

## *2. Roadcuts at Herrling Island Exit on the Trans-Canada Highway, Route 1, 20 km southwest of Hope, B.C. (latitude 49.256°N, longitude 121.677°W)*

Miocene granodiorite of the Mount Barr Pluton (Monger and Journeay, 1994) is exposed in a composite outcrop beside feeder roads onto the two main lanes of the Trans-Canada Highway near Cheam View (Fig. 6). The roadcuts contain preshear boreholes with axial fractures oriented at 11.7° (±18.0°). The newly created rock faces have a jagged aspect because they have opened along two series of breakage fractures characterized by subhorizontal ribs (Fig. 5). As Figure 6 indicates, one set of breakage fractures parallels the axial fractures and shows a mean orientation of 11.7° (±12.5°), whereas the complementary set is aligned almost at right angles 116.2° (±18.5°). We interpret the axial fractures as diagnostic of $S_{Hmax}$, and assume that the breakage fractures are also controlled by in situ horizontal principal stresses that act on the rockmass.

Additional information on stress orientation is provided by five neotectonic microfaults which offset glacially-striated subhorizontal surfaces of the granodiorite (Fig. 7). Figure 8 demonstrates that fault orientations and offsets are compatible with a stress regime in which $S_{Hmax}$ is oriented at approximately 012°, as suggested by both axial and breakage fractures in the adjacent artificial roadcuts.

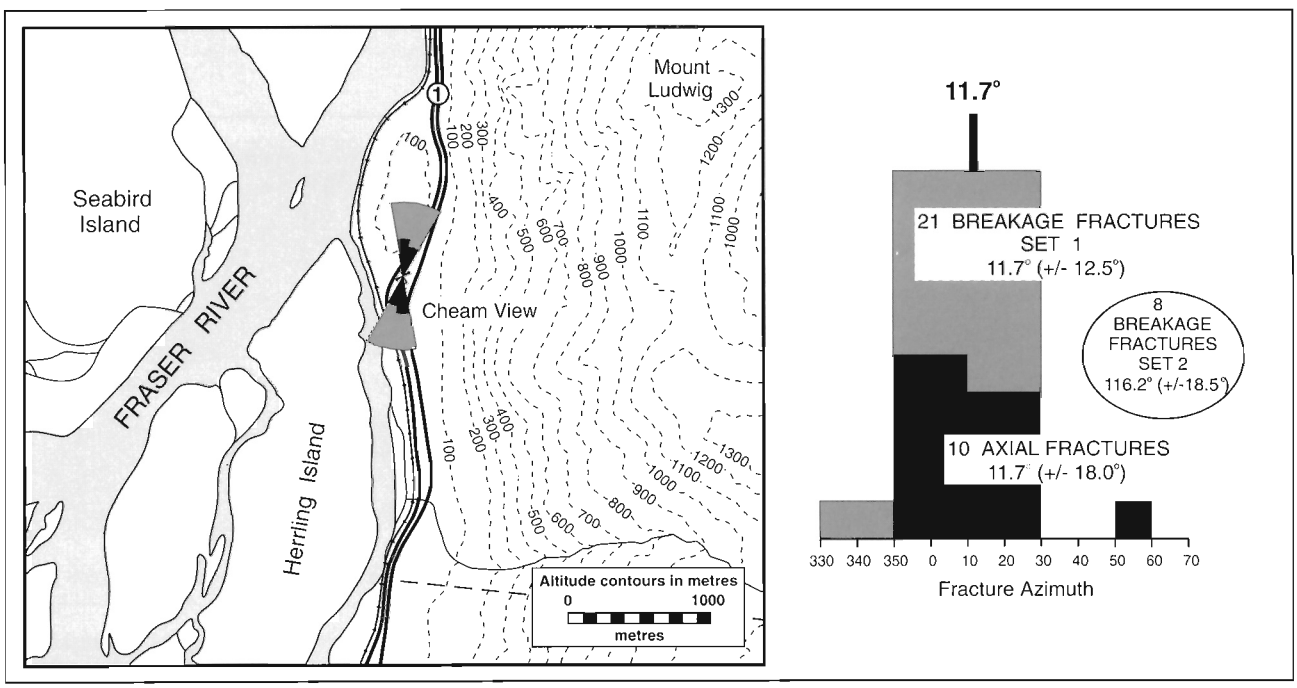


***Figure 6.*** *Stress orientation indicators at Cheam View (Location 2) on the Trans-Canada Highway.*

It is tempting to interpret these observations as evidence for regional north-northeast orientation of $S_{Hmax}$ at Cheam View. Similar orientations have been inferred from focal mechanisms of earthquakes in Washington State to the south (Ma, 1988; Johnson, 1989). However, the roadcuts are located at the base of a steep mountain slope that strikes north, approximately parallel to the inferred axis of $S_{Hmax}$ (Fig. 6). Thus topography could contribute to a reorientation of the regional stress trajectories. In fact, the regional orientation of $S_{Hmax}$ may well be north-northeast to north, and compatible with crustal earthquake displacements. However, the steep slopes at Cheam View suggest that our observations need to be interpreted with care.

***Figure 7.*** *Neotectonic fault at Cheam View (Location 2).*

The evidence that $S_{Hmax}$ is oriented north-northeast to north at Cheam View and that fractures are opening along this axis is of engineering significance. Evans and Savigny (1994) summarize the mountain slope deformation at Wahleach, immediately south of Location 2, where downslope rock slab movement occurs. However, Moore et al. (1992) believe that a large rock slide is, as yet, not imminent.

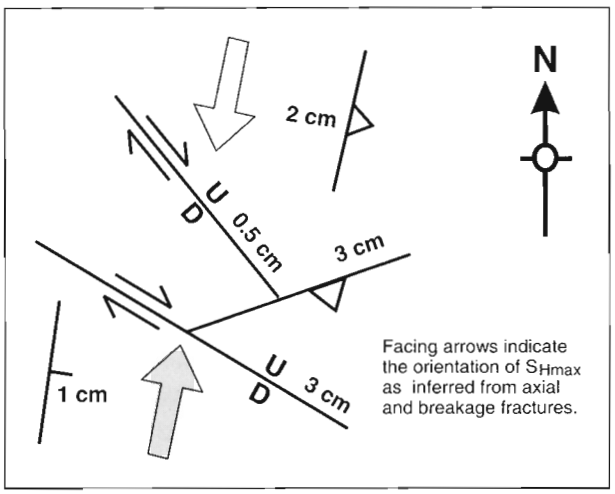


***Figure 8.*** *Orientation of, and offsets along, postglacial faults at Cheam View. Note that the movements observed are compatible with a stress regime where $S_{Hmax}$ is oriented north to north-northeastward as could be inferred from the axial and breakage fractures at the site.*

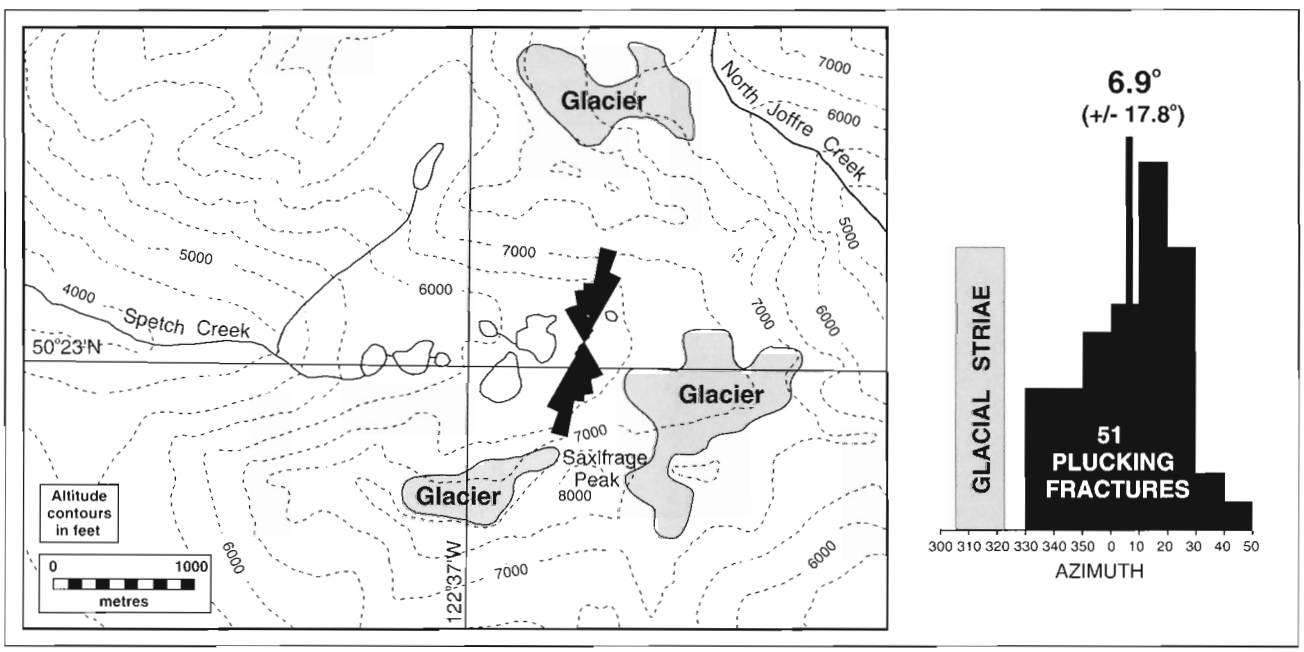


***Figure 9.*** *Plucking fracture orientations from a glacier forefield underlain by quartz diorite of the Spetch Creek Pluton, 16 km northeast of Pemberton, B.C. (Location 3).*

### *3. Glacier forefield south of Saxifrage Peak, Place Glaciers, Cayoosh Ranges, B.C. (latitude 50.385°N, longitude 122.606°W)*

Observations were made on a west-facing low-relief glacier forefield underlain by quartz diorite of the Spetch Creek Pluton (Fig. 9), which is dated as mid-Cretaceous by Friedman and Armstrong (1990). The central part of the forefield has yielded numerous well developed glacial plucking fractures (Bell and Eisbacher, 1995), which exhibit a mean azimuth of 006.3° (±17.8°), oblique to northwest-trending glacial striae (Fig. 9, 10). Two intersecting neotectonic microfaults offsetting glacially striated surfaces were also encountered (Fig. 11). The east-trending fault appears to be an extension of an older fracture set that is visible in cliffs flanking the forefield. Neither fault is believed to be diagnostic of today's stress regime. However, the plucking fracture population is interpreted to define the orientation of $S_{Hmax}$, following the model proposed earlier for glacier forefields in massive sedimentary rocks by Bell and Eisbacher (1995).

### *4. Glacier forefield east of the glacier at the head of Miller Creek, 15 km northwest of Pemberton, B.C. (latitude 50.387°N, longitude 123.003°W)*

This forefield (Fig. 12) is underlain by granodiorite of mid-Cretaceous age (Friedman and Armstrong, 1990), but unlike Location 3, it yielded only a few well developed plucking fractures. However, clean hairline fractures, with jagged surfaces (on a small scale) without any traces of mineralization and cutting older chlorite and quartz-filled fractures, are abundant about 200 m in front of the glacier snout. About 300 m east of the glacier snout, several neotectonic microfaults were found as well. They offset glacially striated surfaces by up to several centimetres. All the post-striae faults are aligned parallel with the hairline fracture population and have been included in the fracture histogram and rose diagram of Figure 12. Both sets of fractures are interpreted as neotectonic stress-relief features. They exhibit a mean azimuth of 10.5° (±10.1°) which we interpret as defining $S_{Hmax}$ at this site. Six plucking fractures with a mean azimuth of 17.2° (±7.6°) support this interpretation. One of the neotectonic faults, striking at 005° and dipping 8° to the west, was associated with Riedel shear fractures that implied dextral movement, which also favours an $S_{Hmax}$ azimuth east of 005°.

### *5. Glacier forefield north of the Cochina Glacier, 27 km southwest of Lytton, B.C. (latitude 50.079°N, longitude 121.867°W)*

The flat glacier forefield north and in front of the Cochina Glacier (Fig. 13), composed of granodiorite of the Scuzzy Pluton of Upper Cretaceous age (Friedman and Armstrong, 1990), was examined. The weakly foliated granodiorite is cut by northeast-striking mineralized fractures. There is also a related set of glacial plucking fractures, which was not measured. An unmetamorphosed diabase dyke was deflected by the northeast-striking fracture set, confirming that these are old structures that would not be diagnostic of today's stress regime. However, a few open, nonmineralized, northwest-oriented, hairline fractures were observed to abut against but not cut the northeast-oriented fracture set, showing that the hairline fractures were younger (Fig. 14). These northwest-trending hairline fractures are interpreted as postglacial stress relief features. Numerous plucking fractures subparallel to these hairline fractures were also observed (Fig. 13, 15); their orientations are unrelated to rock schistosity and to the old mineralized fractures. The mean azimuth of these plucking fractures is 141.1° (±12.1°), essentially parallel to the hairline fractures, and interpreted as the local orientation of $S_{Hmax}$.

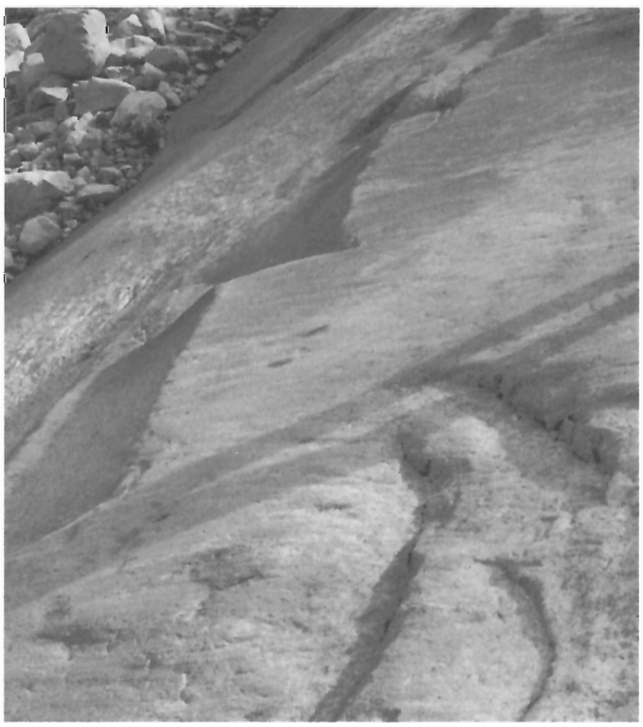

***Figure 10.*** *Neotectonic plucking fractures in quartz diorite of the Spetch Creek Pluton at Location 3.*

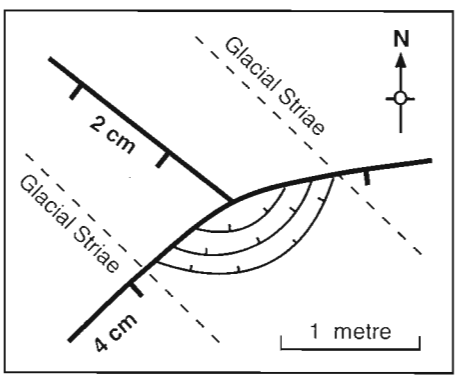


***Figure 11.*** *Sketch of neotectonic faults that offset glacial striae in the quartz diorite surface of Spetch Creek Pluton at Location 3.*

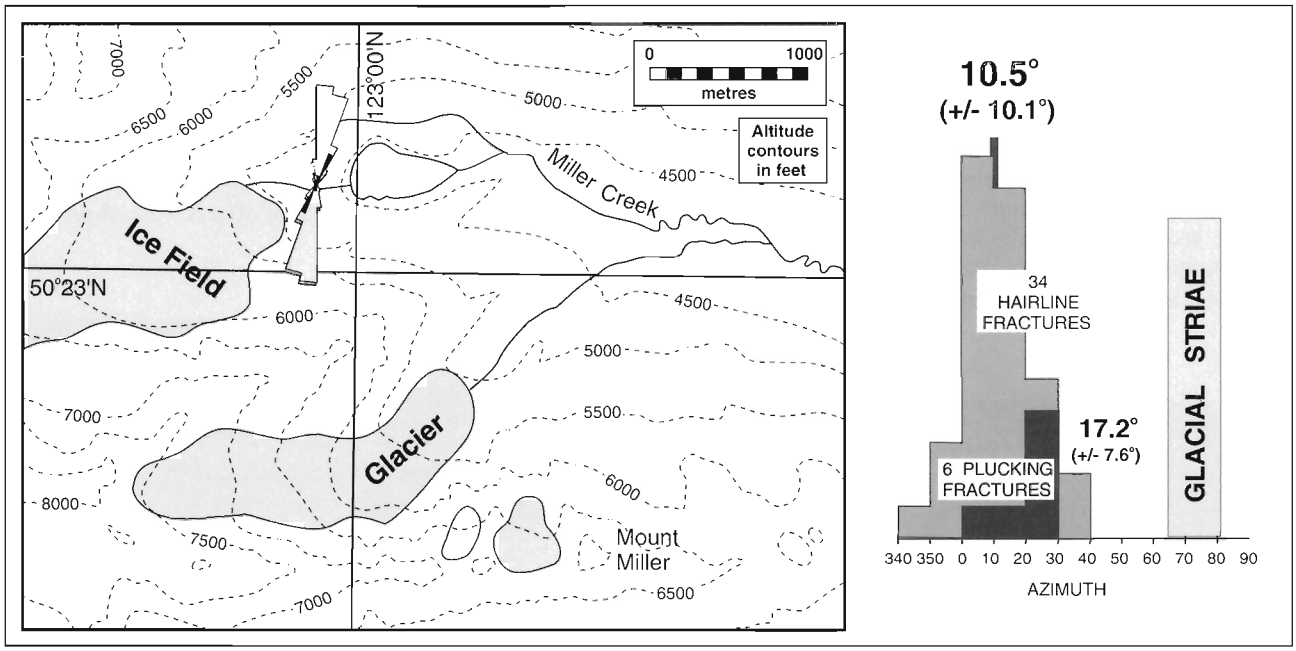


***Figure 12.*** *Hairline fractures and plucking fractures measured in granodiorite of the forefield east of the glacier terminus at the head of Miller Creek, 15 km northwest of Pemberton, B.C. (Location 4).*

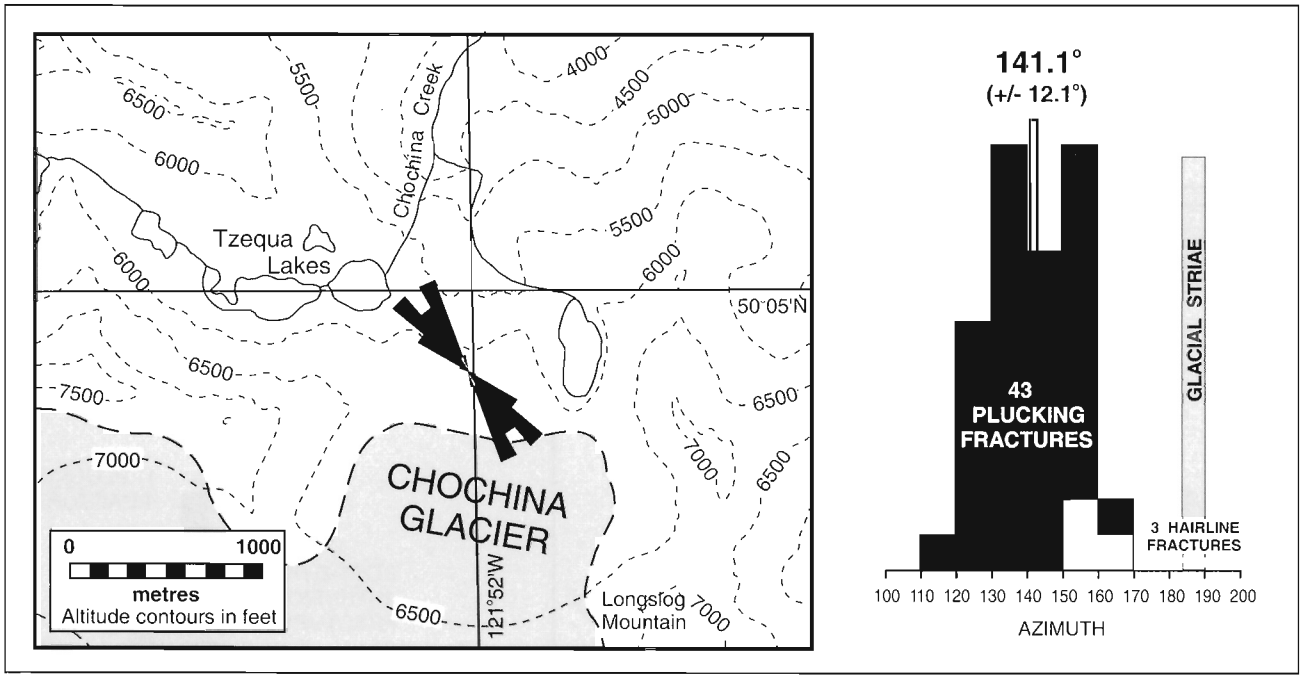


***Figure 13.*** *Map of the glacier forefield north of Cochina Glacier, 27 km southwest of Lytton, with a histogram and rose diagram indicating the orientation of plucking fractures.*

### *6. Glacier forefield north of Armstrong Peak icefield, 25 km south of Revelstoke, B.C. (latitude 50.774°N, longitude 118.222°W)*

On this broadly concave forefield, mica-garnet-sillimanite schist and gneiss of the Monashee Group (Jones, 1959), locally intruded by mafic dykes, outcrop north of the icefields of Armstrong Peak (Fig. 16). Several square kilometres of bedrock exposures were examined carefully for stress-relief features, but few were found. Unmineralized open hairline fractures are present locally in a variety of orientations (Fig. 16), but the most prominent population (azimuth: 3.0° ± 9.4°) is subparallel to a preglacial mineralized fracture set and also to a mafic dyke of presumed Tertiary age. Therefore, the hairline fractures were not used to infer present $S_{Hmax}$ orientation. Plucking fractures are present on glacially striated surfaces. However, they are not abundant and show no preferred orientation (Fig. 16). The most recent features observed are clean hairline fractures that cut both a mafic dyke and the intruded metamorphic country rock (Fig. 17). These fractures exhibit a mean orientation of 92.0° (±12.5°), and might be stress relief features related to the present stress field. No postglacial neotectonic fault offsets were observed.

***Figure 14.*** *A hairline fracture (strike 155°, dip 76°NE) abuts against, but does not cut, a mineralized fracture striking at 45° in granodiorite of the Cochina Glacier forefield at Location 5. The fracture with a 155° azimuth is inferred to be the younger of the two structures.*

***Figure 15.*** *Neotectonic plucking fracture in granodiorite interpreted as being parallel to $S_{Hmax}$ at Location 5. The bergstock poles are parallel to glacial striae.*

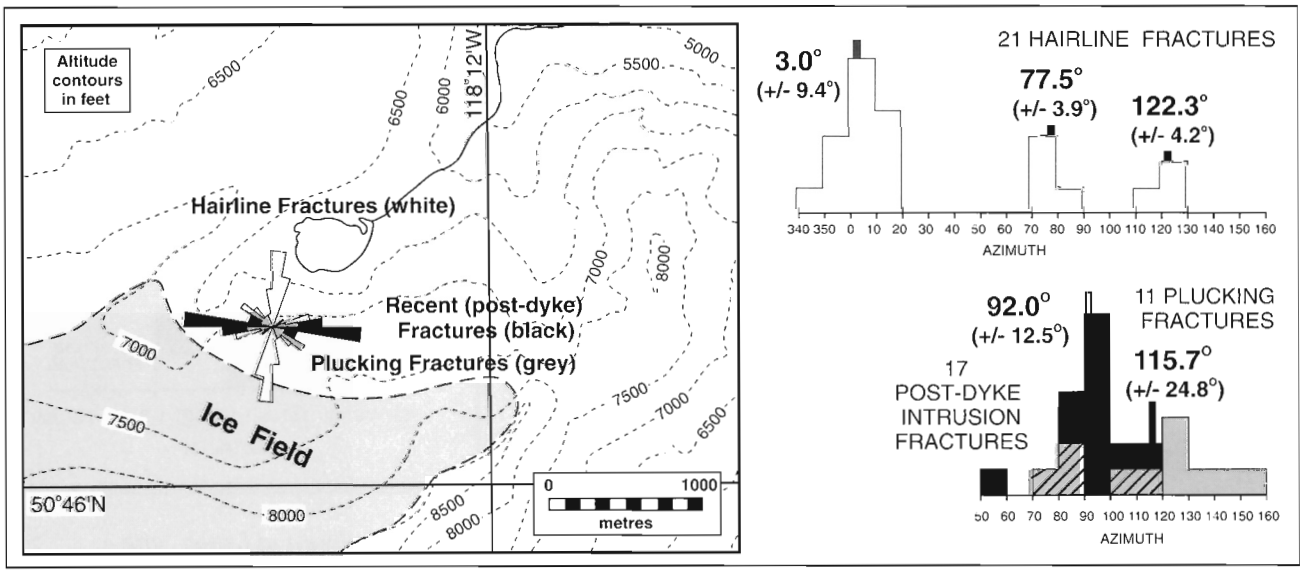


***Figure 16.*** *Map of the glacier forefield north of Armstrong Peak, 25 km south of Revelstoke (Location 6). Histograms and rose diagram of the site measurements are described in the text.*

Large scale exfoliation and surface-parallel splitting occurs in most of the rocks within the highly contorted layered metamorphics of this locality. It is possible that these planes have accommodated almost complete surficial destressing that no hairline fractures, neotectonic faults, or plucking fractures could develop. On the other hand, the ice load may not have been great, its removal may have been too recent, or possibly these high grade metamorphic rocks were too heterogeneous for a surfical stress-relief anisotropy to develop within them.

***Figure 17.*** *Hairline fracture cutting a Tertiary dyke intruded into gneisses of the Monashee Group at Location 6. Such fractures were the most recent features found at the site.*

### *7. Glacier forefield west of Bourne Glacier, 46 km northwest of Revelstoke, B.C. (latitude 51.317°N, longitude 118.633°W)*

The west-sloping forefield, consisting of high-grade gneiss and quartzite of the Shuswap Metamorphic Complex (Wheeler, 1965) was examined downslope and west of the Bourne Glacier (Fig. 18). These massive to foliated rocks are cut by two preglacial fracture sets: an older, northwest-trending set, and a younger, north- to north-northeast-trending set. Northeast-trending plucking fractures occur widely, particularly at distances of more than 200 m and distinctly downslope from the glacier terminus. Sixty-six plucking fractures were measured and yielded a mean azimuth of 58.1° (±18.5°). This is interpreted as the present local orientation of $S_{Hmax}$.

Postglacial faulting was observed locally. Glacially striated surfaces are offset by normal displacements of up to 5 cm along mineralized fractures that strike 135°, 140°, and 151° and dip to the northeast. These neotectonic faults are believed to be stress-relief features, but because the reactivated fractures are clearly preglacial (?Early Tertiary) structures, their strike is not thought to reflect the present day stress regime.

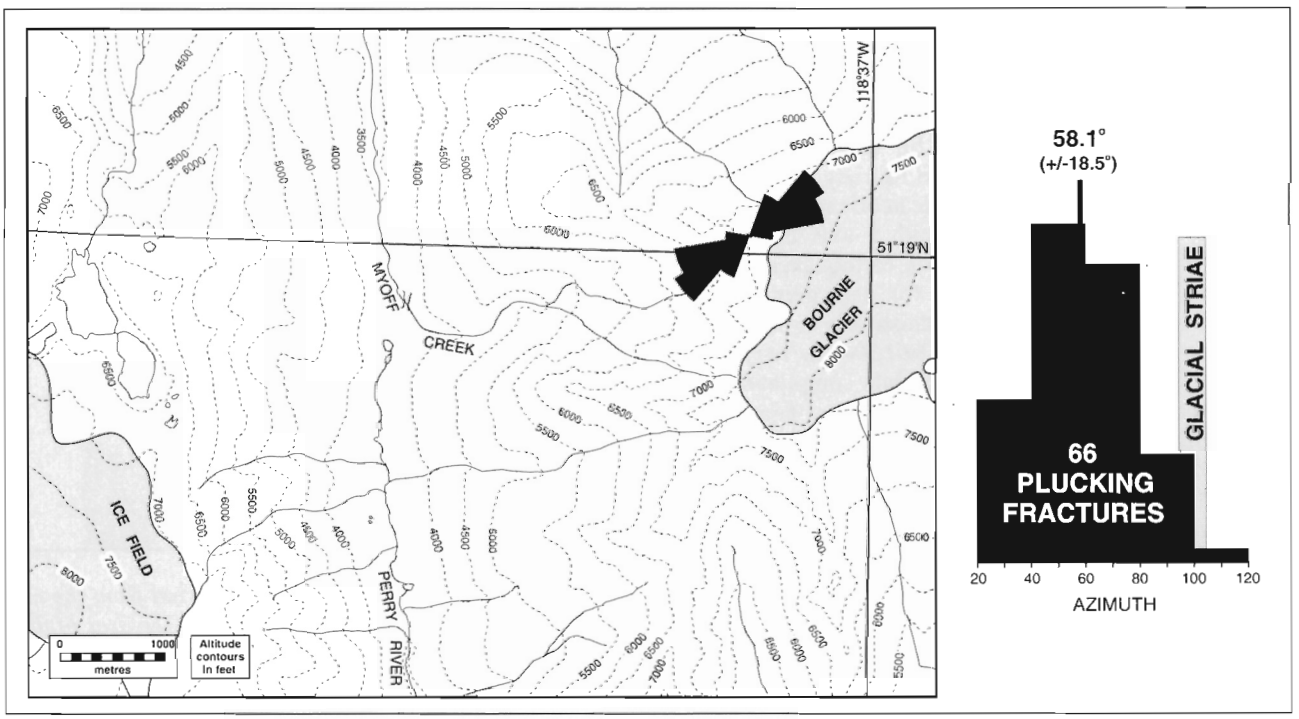


***Figure 18.*** *Map of the glacier forefield west of Bourne Glacier, 46 km northwest of Revelstoke (Location 7), with a histogram and rose diagram for the plucking fractures measured at the site.*

## ADDITIONAL OBSERVATIONS

Within the Pemberton area of the southern Coast Mountains, and across the region sampled by localities 1 to 5, a number of linear scarps cross the mountainsides. Generally, these upward-facing scarps exhibit straight traces, cross ridges, and are commonly oriented approximately north-northeast. Since the topographically lower parts of the slopes cut by the scarps do not appear to have experienced relative outward motion, those features are not likely to be surficial gravitational displacements or sagging bedrock slopes, although unstable sagging slopes also occur in the region. Bovis (1982) and Evans (1987) have invoked a predominantly near-surface toppling process to account for some of the uphill-facing scarps. We do not dispute the involvement of toppling in the detachment of individual slabs from steep bedrock slopes. However, the straightness of the scarps and their disregard for topography, as evidenced by the scarp on Mount Currie (Eisbacher, 1983), suggests that the near-surface offsets are related to displacements on steeply-dipping crustal fractures that extend to significant depths. The linear scarps have every appearance of being neotectonic faults and our brief reconnaisance suggests that there may be far more of these features in the Coast Belt than have been mapped. It is noteworthy that neotectonic regional and local stress fields inferred for near surface faulting within the southern Coast Mountains by Eisbacher (1983, p. 5, 41) are in remarkable agreement with the detached crustal stress field postulated from onshore seismicity in southwestern British Columbia (Wang et al., 1995). Tertiary faults with similar orientations have been mapped elsewhere in the region, particularly in the vicinity of Harrison Lake (Monger and Journeay, 1994). Neotectonic faulting possibly reactivated some of these older fractures.

## RESULTS

The results of this preliminary study are summarized in Figure 19. Five sites were examined for stress indicators in plutonic rocks of the Coast Belt, and four are interpreted in terms of $S_{Hmax}$. Location 1 gave a mean orientation of 60.6° for $S_{Hmax}$, which is compatible with P-axis orientations obtained from focal mechanisms of earthquakes beneath Vancouver Island (Adams, 1995, for data compilation). Locations 3 (6.3°) and 4 (10.5°) are statistically indistinguishable and are similar to north $S_{Hmax}$ orientations reported in Washington State (Adams, 1995, for data compilation). As indicated above, the 11.7° $S_{Hmax}$ orientation obtained from axial and breakage fractures at Location 2 is suspect, because it is aligned with a steep topographic slope to the east. Nevertheless, this orientation compares well with measurements in Washington State (Adams, 1995). Rogers (1979) reports a P-axis determination of 348° at Southgate River, northwest of Locations 3 and 4. The 141° orientation for $S_{Hmax}$ measured in the Cochina Glacier forefield at Location 5 is enigmatic and needs to be supplemented with more data from other, yet to be studied, sites.

Two sites were examined in the high-grade metamorphic rocks of the Omineca Belt. At Location 6, no clear indication of contemporary stress orientations was obtained. On the other hand, Location 7 provided a huge suite of plucking fractures pointing to an $S_{Hmax}$ orientation of 58.1°. This orientation is comparable to the northwest signature in Phanerozoic sediments of the frontal Rocky Mountains and Alberta Plains (Bell et al., 1994).

## OPERATIONAL CONSIDERATIONS

Fieldwork undertaken this summer has emphasized anew that obtaining insights into the contemporary stress regime from rocks which have experienced recent unloading is a tenuous proposition. There are so many reasons why a seemingly clear signal can be distorted, and it is essential to avoid measurements in rocks that are unable to express a regional stress signature during their release from confining pressures.

In artificial or natural outcrops, it is essential to work on massive rocks with minimal internal fabrics or fractures. The locations should be in areas of low topographic relief and distant from hillslopes which could generate local stresses. An *a priori* requirement is that fracturing and offsets are recent, and that outcrop criteria exist to demonstrate this. Naturally-formed glacial striae are ideal, as are manmade features such as preshear boreholes in roadcuts. Furthermore, since the observations are supposed to provide indications of principal horizontal stress orientations, a significant degree of horizontal stress anisotropy is required; if the stress regime is close to isotropic, it is not likely that meaningful measurements can be made.

Judged by these rather stringent criteria, the number of suitable locations for making stress relief measurements is limited. In the Coast Mountains, there are numerous massive granodioritic rocks but, where they are exposed naturally, they are frequently exfoliated, or cut by cooling fractures, and

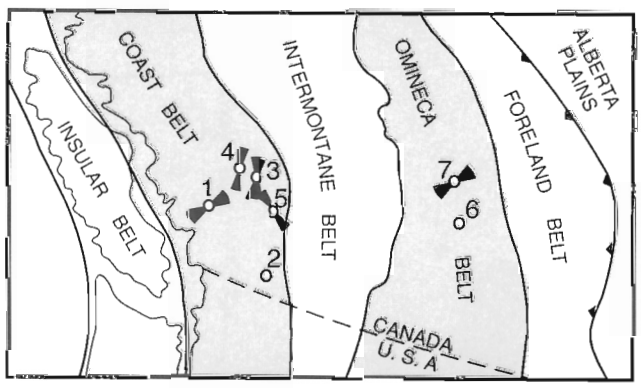


***Figure 19.*** *Orientations of $S_{Hmax}$ inferred from the neotectonic structures examined in this study. The arcs of the bow ties represent two standard deviations centred about the mean azimuths. Open circles denote locations where interpretion of $S_{Hmax}$ was ambiguous.*

therefore have been destressed near the Earth's surface. Roadcuts in the Coast Belt tend to be in areas of high relief, which renders any observations of stress release indicators suspect (see Location 2). The Intermontane Belt is largely composed of crushed and sheared rocks that are totally destressed near the surface whether outcrops are natural or artificial. The Omenica Belt contains high-grade metamorphic rocks, offering hope that enough stress-release features can be found to map the stress regime there. However, more fieldwork will be required to identify suitable localities.

Glacier forefields remain the most encouraging sites because they have experienced recent removal of loads due to the ongoing retreat of the Cordilleran glaciers. In our experience, it is essential to work on wide and flat forefields with low local relief. The rocks should be as mechanically isotropic as possible with minimal fabric anisotropy or preglacial fracturing, a requirement that is very difficult to meet. Thus, it is essential that the most recent set of fractures in the rock be identified and, where possible, be shown to be of postglacial age. Sites several hundred metres downslope from the present glacier snouts appear to provide the best stress release indicators. Factors which are not considered here are the effects of former ice thickness and the time period since the glacier ice melted back. These factors might account in part for the lack of distinctive directional features at Location 6 in the high-grade metamorphic rocks of the Monashee Group.

## FUTURE WORK

Based on the results and observations made during this study, the southern part of the Coast Belt appears to be an excellent candidate for an extensive helicopter-supported study of neotectonic indicators. Such an endeavour could be expected to yield data on stress orientation from glacier forefields underlain by plutonic rocks. As well, fractures and faults that have experienced recent displacements could be mapped and interpreted within a dynamic framework. The huge icefields west and northwest of Pemberton appear to hold potential for glacier forefield studies. Furthermore, it would be most useful to map weakness anisotropy in rocks, that is to say, to record in three dimensions the major potential failure planes in rock masses.

Neotectonic mapping on this scale has many short term and long term benefits. Motion on recent faults tends to trigger slope failure. Thus mapping these fracture zones will assist development of safer road systems and drainage diversions. Stress release from glacial retreat or artificial excavations is also likely to promote slope failure depending on the stress regime, rock types, weakness anisotropy, and specific site topography. A neotectonic study of the type envisaged would also identify areas where potential slope stability problems (e.g., Evans and Savigny, 1994) merge with stress-related rock fracture. The proposed study could incorporate both types of information. In addition, there is the ongoing concern about the direct impact of earthquakes on the mountainous West Coast of Canada and the potential for damage to buildings and urban infrastructure. Neotectonic mapping will help address these issues.

We are less positive about a similar program for the Omineca Belt. Neither population density nor earthquake intensity are high in this region, and potential sites for measuring neotectonic stress indicators appear to be more limited.

## REFERENCES

**Adams, J.**
1995: The Canadian Crustal Stress Database - a compilation to 1994, parts I and II; Geological Survey of Canada, Open File 3122, 194 p. (contains original references to stress studies discussed in this report).

**Bell, J.S. and Eisbacher, G.H.**
1995: Stress orientation indicators (neotectonic plucking fractures) in bedrock of glacier forefields, southeastern Cordillera, western Canada; in Current Research 1995-B, Geological Survey of Canada, p. 151-159.

**Bell, J.S., Price, P.R., and McLellan, P.J.**
1994: In-situ stress in the Western Canada Sedimentary Basin; in Geological Atlas of Western Canada Sedimentary Basin, G.D. Mossop and I. Shetsen (comp.); Canadian Society of Petroleum Geologists and Alberta Research Council, p. 439-446.

**Bovis, M.J.**
1982: Upward-facing (antislope) scarps in the Coast Mountains, southwest British Columbia; Geological Society of America Bulletin, v. 93, p. 804-812.

**Eisbacher, G.H.**
1983: Slope stability and mountain torrents, Fraser Lowlands and southern Coast Mountains, British Columbia; Geological Association of Canada Annual Meeting (Victoria, B.C. ) Field Trip Guidebook, Trip 15, 46 p.

**Evans, S.G.**
1987: Surface displacement and massive toppling on the northeast ridge of Mount Currie, British Columbia; in Current Research, Part A; Geological Survey of Canada, Paper 87-1A, p. 181-189.

**Evans, S.G. and Savigny, K.W.**
1994: Landslides in the Vancouver-Fraser Valley-Whistler region; in Geology and Geological Hazards of the Vancouver Region, Southwestern British Columbia, (ed.) J.W.H. Monger; Geological Survey of Canada, Bulletin 481, p. 251-286.

**Friedman, R.M. and Armstrong, R.L.**
1990: U-Pb dating, Southern Coast Belt, British Columbia; in Project Lithoprobe - Southern Canadian Cordillera Transect Workshop, University of Calgary, 3-4 March, 1990, p. 146-155.

**Johnson, P.A.**
1989: Cluster analysis of eastern Washington seismicity; MSc. thesis, University of Washington, Seattle, Washington, 79 p.

**Jones, A.G.**
1959: Vernon map-area, British Columbia; Geological Survey of Canada, Memoir 296, 186 p.

**Ma, L.**
1988: Regional tectonic stress in western Washington from focal mechanisms of crustal and subcrustal earthquakes; MSc. thesis, University of Washington, Seattle, Washington, 84 p.

**Monger, J.W.H. and Journeay, J.M.**
1994: Guide to the Geology and Tectonic Evolution of the Southern Coast Mountains; Geological Survey of Canada, Open File 2490, 77 p.

**Moore, D.P., Ripley, B.D., and Groves, K.L.**
1992: Evaluation of mountainslope movements at Wahleach; in Geotechnique and Natural Hazards, Bitech Publishers, Vancouver, p. 99-107.

**Rogers, G.C.**
1979: Earthquake fault plane solutions near Vancouver Island; Canadian Journal of Earth Sciences, v. 16, p. 523-531.

**Wang, K., Mulder, T., Rogers, G.C., and Hyndman, R.D.**
1995: Case for very low coupling stress on the Cascadia subduction fault; Journal of Geophysical Research, v. 100, p. 12, 907-12, 918.

**Wheeler, J.O.**
1965: Big Bend map-area, British Columbia, 82M (East half); Geological Survey of Canada, Paper 64-32, 37 p.

Geological Survey of Canada Project 870039

# Shoreface of the Bearpaw Sea in the footwall of the Lewis Thrust, southern Canadian Cordillera, Alberta[1]

T. Jerzykiewicz, A.R. Sweet, and D.H. McNeil
GSC Calgary, Calgary

*Jerzykiewicz, T., Sweet, A.R., and McNeil, D.H., 1996: Shoreface of the Bearpaw Sea in the footwall of the Lewis Thrust, southern Canadian Cordillera, Alberta; in Current Research 1996-A; Geological Survey of Canada, p. 155-163.*

**Abstract:** The youngest strata exposed in the footwall of the Lewis Thrust, south of Beaver Mines Lake, contain upper shoreface and coastal marsh sediments. Facies, microflora, and microfauna indicate that these strata are correlative with the regressive phase of the Bearpaw Seaway dated at approximately 71 Ma. This date is the maximum age for the emplacement of the Lewis Thrust in the southeastern Cordillera. The occurrence of the Bearpaw and the St. Mary River formations in the footwall of the Lewis Thrust must be taken into account for geological mapping of the southern Foothills.

**Résumé :** Les strates les plus récentes affleurant dans le compartiment inférieur du chevauchement de Lewis, au sud du lac Beaver Mines, contiennent des sédiments d'avant-plage supérieure et de marais littoral. Les faciès, la microflore et la microfaune indiquent que ces strates sont corrélatives de la phase régressive du canal maritime Bearpaw, daté à 71 Ma environ, ce qui correspond à l'âge maximal du chevauchement de Lewis dans le sud-est de la Cordillère. Il faut tenir compte de la présence des formations de Bearpaw et de St. Mary River dans le compartiment inférieur du chevauchement de Lewis lorsqu'on établit la cartographie géologique des contreforts méridionaux.

[1] Contribution to the Eastern Cordillera NATMAP Project

## INTRODUCTION

The Proterozoic and Paleozoic rocks of the Lewis thrust sheet in the southern Foothills were emplaced onto a succession of Upper Cretaceous clastic rocks traditionally referred to as the "Belly River Formation". This succession of sandstone and mudstone units containing some coalbeds is at least 1 km thick. It is very intensively deformed in the footwall of the Lewis Thrust and nowhere is it exposed in its entirety.

The "Belly River Formation" has been mapped as one stratigraphic unit although some authors realized that the youngest beds beneath the Lewis Thrust may in fact belong to the Bearpaw Formation or even to the St. Mary River Formation (Clow and Crockford, 1951; Price, 1962; Norris, 1993a, b).

This paper provides lithostratigraphic, sedimentological, and paleontological evidence that the youngest beds exposed in the footwall of the Lewis Thrust, south of Beaver Mines Lake, contain an interval of strata correlative with the Bearpaw to lowermost St. Mary River formations of the outer Foothills and plains. This fact is important for constraining the timing of deformation in the southern Foothills, and must be considered during any future mapping or map revisions containing the footwall of the Lewis Thrust on Beaver Mines, Crowsnest, Tornado Mountain, Fording River, and Mount Head map areas.

## GEOLOGICAL SETTING

Outcrops analyzed in this paper are located on north-westward-facing slopes of Table and Whistler mountains, about 1.5 km southeast of Beaver Mines Lake in Lsd. 9-2-5-3W5.

According to Norris (1993a), the footwall of the Lewis Thrust in the vicinity of Beaver Mines Lake is folded into two synclines and an intervening anticline (Fig. 1). These folds are overturned toward the northeast and built up with Blairmore, Alberta Group, and Belly River strata. The core of Lost Syncline, immediately beneath the Lewis Thrust, contains the youngest strata, which are correlative to the lower, brackish-water member of the St. Mary River Formation (outcrop 1). These strata are underlain by a black shale (outcrop 2; Fig. 1) containing foraminifers which, although impoverished, suggest a correlation with the middle to upper Bearpaw Formation.

## LITHOSTRATIGRAPHY

The section designated as outcrop 1 (Fig. 1-3) consists of interstratified sandstone, mudstone, oyster beds, and coal. The sandstone layers vary in thickness from 1.2 to 2.5 m. The sandstone is medium to fine grained and well sorted. Stratification types include low-angle crossbedding, and swash crossbedding typical of backshore and beach deposits.

The uppermost layer of sandstone (Fig. 2) is rooted and contains well preserved *Ophiomorpha* burrows (Fig. 3B) which are very similar to those illustrated by Jerzykiewicz (in prep.) from the Blood Reserve Formation. The sandstone layers resemble those of an upper shoreface origin found in the Blood Reserve Formation described from the Cardston and Pincher Creek map areas (Williams, 1949; Douglas, 1951; Nadon, 1988; Jerzykiewicz, in prep.). The sandstone corresponds closely to facies 8 of Nadon (1988), which was interpreted as being deposited during upper flow plane bed conditions.

The sandstone layers are interstratified with dark grey mudstone containing abundant plant fragments, some coaly material, and traces of rootlets. A conspicuous layer of coal, which occurs in the lower part of the section (Fig. 2), is interpreted as an in situ accumulation of plant material in a coastal marsh environment typified palynologically as being fern dominated (Fig. 3).

Two oyster beds that occur in outcrop 1 closely resemble those described by Jerzykiewicz and Sweet (1988, Fig. 14) from the lower, brackish-water member of the St. Mary River Formation. They consist mainly of closely packed shells of *Ostrea glabra* Meek and Hayden, and other oyster, gastropod

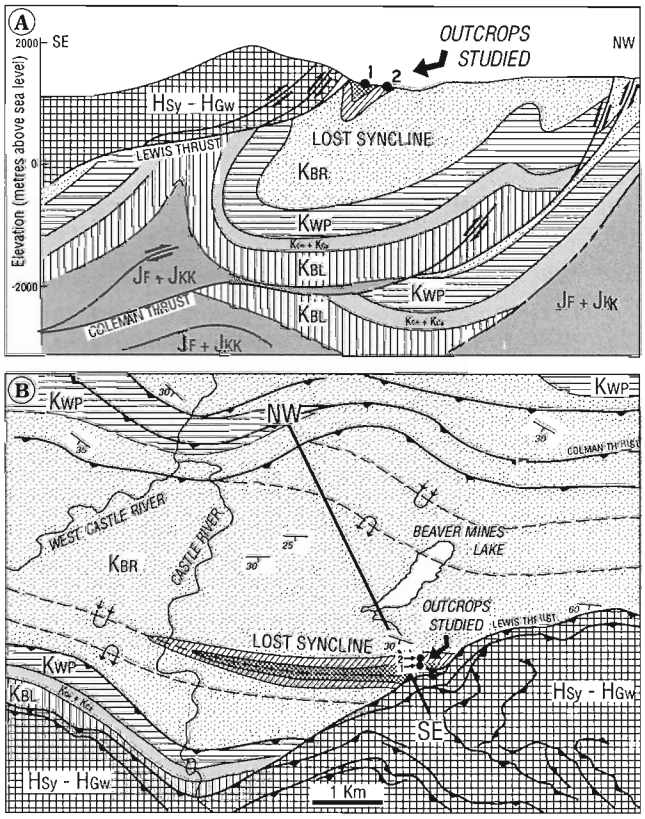


***Figure 1.*** *The structural setting of the outcrops studied in the core of the Lost Syncline in the footwall of the Lewis Thrust. Geology modified after Norris (1993a).*

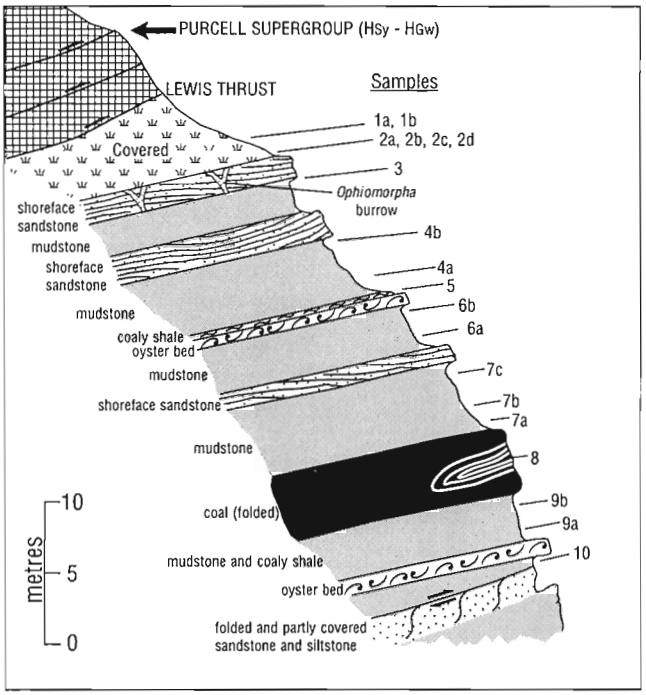


***Figure 2.*** *Shoreface sandstone layers interstratified with mudstone, oyster beds and coal in the footwall of the Lewis Thrust. Outcrop 1.*

and bryozoa shells and are interpreted as oyster bioherms. Communities of oysters, thick-shelled epifaunal bivalves capable of producing bioherms, are highly tolerant of salinity fluctuations. They may occur in marginal-marine hypersaline environments as well as in brackish waters. Present-day oyster bioherms occur in the intertidal and shallow subtidal zones as well as in supratidal marsh settings (for references see Jerzykiewicz and Sweet, 1988).

The association of sedimentary structures and macrofossils found in outcrop 1 strongly suggests deposition in an upper shoreface and coastal marsh environment. Analogous environments developed during the regression of the Bearpaw Seaway from the Alberta basin, which is recorded in the Blood Reserve and St. Mary River formations of southern Alberta. This conclusion is consistent with the position of outcrop 1 above a shallow marine black shale (outcrop 2), which yielded an assemblage of foraminifers that suggests correlation with the middle to upper part of the Bearpaw Formation to the northeast.

## PALEONTOLOGY

### *Palynology*

Palynomorph recovery was consistently good throughout outcrop 1, except for units 1 and 2 at the top of the section (Fig. 2, 4). The two mudstone samples from unit 1 were

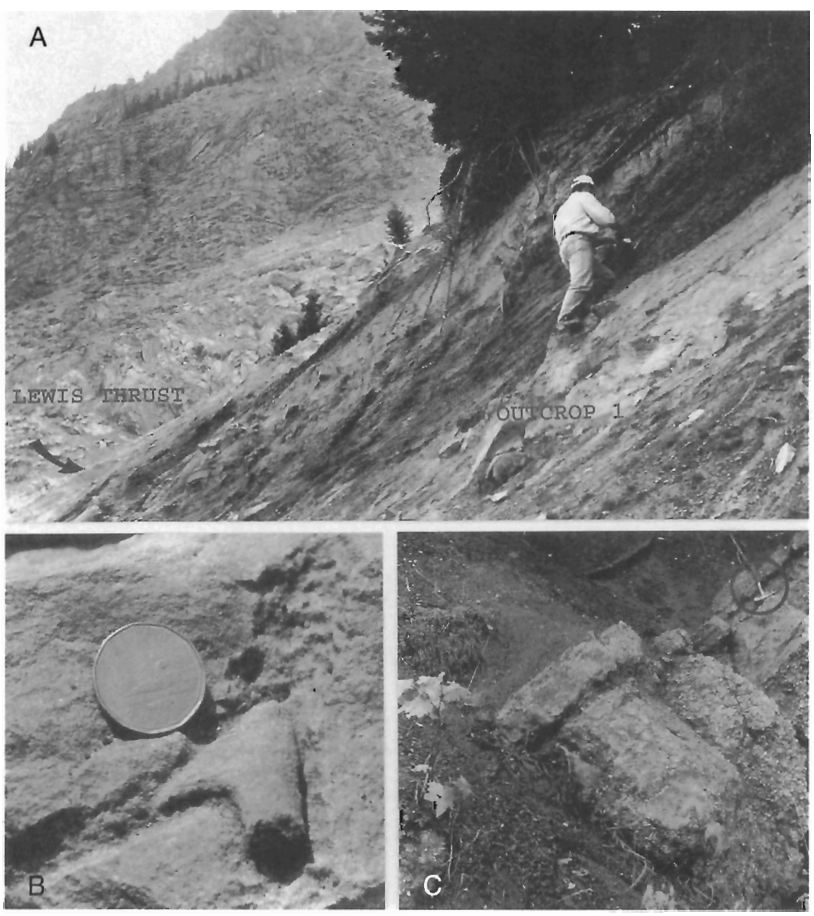


***Figure 3.***

*Shoreface deposits in the footwall of the Lewis Thrust. Outcrop 1.*

***A.*** *View from outcrop 1 toward the hanging wall of the Lewis Thrust. ISPG Photo 43967*

***B.*** *Close-up view of an Ophiomorpha burrow. ISPG Photo 43965*

***C.*** *Oyster layer. Hammer for scale. ISPG Photo 43968*

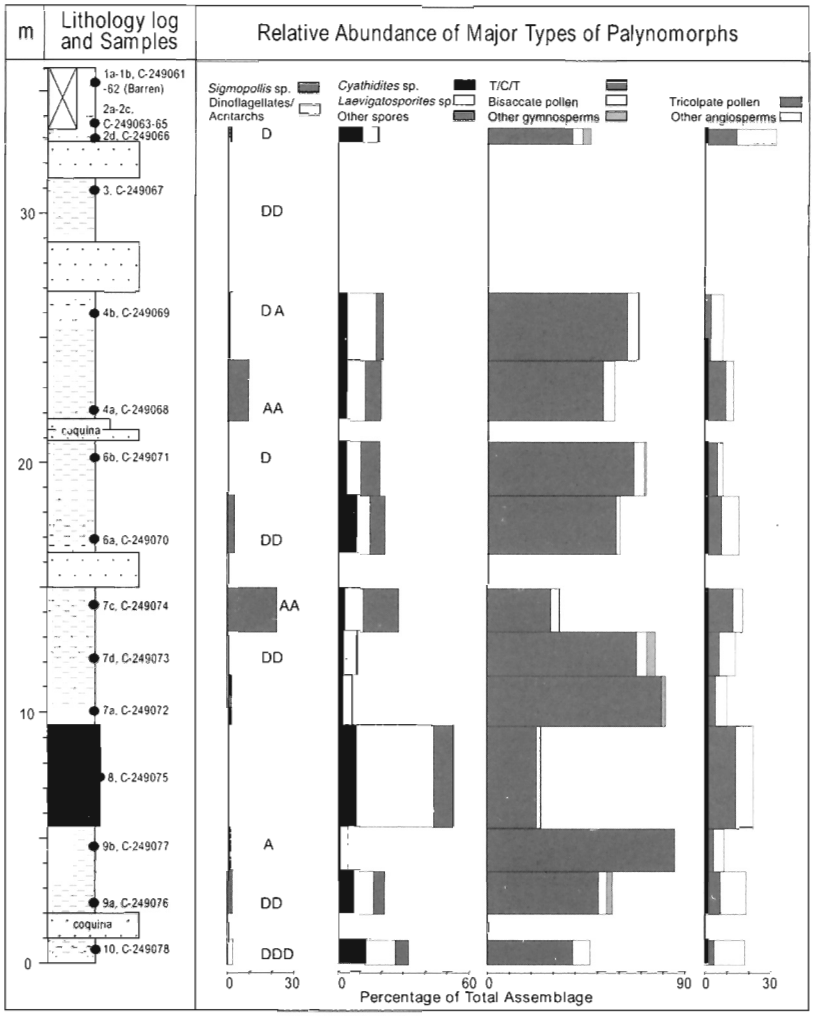


***Figure 4.***

*Relative abundance of major types of palynomorphs. D, rare, DD, common and DDD, abundant dinoflagellates; A, rare and AA, common acritarchs; both types of palynomorphs indicate a marine depositional environment.*

## PLATE 1

Selected biostratigraphically significant palynomorphs from outcrop 1 (JO-94-BR-10; NTS 82G/8 W, UTM zone 11, 696500 E, 5470700 N; LSD 9-2-5-3 W5). All figures x1000. Microscope coordinates from Olympus Vanox-T microscope 606009.

**1.** *Aquilapollenites trialatus* Rouse, 1957; C-249071; P4024-11b, 132.2x15.3; GSC 112303.
**2.** *A. drumhellerensis* Srivastava, 1969; C-249066; P4024-6b, 126.4x16.7; GSC 112304.
**3.** *A. leucocephalus* Srivastava, 1968; C-249077; P4024-17c, 124.3x18.7; GSC 112305.
**4.** *A. funkhouseri* Srivastava, 1966; C-249073; P4024-13c, 134.3x20.2; GSC 112306.
**5.** *A. senonicus* (Mtchedlishvili) Tschudy & Leopold, 1971; C-249071; P4024-11a, 119.3x8.6; GSC 112307.
**6.** *Grewipollenites radiatus* Tschudy, 1973; C-249075, P4024-15c, 128.6x18.8; GSC 112308.
**7.** *Cranwellia rumseyensis* Srivastava, 1966; C-249073; P4024-13c, 131.6x15.3; GSC 112309.
**8.** *Sindorapollis granulatus* Tschudy, 1973; C-249071; P4024-11c, 131.8x15.3; GSC 112310.
**9.** *Mancicorpus tripodiformis* (Tschudy & Leopold) Tschudy, 1973; C-249078; P4024-18b, 113.6x6.2; GSC 112311.
**10.** *Mancicorpus calvus* (Tschudy & Leopold) Tschudy, 1973; C-249072; P4024-12c, 124.8x3.7; GSC 112312.
**11.** *Aquilapollenites stelckii* Srivastava, 1968; C-249071; P4024-11b, 134.3x20.2; GSC 112313.
**12.** *Expressipollis* sp. cf. *E. barbatus* Chlonova 1961; C-249066; P4024-6b, 119.0x10.2; GSC 112314.
**13.** *Syncolporites minimus* Leffingwell, 1971; C-249072; P4024-12d, 113.5x7.6; GSC 112315.
**14.** *Ulmipollenites granulatus* Stone, 1973; C-249071; P4024-11c, 125.5x11.9; GSC 112316.
**15.** *Gunnaripollis superbus* Srivastava, 1969; C-249073; P4024-13c, 122.6x17.7; GSC 112317.
**16.** *Ilexpollenites compactus* Stone, 1973; C-249070; P4024-10c, 127.7x22.2; GSC 112318.
**17.** *Siberiapollis* sp.; C-249073; P4024-13c, 135.4x17.8; GSC 112319.

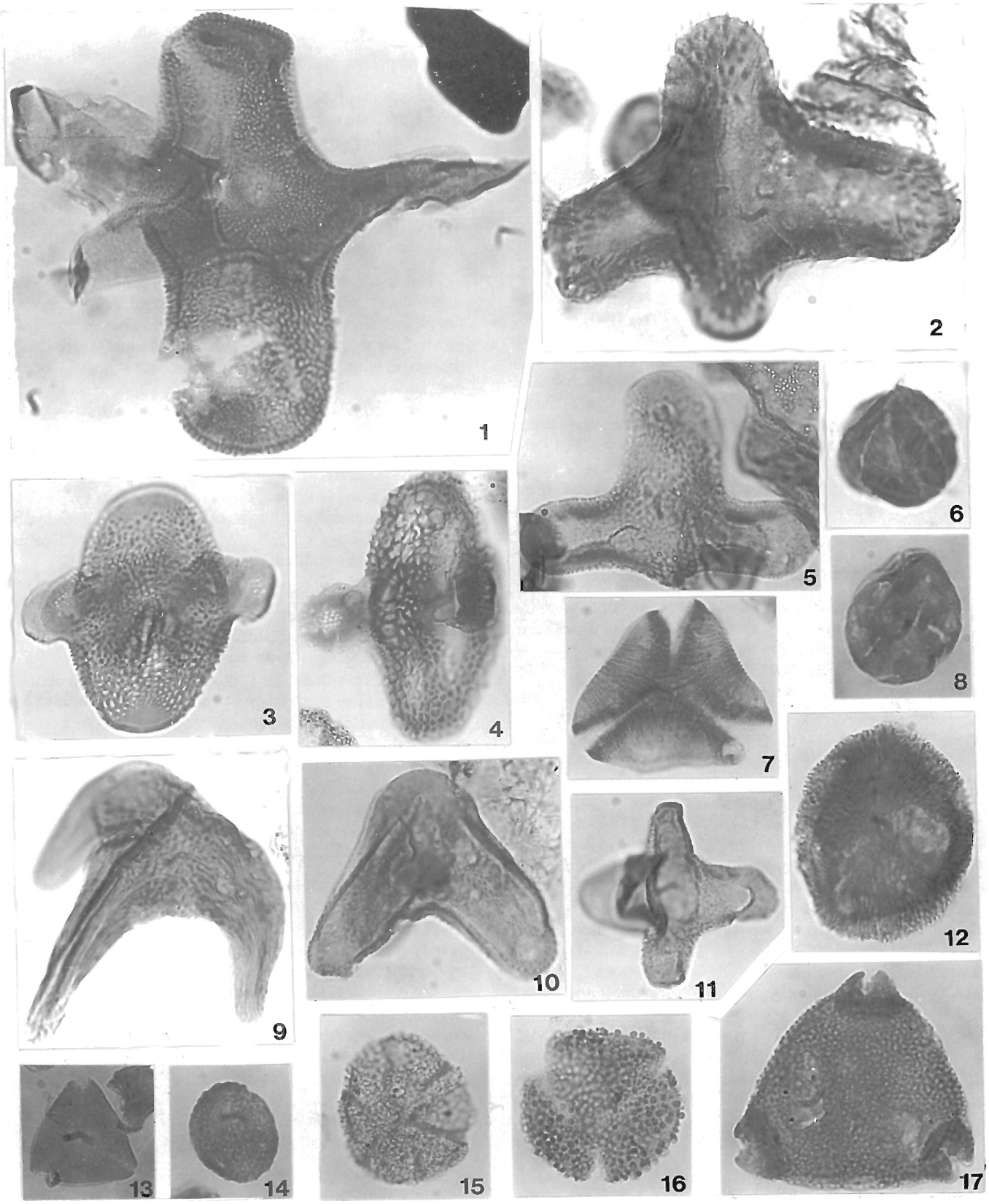
1
2
3
4
5
6
7
8
9
10
11
12
13
14
15
16
17

almost barren, and the four processed from unit 2 ranged from being almost barren to having sparse to good recoveries. Low recovery is the rule rather than the exception for samples of mudstone above the "lower St. Mary River Formation" of Douglas (1952), presumably reflecting a relatively low water table (at least periodically), and oxidizing conditions within a floodplain setting. This suggests that the top of the section corresponds to "upper St. Mary River Formation" strata. All samples (coal and mudstone) from the lower portion of the section yielded rich assemblages. This was also true for samples from the lower portion of the St. Mary River Formation on Castle River (Jerzykiewicz and Sweet, 1988) in a section with similar facies associations.

The overall aspect of the assemblage (Fig. 4, Pl. 1, Table 1) from outcrop 1 compares most closely with that of the latest Campanian *Aquilapollenites leucocephalus* Zone of Srivastava (1970). *Aquilapollenites leucocephalus* is present in most of the productive samples, although there is considerable variation in its relative abundance and that of other species (Table 1). An abundance of this species has also previously been recorded in the lower portion of the St. Mary River Formation on Castle River (Jerzykiewicz and Sweet, 1988). In the Horseshoe Canyon Formation in the Red Deer River Valley *Aquilapollenites leucocephalus* has a stratigraphic range restricted to an interval immediately below the #4 coal (Srivastava, 1970). However, it has also been reported from pre-Bearpaw strata, although in this instance the reticulum is quite fine (Eberth et al., 1990, Pl. 2, fig. 5; note the finer reticulum compared to that of Plate 1, fig. 3).

The *Aquilapollenites leucocephalus* Zone falls within the upper part of polarity chron 33 normal, based on the relative position of the coal zones and polarity chrons given in Lerbekmo and Coulter (1985, fig. 17), the position of coal zones within individual sections given in Gibson (1977), and the zonal reference section given in Srivastava (1970). The overlying *Wodehouseia edmonticola (jacutense)* Zone (Srivastava, 1970) starts just below the #5 coal (Lerbekmo and Coulter, 1985), and is distinguished from the *Aquilapollenites leucocephalus* Zone by the occurrence of *Wodehouseia*. Lerbekmo and Coulter (1985) considered the base of the *Wodehouseia edmonticola (jacutense)* Zone to be more or less correlative to the base of the *Baculites baculus* Zone with an inferred absolute age of about 71 Ma. Given the above, the upper part of the *Aquilapollenites leucocephalus* zone must be correlative to the *Baculites eliasi* Zone, the base of which is currently taken to be 71.3 Ma, and marks the Campanian-Maastrichtian boundary (Obradovitch, 1993). The *Aquilapollenites leucocephalus* Zone extends downward from the lower St. Mary River Formation into the upper part of the Bearpaw Formation in the Alberta Foothills (unpublished data), and therefore 71.3 Ma is to be considered a minimum age for the zone. *Aquilapollenites leucocephalus* is scarce in the underlying Belly River Formation.

The palynological assemblage is dominantly of terrestrial origin but the consistent presence of dinoflagellates (Fig. 4), especially in the lower portion of the section, indicates a nearshore marine environment of deposition for the mudstone facies. This is consistent with the presence of oysters, *Ophiomorpha* burrows, and inorganic sedimentary structures found in sandstone layers.

### *Foraminifers and other microfossils*

Examination of seventeen microfossil samples from outcrop 1, and one sample from outcrop 2, yielded sparse assemblages of foraminifers, diatoms, ostracods, charophytes, gastropod fragments, and amber and coaly debris. Marine microfossils (foraminifers) were recovered from outcrop 2. Terrestrial microfossils were recovered through most of outcrop 1, but a few marine microfossils (foraminifers) were recovered from the lower part.

The black shale from outcrop 2 yielded ten species of foraminifers, eight of which are illustrated in Plate 2, and a few specimens of the marine diatom *Coscinodiscus*?. The biostratigraphic position of this microfauna is difficult to determine with complete assurance because most of the species, such as *Saccammina placenta*, *Haplophragmoides rota*, *Trochammina albertensis*, *Verneuilinoides* cf. *V.* verneuilinoides, and *Quinqueloculina sphaera* could range through the Pakowki and Bearpaw formations. The small, unnamed species of *Ammodiscus* (*Spirillina*? of Rosene, 1972) illustrated in Plate 2, however, is known only from the middle and upper Bearpaw Formation based on unpublished data from Rosene's (1972) M.Sc. thesis on the Bearpaw Formation of the southwestern Foothills of Alberta.

Rosene (1972) and Wall and Rosene (1977) recognized three microfossil zones within the Bearpaw Formation of southwestern Alberta (Oldman River, Lundbreck, Castle River, and Waterton River areas): an ostracod zone in the lower 12 m; an arenaceous foraminiferal zone from about 12 to 120 m; and an agglutinated-calcareous foraminiferal zone (*Gavelinella talaria* assemblage) from 120 to 270 m (top of measured section at Lundbreck). The assemblage from outcrop 2 is impoverished compared to the Bearpaw assemblages documented by Rosene (1972), but the similarities that do exist suggest correlation with the *G. talaria* zone, based on the ranges of *Saccammina* spp., *Ammodiscus* sp. (*Spirillina*? sp. of Rosene, 1972), and *Quinqueloculina sphaera*.

The foraminiferal assemblage in outcrop 2 (one sample) suggests a shallow inner shelf marine environment of deposition in water of less than normal marine salinity. This is based on the low species diversity and the presence of only two species of calcareous benthic foraminifers of the genus *Quinqueloculina*. The absence of planktonic foraminifers and the diversity of calcareous benthic foraminifers indicate that normal marine conditions were probably not present at this site. The assemblage is also not typical of marginal marine environments (lagoon, marsh, estuary) which are usually dominated by abundant *Miliammina*, *Ammobaculites*, *Ammotium*, *Haplophragmoides*, *Trochammina*, and *Verneuilinoides* and *Eggerella* (Murray, 1991; Wall, 1976).

Samples from the stratigraphically higher outcrop 1 were mostly either barren of microfossils or yielded terrestrial indicators such as charophytes, amber, coaly debris, and fresh

**Table 1.** Occurrence chart of taxa not shown individually in Figure 4. R, rare, 1 to 2 specimens; S, scarce, 3 to 4 specimens; C, common, 5 to 8 specimens; A, abundant, over 8 specimens seen in area of slides outside that counted. Numbers indicate number of specimens recorded in counted population.

| DISTRIBUTION OF TERRESTRIAL PALYNOMORPHS | | | | | | | | | | | | | | | |
|---|---|---|---|---|---|---|---|---|---|---|---|---|---|---|---|
| **TAXA** | **2b** | **2c** | **2d** | **3** | **4a** | **4b** | **6a** | **6b** | **7a** | **7d** | **7c** | **8** | **9a** | **9b** | **10** |
| **Spores** | | | | | | | | | | | | | | | |
| *Cicatricosisporites ornatus* | | R | | R | 18 | 3 | S | 2 | C | 1 | 33 | | 2 | C | |
| *Ghoshispora* spp. | | | | | | | | | | A | | | 6 | | |
| *Gleicheniidites* sp. | | | | | | | R | 4 | 1 | | 1 | 18 | | | 3 |
| *Hamulatisporites* sp. | R | | | | | | | 2 | | | R | | 2 | | |
| *Hazaria* sp. | C | | | R | 4 | R | 1 | 7 | | | 1 | 2 | | | 3 |
| *Libumisporis adnacus* | | | | | | | | | R | | | | R | R | R |
| *Matonisporites* sp. | R | | | | | 5 | 17 | 6 | 1 | 1 | 5 | | 2 | | 7 |
| *Osmudacidites* sp. | | | 1 | | | 1 | | R | R | R | | 1 | | | 1 |
| *Reticulosporis* sp. | | | | | | | | R | | | | | | | |
| *Stereisporites* sp. | | | 1 | | | | | 1 | | | | | | | |
| *Triporoletes* sp. | | | | | | | R | | | | 1 | | R | R | |
| **Gymnosperm pollen** | | | | | | | | | | | | | | | |
| *Classopollis* sp. | R | R | 4 | | | | | 2 | R | R | | | 4 | | |
| *Equisetosporites* sp. | | | R | | | | R | | R | R | R | | S | | |
| *Ginkgo* sp. | | | 4 | | | 1 | | | 5 | 9 | 1 | 1 | 2 | R | |
| **Angiosperm pollen** | | | | | | | | | | | | | | | |
| *A. clarireticulatus* | S | | R | | | | R | R | | | | | R | 1 | R |
| *A. drumhellerensis* | R | R | R | R | | R | S | S | | | | | 1 | | |
| *A. eurypteronus* | | | | | | | | | | R | | | | | |
| *A. formosus* | | | | | | | | R | | R | | | | | |
| *A. funkhouseri* | | | R | S | 1 | 1 | R | 1 | R | R | R | | | | S |
| *A. leucocephalus* | R | | R | | | 5 | | R | 1 | 1 | | S | | A | 1 |
| *A. oblatus* | S | S | | R | | R | | | | | | | | | 1 |
| *A. quadrilobus* | | | | | | | | S | | R | | | R | | R |
| *A. rectus* | R | | | R | | | R | R | | | | | | | |
| *A. senonicus* | | | | | | | | R | | R | | | | | |
| *A. sentus* | | | | | | | | | | | | | | | |
| *A. trialatus* | S | | 2 | | | | | R | | | 1 | | | | |
| *A. vinosus* | | | 1 | | | | | | | | | | | | |
| *Arecipites* spp. | | | 3 | R | | 1 | | | | | 1 | | 1 | | 1 |
| *Callistopollenites* sp. | | | | | | | | | | | | | R | | |
| *Cranwellia rumseyensis* | R | R | S | R | | 3 | 4 | 3 | R | S | R | 1 | 7 | | 6 |
| *Cupanieidites* sp. | | | | R | | | | | | | | | | R | |
| *Dyadonapites reticualatus* | | | | | R | | 2 | | | | | | 5 | | 6 |
| *Erdtmanipollis procumbentiformis* | | R | A | S | R | | R | 1 | | S | | R | S | R | R |
| *Expressipollis* sp. cf. *E. barbatus* | R | R | A | | | | | | | | | | | | |
| *Fibulapollis* sp. | | | | | R | | R | | | | | | | | |
| *Grewipollenites radiatus* | | | | | | | | | | | | R | | | |
| *Gunnaripollis superbus* | | | | | | | | | | R | | | | | |
| *Ilexpollenites compactus* | R | | | R | A | | 7 | | S | 2 | R | 1 | R | R | 1 |
| *Inaperturotetradites scabratus* | | | R | | | | | | | | R | | S | | 1 |
| *Liliacidites complexus* | | | | R | | | 1 | R | | 1 | 1 | 1 | | | |
| *Liliacidites* sp. (spinate) | R | R | R | | | | R | R | R | | 1 | | 2 | | 1 |
| *Liliacidites* spp. | | | 3 | | | 1 | | | 1 | | | 2 | 1 | | |
| *Mancicorpus albertensis* | S | C | R | | | | | | | | | | R | | |
| *Mancicorpus calvus* | A | R | 1 | R | R | 1 | | R | A | S | R | | A | 2 | |
| *M.* sp. cf. *M. glabra* | | | | | | | | R | | R | | | | | |
| *M. tripodiformis* | | | R | S | | | | R | | | | | | | R |
| *Nyssapollenites bindae* | | | | | | | | | R | | | | R | | |
| *Nyssoidites* sp. | | | R | | | | | | | | | R | | S | |
| *Penetetrapites inconspicuus* | | | R | | | | | | | | | | R | | |
| *Pleurospermaepollenites* sp. | R | | | | | | | | C | R | | R | | C | |
| *Proteacidites* sp. | | | R | | | | | | | | | | | | |
| *Pulcheripollenites narcissus* | | | | | | | | | R | S | | | | | |
| R*Retibrevitricolporites* sp. | | | | | | R | | R | | | | | | | |
| *Scabratriporites legibilis* | | | | | | | R | | | | | | S | | |
| *Senipites* sp. | R | | R | | | | | R | | | | | | | |
| *Siberiapollis* sp. | | R | R | R | | | | S | | R | | | R | | |
| *Sindorapollis granulatus* | | | | | | | | R | | | | | | 1 | 2 |
| *Syncolporites minimus* | R | | | | 1 | R | | R | 3 | 3 | | R | 3 | 2 | 2 |
| *Tricolpites interangulas* | | A | 16 | | | | | R | | 2 | | | | | 3 |
| *Tricolporopollenites* sp. | | | | | | | S | | 3 | R | 1 | 5 | 1 | 2 | 2 |
| *Trifossapollenites ellipticus* | | | 2 | | 1 | | | | A | | | | | S | |
| *Triporopollenites* sp. | | | 6 | | 4 | 2 | R | | 1 | | | | 1 | | 1 |
| *Ulmipollenites granulatus* | | | 5 | | 3 | 1 | 6 | 1 | 5 | 8 | 6 | R | 6 | 4 | 4 |
| *Virgo rallus* | R | | | | | | | | 1 | R | 1 | R | | | |
| **TOTAL SPECIMENS COUNTED** | **0** | | **221** | **0** | **31** | **286** | **262** | **259** | **294** | **236** | **269** | **24** | **244** | **262** | **230** |

water ostracods. One sample at the base of outcrop 1 did, however, yield specimens of *Saccammina* and *Haplophragmoides*? which suggests a marginal marine influence at time of deposition. The recovery of dinoflagellates at several levels through all but the uppermost part of outcrop 1 (Fig. 4) similarly indicates marginal marine conditions of sedimentation.

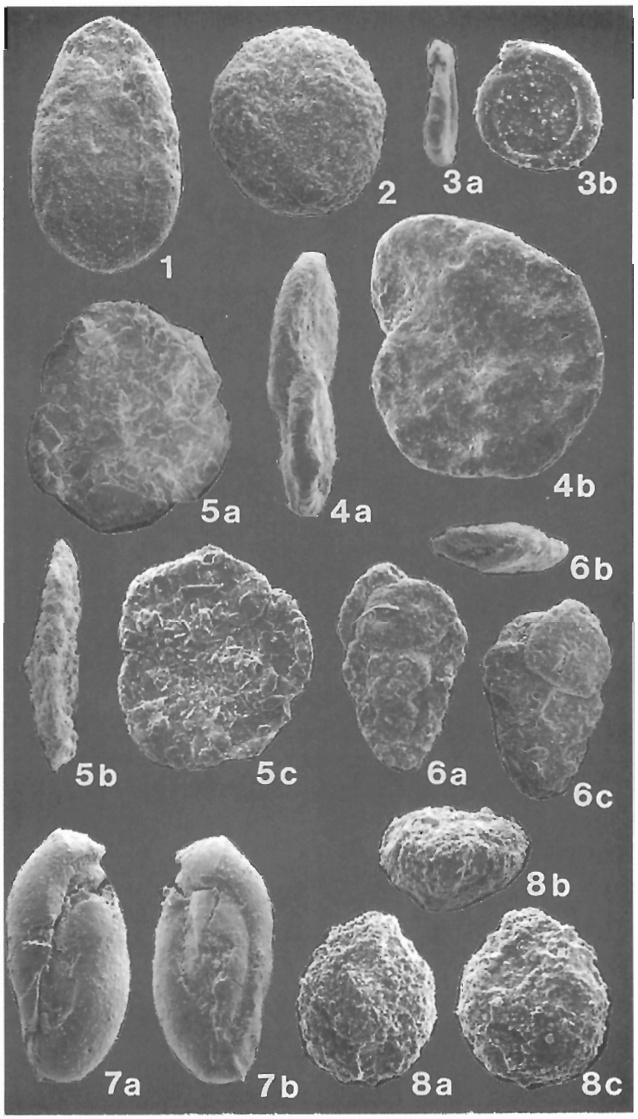


**PLATE 2**

Foraminifers from outcrop 2 (field section JO-94-BR-11, sample C-249074). **1**. *Saccammina* sp., 75x, GSC 89629. **2.** *Saccammina placenta* (Grzybowski), 100x, GSC 89630. **3a, b**. *Ammodiscus* sp., 137x, GSC 89631. **4a, b.** *Haplophragmoides rota* Nauss, 102x, GSC 89632. **5a-c**. *Trochammina albertensis* Wickenden, 97x, GSC 89633. **6a-c**. *Verneuilinoides* cf. *V. bearpawensis* (Wickenden), 112x, GSC 89634. **7a, b**. *Quinqueloculina* sp., 74x, GSC 89635. **8a-c**. *Quinqueloculina sphaera* Nauss, 110x, GSC 89636.

## CONCLUSIONS

1. The succession of sandstone, mudstone, oyster beds, and coal that occurs in the footwall of the Lewis Thrust, south of Beaver Mines Lake (outcrop 1), contains sedimentological features of upper shoreface and coastal marsh environments.
2. Palynological assemblages found in the mudstone and coal at outcrop 1 are similar to those known from the lower (brackish) member of the St. Mary River Formation on Castle River (outcrop 4 in Jerzykiewicz and Sweet, 1988).
3. The black shale from outcrop 2 contains a shallow marine assemblage of benthic foraminifers that shows some similarities to the *Gavelinella talaria* assemblage of Wall and Given (1977) and thus suggests correlation with the middle or upper Bearpaw Formation at Lundbreck.
4. The Lewis Thrust sheet overlies a succession of shoreface-to-brackish water deposits that represent the regressive phase of the Bearpaw Sea, which is dated in the Foothills at approximately 71 Ma. This date should be considered as a maximum age for the time of emplacement of the Lewis Thrust in the southern Canadian Cordillera.
5. Correlatives to the marginal marine sediments described above, containing oysters and coal, occur farther north in the footwall of the Lewis Thrust in the Crowsnest, Tornado Mountain, and Fording River map areas, and must be taken into account during future mapping of the foothills.

## ACKNOWLEDGMENTS

The first author is grateful to D.K. Norris for turning his attention to the outcrop 1, and to D. Van Helden for help in the field work. Discussions with J.H. Wall on the foraminiferal assemblages of the southern Foothills are gratefully acknowledged.

## REFERENCES

**Clow, W.H.A. and Crockford, M.B.B.**
1951: Geology of Carbondale River area, Alberta; Research Council of Alberta, Report No. 59, 70 p.

**Douglas, R.J.W.**
1951: Pincher Creek, Alberta; Geological Survey of Canada, Paper 51-22.
1952: Waterton, Alberta; Geological Survey of Canada, Paper 52-10.

**Eberth, D.A., Braman, D.R., and Tokaryk, T.T.**
1990: Stratigraphy, sedimentology and vertebrate paleontology of the Judith River Formation (Campanian) near Muddy Lake, west-central Saskatchewan; Bulletin of Canadian Petroleum Geology, v. 38, p. 387-406.

**Gibson, D.W.**
1977: Upper Cretaceous and Tertiary coal-bearing strata in the Drumheller-Ardley region, Red Deer valley, Alberta; Geological Survey of Canada, Paper 76-35.

**Jerzykiewicz, T. and Sweet, A.R.**
1988: Sedimentological and palynological evidence of regional climatic changes in the Campanian to Paleocene sediments of the Rocky Mountain Foothills, Canada; Sedimentary Geology, v. 59, p. 29-76.

**Lerbekmo, J.F. and Coulter, K.C.**
1985: Late Cretaceous to early Tertiary magnetostratigraphy of a continental sequence: Red Deer Valley, Alberta, Canada; Canadian Journal of Earth Sciences, v. 22, p. 567-583.

**Murray, J.W.**
1991: Ecology and Palaeoecology of Benthic Foraminifera; Longman Group UK Limited, 397 p.

**Nadon, G.**
1988: Tectonic controls on sedimentation within a foreland basin: The Bearpaw, Blood Reserve and St. Mary River formations, southwestern Alberta; Field Trip Guide to: Sequences, stratigraphy, sedimentology: Surface and subsurface; Canadian Society of Petroleum Geologists, 84 p.

**Norris, D.K.**
1993a: Geology and structure cross-sections, Beaver Mines (West Half), Alberta-British Columbia; Geological Survey of Canada, Map 1838A, scale 1:50 000.
1993b: Geology and structure cross-sections, Fording River (East Half), British Columbia-Alberta; Geological Survey of Canada, Map 1831A, scale 1:50 000.

**Obradovich, J.D.**
1993: A Cretaceous time scale; *in* Evolution of the Western Interior Basin, (ed.) W.G.E. Caldwell and E.G. Kauffman; Geological Association of Canada, Special Paper 39, p. 379-396.

**Price, R.A.**
1962: Fernie map-area, east half, Alberta and British Columbia, 82 GE 1/2; Geological Survey of Canada, Paper 61-24.

**Rosene, R.K.**
1972: Micropaleontology of the Bearpaw Formation, southwestern Alberta Foothills; Master's Thesis, University of Alberta, Edmonton, Alberta, 133 p.

**Srivastava, S.K.**
1970: Pollen biostratigraphy and paleoecology of the Edmonton Formation (Maestrichtian), Alberta, Canada; Palaeogeography, Palaeoclimatology, Palaeoecology, v. 7, p. 221-276.

**Wall, J.H.**
1976: Marginal marine foraminifera from the Late Cretaceous Bearpaw-Horseshoe Canyon transition, southern Alberta, Canada; Journal of Foraminiferal Research, v. 6, p. 193-201.

**Wall, J.H. and Rosene, R.K.**
1977: Upper Cretaceous stratigraphy and micropaleontology of the Crowsnest Pass - Waterton area, southern Alberta Foothills; Bulletin of Canadian Petroleum Geology, v. 25, no. 4, p. 842-867.

**Williams, E.P.**
1949: Cardston, Alberta; Geological Survey of Canada, Paper 49-3.

Geological Survey of Canada Project 930006

# A re-evaluation of the paleoglaciology of the maximum continental and montane advances, southwestern Alberta[1]

Lionel E. Jackson, Jr., Edward C. Little[2], Elizabeth R. Leboe[3], and Philip J. Holme[4]

Terrain Sciences Division, Vancouver

*Jackson, L.E., Jr., Little, E.C., Leboe, E.R., and Holme, P.J., 1996: A re-evaluation of the paleoglaciology of the maximum continental and montane advances, southwestern Alberta; in Current Research 1996-A; Geological Survey of Canada, p. 165-173.*

**Abstract:** Controversy over the age of the maximum known advances of continental and montane glaciers in southwestern Alberta rests largely on the paleoglaciology of the maximum montane piedmont glacier. Reconstruction of it, based upon features that mark the former glacier surface in the Foothills, indicate that the glacier had a maximum surface gradient of 0.4-0.6° – less than half the value assumed by previous workers. The continental ice sheet that was roughly coeval with the piedmont glacier and coalesced with it in the Foothills. Paleoglaciological evidence favours a Late Wisconsinan age for maximum extent of continental and montane ice.

**Résumé :** Dans le sud-ouest de l'Alberta, la controverse soulevée par l'âge des avancées maximales connues des glaciers continentaux et subalpins est en grande partie attribuable à la paléoglaciologie de la phase maximale du glacier de piémont subalpin. Sa reconstitution, basée sur les caractéristiques qui marquent l'ancienne surface glaciaire dans les contreforts, indique que le gradient de surface maximal du glacier (0,4-0,6°) correspondait à moins de la moitié de la valeur présumée auparavant. La nappe glaciaire continentale était à peu près contemporaine du glacier de piémont et a fusionné avec lui dans les contreforts. Les indices paléoglaciologiques font pencher en faveur de l'attribution d'un âge du Wisconsinien tardif à l'étendue maximale des glaciers continentaux et subalpins.

[1] Contribution to the Eastern Cordillera NATMAP Project

[2] Department of Earth and Atmospheric Sciences, University of Alberta, 26 Earth Sciences Building, Edmonton, Alberta T6G 2E3

[3] Department of Geography, Simon Fraser University, Burnaby, British Columbia V5A 1S6

[4] Department of Geography, University of British Columbia, Vancouver, British Columbia V6T 1W4

## INTRODUCTION

A third season of field mapping of the surficial geology of the Foothills of southwestern Alberta and contiguous areas of the Interior Plains and the Rocky Mountain Front Ranges was undertaken during the period June-August, 1995 as a part of the larger National Geoscience Mapping Program (NATMAP) aimed at integrating bedrock and surficial geology for this region. At the conclusion of the 1995 summer field season, preliminary digital surficial geology maps of eleven for the twelve 1:50 000 areas were completed. All field notes were entered into a relational database (FIELDLOG). Only one-half of the Beaver Mines map area (82G/8) remains to be covered. With the near completion of surficial geology mapping, the Quaternary geology and stratigraphy of the southwestern Foothills can now be considered in their totality. This paper represents the first in a series to report on new insights into the Quaternary history of this region based upon our detailed mapping and stratigraphic investigations.

Evidence for extensive advances of glacier ice from the Rocky Mountains and the continental interior in the southern Alberta Foothills (Fig. 1) was recognized initially by Dawson and McConnell (1895). They noted a basal boulder clay (till) of montane origin (Albertan Till) that extended from the Rocky Mountains to the Lethbridge area changing facies to gravels and sand over this distance. This was in turn overlain by two boulder clays bearing stones from the Canadian Shield. The two continental boulder clays were separated by intervening silt beds which they considered interglacial (their fig. 3). They also noted that boulders from the Canadian Shield as high as 1610 m in the Porcupine Hills which were coeval with the younger (upper) continental boulder clay. They assigned a "pre-Kansan" age to the lower continental boulder clay and the Albertan Till. This stratigraphy was modified by Horberg (1952, 1954) who subdivided the lower continental boulder clay at Lethbridge into two units (basal and lower tills) and discounted the interglacial nature of the silt beds separating the upper and lower tills. He concluded that all of these continental tills, and the stratigraphically lower Albertan Till farther west could be assigned to the Wisconsin Glaciation. This finding was corroborated by Wagner (1966) who described and correlated natural cliff exposures throughout the Oldman and Belly River basins upstream from Lethbridge. He also demonstrated that the continental ice sheet that deposited the most extensive (lower) till was at least partly synchronous with the waning stages of the montane glacier that deposited the Albertan Till. Horberg (1954) and Wagner (1966) also concurred in their division of the region's glacial deposits into two temporal groupings:

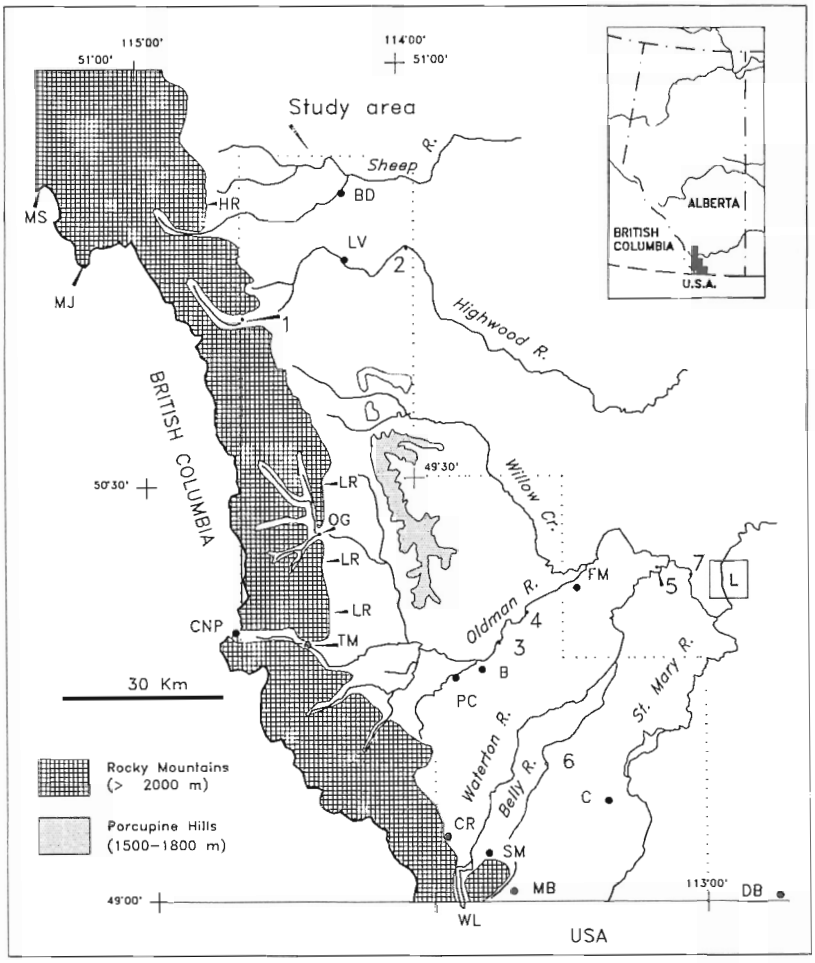


*Figure 1.*

*Geography of the Foothills NATMAP study area and the surrounding region and locations discussed in the text: WL – Waterton Lakes, MB – Mokowan Butte, C – Cardston, DB – Del Bonita, SM – Sofa Mountain, CR – Cloudy Ridge, PC – Pincher Creek, L – Lethbridge, B – Brocket, FM – Fort Macleod, TM – Turtle Mountain, CNP – Crowsnest Pass, OG – Oldman Gap, LV – Longview, BD – Blackdiamond, MJ – Mt. Joffre, MS – Mt. Sir Douglas, HR – Highwood Range, LR – Livingstone Range. The numbers identify cliff bank exposures described in the text.*

1. The entire valley fill seen by Dawson and McConnell from Lethbridge into the Foothills along with the high erratics on the Porcupine Hills were assigned to the Wisconsin Glaciation.
2. The interstratified drift/paleosol sequences of the Kennedy Drift (Alden, 1932; Alden and Stebinger, 1913) seen on Mokowan Butte and a unit thought to be a till below a paleosol on Cloudy Ridge (Fig. 1) were assigned to montane glaciations prior to the Wisconsin.

In contrast, Stalker (1963), Alley (1972, 1973), Alley and Harris (1974), and Stalker and Harrison (1977) came to considerably different conclusions based upon the interpretation of the same natural exposures but particularly on the interpretation of the extensive cliff bank exposure near Brocket (Fig. 1, Location 3). They concluded that the till units within the valley fills exposed in the Oldman and Belly River basins represented multiple glaciation extending back to the Illinoian Glaciation or before. Stalker and Harrison assigned the informal name "Great Glaciation" to the glaciation responsible for the deposition of the first montane (Albertan) till and the most extensive continental till (Labuma; Stalker, 1963). One of the cornerstones of their argument was their correlation of the Albertan Till with the uppermost till unit of the Kennedy drift on Mokowan Butte and a unit described as till by Horberg (1954) on Cloudy Ridge. Both of these units are capped by paleosols developed under climates significantly warmer and over periods more than an order of magnitude longer than the present (Holocene) interglacial (Horberg, 1954; Karlstrom, 1987).

The purpose of this paper is to the test the paleoglaciological reconstructions of the maximum montane and continental glaciers of Stalker and Harrison (1977) against our observations of glacial limits. We apply these findings to reconciliation of their age assignments to this glaciation with those of Wagner (1966), Clayton and Moran (1983), Fullerton and Colton (1986), and Little (1995) and others. The term "Maximum Glaciation" will be used throughout this paper to refer to this glaciation.

## THE GREAT MONTANE GLACIER

### *Stalker and Harrison model*

Stalker and Harrison (1977) reconstructed the montane glacier responsible for depositing the Albertan Till between Waterton Lakes and Lethbridge. They arrived at an estimate of ice thickness at the mountain front ranging between 1200 and 1500 m and ice surface gradients of between 16.4 and 19.6 m/km based upon the compilation of extant glacier gradients made by Buckley (1969). These values were arrived at assuming:

1. Alpine landforms within the Lewis and Clark Ranges of what is now Waterton Lakes National Park in Alberta and Glacier National Park in Montana were sculpted as nunataks projecting through an ice dome over the region.
2. The maximum areal extent of the piedmont glacier could be inferred from the subsurface distribution of the Albertan Till.

The Albertan Till can be traced to the eastern margin of the Foothills in cliff bank exposures (Fig. 1, locations 3, 4, and 6) where it overlies gravels of purely montane provenance (Saskatchewan Gravels). Stalker (1963) and Wagner (1966) reported montane diamicton and ice-contact montane gravels in the Monarch and Lethbridge areas (Fig. 1, locations 5 and 7 respectively). These units also overlie the Saskatchewan Gravels directly. They computed ice thicknesses at the Rocky Mountain front by applying assumed regional slope values to the piedmont lobe with a terminus in the Lethbridge area. The resulting surface elevation of about 2400 m is more than sufficient to overrun Mokowan Butte (maximum elevation 1800 m; Fig. 1). This led them to the conclusion that the uppermost diamicton of the Kennedy Drift (Alden, 1932), which caps this upland, correlates to the Albertan Till. Furthermore, it followed that the paleosol developed upon the uppermost Mokowan Butte diamicton was proof that one or more periods of interglacial climate occurred between the deposition of the Albertan Till and subsequent montane advances. Because stratigraphic evidence clearly shows the continental Labuma Till to be coeval with the Albertan Till, it follows that the maximum continental advance must have have occurred prior to the Wisconsin Glaciation as well (Stalker and Harrison, 1977).

### *Montane "Maximum Glaciation" ice limits determined from the present study*

The former upper limits of glacial ice of montane origin in the area of the Rocky Mountain front was determined from the elevations of the highest occurrence of erratic boulders of montane origin and the upper limits of glacial and glaciofluvial erosion such as former ice-walled channels. Limits associated exclusively with the maximum montane glaciation can only be determined near the mountain front where ridges were sufficiently high to protrude above the surfaces of montane and continental glaciers. Table 1 lists elevations of the uppermost ice-related features along the Mountain Front. Table 2 lists the locations and former ice surface markers on high Foothills ridges in the Oldman River basin above the confluence with the Crowsnest River. These data indicate that ice thickness at the Rocky Mountain Front did not exceed 550 m, with the glacier surface no higher that 1800 m. The highest elevations were recorded at Oldman Gap and Turtle Mountain where outlet glaciers passed through bottlenecks of about a 1 km in width. Gradients had to have been steep across these constrictions. Consequently, these elevations are probably significantly above the general level of ice over the adjacent Foothills. The coalesced network of valley glaciers traversing the Foothills did not exceed thicknesses of approximately 300 m.

### *Firn lines associated with the Great Montane Glacier*

The paleo-firn line during the climax of the advance of the Great Montane Glacier was approximated by measuring the elevations of the lowest cirque floors and the highest ridges without cirques within the study area north of the Crowsnest River. The lowest cirque floors range down to an elevation of

1680 m in the Highwood Range and 1780 m in the Livingstone Range. The Porcupine Hills have no apparent cirque features and range up to 1820 m. Consequently, the paleo-firn line fell to the range of 1680 to 1820 m. It is consistent with the estimates of the paleo-firn line during the acme of the Pinedale and Bull Lake glaciations at 49°N by Richmond (1965; his fig. 3). The closest large extant glaciers to the study area north of 49° are in the areas of Mt. Sir Douglas and Mt. Jofre (Fig. 1: MS and MJ). These have firn lines in the range of 2590 m elevation. These observations permit an estimate of firn line depression of between 770 and 910 m during the montane advance of the Great Glaciation. This range exceeds the value of 600 m for depression of the snowline in the northern Rocky Mountains of the United States during the Pinedale and Bull Lake glaciations by Richmond (1965) who also used cirque floor elevations to arrive at his estimate. However, other methodologies have yielded values for firn line depression in the same region of as much as 1200 m (Richmond, 1965).

Jackson (1994) cited evidence for two paleo-firn lines in the Rocky Mountains within the northern portion of the study area. He noted that cirques in the Rocky Mountains of this region could be classified by age based upon their apparent

**Table 1.** Maximum thicknesses of montane ice at the Rocky Mountain front and estimates of piedmont glacier gradients.

| Location (Figure 2) | Feature | Elevation (m) | Inferred former ice thickness at Rocky Mountain Front (m) | Most distant till exposure (Figure 2) / distance from exposure to highest related ice limit feature at the Rocky Mountain Front (m) | Average ice slope m/km (degrees)[1] |
|---|---|---|---|---|---|
| South end of Highwood Range (HW) | meltwater channel | 1740 | 260 | 2/42 | 16 (0.9) |
| Oldman Gap (OG) | upper limit of glacial erosion | 1770 | 400 | 5/132 | 6.6 (0.4) |
| Turtle Mountain (TM) | upper limit of glacial erosion | 1800 | 550 | 5/105 | 8.6 (0.5) |
| Cloudy Ridge (TM ) | upper limit of moraine | 1680 | 125 | 5/91 | 8.5 (0.5) |
| Ridge north of Sofa Mountain (SM ) | upper limit of lateral moraine | 1770 | 490 | 5/95 | 9.1 (0.5) |

[1] Values rounded to the nearest tenth of m/km and tenth of degree.

**Table 2.** Ice-limit features in the Foothills.

| Feature | Location | Elevation | Comments |
|---|---|---|---|
| Cross-ridge meltwater channels | Whaleback Ridge between 49°52' and 50°00' north 114°13' west | Common up to 1680 m. | Upper limit of montane glacial ice |
| Montane erratics on ridge top and cross ridge meltwater channels | Unnamed ridge west of Callum Cr. between 49° 52' and 49°53', 114°9.5' west | Montane erratics to 1520 m, meltwater channels to same elevation | Upper limit of Canadian Shield erratics to about 1500 m (point C, Figure 4) |
| Cross-ridge meltwater channel | Unnamed ridge north of Tod Creek area of 49°47.5' north 114°16' west | Channels up to 1680 m | Upper limit of montane ice |
| Highest montane erratic, cross ridge meltwater channel | Unnamed ridge, headwaters Wildcat Cr. 49°44' north, 114°15' west | Montane erratics to 1520 m, cross ridge channel at 1590 m. | Upper limit of montane ice |
| Cross-ridge meltwater channels | Unnamed ridge east of Centre Peak 49°43.5' north, 114°17' west | Meltwater channels up to 1650 m | Upper limit of montane ice |
| Cross-ridge meltwater channels | Unnamed ridge north of Ross Lake 49°41' north, 144°14' west | Meltwater channel at 1520 m | Upper limit of montane ice |
| Highest erratics | South end of Porcupine Hills, area of 49°44' to 49°44.5' north and 113°49' and 114°3' west | Highest Canadian Shield erratic 1585 m; highest limestone 1598 m; highest quartzite 1611 m. | Upper limit of continental ice and possibly montane ice although highest montane erratics could have been reworked and emplaced by continental ice (point B, Figure 4) |

freshness or degradation, i.e. the presence of dendritic drainage within the cirque headwall. He observed that fresh cirques occur above 2050 m elevation, whereas degraded cirques range as low as 1680 m. He concluded that this was evidence of two glaciations separated by an extended period of erosion. He referred the younger and less extensive event with the high paleo-firn line to the Late Wisconsinan Erratics Train Glaciation (Jackson, 1980; Jackson et al., 1989) whereas the lower paleo-firn line was correlated to a more extensive penultimate glaciation.

Further examination of cirques in the study area has allowed a re-interpretation of the development of drainage systems in cirque headwalls. Neither the lithology of bedrock in which these cirques have developed nor the presence of apparently degraded cirques at higher elevations were taken into consideration in Jackson's analysis. Bedrock lithology in the region varies directly with age. Paleozoic bedrock consists of resistant and thickly bedded limestone, dolostone, and quartzite. These units outcrop almost entirely above 1800 m whereas Mesozoic units consisting of sandstone, shale, conglomerate, and coal, outcrop below 2100 m. Figure 2 shows freshness and the presence of integrated channels within cirque head walls to be related to lithology as well as elevation rather than to elevation only. Eroded cirques developed in Mesozoic rocks occur at all levels as do uneroded ones. Airphoto interpretation indicates that the lack of development of dendritic drainage in cirques developed in Paleozoic rock units is associated with the accumulation of porous talus aprons that protect cirque head walls from erosion by running surface water. This armouring is particularly effective within cirques developed in the Paleozoic carbonates and quartzites which yield coarse, resistant talus. In contrast, the Mesozoic clastics yield more friable talus and scree which is more erodible. Figure 2 shows a general trend for cirques developed in all lithologies to increase in freshness with elevation. This appears to be related to the increase of mass wasting processes over fluvial erosion processes with elevation. Consequently, clear cut evidence does not exist to infer two ages of cirques in the Rocky Mountains within the study area.

## *Discussion*

The paleo-ice surface reconstructed by Stalker and Harrison (1977) for the Great Piedmont Glacier is incompatible with the observable ice limit data (Tables 1 and 2). If glacier ice ever reached the thickness at the Rocky Mountain Front that they proposed, no ridges within the Foothills of the study area including the highest summits of Porcupine Hills (about 1820 m) would have escaped inundation beneath montane ice. Even assuming that the Foothills within Oldman River basin were affected only by ice originating from Waterton Lakes area, montane erratics should be found over 100 m higher than the upper limits of erratics of either montane or Canadian Shield provenance at the southern end of Porcupine Hills (see below).

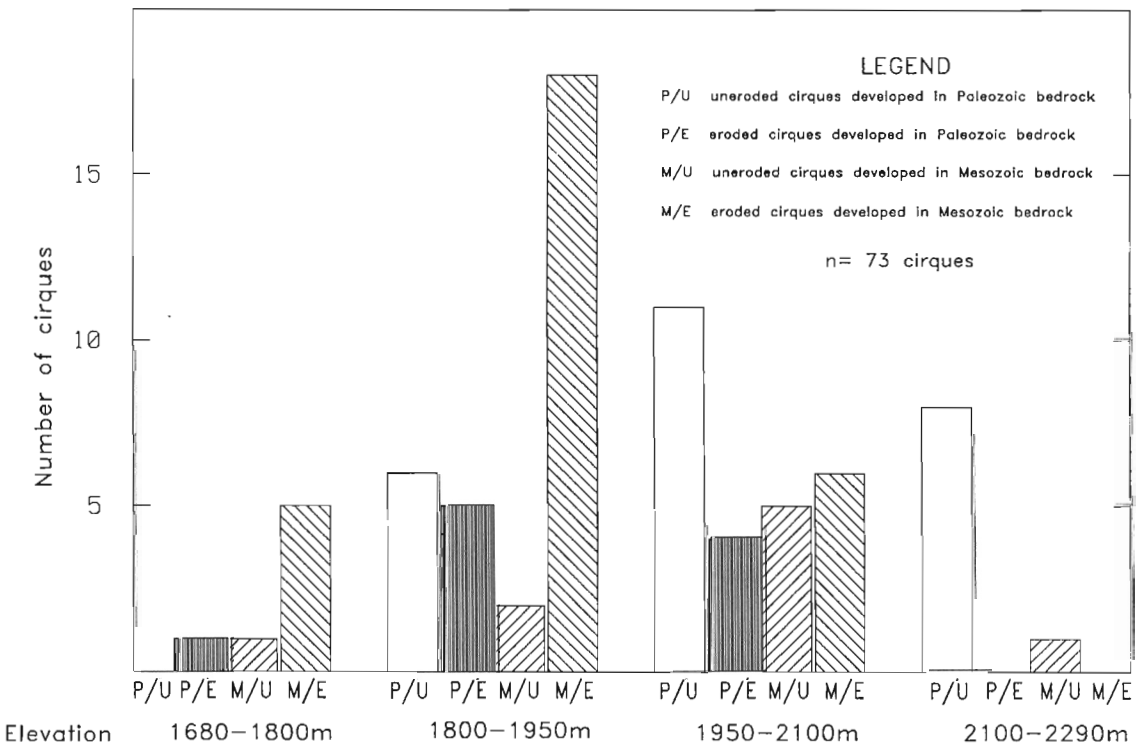


***Figure 2.*** *The frequency of eroded and noneroded cirque headwalls with elevation in the Rocky Mountains of Langford Creek (82J/1), Maycroft (82G/16), and Blairmore (82G/9) map areas. Elevations were determined from topographic maps with an error range of approximately 30 m.*

Excluding the data from the Highwood Range, ice gradients between ice limit control points at the Rocky Mountain Front (Tables 1 and 2) and Lethbridge were calculated along flow paths shown in Figure 3. These followed main valleys in the Foothills and the shortest distance over the Plains. The gradients calculated best fit a low profile complex of valley glaciers within the ridge and valley terrain of the Foothills and a low profile piedmont glacier on the adjacent Plains with an overall surface gradient of about one-half to one-third the value of that assumed by Stalker and Harrison (approximately 0.4 to 0.6° versus 0.9 to 1.1°). This low profile is in agreement with reconstruction of other Pleistocene montane ice sheets which advanced into lowland areas. For example, Jackson et al. (1991) found that the outer 50 km of the last Cordilleran Ice Sheet in central Yukon had an overall gradient of 0.5°, with the profile flattening to 0.3° further inboard (eastward). Reconstructed contours on the outer (southernmost) 100 km of the Puget lobe of the Cordilleran Ice Sheet yielded a gradient of about 0.6° (Booth, 1991, his fig. 3). The gradient calculated for the equivalent advance of piedmont ice from the from the Highwood Range (Table 1, Fig. 3) is anomalously steeper. However, no sections east of the location 2, (which exposes the equivalent to the Albertan Till) have been examined in this basin (Jackson, 1994, lower till in his fig. 4). It is likely, based upon gradients calculated in the Oldman River basin, that the piedmont lobe originating in the Highwood Range extended well beyond location 2 in Figure 1.

## THE GREAT LAURENTIDE GLACIER

### *Stalker and Harrison model*

The advance of the Great Laurentide Glacier of Stalker and Harrison (1977) represented the all time limit of continental ice in the Foothills of Alberta. Their reconstruction of this glacier was based entirely on the upper and westernmost limits of erratics from the Canadian Shield. The reconstruction was limited to the Foothills and the Rocky Mountain Front south of approximately 49°50′. They recognized that the upper limit of erratics rises from east to west from the Plains (1310 m south of Lethbridge) to the Rocky Mountain Front (as high as 1585 m west of Waterton Lakes) and from south to north. This pattern has been corroborated by the regional study of Wagner (1966) and other less expansive studies. This advance is linked to the stratigraphically lowest continental till found in the Foothills originally called the "lower till" by Horberg (1952) and named Labuma by Stalker (1963) through correlation with a till he named in the Red Deer area several hundred kilometres to the north. The Labuma Till either conformably overlies the Albertan Till or is separated from it by lacustrine deposits bracketed by conformable contacts. No evidence of fluvial erosion deposits such as lag gravels or weathered profiles have been found

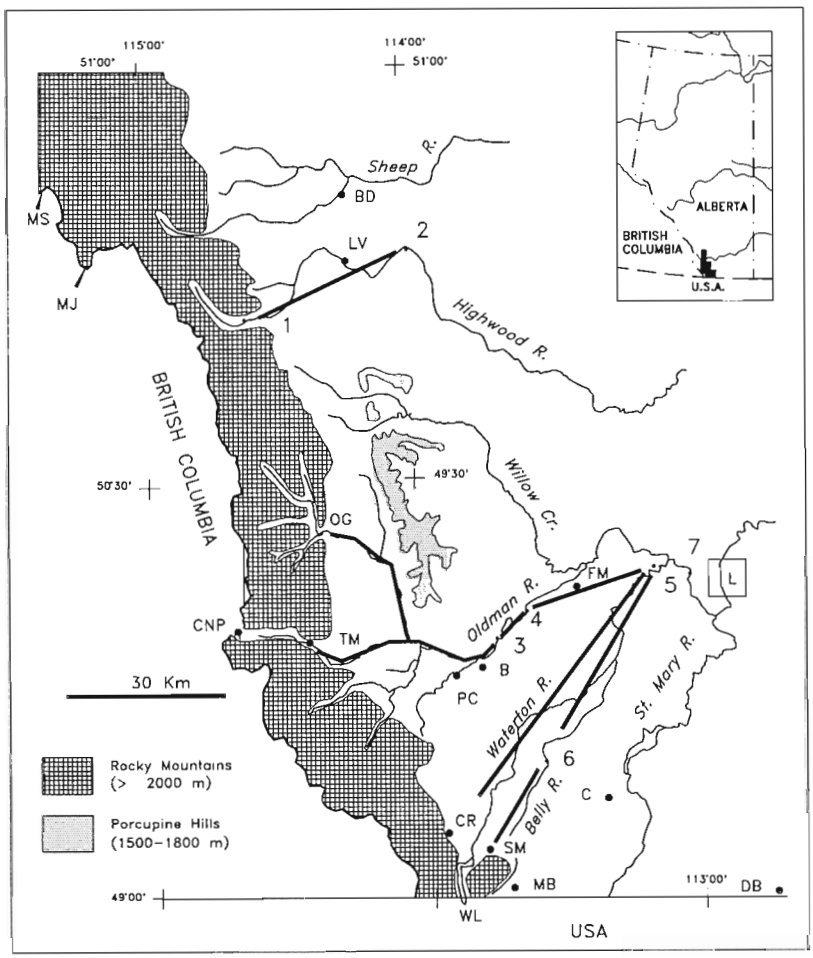


***Figure 3.***

*Heavy lines denote paths along which paleo-ice surface gradients listed in Table 2 were calculated. See Figure 1 caption for location key.*

between the two tills. This led Stalker and Harrison (1977) to conclude that the Great Laurentide Glacier was roughly time equivalent to the Great Montane Glacier.

### *Findings from the present study*

The general picture of the Great Laurentide Glacier remains the same as that of Stalker and Harrison (1977). However, the present study has served to better define its limits, particularly north of the area addressed by Stalker and Harrison, and its relationship with coeval montane ice. Our observations combined with those of Day (1971) and Douglas (1950) indicate that during the climax of this advance, continental ice reached and may have overtopped the northern end of the Porcupine Hills, depositing erratics on summits presently as high as 1750 m (50°04′20″, 114°04′30″; Day, 1971). Shield erratics completely encircle the Porcupine Hills south of Willow Creek. Ice pressed up the south fork of Willow Creek (arrow north of Point C, Fig. 4) on the north flank of the Porcupine Hills and pressed up the Oldman River along the south and west side of them (arrow south of B, Fig. 4) to apparently meet the South Willow Creek lobe at the base of the Rocky Mountain Front (Point C, Fig. 4). The gradient of the ice sheet, uncorrected for any differential isostatic rebound, can be roughly approximated. Assuming that erratics were close to the ice surface, then the highest erratics at 1750 m at the north end of the Porcupine Hills and those at 1585 m at the south end describe a gradient of approximately 160 m over 40 km or 4 m/ km (approximately 0.2°). The distance between these points was measured in a straight line (Fig. 4, A-B). The actual path of flow is not known but it was likely longer. If so, the ice surface gradient was gentler. For example, Stalker (1965) determined an upper value of approximately 2.5 m/km for the slope of the maximum continental advance in southern Alberta and Saskatchewan. This is steeper than other regional slope values found for last continental ice sheet in western Canada: Mathews (1974) approximated the profiles for various lobes of the maximum Laurentide Ice Sheet in southern Alberta and Saskatchewan and northern Montana and North Dakota using the parabolic formula:

$$h=Ax^{0.5}$$

where h is ice thickness at distance x from the terminus. For distances in metres, he found A values in the range of 0.46 to 1.0. For distances more than 100 to 200 km from the ice terminus (representative for the Porcupine Hills), the highest (A = 1.0) value yields a gradient of 1.3 m/km or about 0.07°. This low gradient has been corroborated elsewhere. Duk-Rodkin and Hughes (1995) found a regional surface gradient of less than 1 m/km for the Laurentide Ice Sheet along its northwestern extremity east of the Mackenzie Mountains.

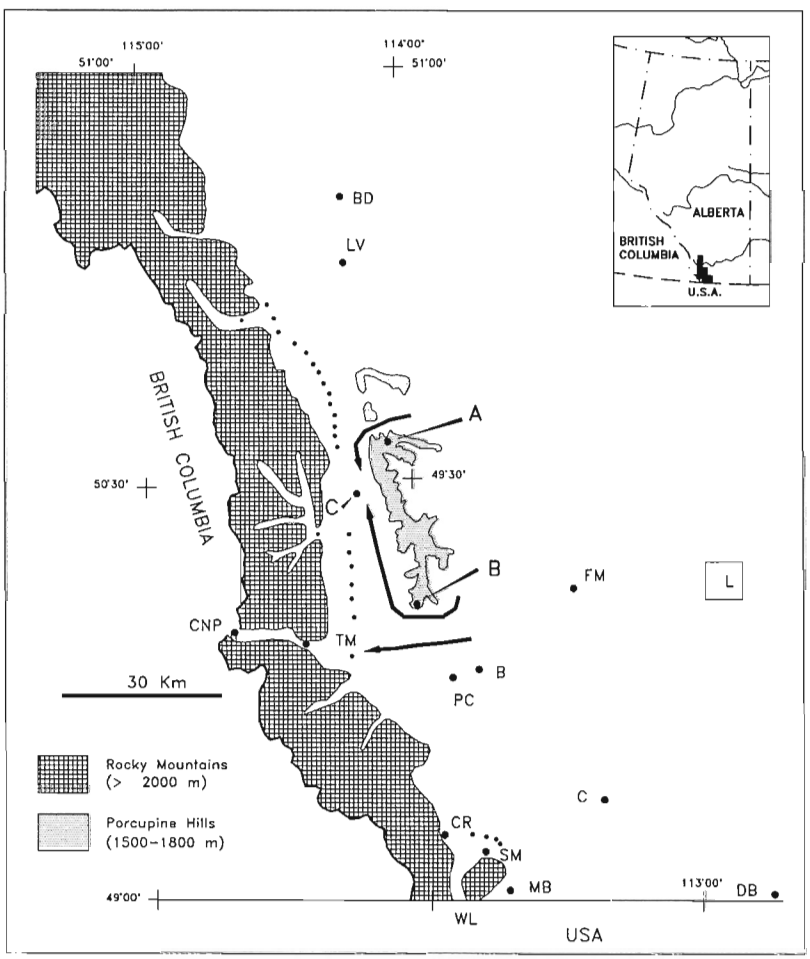


***Figure 4.***

*Locations of erratics (points A, B, C) from which surface gradients upon the maximum extent of the continental ice sheet were calculated and areas of contact between continental and montane ice (heavy dotted lines) during the same glaciation. See Figure 1 caption for location key.*

The upper limit of Shield erratics descends approximately 80 m over 23 km west of the Porcupine Hills (Fig. 4, B-C; lat. 49°42′ to 49°52′) or about 4 m/km (approximately 0.4°). Again, this gradient was measured over a straight line and should be regarded as a maximum figure.

In many areas, particularly within major valleys, the western limit of Canadian Shield erratics is offset east and depressed in elevation compared to the upper limits of Shield erratics between valleys. Wagner (1966) suggested that these were areas where montane and continental ice were in contact preventing continental ice from penetrating deeper into the Foothills. These areas are portrayed by heavy dotted lines in Figure 4. Our mapping of till pebble lithology corroborates Wagners interpretation. Although the climax of the maximum montane advance preceded the continental climax, the two advances were not as asynchronous as was portrayed by Stalker and Harrison (although they too (p. 896) postulated at least local contact).

## AGE OF THE MAXIMUM GLACIATION

The interpretation of ice limit evidence presented in this paper rejects the paleoglaciological reconstruction of the Great Montane Glacier of Stalker and Harrison (1977). Montane ice near the front of the Rocky Mountains was never thick enough to reach the top of Mokowan Butte during the maximum montane advance associated with the Albertan Till. The reconstruction of the Great Montane Glacier documented in this paper is comparable to the Pinedale (late Wisconsinan) piedmont glaciers in northern Montana. The Two Medicine Glacier (Alden, 1932) which existed about 75 km south of the Canada-United States border, advanced up to 64 km from the Rocky Mountain front and covered approximately 2200 square kilometres during its maximum extent. It had an iceshed of less than 20% of that of the combined St. Mary, Belly, and Oldman River basins that fed the Great Montane piedmont glacier in the Lethbridge area which advanced 100 km from the mountain front. Although it can be argued that the Two Medicine Lobe was partly fed by ice crossing the Continental Divide (Carrara, 1989, p. 8), our mapping has shown that large volumes of ice also crossed the Continental Divide at Crowsnest Pass and contributed to the Great Montane Glacier. Furthermore, the paleo-firn line was apparently at the same elevation during the Pinedale and Maximum Glaciation. We conclude that the piedmont advance of the Great Glaciation of Stalker and Harrison (1977) is equivalent in age to the Two Medicine Lobe and can be assigned to the Pinedale (Late Wisconsinan) Glaciation as was originally envisioned by Alden (1932; his Plate 37). Consequently, it follows that all of the glacial deposits overlying the Albertan and Labuma tills glacial deposits must be of Late Wisconsinan age as well. This is consistent with the chronologies of Horberg (1954), Wagner (1966), Bayrock (1969), Clayton and Moran (1983), Fullerton and Colton (1986),Young et al. (1994), and Little (1995). Further supporting stratigraphic evidence will be presented in a forthcoming paper.

## CONCLUSIONS

Ice limit features and the upper limits of montane erratics in the Foothills can be used to reconstruct the surface of the maximum montane glacier near the Rocky Mountain front. The maximum thickness of ice there was less than 550 m and probably never reached more that 300 m over most of the Foothills. The average gradient on the ice surface between the Rocky Mountain front and Lethbridge was one-half to one-third of that previously estimated by Stalker and Harrison (1977). The firn line during this event was comparable to that estimated by Richmond (1965) for the maxima of the Pinedale and Bull Lake glaciations at 49°N. The argument for two ages of cirques in the southern Rocky Mountains proposed by Jackson (1994) was found to be incorrect due to a lack of consideration of lithological controls on erodability when assigning an apparent age.

The maximum advance of the continental ice sheet was coeval with the maximum montane advance but climaxed slightly later. Sufficient montane ice remained in the Foothills to prevent its penetration up major valleys. Apparent surface gradients of this ice sheet are steeper than those measured elsewhere; this may be the result of straight line measurements where flow was sinuous or oblique to the measured direction.

The maximum advance of montane ice is not related to the uppermost drift unit on Mokowan Butte. The scale of the advance and associated paleo-firn line is similar to the Pinedale (Late Wisconsinan) Glaciation and is assigned to it along with the maximum continental advance.

## REFERENCES

**Alden, W.C.**
1932: Physiography and glacial geology of eastern Montana and adjacent areas; United States Geological Survey, Professional Paper 174, 133 p.

**Alden, W.C. and Stebinger, E.**
1913: Pre-Wisconsin glacial drift in the region of Glacier National Park, Montana; Geological Society of America Bulletin, v. 23, p. 687-708.

**Alley, N.F.**
1972: The Quaternary history of part of the Rocky Mountains, Foothills, Plains and western Porcupine Hills; PhD. thesis, Department of Geography, University of Calgary, Calgary, Alberta, 201 p.
1973: Glacial stratigraphy and the limits of Rocky Mountain and Laurentide ice sheets in southwestern Alberta, Canada; Bulletin of Canadian Petroleum Geology, v. 21, p. 153-177.

**Alley, N.F. and Harris, S.A.**
1974: Pleistocene glacial lake sequences in the Foothills, southwestern Alberta, Canada; Canadian Journal of Earth Sciences, v. 11, p. 153-177.

**Bayrock, L.A.**
1969: Incomplete continental glacial record of Alberta, Canada; Quaternary Geology and Climate, Publication 1701, National Academy of Sciences, Washington, D.C., p. 99-103.

**Booth, D.B.**
1991: Glacier physics of the Puget Lobe, southwest Cordilleran Ice Sheet; in The Cordilleran Ice Sheet, (ed.) L.E. Jackson Jr. and J.J. Clague; Géographie physique et Quaternaire, v. 45, p. 301-316.

**Buckley, J.T.**
1969: Gradients of past and present outlet glaciers; Geological Survey of Canada, Paper 69-29, 13 p.

**Carrara, P.E.**
1989: Late Quaternary glacial and vegetative history of the Glacier National Park region, Montana; United States Geological Survey, Bulletin 1902, 64 p.

**Clayton, L. and Moran, S.R.**
1983: Chronology of late Wisconsinan glaciation in middle North America; Quaternary Science Reviews, v. 1, p. 55-82.

**Dawson, G.M. and McConnell, R.G.**
1895: Glacial deposits of southwestern Alberta in the vicinity of the Rocky Mountains; Bulletin of the Geological Society of America, v. 7, p. 31-66.

**Day, D.L.**
1971: The glacial geomorphology of the Trout Creek area, Porcupine Hills, Alberta; MSc. thesis, Department of Geography, University of Calgary, Calgary, Alberta, 158 p.

**Douglas, R.J.W.**
1950: Callum Creek, Langford Creek, and Gap map areas, Alberta; Geological Survey of Canada, Memoir 255, 123 p.

**Duk-Rodkin, A. and Hughes, O.L.**
1995: Quaternary geology of the northeast part of the central Mackenzie valley corridor, Northwest Territories; Geological Survey of Canada, Bulletin 458, 45 p.

**Fullerton, D.S. and Colton, R.B.**
1986: Stratigraphy and correlation of the glacial deposits on the Montana plains; Quaternary Science Reviews, v. 5, p. 69-82.

**Horberg, L.**
1952: Pleistocene drift sheets in the Lethbridge region, Alberta, Canada; Journal of Geology, v. 60, p. 303-330.
1954: Rocky Mountain and continental Pleistocene deposits in the Waterton region, Alberta, Canada; Geological Society of America Bulletin, v. 65, p. 1093-1150.

**Jackson, L.E., Jr.**
1980: Glacial history and stratigraphy of the Alberta portion of the Kananaskis Lakes map area; Canadian Journal of Earth Sciences, v. 17, p. 459-477.
1994: Quaternary geology and terrain inventory, Foothills and adjacent plains, southwestern Alberta: some new insights into the last two glaciations; in Current Research 1994-A; Geological Survey of Canada, p. 237-242.

**Jackson, L.E., Jr., Rutter, N.W., Hughes, O.L., and Clague, J.J.**
1989: Glaciated fringe (Quaternary stratigraphy and history, Canadian Cordillera); in Chapter 1 of Quaternary Geology of Canada and Greenland, (ed.) R.J. Fulton; Geological Survey of Canada, Geology of Canada, no. 1 (also Geological Society of America, The Geology of North America, v. K-1).

**Jackson, L.E., Jr., Ward, B., Duk-Rodkin, A., and Hughes, O.L.**
1991: The last Cordilleran Ice Sheet in Yukon Territory; in The Cordilleran Ice Sheet, (ed.) L.E. Jackson Jr. and J.J. Clague; Géographie physique et Quaternaire, v. 45, p. 301-316.

**Karlstrom, E.T.**
1987: Stratigraphy and genesis of five superposed paleosols in pre-Wisconsinan drift on Mokowan Butte, southwestern Alberta; Canadian Journal of Earth Sciences, v. 24, p. 2235-2253.

**Little, E.C.**
1995: A single maximum-advance hypothesis of continental glaciation restricted to the late Wisconsinan, southwestern Alberta; MSc. thesis, Department of Earth Sciences, University of Western Ontario, London, Ontario, 229 p.

**Mathews, W.M.**
1974: Surface profiles of the Laurentide Ice Sheet in its marginal areas; Journal of Glaciology, v. 13, p. 37-43.

**Richmond, G.M.**
1965: Glaciation of the Rocky Mountains; in The Quaternary of the United States, (ed.) H.E. Wright and D.G. Frey; Princeton University Press, Princeton, New Jersey, p. 217-230.

**Stalker, A.MacS.**
1963: Quaternary stratigraphy in southern Alberta; Geological Survey of Canada, Paper 62-34, 52 p.
1965: Pleistocene ice surfaces, Cypress Hills area; in Cypress Hills Plateau, Alberta and Saskatchewan: 15th Annual Field Conference, (ed.) R.L. Zell; Canadian Society of Petroleum Geologists, p. 116-130.

**Stalker, A.MacS. and Harrison, J.E.**
1977: Quaternary glaciation of Waterton-Castle River region of Alberta; Bulletin of Canadian Petroleum Geology, v. 25, p. 882-906.

**Wagner, W.P.**
1966: Correlation of Rocky Mountain and Laurentide glacial chronologies in southwestern Alberta, Canada; PhD. thesis, University of Michigan, Ann Arbour, Michigan, 141 p.

**Young, R.R., Burns, J.A., Smith, D.G., Arnold, L.D., and Rains, R.B.**
1994: A single, late Wisconsin, Laurentide glaciation, Edmonton area and southwestern Alberta; Geology, v. 22, p. 683-686.

Geological Survey of Canada Project 930043

# AUTHOR INDEX

## NOTE TO CONTRIBUTORS

Submissions to the Discussion section of Current Research are welcome from both the staff of the Geological Survey of Canada and from the public. Discussions are limited to 6 double-spaced typewritten pages (about 1500 words) and are subject to review by the Chief Scientific Editor. Discussions are restricted to the scientific content of Geological Survey reports. General discussions concerning sector or government policy will not be accepted. All manuscripts must be computer word-processed on an IBM compatible system and must be submitted with a diskette using WordPerfect. Illustrations will be accepted only if, in the opinion of the editor, they are considered essential. In any case no redrafting will be undertaken and reproducible copy must accompany the original submissions. Discussion is limited to recent reports (not more than 2 years old) and may be in either English or French. Every effort is made to include both Discussion and Reply in the same issue. Current Research is published in January and July. Submissions should be sent to the Chief Scientific Editor, Geological Survey of Canada, 601 Booth Street, Ottawa K1A 0E8 Canada.

## AVIS AUX AUTEURS D'ARTICLES

Nous encourageons tant le personnel de la Commission géologique que le grand public à nous faire parvenir des articles destinés à la section discussion de la publication Recherches en cours. Le texte doit comprendre au plus six pages dactylographiées à double interligne (environ 1500 mots), texte qui peut faire l'objet d'un réexamen par le rédacteur scientifique en chef. Les discussions doivent se limiter au contenu scientifique des rapports de la Commission géologique. Les discussions générales sur le Secteur ou les politiques gouvernementales ne seront pas acceptées. Le texte doit être soumis à un traitement de texte informatisé par un système IBM compatible et enregistré sur disquette WordPerfect. Les illustrations ne seront acceptées que dans la mesure où, selon l'opinion du rédacteur, elles seront considérées comme essentielles. Aucune retouche ne sera faite au texte et dans tous les cas, une copie qui puisse être reproduite doit accompagner le texte original. Les discussions en français ou en anglais doivent se limiter aux rapports récents (au plus de 2 ans). On s'efforcera de faire coïncider les articles destinés aux rubriques discussions et réponses dans le même numéro. La publication Recherches en cours paraît en janvier et en juillet. Les articles doivent être envoyés au rédacteur en chef scientifique, Commission géologique du Canada, 601, rue Booth, Ottawa K1A 0E8 Canada.

Geological Survey of Canada Current Research, is released twice a year, in January and July. The four parts published in January 1996 (Current Research 1996-A to D) are listed below and can be purchased separately.

Recherches en cours, une publication de la Commission géologique du Canada, est publiée deux fois par année, en janvier et en juillet. Les quatre parties publiées en janvier 1996 (Recherches en cours 1996-A à D) sont énumérées ci-dessous et sont vendues séparément.

Part A: Cordillera and Pacific Margin
Partie A : Cordillère et marge du Pacifique

Part B: Interior Plains and Arctic Canada
Partie B : Plaines intérieures et région arctique du Canada

Part C: Canadian Shield
Partie C : Bouclier canadien

Part D: Eastern Canada and national and general programs
Partie D : Est du Canada et programmes nationaux et généraux